

2021

## Thermal Performance of Case-study Apartment Buildings in Temperate Climate Zones in Australia: Measurements, Modelling, and Codes

Steven Beltrame

Follow this and additional works at: <https://ro.uow.edu.au/theses1>

### University of Wollongong

#### Copyright Warning

You may print or download ONE copy of this document for the purpose of your own research or study. The University does not authorise you to copy, communicate or otherwise make available electronically to any other person any copyright material contained on this site.

You are reminded of the following: This work is copyright. Apart from any use permitted under the Copyright Act 1968, no part of this work may be reproduced by any process, nor may any other exclusive right be exercised, without the permission of the author. Copyright owners are entitled to take legal action against persons who infringe their copyright. A reproduction of material that is protected by copyright may be a copyright infringement. A court may impose penalties and award damages in relation to offences and infringements relating to copyright material.

Higher penalties may apply, and higher damages may be awarded, for offences and infringements involving the conversion of material into digital or electronic form.

Unless otherwise indicated, the views expressed in this thesis are those of the author and do not necessarily represent the views of the University of Wollongong.

Research Online is the open access institutional repository for the University of Wollongong. For further information contact the UOW Library: [research-pubs@uow.edu.au](mailto:research-pubs@uow.edu.au)



UNIVERSITY  
OF WOLLONGONG  
AUSTRALIA

**Thermal Performance of Case-study Apartment Buildings in  
Temperate Climate Zones in Australia: Measurements,  
Modelling, and Codes**

Steven Beltrame

This thesis is presented as part of the requirement for the conferral of the degree:  
Doctor of Philosophy

This research has been conducted with the support of an Australian Government  
Research Training Program Scholarship

University of Wollongong  
Sustainable Buildings Research Centre  
Faculty of Engineering and Information Sciences

June 2021

## **Abstract**

Population growth and lifestyle incentives have led to an increase in the amount and proportion of people living in apartment dwellings in Australia's capital and major regional cities. Concurrently, there have been ongoing increases in energy efficiency regulations for residential buildings in Australia in efforts to reduce greenhouse gas emissions generated through energy used for space conditioning to maintain thermal comfort. However, there is uncertainty as to whether the intended benefits of these energy efficiency regulations are being realised due to uncertainties in the simulation-based compliance process. This issue is particularly significant for apartments as there is very little quantitative evidence of the thermal performance of Australian apartments, despite the introduction of energy efficiency regulations in 2005 and the significant apartment development boom that has occurred since then.

The underlying operating mechanism of these regulations is to enforce improvements to thermal performance of the building envelope. While regulations have increased the amount of insulation installed in dwellings, the estimated performance benefits may be overstated as, at the time of writing, thermal bridging effects are not considered in residential buildings.

The aims of this study were therefore to understand and quantify the thermal performance of a set of case-study apartments in Australia, and to compare this measured thermal performance to that simulated using the Nationwide House Energy Rating Scheme (NatHERS) mandated building performance simulation (BPS) software and protocol of assumptions. The study also aimed to assess the impact of uncertainties associated with assumptions in the NatHERS protocol regarding thermal conditions, occupant behaviour, weather conditions, and building envelope performance. Finally, the study sought to quantify the impact of thermal bridging in apartments.

The research was carried out on nine case-study apartment dwellings that were located in Wollongong, Sydney, and Canberra. Air conditioning was present in seven of the apartments, but was only monitored in six apartments. Data collection involved a range of methods including: energy efficiency audits that involved airtightness testing and thermographic analysis; and longitudinal monitoring of indoor environmental conditions, window state, circuit-level electricity consumption, and local weather conditions for up to a nine-month period.

Electricity consumption of the apartments was evaluated against several notable Australian benchmarks. Air conditioning energy consumption of the apartments was automatically classified as heating, cooling, or standby consumption using a rule-based algorithm developed in this study. Thermal energy delivered by air conditioning for heating and cooling was then estimated using the nominal COP and EER values, respectively, of the installed air conditioning systems.

Thermal conditions in the apartments were assessed with respect to the 80% acceptability limits of the adaptive comfort model. The majority of the apartments were comfortable for more than 90% of occupied hours. However, overheating was observed in the two naturally ventilated apartments in summer. In addition, over 50% of the occupied hours in winter for one apartment were below the 80% acceptability limits.

Occupant behaviour was characterised in terms of heating, cooling and natural ventilation use as a function of indoor and outdoor temperature. Several distinct usage strategies were observed. In particular, two apartments used air conditioning regardless of outdoor conditions and rarely utilised natural ventilation opportunities, whereas the remaining four air conditioned apartments prioritised natural ventilation when outdoor temperatures were below 31.7°C. Occupants frequently operated air conditioning at lower indoor and outdoor temperatures compared to the occupant cooling strategy assumed in the NatHERS protocol. In such instances, indoor and outdoor conditions were considered by the protocol to be thermally acceptable or suitable for cooling via natural ventilation.

Weather conditions measured in reality were significantly warmer than the NatHERS prescribed representative meteorological year (RMY) weather data, with an average of 51% more cooling degree days and 12% less heating degree days. While the monitoring period was during a warmer than average year, it was consistent with weather trends observed in recent years.

Airtightness testing revealed that the apartments were significantly more airtight than recently constructed detached dwellings in Australia. Previous studies have shown that the infiltration model used in NatHERS simulations produces infiltration rates that are typical of detached dwellings. Thus, this model could not be considered accurate for apartments. Thermographic analysis revealed that wall insulation was present and was installed well, although thermal bridging caused by steel framing was prevalent. Ceiling insulation was poorly installed in the sole top-floor apartment.

NatHERS simulation models were developed for each of the apartments in accordance with the NatHERS Assessor Handbook and were calibrated against measured indoor temperature data and local weather conditions. Cooling consumption measured in the apartments was 105% greater than the simulated cooling loads determined in accordance with the NatHERS protocol (which specifies the use of representative weather conditions). Conversely, the measured heating consumption was 37% lower than the simulated heating loads. The overall space conditioning consumption was 27% greater in reality than simulated.

Uncertainties were quantified by examining the variation in simulated energy consumption of the apartments when simulated with input values determined from on-site measurements. The



greatest sources of uncertainties for simulated cooling loads were differences in natural ventilation usage followed by warmer weather conditions in reality as compared to NatHERS weather data. The most significant uncertainties for simulated heating consumption regarded occupant thermal comfort preferences and infiltration rates.

The impacts of thermal bridging caused by steel framing were investigated for an external wall assembly that was considered to be typical of Australian apartments. Steady-state conjugate heat transfer analysis using computational fluid dynamics (CFD) simulations showed that thermal bridging reduced the total wall resistance by 27%. In comparison, the NZS 4214 Isothermal Planes method and Gorgolewski method overestimated the impact of thermal bridging.

Thermal bridging effects were also shown to significantly change air flow patterns and increase convective heat transfer coefficients in the air-filled cavity within the wall. However, as heat transfer across the cavity examined in the present study was dominated by surface-to-surface radiation, there were negligible differences in the overall thermal resistance of the air cavity. The impact was expected to be significantly more prominent in reality, particularly when reflective membranes were used to reduce radiative heat transfer across the cavity.

The research described in this thesis has provided an in-depth understanding of the actual thermal performance of a small cohort Australian apartment dwellings. It also provides insights into typical indoor environmental conditions within occupied apartments and the associated occupant preferences and strategies used to maintain their preferred indoor environmental conditions. Such apartments are representative of a building typology that is rapidly increasing in number in Australia, but which has previously received relatively little attention in the literature concerning thermal performance. It is hoped that this thesis makes a significant contribution to our knowledge of heating and cooling energy consumption in apartments as simulated with the NatHERS protocol as compared with reality, which therefore has an important impact on appropriate thermal design of apartment buildings.

## **Acknowledgments**

First of all, I would like to thank my supervisors, Prof Paul Cooper and A/Prof Zhenjun Ma, for their feedback and guidance during this project, and for their transfer of knowledge that has been imparted into this body of work. I would like to express my sincerest gratitude towards Prof Paul Cooper for his unwavering support during this journey.

I would like to acknowledge the Australian Research Council (ARC), in particular, the Research Hub for Steel Manufacturing in Australia, for the provision of resources that enabled this research to be realised. I would like to specifically acknowledge the Director of the Research Hub, Dr Paul Zulli, for his mentorship throughout my PhD and for his encouragement to take on additional roles during my PhD.

I would like to extend my acknowledgements to the industry representatives from BlueScope Steel that were involved in this project: Mr Lloyd Niccol, Mr Mark Eckermann, and Mr Jamie Adams. I would like to thank each of you for your feedback, advice, and consultation over the course of this PhD.

I would also like to thank each of the participants that were involved in this study. Thank you for facilitating this research.

I would like to acknowledge the PhD candidates of the Sustainable Buildings Research Centre (SBRC) with whom I had the pleasure of sharing this journey. I will forever cherish the camaraderie we developed and would like to thank you all for your advice and support during this PhD. I would also like to extend this gratitude and commendation to the staff members that worked at the SBRC throughout my PhD.

Finally, I would especially like to acknowledge my family and friends, who have offered me love, support, and encouragement as well as helped me to relax and find comfort over this long path.

## **Certification**

*I, Steven Beltrame, declare that this thesis submitted in fulfilment of the requirements for the conferral of the degree Doctor of Philosophy, from the University of Wollongong, is wholly my own work unless otherwise referenced or acknowledged. This document has not been submitted for qualifications at any other academic institution.*

---

***Steven Angelo Beltrame***

*16<sup>th</sup> June 2021*

# Table of Contents

Abstract.....	2
Acknowledgments.....	5
Certification .....	6
Table of Contents.....	7
List of Figures .....	11
List of Tables .....	17
<b>Chapter 1 Introduction.....</b>	<b>20</b>
1.1 Background and Motivations .....	20
1.2 Aims, Research Questions, and Objectives.....	23
1.3 Thesis Structure .....	25
1.4 Declarations .....	26
<b>Chapter 2 Literature Review .....</b>	<b>27</b>
2.1 Introduction.....	27
2.2 Australian Residential Urban Development.....	27
2.3 Impact of Dwelling Type on Energy Consumption .....	29
2.4 Australian Apartment Thermal Performance Regulations .....	31
2.4.1 NatHERS Tools.....	33
2.5 Purpose of Residential Thermal Performance Rating Systems.....	35
2.6 The Performance Gap .....	37
2.6.1 Available Data on the Performance Gap of Australian Dwellings .....	37
2.6.2 Performance Gap of Residential Dwellings in Other Countries Outside Australia	40
2.7 Key Factors that Contribute to the Performance Gap .....	42
2.7.1 Thermal Comfort.....	43
2.7.2 Occupant Behaviour.....	48
2.7.3 Weather Variations .....	53
2.7.4 Building Envelope.....	56
2.8 Thermal Bridging in Apartment Buildings .....	58
2.8.1 The Australian Context .....	59
2.8.2 Thermal bridges caused by Steel Framing .....	59
2.8.3 Simple Calculation Methods .....	60
2.8.4 Methods to Simulate Thermal Bridges .....	65
2.9 Summary .....	67
<b>Chapter 3 Thermal Performance Evaluation of Existing Apartment Buildings: Experimental Methodology .....</b>	<b>68</b>
3.1 Introduction.....	68
3.2 Participant Recruitment and Apartment Selection Methodology .....	70

3.2.1	Selection of Case-Study Buildings .....	70
3.2.2	Recruitment Procedure .....	70
3.2.3	Ethics .....	71
3.3	Inspection of Apartment General Characteristics .....	71
3.4	Electricity Consumption .....	73
3.4.1	Electricity Monitoring Equipment .....	73
3.4.2	Characterisation of Air Conditioning Energy Consumption .....	74
3.5	Indoor Thermal Conditions .....	79
3.5.1	Indoor Environment Monitoring Equipment .....	80
3.5.2	Assessment of Thermal Conditions .....	83
3.6	Occupant Behaviour .....	85
3.6.1	Monitoring Occupant Behaviour .....	85
3.6.2	Assessment of Occupant Behaviour .....	87
3.6.3	Semi-Structured Interview .....	89
3.7	Building Envelope .....	89
3.7.1	Air Permeability Test .....	89
3.7.2	Thermographic Survey .....	91
3.8	Climate .....	91
3.8.1	BOM Weather Station .....	91
3.9	Occupant Detection .....	92
3.9.1	Rule-Based Classification .....	92
3.9.2	k-Nearest Neighbours Classification .....	94
3.9.3	Combining and Applying the Occupancy Detection Models .....	98
3.10	Summary .....	100

**Chapter 4 Thermal Performance Evaluation of Existing Apartment Buildings: Results and Discussion..... 102**

4.1	Introduction .....	102
4.2	Description of Case-study Apartments .....	102
4.3	Energy Consumption .....	106
4.3.1	Overall Electricity Consumption .....	106
4.3.2	Electricity End-Use Patterns .....	107
4.3.3	Air Conditioning Consumption .....	109
4.3.4	Summary of Air-Conditioning Energy Consumption Findings .....	118
4.4	Thermal Conditions .....	119
4.4.1	Indoor Air Temperature .....	119
4.4.2	Adaptive Thermal Comfort Model .....	121
4.5	Occupant Behaviour .....	125
4.5.1	Air Conditioning and Natural Ventilation use .....	125
4.5.2	Air Conditioning On and Off Events .....	132

4.6	Building Envelope .....	136
4.6.1	Airtightness .....	136
4.6.2	Building Envelope Thermal Characteristics .....	139
4.7	Summary .....	142
<b>Chapter 5</b>	<b>NatHERS Building Performance Simulation Assessments .....</b>	<b>144</b>
5.1	Introduction.....	144
5.2	Building Performance Simulation Methodology .....	145
5.2.1	Software Tools .....	145
5.2.2	Building Configuration, Boundary Conditions, and Zoning.....	146
5.2.3	Building Envelope Structure .....	146
5.2.4	Glazing Specifications .....	151
5.2.5	Infiltration and Ventilation Specifications .....	152
5.2.6	Climate Settings .....	152
5.2.7	Internal Heat Load Settings.....	153
5.2.8	Heating and Cooling Logic .....	153
5.3	Measured vs Simulated Performance Comparison: Methodology.....	157
5.3.1	Heating and Cooling Energy Methodology .....	157
5.3.2	Indoor Environmental Conditions Comparison Methodology.....	158
5.3.3	Occupant Behaviour Impact on Energy Consumption Methodology .....	159
5.3.4	Weather Data Impact on Energy Consumption Methodology .....	160
5.3.5	Building Envelope Airtightness Impact Methodology.....	163
5.4	Model Validation and Calibration.....	165
5.5	Measured vs Simulated Performance Comparison: Results and Discussion .....	172
5.5.1	Heating and Cooling Energy Results .....	172
5.5.2	Comparison of Simulated and Actual Indoor Environmental Conditions .....	174
5.5.3	Impact of Occupant Behaviour on Energy Consumption .....	178
5.5.4	Impact of Weather on Energy Consumption.....	180
5.5.5	Impact of Building Envelope Airtightness on Energy Consumption.....	183
5.5.6	Discussion .....	185
5.6	Legislative Energy Efficiency Performance Assessment.....	186
5.6.1	Methodology .....	187
5.6.2	Results.....	189
5.6.3	Discussion .....	195
5.7	Summary .....	196
<b>Chapter 6</b>	<b>Numerical Modelling of Thermal Bridges .....</b>	<b>199</b>
6.1	Introduction.....	199
6.1.1	Background .....	199
6.1.2	Aims and Objectives .....	200
6.2	Methodology .....	201

6.2.1	Base Case (Case 1) .....	201
6.2.2	Alternative Case (Case 2) .....	204
6.2.3	Material Properties .....	205
6.2.4	Boundary Conditions .....	205
6.2.5	Simulation Methodology .....	206
6.2.6	Analysis of Results .....	208
6.3	Results and Discussion .....	210
6.3.1	Mesh Sensitivity .....	210
6.3.2	Total Thermal Resistance .....	212
6.3.3	Thermal Characteristics of the Air Cavity .....	213
6.4	Summary .....	218
<b>Chapter 7</b>	<b>Conclusions .....</b>	<b>219</b>
7.1	Recommendations for Future Work .....	225
	<b>List of References .....</b>	<b>226</b>
	<b>Appendix A – Case-study apartment floor plans and sensor locations .....</b>	<b>245</b>

## List of Figures

Figure 2-1 Residential building approvals in Sydney, Melbourne, and Brisbane between 2001 and 2016, contrasting the approval rate of apartments and detached houses, grouped by suburb location (Rosewall and Shoory, 2017).....	28
Figure 2-2 Historic and future housing supply in Greater Sydney (Greater Sydney Commission, 2018).....	29
Figure 2-3 Predicted Percentage Dissatisfied (PPD) as a function of Predicted Mean Vote (PMV) (ANSI/ASHRAE, 2017). ....	44
Figure 2-4 Acceptable indoor operative temperature ranges for naturally ventilated buildings as a function of prevailing mean outdoor air temperature as defined by the adaptive comfort model (ANSI/ASHRAE, 2017). ....	45
Figure 2-5 Scheme of the discrete-time Markov process model developed by Haldi and Robinson (2009) that highlights the three sub-models for arrival, during presence, and departure.....	51
Figure 2-6 Schematic representation using a resistance network to illustrate how the parallel paths method treats thermal bridges. The distribution of the heat flow amongst the heat flow paths is determined by area-weighting.....	61
Figure 2-7 Schematic representation using a resistance network to illustrate how the isothermal planes method treats thermal bridges. The distribution of the heat flow amongst the heat flow paths is determined by area-weighting. Note that the isothermal planes in the figure have been positioned in accordance with NZS 4214. ....	62
Figure 3-1 Flowchart indicating sequence of activities associated with apartment thermal performance monitoring. Blue rectangles indicate interactions with the participants, green indicates instrumentation preparation, red indicates research activities conducted within the apartments, yellow indicates work conducted by the electrical contractor, and purple indicates data processing.....	69
Figure 3-2 Wattwatchers Auditor 6M device installed within the circuit-breaker panel in an apartment.....	74
Figure 3-3 HOBO Temp/RH logger in a typical installation location within the apartment. ....	81
Figure 3-4 Close-up of the Raspberry Pi IEQ monitoring device.....	81
Figure 3-5 Raspberry Pi IEQ monitoring devices and the reference temperature sensors within the climate chamber prior to calibration. ....	82
Figure 3-6 HOBO state logger installed on a sliding door in closed position .....	86



Figure 3-7 HOBO state logger installed on an awning window in opened position ..... 86

Figure 3-8 Typical blower door setup. .... 90

Figure 3-9 Relative frequency distribution of the labelled unoccupied and occupied states for the features derived from the ‘general power’ circuit energy consumption in Apartment #1..... 95

Figure 3-10 Diagram depicting the model selection and evaluation process. .... 97

Figure 3-11 Plot of the occupancy status of Apartment #6 that resulted from the combination of the rule-based and KNN models, including the assumption of sleeping periods. .... 99

Figure 4-1 Images of each of the monitored apartment blocks. The specific apartments monitored are outlined in red. .... 103

Figure 4-2 Monitoring periods for each of the nine participating apartments, indicated by the area shaded in grey. Daily HDDs and CDDs are shown in red and blue, respectively, as calculated using data from the nearest BOM weather station..... 104

Figure 4-3 Average daily electricity consumption for each apartment in summer..... 106

Figure 4-4 Electricity consumption by end-use in summer for all apartments, expressed as a fraction of total consumption. Power includes all other electrical appliances not individually monitored, e.g. refrigeration, washing and drying appliances, television, entertainment devices, etc. .... 108

Figure 4-5 Proportion of household energy consumption end-use based on a typical three-person home in Sydney with all electric powered appliances (i.e. No gas or other energy sources) (Ausgrid, 2020). Note that the hot-water consumption has been removed from the chart for the purposes of comparison. .... 109

Figure 4-6 Average proportion of household electricity consumption end-use from a mixed cohort of detached and attached dwellings across the Sydney Metropolitan area monitored from September 2015 until June 2018 (Ding et al., 2019). Note that hot-water system consumption was not monitored within this study. .... 109

Figure 4-7 Average daily air conditioning usage profile in terms of average hourly energy consumption amongst the six air conditioned apartments for each month within the monitoring period. The colours indicate the predominant air conditioning operation for each month i.e. orange for heating only, green for mixed, and blue for cooling only. .... 110

Figure 4-8 Energy Signatures for each of the monitored apartments in which air conditioning was separately monitored. Each data-point represents a day within the monitoring period and the line of best fit was determined via piecewise regression using the methodology outlined in Section 3.4.2.1. .... 112

Figure 4-9 Seasonal daily average air conditioning consumption for standby and active consumption in each of the monitored apartments with independently monitored reverse-cycle air conditioning. ....	115
Figure 4-10 Distribution of air conditioning operating modes in terms of electricity consumption using four different classification methods/algorithms. ....	117
Figure 4-11 Daily average air conditioning energy consumption for each apartment as a function of operating mode, and the proportion of the air conditioning energy consumption used in each operating mode. ....	118
Figure 4-12 Box plot of the average hourly indoor air temperature data measured in the living rooms (left) and bedrooms (right) of the nine case study apartments in summer (01/12/2018 – 28/02/2019) during occupied periods. The chart also shows the overall mean, mean daily minimum, and mean daily maximum temperatures measured in each apartment. ....	119
Figure 4-13 Box plots of the average hourly indoor air temperatures measured in the living rooms (left) and bedrooms (right) of the four case-study apartments that were monitored during winter. The chart also shows the overall mean, mean daily minimum, and mean daily maximum temperatures measured in each apartment. ....	120
Figure 4-14 Hourly indoor operative temperature measured in the living room during occupied hours against the prevailing daily mean outdoor temperature. The 80% acceptability limits defined by the adaptive model from ASHRAE Standard 55-2017 is shown in grey. ....	123
Figure 4-15 Probability of heating, cooling, and window operation as a function of outdoor temperature, determined using logistic regression. The data used in the above plots included all occupied hours within the monitoring periods for the six mixed-mode conditioned apartments. ....	126
Figure 4-16 Probabilities of heating, cooling, and window operation during occupied hours as a function of outdoor temperature, determined using logistic regression. Note that Apartments #8 and #9 did not have air conditioning. While Apartment #4 did have air conditioning this was not individually monitored. ....	127
Figure 4-17 Box-plot distribution of indoor temperatures at which reverse-cycle heating and cooling was turned on and off in each apartment. ....	133
Figure 4-18 Indoor temperatures at which heating and cooling was turned on and off with respect to the adaptive comfort model 80% and 90% acceptability boundaries as a function of prevailing mean outdoor temperature. ....	136

Figure 4-19 Air change rates (n50) of each apartment using the Fan Pressurisation Method from ISO 9972. The average air change rate of 5.9 ACH@50 Pa is indicated by the red line. .... 137

Figure 4-20 Air permeability rates (q50) through the envelope within each of the apartments using the Fan Pressurisation Method from ISO 9972. The envelope area is measured as the entire boundary of the apartment including external, intertenancy, and corridor walls, floors, and ceilings. The average air permeability rate, indicated by the red line, was 5 m<sup>3</sup>/h/m<sup>2</sup>. .... 137

Figure 4-21 Condition of the ceiling cavity of Apartment #4, which was the least airtight apartment amongst the cohort. This building had been converted from an inner-city warehouse to a multi-unit residential building around 2000. .... 138

Figure 4-22 Smoke puffer testing used to visualise the air leakage paths between the sliding door and the door tracks. This was the most common leakage path witnessed amongst the tested apartments along with the exhaust fan ducting..... 138

Figure 4-23 Thermographic and visual images of an external wall in Apartment #5. The thermographic image highlights the thermal bridging caused by steel framing. This image was taken on 12/09/2018 at 10:10 am. .... 140

Figure 4-24 Thermographic image of the top floor of Apartment #3, indicating unsatisfactory ceiling insulation above the living room. The visual image is presented on the right for comparison. This image was taken on 23/07/2018 at 09:01am..... 140

Figure 4-25 Thermographic and visual images of an internal wall in Apartment #2. The thermographic image highlights the thermal mass of a concrete column at the confluence of the living room and the bedrooms. This image was taken on 12/07/2018 at 02:10pm. .... 141

Figure 4-26 Thermographic and visual images of an external wall in Apartment #9. The thermographic image highlights the presence of thermal bridging from steel framing effects and the influence of a concrete column. The green spots are caused by small thermal bridges of plasterboard adhesive. This image was taken on 28/11/2018 at 03:15pm..... 141

Figure 5-1 NatHERS software thermal comfort boundaries based on the climate in Wollongong and Eastern Sydney (Climate Zone 56; Neutral temperature = 24.5°C) for a living room during daytime active hours (07:00 – 00:00). The comfort region and extended comfort regions are presented for air speeds (v) of 0.2 m/s and 0.5, 1.0, and 1.5 m/s. .... 155

Figure 5-2 Heating and cooling schedules defined in NatHERS for daytime (e.g. living) and night-time (e.g. bedroom) zone types. .... 155

Figure 5-3 Comparison of the cumulative heating and cooling degree days from BOM data between April 2018 and March 2019 and within the Representative Meteorological Year (RMY) climate files used within NatHERS. ....161

Figure 5-4 Comparison of modelled indoor air temperature from the calibrated models with measured air temperature during the longest unoccupied period in each apartment. Outdoor temperature and global horizontal irradiance are also shown. ....171

Figure 5-5 Average measured thermal energy consumption of the air conditioned apartments compared to NatHERS simulations performed in accordance with the NatHERS protocol.....172

Figure 5-6 Comparison of the measured and simulated thermal energy consumption during the monitoring period using default input assumptions within AccuRate. Only apartments in which the air conditioning energy was individually monitored are shown. ....173

Figure 5-7 Distributions (binned into 1°C intervals) of the hourly air temperature from measurements (blue) and from NatHERS simulations (red) within the monitoring period.....176

Figure 5-8 Cooling, heating, and total space conditioning intensities as measured compared to NatHERS simulations using different weather conditions based on: i) NatHERS Default RMY climate files (RMY) and ii) climate files derived from real weather data (real). Results presented for the air conditioned apartments during the monitoring period. ....181

Figure 5-9 Percentage change in simulated cooling load as a function of the change in CDDs for each apartment. The dashed blue line is the linear regression line of best fit. ....182

Figure 5-10 Cooling, heating, and total space conditioning intensities as measured compared to NatHERS simulations using different infiltration rates based on: i) the NatHERS Default method (Def) and ii) the blower door test results using the method from the NCC Trajectory Project. Results presented for the air conditioned apartments during the monitoring period. ....184

Figure 5-11 Comparison between the area-adjusted thermal energy consumption from the original DAs to the simulations performed in this study for each Apartment where available. Apartment #7 has been marked red to highlight that the DA simulation used outdated first-generation NatHERS tools.....189

Figure 5-12 Simulated heating and cooling loads obtained from the original Development Applications where available compared with the simulated heating and cooling loads determined from NatHERS remodelling. ....190

Figure 5-13 Simulated area-adjusted thermal energy consumption of the apartments subject to NatHERS performance requirements (i.e. Apartments #1 and #2 in the ACT). NatHERS heating

and cooling limits at the time of construction are shown as horizontal lines. Note: the individual heating and cooling performance and limits shown on the right were introduced in 2019. .... 192

Figure 5-14 Comparison of the simulated heating and cooling loads from the modelling conducted in this study and those from the original Development Application. The BASIX heating and cooling load limits are shown as horizontal lines. .... 194

Figure 6-1 Cross-section of the brick veneer wall assembly examined in this study. Dimensions given in millimetres. .... 202

Figure 6-2 Graphical representation of boundary conditions within the numerical simulation. Note that the plan view and side view are not in comparable scales. .... 206

Figure 6-3 External wall geometry used in the CFD simulations. The full domain is shown on the left and a close-up is shown on the right. .... 206

Figure 6-4 A collection of key variables as a function of mesh size. Plot a) corresponds to the heat flux at the interior boundary; b) corresponds to the temperature at the interface between the steel stud flange and the air cavity; and c) corresponds to the maximum air velocity magnitude within the air cavity. .... 211

Figure 6-5 Comparison of temperature distributions for Case 1 (bridged) and Case 2 (unbridged) at a cross-section of the wall assembly corresponding to the mid-height of the cavity ( $y=1.35\text{m}$ ). .... 212

Figure 6-6 Two-dimensional flow streamlines in a plane at the mid-width of the cavity (Case 1). .... 214

Figure 6-7 Three-dimensional visualisation of the air cavity flow vectors at the mid-height of the cavity (Case 1). The geometry and vectors have been repeated to highlight the flow in between adjacent studs. The stud flange and insulation surfaces of the interior wall have been indicated in grey and yellow, respectively. Note that the interior side of the cavity is cooler than the exterior side (not shown). .... 215

Figure 6-8 Velocity profiles at the mid-height of the cavity ( $y=1.35\text{m}$ ) for Case 1 and Case 2. The two profiles shown for Case 1 represent the velocity profiles at the stud centroid plane (i) and at the mid-plane between adjacent studs (ii). .... 215

Figure 6-9 Field vectors for flow at the top (a), central (b, and bottom (c) regions of the air cavity indicated by the red, shaded regions on the right side of the figure. The vectors in Case 1 ii) and Case 2 have been enlarged by a factor of 3 and 6, respectively, relative to Case 1 i), to better illustrate key features of the flow. .... 216

## List of Tables

Table 3-1 List of rules used in the score-based classification method to determine whether an air conditioning event was providing heating or cooling. ....	78
Table 3-2 Accuracy of indoor thermal environment monitoring equipment extracted from ISO 7726 (ISO, 1998) .....	80
Table 3-3 Specific instruments installed on the IEQ monitoring device. ....	81
Table 3-4 Summary of measurements collected within the case study apartments over the duration of the monitoring period. ....	101
Table 3-5 Summary of the parameters of interest and assessment methods used within the experimental case-study. ....	101
Table 4-1 Fraction of annual HDD and CDDs within each apartment’s monitoring period. ....	104
Table 4-2 Summary of the key characteristics for each of the case-study apartments. ....	105
Table 4-3 Average total daily air conditioning energy consumption in each air conditioned apartment and consumption intensity, i.e. normalised by floor area. ....	109
Table 4-4 Key parameters of the energy signatures for each of the air conditioned apartments as determined using the methodology outlined in Section 3.4.2.1. ....	113
Table 4-5 Proportion of time that the air conditioner was actively conditioning each apartment in each season, and overall throughout the monitoring period. ....	116
Table 4-6 Seasonal exceedance hours determined using the adaptive model and expressed as a fraction of the total occupied hours. ....	123
Table 4-7 Logistic regression modelling results for natural ventilation using outdoor temperature as the independent variable. ....	127
Table 4-8 Logistic regression modelling results for cooling using outdoor temperature as the independent variable. ....	128
Table 4-9 Logistic regression modelling results for heating using outdoor temperature as the independent variable. ....	128
Table 4-10 Proportion of time that at least one of the windows was open while cooling was in operation. ....	131
Table 5-1 Summary of the building envelope structural details used to model the thermal performance of the apartments in AccuRate Sustainability. Total thermal resistance values are	

calculated without the effects of thermal bridging nor the air-film resistances on the superficial surfaces. Air gaps have been specified using default nominal widths provided by AccuRate. . 147

Table 5-2 Window specifications used within the AccuRate building models. Properties were sourced from the built-in AccuRate Sustainability window library. .... 151

Table 5-3 NatHERS Heating thermostat settings and heating schedules as a function of zone type. .... 153

Table 5-4 Cooling thermostat settings and natural ventilation trigger temperature for each of the NatHERS climate zones in this study (NatHERS National Administrator, 2012) ..... 154

Table 5-5 Manufacturer EER and COP values for the air conditioning systems identified in each apartment. .... 158

Table 5-6 List of weather data sources for the measured weather data (BOM) and NatHERS Climate Zones corresponding to each of the monitored regions. .... 161

Table 5-7 Simulated airtightness (expressed as air change rates at 50 Pa) for each apartment determined by: i) the NatHERS default method, and ii) NCC Trajectory Project method. Also shown is the measured air change rate at 50 Pa..... 165

Table 5-8 Parameters varied during calibration to identify the most realistic properties of the building envelope. .... 168

Table 5-9 RMSE between the calibrated models and measurements during the longest unoccupied period for hourly indoor temperatures in the bedroom and living room. Note that the calibrated model corresponds to the parameter set with the minimum value of  $RMSE_{ave}$ ..... 170

Table 5-10 Building envelope characteristics for the calibrated models used in each apartment. .... 170

Table 5-11 Exceedance rates of the NatHERS thermal comfort region and extended comfort region (assuming an indoor air velocity of 0.5 m/s) for occupied periods within the NatHERS scheduled conditioned hours during: a) the entire monitoring period; and b) exclusively within summer (shown in brackets)..... 176

Table 5-12 Exceedance rates of the NatHERS heating thermostat settings for the appropriate zones for occupied periods within the respective NatHERS scheduled heating hours during: a) the entire monitoring period; and b) exclusively within winter (shown in brackets). .... 177

Table 5-13 NatHERS legislative thermal performance requirements for apartment developments. The table presents the maximum total load limits and separate heating and cooling load limits for the relevant climate zones. Note that NatHERS does not specify heating and cooling load limits for climate zones within NSW as they have already been included within BASIX..... 188

Table 5-14 BASIX legislative thermal performance requirements. The table presents the maximum loads for units of multi-unit dwellings for the climate zones considered in the study. ....	189
Table 6-1 Prevalence of the three most common external wall systems used in apartment buildings in Australia between 2016 and 2021. Data sourced from the Australian Housing Data portal (CSIRO, 2021a). ....	202
Table 6-2 Specifications of the steel stud used in the wall assembly. ....	203
Table 6-3 Material properties of the solid materials used in the wall assembly. ....	205
Table 6-4 Boundary conditions specified in accordance with AS/NZS 4859.2 for summer conditions in Australia. ....	205
Table 6-5 Total thermal resistance of the brick veneer wall assembly calculated using the examined methods with and without consideration for thermal bridges. ....	212
Table 6-6 Thermal characteristics of the air cavity determined using CFD. ....	217



# Chapter 1

## 1 Introduction

### 1.1 Background and Motivations

Ongoing population growth, coupled with financial imperatives and improved access to amenities have led to an increase in the urban density of Australia's capital and major regional cities. This is changing the residential landscape of Australia, which has been historically dominated by detached dwellings. Increased development and occupation of higher-density residential buildings throughout Australia's major metropolitan areas has been ongoing in recent years as Australians start to embrace higher-density living (Newton, 2017; Australian Bureau of Statistics, 2019). The populations of Australia's capital cities are expected to continue to sustain significant growth. Sydney, Melbourne, Brisbane, and Perth are expected to constitute three-quarters of Australia's population growth between 2011 and 2061 (Coleman, 2017), placing ongoing pressure on housing supply in these cities.

Most of the urban density increase can be attributed to infill development of inner-city regions, in which vacant, non-residential or low-density dwelling areas have been replaced with higher-density dwellings (NHSC, 2013; Coleman, 2017; Australian Bureau of Statistics, 2019). Infill has been favoured by the housing market due to reduced commute times, proximity to services, and financial reasons, and is prioritised by city planning over continued urban fringe expansion (NHSC, 2013). Government planning targets and housing development projections anticipate higher-density infill developments to be responsible for at least half of dwelling developments in Australia's most populous cities, with infill projected to account for 60% to 70% of dwelling developments in Sydney and Melbourne between 2011 and 2031 (Coleman, 2017; Greater Sydney Commission, 2018).

Concurrently, a significant reduction in greenhouse gas emissions is required to mitigate the projected impacts and severity of anthropogenic climate change, which is considered to be one of the main challenges facing humanity in the 21st century (de Wilde and Coley, 2012; Foo, 2020). While a multifaceted approach is required for Australia to realise its emissions reduction targets set as part of the Paris Agreement (i.e. to reduce emissions by 26% to 28% below 2005 levels by 2030 (Department of Industry, 2021)), improving the energy efficiency of the built environment has been identified as one of the most cost-effective mechanisms to abate emissions (ClimateWorks, 2010; COAG Energy Council, 2015b). The Council of Australian Governments (COAG) also recognised that improving the energy efficiency of buildings provides many secondary benefits including improved occupant comfort, health and productivity; improved

resilience to extreme weather and blackouts; reduced energy bills; and greater energy availability for the benefit of the wider economy (COAG Energy Council, 2018; ABCB, 2019a).

Residential buildings account for approximately 11% to 12% of Australia's final energy consumption (IEA, 2018; Department of the Environment and Energy, 2019a), of which 40% to 50% is used for space conditioning (EnergyConsult, 2015). Energy efficiency regulations for detached dwelling developments were introduced into the Building Code of Australia (BCA), which now forms part of the National Construction Code (NCC), in 2003 and applied to apartment developments from 2005. The objective of these initiatives being the reduction of emissions associated with energy used for space conditioning to maintain thermal comfort (NatHERS National Administrator, 2015).

There are two deemed-to-satisfy (DTS) methods available to demonstrate that a new residential dwelling complies with energy efficiency regulations. One method is to comply with the relevant DTS elemental provisions detailed in the NCC, including the Building Sustainability Index (BASIX) requirements in NSW. However, the most common method involves using Building performance simulation (BPS) to demonstrate that the building exceeds minimum thermal performance targets i.e. remains below annual maximum simulated space conditioning consumption limits (NatHERS National Administrator, 2021). This method is regulated by the Nationwide House Energy Rating Scheme (NatHERS) (ABCB, 2009, 2019c), which specifies the simulation methodology that must be used with certified software to produce a valid compliance report. This approach must be used for apartment buildings seeking to follow the DTS solution pathway as there are no alternative DTS methods (i.e. no elemental provisions) available for sole-occupancy units within apartment buildings despite being available for common areas of apartment buildings (ABCB, 2019c; NSW Department of Planning Industry and Environment, 2021).

While the NatHERS simulation engine has been validated as a sound BPS tool (Delsante, 2005), simulated energy consumption may significantly differ from reality due to uncertainties of assumptions specified in the NatHERS protocol. The key sources of uncertainty are occupant indoor environmental preferences, occupant heating, cooling, and natural ventilation practices, weather conditions, and building envelope performance (Stein and Meier, 2000; Ambrose *et al.*, 2013; De Wilde, 2014; Pitt&sherry, 2016). This is a fundamental issue with BPS software that has been analysed in literature around the world since being used in House Energy Rating Schemes (HERS) (Stein and Meier, 2000). While HERS, including NatHERS, are not intended to accurately predict the actual energy use of residential buildings, they are intended to rank the energy-efficiency of the building design and building envelope when modelled under standard operating conditions. However, previous comparisons have shown poor correlation between the

rating of houses and their actual energy usage (Stein and Meier, 2000; Williamson, 2005a; Ambrose *et al.*, 2013). This implies that the use of standard operating conditions in such schemes limits their ability to accurately rate the energy efficiency of non-typical dwelling designs or occupant practices, which are often context-specific (Soebarto, 2000; Williamson, 2005b). These uncertainties have been identified as barriers to assessing whether or not the intended benefits of energy efficiency regulations have been realised (COAG Energy Council, 2015a).

Of the small number of studies that have examined the thermal performance of Australian detached dwellings, the majority have recognised these uncertainties as causes for significant differences in the thermal performance in reality compared to simulations conducted in accordance with the NatHERS protocol (Saman *et al.*, 2008; Ambrose *et al.*, 2013; O’Leary *et al.*, 2016; Ren, Chen and James, 2018; Ding *et al.*, 2019). One particularly consistent finding was that measured annual cooling consumption was significantly greater than simulated. In contrast, at least one key assumption, that of airtightness, has been demonstrated to be representative of detached dwellings (Ambrose and Syme, 2017).

However, there is very little quantitative evidence concerning the actual thermal performance of Australian apartments. Therefore, there is currently a lack of evidence to determine whether key assumptions specified in the NatHERS protocol are representative of Australian apartment dwellings. By extension, there has been little research to evaluate if apartments constructed in accordance with the current energy efficiency regulations are comfortable and energy efficient.

Despite these uncertainties, the underlying operating mechanism of such energy efficiency regulations is to enforce energy efficiency improvements to building design, particularly in respect of the thermal properties of the building envelope (Pitt&sherry, 2016). In order of significance, insulation and glazing were the most crucial aspects of the envelope, which have been addressed by DTS provisions and are considered during NatHERS simulations. By comparison, the impact of structural elements on the thermal performance of the envelope (e.g. framing that can form thermal bridges through the insulation layer) has historically received less attention. However, as building construction practices have improved in response to increased stringencies, considerations regarding the building envelope have become more comprehensive.

In 2019 the NCC introduced provisions for commercial buildings that thermal bridging effects caused by repeating structural elements (i.e. framing) must be included when demonstrating compliance of building envelope elements with minimum total thermal resistance requirements (ABCB, 2019c). However, at the time of writing, thermal bridging effects are not considered for residential buildings, including apartments. Previous reports indicate that the impacts of thermal bridging caused by structural elements vary considerably and are dependent on building envelope construction details. These reports show that consideration of thermal bridges can reduce the total

thermal resistance of building assemblies by up to 50% (Trethowen, 2004; Gorgolewski, 2007; Finch, Wilson and Higgins, 2013). The impacts of thermal bridges are not taken into account in formal NatHERS assessments (i.e. regulatory building performance simulations) as decreed by the NatHERS protocol. This is despite AccuRate (one of the three software tools used for NatHERS assessments) already containing the capability to model repeating thermal bridges. This omission represents a potentially significant source of uncertainty in the thermal performance of the building envelope that may significantly contribute to the performance gap.

Furthermore, there are several accuracy issues with the current NCC provisions for thermal bridging. The primary issue is that they utilise simple methods to calculate the impact of thermal bridging. These methods represent heat transfer through the envelope via calibrated one-dimensional thermal resistance network models, which are less accurate than detailed two- or three-dimensional calculations. Moreover, these methods utilise simplistic representations of air-filled cavities. The thermal resistance of air cavities is calculated using a semi-analytical model to approximate the convective and radiative resistances. This approach is likely to be accurate for relatively simple cavity situations, e.g. those where surface temperatures are relatively uniform. However, such approaches could fail to capture important physical processes in air-filled cavities that are adjacent to thermally bridged layers where surface temperatures of the cavity are non-uniform. In general, the effect of periodic surface temperature variations along the wall on the thermodynamics of enclosed air-filled cavities does not appear to have been investigated previously. Finally, these simplified methods are unable to account for thermal bridges in which there is more than one primary direction of heat transfer, such as wall corners and wall/floor junctions. These methods are also unable to account for protrusions beyond the plane of the outdoor or indoor surface of the building assembly, such as a balcony.

Steel framing is commonly used in external walls within apartments, which are predominantly constructed using reinforced concrete structures. The prevalent use of steel framing within Australian apartment buildings suggests that thermal bridging may be a significant and emerging issue as apartments become more prevalent and as the minimum required thermal performance of buildings continues to increase.

## **1.2 Aims, Research Questions, and Objectives**

The primary aim of this research project was to understand and quantify the actual thermal performance of a small case-study cohort of occupied Australian medium-rise apartment dwellings located in warm temperate and cool temperate climates and compare this measured performance with that simulated using NatHERS software and protocols. In addition, this research project sought to measure and characterise the indoor environment, occupant behaviour, weather conditions, and building envelope performance of the apartments to quantify the key sources of

uncertainty for simulation/regulatory tools. This included assessing the significance of thermal bridges in Australian apartments caused by repeating structural elements.

The key research questions for this study were as follows.

1. What is the actual thermal performance of a set of case-study apartments in Australia, and how does the actual thermal performance compare to the simulated thermal performance determined in accordance with NatHERS?
2. Are default assumptions specified in the protocol defined by NatHERS for uncertain parameters representative of observations from actual apartments, or are they a significant cause of differences between the actual thermal performance and simulated thermal performance determined in accordance with NatHERS?
3. What are the impacts of repeating thermal bridging caused by metal framing in external wall assemblies that are typical of Australian apartment construction, including the effects on air-filled cavities, and are the simplified methods for the treatment of thermal bridging currently adopted or proposed by Australian regulatory bodies sufficiently accurate relative to more comprehensive methods?

The specific objectives of this research project were as follows.

1. Conduct a comprehensive literature review of:
  - a. the Australian residential building sector, specifically with respect to apartments, including relevant policies and standards;
  - b. the significance of dwelling type on energy consumption;
  - c. thermal performance of existing residential buildings, including the relevant assessment methods used;
  - d. the key sources of uncertainty within BPS that contribute to differences between simulated and actual thermal performance of residential dwellings; and
  - e. methods available to quantify the effects of thermal bridging.
2. Develop and implement a comprehensive methodology to recruit, monitor, and test a set of case-study apartments (and occupants) for the purposes of assessing thermal performance, including assessing the impact of thermal comfort perceptions, occupant behaviour, building envelope performance, and environmental influences.
3. Analyse longitudinal measurements within the case-study apartments to determine heating and cooling loads and usage patterns of air conditioning.

4. Characterise the associated building and occupant characteristics observed in the case-study apartments using appropriate methods to facilitate comparison with typical assumptions specified in the NatHERS protocol.
5. Determine the simulated thermal performance of the case-study apartments using NatHERS approved BPS software and associated protocol.
6. Compare the actual and simulated thermal performances of the case-study apartments and quantify the level of uncertainty in the simulations attributable to assumptions of the various uncertain parameters within the NatHERS protocol compared to actual measurements of these parameters within the case-study apartments.
7. Identify a representative external wall assembly of Australian apartments to evaluate the impact of repeating thermal bridges within such walls using several recognised simple calculation methods; and to carry out computational fluid dynamics (CFD) simulations of the details of heat transfer and air flow within such walls for the purposes of comparison.

### 1.3 Thesis Structure

An overview of each chapter is provided below.

**Chapter 1 – Introduction** describes the background of the project and the motivation for determining the scope of work conducted as part of this research project.

**Chapter 2 – Literature Review** provides an overview of residential urban development in Australia with a focus on apartments and discusses energy consumption and thermal performance of Australia’s residential built environment. Primary sources of uncertainties associated with building performance simulation are outlined, and the review identifies and examines the primary methods used to account for thermal bridges within building envelope elements.

**Chapter 3 – Thermal Performance Evaluation of Existing Apartment Buildings: Experimental Methodology** describes the recruitment, data collection, and analysis methods used to assess the key thermal performance characteristics within a set of case-study apartments in order to evaluate actual thermal performance and to characterise sources of uncertainty when compared to NatHERS simulations.

**Chapter 4 – Thermal Performance Evaluation of Existing Apartment Buildings: Results and Discussion** provides an overview of the general characteristics of the case study apartments and analyses the total energy consumption, indoor environmental conditions, occupant behaviour, and building envelope characteristics observed within the case-study apartments.

### **Chapter 5 – Legislative Thermal Performance Assessment of the Case-Study Apartments**

describes the method used to determine the simulated thermal performance of the case-study apartments in accordance with the NatHERS protocol and the methods used to compare the resulting simulated thermal performance with the actual thermal performance. This chapter then presents the findings from this comparison, which included quantifying the impacts of differences in indoor environmental conditions, occupant behaviour, weather, and building envelope performance specified by NatHERS and as measured in reality. Finally, this chapter compares the NatHERS simulations performed in this study to those provided in the original Development Applications, with respect to the relevant thermal performance regulations.

### **Chapter 6 – Thermal Bridging of External Walls in Apartment Buildings**

evaluates the impact of thermal bridging within a case-study external wall assembly that is representative of those commonly used in Australian apartment buildings using several different calculation methods. The chapter also quantifies the effects of a thermal bridge on the thermal characteristics of an adjacent enclosed air cavity using computational fluid dynamics (CFD) simulations of the case-study external wall assembly.

**Chapter 7 – Conclusion** outlines the conclusions and major contributions of this research project, including its limitations and recommendations for future work.

## **1.4 Declarations**

While this project was part of the ARC Research Hub for Steel Manufacturing, all work presented in this thesis was independently undertaken by the PhD candidate and this thesis manuscript has been composed entirely by the candidate.

## Chapter 2

### 2 Literature Review

#### 2.1 Introduction

This literature review begins with an overview of the current Australian urban residential context, with a focus on apartment development. The literature regarding energy consumption within the residential built environment of Australia is then presented, with a key finding being that a wealth of information exists on the simulated and actual thermal performance of detached dwellings but extremely limited data on the actual thermal performance of apartments. There then follows a critical review of the most significant sources of uncertainty identified in literature that result in disparities between simulated and actual thermal performance. These sources include: thermal comfort, occupant behaviour, weather variations, and building envelope. The review then concludes with a brief overview of the calculation methods used to account for thermal bridges, and identifies the key limitations and knowledge gaps in this area relevant to Australian apartments.

#### 2.2 Australian Residential Urban Development

The resident population of Australia was estimated to be 24 million in March 2016, with an average annual growth rate of 1.3% over the past twenty years (Coleman, 2017). Over two-thirds of the Australian population reside within one of the eight capital cities, which experienced a growth rate of 10.5% between the 2011 and 2016 censuses i.e. approximately twice the growth rate of the population living outside capital cities (Australian Bureau of Statistics, 2017). This population growth has placed increasing pressure on the residential housing supply within the capital cities, which have traditionally seen growth predominately on greenfield sites along the urban fringes (Infrastructure Australia, 2016). However, increasing commute times, remoteness of amenities, and rising land costs have shifted home-buyer interests from the detached dwellings along urban fringes towards higher-density dwellings nearer to city centres (NHSC, 2013; Shoory, 2016).

From 2009 to 2016, the number of apartments constructed each year in Australia tripled, and in 2016 accounted for around one-third of residential building approvals (Rosewall and Shoory, 2017). According to the 2016 census, around 14% of Australians then resided in flats or apartments (Australian Bureau of Statistics, 2017). Figure 2-1 displays the residential building approvals of both apartments and detached homes in Sydney, Melbourne, and Brisbane from 2001 to 2016. Whilst detached housing development of greenfield sites in outer suburbs has sustained



growth, infill development of higher-density living within inner and middle suburbs has increased significantly in recent years.

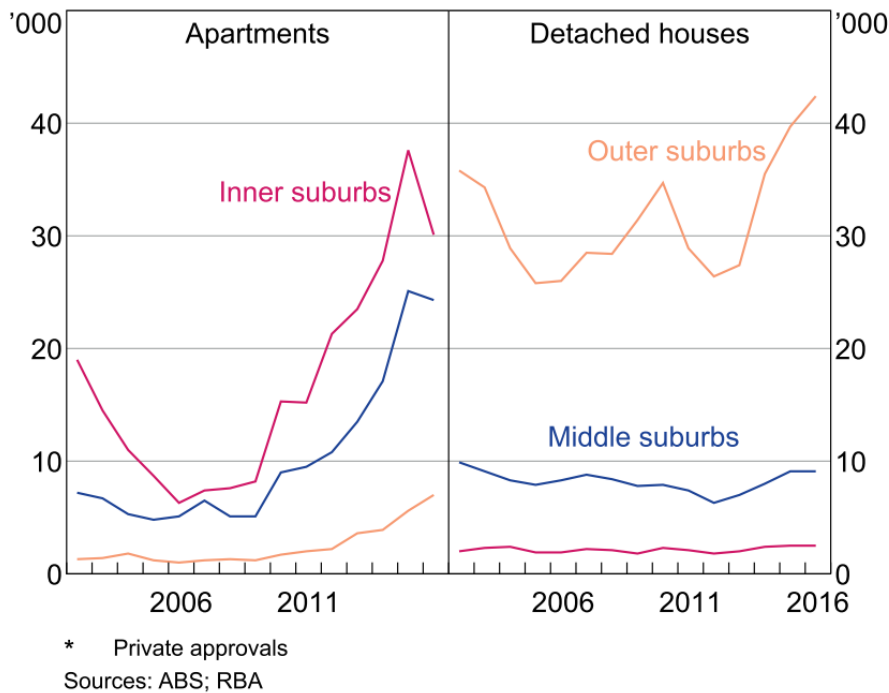


Figure 2-1 Residential building approvals in Sydney, Melbourne, and Brisbane between 2001 and 2016, contrasting the approval rate of apartments and detached houses, grouped by suburb location (Rosewall and Shoory, 2017).

In order to support the future growth of these cities, local and state governments have developed housing supply targets and associated strategies designated to facilitate well planned precincts. For example, the NSW Department of Planning and Environment has projected that 725,000 additional dwellings will be required in Sydney between 2016 and 2036 (Greater Sydney Commission, 2018; NSW Environmental Protection Authority, 2018). The NSW Government has enacted the Greater Sydney Region Plan to support integration of housing supply with health, education, and transport services, which anticipates that infill projects will comprise 60-70% of the additional dwellings required (Greater Sydney Commission, 2018). Figure 2-2 outlines the recent and near future housing supply and urban corridor development of Sydney.

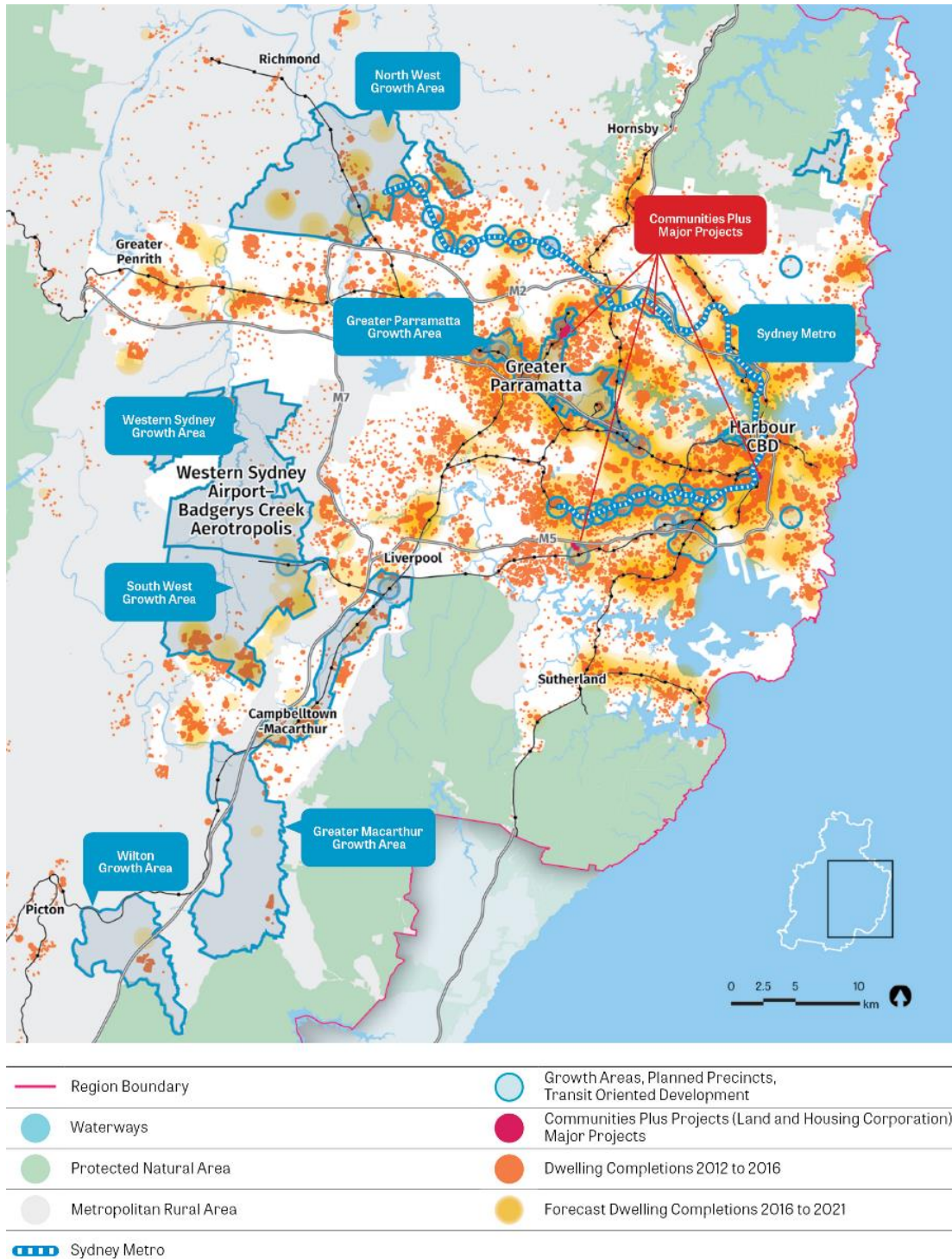


Figure 2-2 Historic and future housing supply in Greater Sydney (Greater Sydney Commission, 2018).

### 2.3 Impact of Dwelling Type on Energy Consumption

There have been numerous Australian studies seeking to quantify and characterise energy consumption in residential dwellings through the examination of individual dwelling energy usage and associated driving factors. Residential energy consumption has been shown to be dependent on multiple factors including climate, dwelling design characteristics, occupant

demographics, appliance ownership, and occupant behaviour (Rickwood, 2009; Fan, Macgill and Sproul, 2015; Roberts *et al.*, 2019).

Two separate and commonly cited Australian studies published by Energy Australia and Independent Pricing and Regulatory Tribunal (IPART) provided conflicting conclusions in regards to the impact of dwelling type on residential energy demand (Myors, O’Leary and Helstroom, 2005; IPART, 2007). The IPART study results indicated that the average annual energy consumption per capita in detached dwellings was 30% greater than in apartments (IPART, 2007). In contrast, Energy Australia reported that average annual per capita greenhouse emissions based on average census occupancy rates were greater in apartments than in detached and semi-detached dwellings, due in part to the common area loads within apartment buildings, which were not measured in the IPART study (Myors, O’Leary and Helstroom, 2005).

In 2009, the IPART data was reanalysed using regression analysis techniques to determine the independent influence several factors including dwelling type on residential energy consumption. The study concluded that apartments consume between 15 and 20% less energy than a detached home, all else being equivalent (Rickwood, 2009). This study also re-examined the Energy Australia dataset, and postulated that the common area energy consumption is only likely to be significant for large apartments with lifts and especially those with pools or spas. Only 8% of apartments surveyed in the IPART study were greater than three-storeys. Thus, the study concluded that the exclusion of common area consumption would not significantly alter the results generated from the IPART data (Rickwood, 2009).

More recent regression analysis studies have been performed using the Smart Grid Smart City high temporal resolution residential energy consumption data (Fan, Macgill and Sproul, 2015; Roberts *et al.*, 2019). Within the dataset, the average daily energy consumption of apartments and detached dwellings were 11.2 kWh and 22.3kWh, respectively. The overall average daily energy consumption was 19.2 kWh, which was in close agreement with the NSW average determined from the IPART and Energy Australia data of 18.9 kWh (Fan, Macgill and Sproul, 2015). The regression model developed from the monitored data indicated that the predicted daily average energy consumption per capita of an apartment was 21% less than for an equivalent detached dwelling (Fan, Macgill and Sproul, 2015; Roberts *et al.*, 2019).

The impact of dwelling type was statistically significant in each of the above studies. However, the authors of these studies highlighted that dwelling type might have been confounded with dwelling size in the regression analysis. While dwelling size was accounted for in the regression, it was measured in terms of the number of bedrooms and not in terms of floor area. The authors thought that the floor area was likely to be smaller in apartments than in detached homes, given the same number of bedrooms. However, this was not confirmed with additional measurements.

Nonetheless, the reduction in energy consumption in apartments relative to detached dwellings was thought to be due to smaller space conditioning loads resulting from the smaller conditioned volume and the smaller fraction of the walls, floors, and ceiling of the occupied space being exposed to external conditions. (Rickwood, 2009; Roberts *et al.*, 2019). This was supported by a study from the United States that concluded that space-heating and space-cooling loads were 53% and 27% greater, respectively, in otherwise equivalent detached homes in comparison to apartment buildings (Ewing and Rong, 2008).

It was also evident that ownership of an air conditioning system was strongly correlated with higher residential energy consumption in each of the aforementioned studies (IPART, 2007; Rickwood, 2009; Fan, Macgill and Sproul, 2015). From the Smart Grid Smart City dataset, dwellings with a ducted or a split-system air conditioner consumed 79% and 34%, respectively, more energy on average than those without an air conditioning system (Fan, Macgill and Sproul, 2015). The impact of the climate on the energy consumption was also examined by using heating and cooling degree-days, calculated from the nearest BOM weather station, as proxies for the space-conditioning loads (Fan, Macgill and Sproul, 2015). The results highlighted that average energy consumption profiles were well matched with superimposed cooling degree day (CDD) and heating degree day (HDD) profiles (Fan, Macgill and Sproul, 2015). Amongst the study cohort, which was in a heating-dominated climate, regression analysis determined that heating was a significant indicator of residential energy loads whereas cooling was not considered to be significant, and was not included in the regression model. However, the authors acknowledged that cooling was very significant driver of peak loads (Fan, Macgill and Sproul, 2015).

Infiltration rates have also been shown to be significantly lower in apartments compared to detached dwellings. This further reduces the thermal loads on apartments compared to otherwise equivalent detached dwellings. Infiltration rates are discussed in greater detail in Section 2.7.4.2.

The results above indicate that the thermal performance of a residential dwelling is a significant indicator of the overall residential energy use, and that lower electrical energy consumption identified in apartments relative to otherwise equivalent detached homes is likely to be due to smaller thermal loads, which are a consequence of lower envelope area exposed to outdoor conditions and lower infiltration rates.

## **2.4 Australian Apartment Thermal Performance Regulations**

There are numerous regulatory frameworks in place at various levels of government in Australia that are designed to ensure that apartment buildings are designed and constructed to provide safety, amenity, and equity to occupants. The introduction of minimum thermal performance design requirements for residential dwellings was prompted by the need to reduce greenhouse gas emissions in an effort to mitigate climate change (NatHERS National Administrator, 2015;

Moore, Berry and Ambrose, 2019). It is also recognised that improved thermal performance can also have positive health and financial implications for occupants (Cooper *et al.*, 2016; Trombley and Halawa, 2017; Ren, Chen and James, 2018; Moore, Berry and Ambrose, 2019).

The National Construction Code (NCC) of Australia contains minimum design requirements for energy efficiency within Section J that aim to reduce the energy consumption of all building types while maintaining thermally comfortable indoor conditions. Energy performance requirements within the NCC were introduced for multi-unit residential buildings in 2005. Section J specifies that the heating and cooling loads of apartment buildings must be assessed using Nationwide House Energy Rating Scheme (NatHERS) approved software, which predict the annual heating and cooling loads based upon the local climatic conditions and standard building usage assumptions. Nationally, individual apartments must meet a minimum NatHERS rating of five stars, and an entire apartment building must meet an average rating of six stars (ABCB, 2019c). However, individual states and territories can and have adopted modified performance requirements as discussed below. A NatHERS or BASIX Certificate is a mandatory inclusion within a Development Application, which must be approved by local council before development can proceed. Separate load limits for heating and cooling have recently been adopted within the 2019 NCC Volume One (ABCB, 2019c, 2019b), which apply to Class 2 sole occupancy units i.e. apartment dwellings amongst other building classes. The limits vary according to the climate zone of the proposed site of the development. As is the case of overall thermal performance, individual apartments have less stringent maximum separate heating and cooling load requirements than the average requirements of the entire apartment building.

The NCC is given legal effect by relevant legislation within each state and territory, and as such there are regional variations, particularly for NSW (ABCB, 2019c). In NSW, portions of Section J are superseded by the Building Sustainability Index (BASIX), also implemented for multi-unit residential buildings in 2005. Under BASIX, apartments must still exhibit satisfactory thermal performance requirements using NatHERS software, however there are alternative performance targets and the heating and cooling loads are integrated into a whole-building greenhouse gas emissions assessment (NSW Department of Planning, 2011; NSW Department of Planning and Environment, 2019). BASIX has individual load limits for heating and cooling (NSW Department of Planning and Environment, 2016; ABCB, 2019b). The limits vary based on the climate zone of the proposed site and, as with NatHERS, there are individual apartment performance requirements and whole-building apartment average performance requirements.

NSW and Victoria have also introduced legislation to improve the design quality of apartments through the specification of design quality principles that must be considered including built form and scale, sustainability, landscape, and amenity (Heffernan *et al.*, 2017). In NSW, the State

Environmental Planning Policy (SEPP) 65, and the Victorian equivalent, the Victoria Planning Provisions (VPP) Amendment VC136, specify their corresponding design principles within the Apartment Design Guide, and Apartment Design Guidelines for Victoria respectively (NSW Department of Planning and Environment, 2015; DELWP, 2016).

There are also local government initiatives in place to improve the design and minimise the environmental impact of residential developments. The city of Sydney has provided non mandatory benchmarks on the predicted energy consumption of new residential developments, included within their Environmental Action Plan 2016-2021 (City of Sydney, 2017). While not enforced, the City of Sydney may consider these benchmarks when proponents are seeking to enter into a Voluntary Planning Agreement with the City, or where a design excellence competition will be undertaken (City of Sydney, 2017). The city of Sydney is also advocating for mandatory disclosure of energy ratings and increased BASIX targets for existing and newly built apartments within the state government. The City of Sydney stated that mandatory disclosure has the most significant GHG emission abatement potential out of a range of cost-effective policy measures (City of Sydney, 2015).

Other non-mandatory rating tools include Green Star and the National Built Environment Rating System (NABERS) (Mitchel, 2010). Green Star was first launched in 2003 by the Green Building Council of Australia (GBCA) (GBCA, 2009). While it has primarily been used as a design rating tool, there is also an as-built version of this performance rating tool. GBCA launched the Multi-Unit Residential Rating tool V1 in 2009 tailored to the rating of apartment buildings. The rating tool holistically evaluates a proposed building design by independent consideration of management, indoor environmental quality, energy, transport, water, materials, land use and ecology, emissions, and innovation. NABERS is a national initiative managed by the NSW Department of Planning, Industry and Environment that was first launched in 1998. NABERS is a performance-based rating tool that requires at least 12 months of occupied data and is conducted by a NABERS approved assessor. NABERS Energy and Water for Apartment Buildings was introduced in 2018 to evaluate the energy and water usage of the common property of an apartment building (NABERS, 2018a, 2018b).

#### **2.4.1 NatHERS Tools**

The Nationwide House Energy Rating Scheme (NatHERS) is a rating system that evaluates the energy efficiency of a dwelling based on its design using building performance simulation. In order to demonstrate NCC compliance using NatHERS tools, simulations must be performed in accordance with the NatHERS protocol. Such simulations are generally termed “NatHERS assessments”. There are three building performance simulation tools currently approved by the NatHERS protocol: AccuRate Sustainability, BERSPro, and FirstRate (Ren, Chen and James,

2018). Each of these tools utilise the Chenath engine as the underlying calculation engine for building thermal performance simulation (Ren, Chen and James, 2018).

The Chenath engine was developed by the Commonwealth Scientific and Industrial Research Organisation (CSIRO) and is the descendant of several thermal performance simulation tools developed by the CSIRO that began in the 1960s (Chen, 2016; Ren, Chen and James, 2018). The Chenath engine couples a frequency response multi-zone thermal model and a multi-zone air flow model to simulate the dynamic thermal performance of the building (Muncey, 1953; Walsh and Delsante, 1983; Li, Delsante and Symons, 2000; Ren and Chen, 2010; Chen, 2016). The Chenath engine was analytically verified for simple cases during its development and has been validated through inter-program performance comparison using the International Energy Agency (IEA) BESTEST protocol (Delsante, 2005; Ren, Chen and James, 2018). The engine has also been updated periodically to improve calculation accuracy, including the integration of improved air flow and ground heat loss models (Ren and Chen, 2010; Ren, Chen and James, 2018). Use of the same calculation engine ensures that the underlying building physics is being modelled using the same processes for all NatHERS assessments.

The NatHERS protocol also specifies a set of default assumptions that are intended to facilitate parity amongst NatHERS assessments to assess the building design independently of operational characteristics. The default assumptions pertain to the following simulation inputs:

- Climatic data;
- Modelling zones;
- Infiltration rates;
- Internal heat gains;
- Heating and cooling thermostat settings;
- Use of natural ventilation; and
- Use of adjustable shading.

The default assumptions for each of these simulation inputs is described in greater detail in Section 5.2.

A NatHERS assessment predicts the area-adjusted annual heating and cooling load intensities [MJ/m<sup>2</sup>.annum] required to maintain indoor temperatures within a comfortable range, assuming the building is operated in accordance with the protocol. These loads are compared with climate zone-specific maximum acceptable heating and cooling load limits to ensure that the design performs sufficiently well in both heating and cooling seasons. The sum of these loads is

compared to a set of benchmarks, which have been established for 69 NatHERS Climate Zones across Australia to account for the variability of weather conditions across the country. For each climate zone, these benchmarks correspond to a national star rating system to facilitate rapid assessment and comparison between building designs regardless of location. The NatHERS star rating system rates the building performance from 0 to 10 stars, where 0 stars corresponds to an extremely poor performance and 10 corresponds to an extremely good performance. The NatHERS assessment automatically outputs the star rating based on the proposed location of the building. As mentioned in Section 2.4, the NCC specifies minimum NatHERS star ratings that are deemed-to-satisfy the NCC performance requirements.

The outputs from a NatHERS assessment are compiled into a brief report, known as a NatHERS Certificate. A NatHERS Certificate is required to demonstrate compliance via the NCC NatHERS pathway or via BASIX (NatHERS National Administrator, 2019a; NSW Department of Planning and Environment, 2019). A NatHERS Certificate includes the predicted heating and cooling load intensities, NatHERS star rating, and NatHERS climate zone as well as information about the building location, building type, building materials used, and the assessor (NatHERS National Administrator, 2019a).

The NatHERS Benchmark Study in 2014 evaluated the consistency and accuracy of NatHERS assessments produced by a cohort of NatHERS accredited and experienced but non-accredited NatHERS assessors (Floyd, Isaacs and Hills, 2014). The assessors were tasked to assess one of four archetype dwellings of varying complexities, one of which was an apartment. The assessors found rating the apartment very difficult, with less than half the sample obtaining a rating within one star of the correct result, despite 77% of the total ratings produced across all building types being within one star of the correct result. The assessors also demonstrated a significant degree of uncertainty in the data entry component, with assessors able to correctly answer only 65% of the associated questionnaire. The most prevalent data entry issues were incorrect assignment of zone-type and incorrect external shading details. The NatHERS Assessor Handbook, which was informed by the benchmark study, was developed to improve the consistency of NatHERS Ratings amongst assessors (Department of the Environment and Energy, 2019b).

## **2.5 Purpose of Residential Thermal Performance Rating Systems**

The purpose of thermal performance modelling of residential dwellings is to:

- Inform the design of energy-efficient dwellings;
- Rate the energy-efficiency of dwellings;
- Predict energy and cost savings from energy efficiency upgrades (i.e. retrofits);
- Evaluate the cost and performance benefits for new energy-efficient building technologies; and



- Provide quantitative analysis and data to guide policy-related decisions.

In this study, the primary focus is the use of BPS as a tool to rate the energy efficiency of dwellings. However, it is important to note that BPS is also used to implement and inform policy in Australia, as evidenced by the reports by Acil Allen Consulting (2021) and earlier studies (Commonwealth of Australia, 2005).

Rating schemes serve to assess the energy efficiency of a dwelling design by estimating energy consumption for space conditioning required to maintain a satisfactory level of thermal comfort under standard operating conditions (Stein, 1997). This assessment is based on a large number of assumptions for a wide range of variables. Many of these variables can be difficult to ascertain in advance, such as the airtightness of the building envelope, the weather conditions experienced during a particular period, or the actual behaviour and thermal comfort preferences of occupants. Furthermore, many simplifications regarding the associated building physics are necessary to facilitate the computer simulations. All these uncertainties and simplifications combine to make it very difficult to accurately predict the actual energy consumption of a particular household.

However, a rating scheme, such as NatHERS, cannot be expected to accurately predict the energy consumption of a particular household (Stein, 1997; Tony Isaacs Consulting, 2005). Instead, it is designed to rank the energy efficiency of a dwelling design relative to alternative designs (particularly for dwellings with similar floor areas) according to a particular set of criteria and assumptions (Stein, 1997). Therefore, a rating system ranks the order of dwelling designs from the least energy efficient to the most energy efficient (Stein, 1997).

The expectation of an accurate rating system is, at some aggregate level, that higher rated dwellings should use less energy for space conditioning than lower rated dwellings. However, no rating system is perfectly accurate in reality. Issues can arise when ratings diverge from the performance of dwelling designs in reality, particularly if higher rated dwellings perform worse than lower rated dwellings or lower rated buildings perform better than higher rated buildings. An example of such an issue with NatHERS was reported by Soebarto (2000), who demonstrated that a house that was designed to utilise natural ventilation and other passive heating and cooling design principles received a very low (1 star) NatHERS rating despite maintaining reasonably comfortable indoor conditions while using very little energy for heating and no energy for cooling. The core issue was that NatHERS did not consider natural ventilation for cooling as an alternative to mechanical cooling, which meant that houses designed to utilise natural ventilation for cooling could be rated as being low-performing despite the opposite being the case in reality. NatHERS has since integrated use of natural ventilation as a prioritised method for cooling if certain thermal conditions are satisfied (Delsante, 2005; Ren and Chen, 2010; AccurateSustainability, 2018a). Other inaccuracies of the rating system can arise from inappropriate assumptions made about

occupant preferences and behaviours. For example, current rating tools do not assess the adaptability provided by building designs that promote active occupant management and control of the indoor environment, such as through more easily understood control systems, which can result in dwellings that are energy-efficient if used correctly, but may not be operated in the intended manner (Stevenson and Rijal, 2010).

Evaluating the accuracy of a rating tool is a difficult task due to the high degree of uncertainties. The current method of evaluating the accuracy of rating tools, or more specifically, the efficacy of policy-mandated use of rating tools, is by comparing predicted energy consumption against measurements. However, rating tools such as NatHERS have generally not been designed to predict actual end-use energy consumption for any particular household. This has led to a “performance gap” between predicted and measured energy consumption, which is discussed further in the following sections.

## **2.6 The Performance Gap**

Uncertainty in the inputs utilised by Building Performance Simulation (BPS) tools to estimate the thermal performance of buildings may result in significant differences between the simulated energy consumption and the actual energy consumption used for space conditioning (Ryan and Sanquist, 2012; De Wilde, 2014; Ren, Chen and James, 2018). This disparity is known as the ‘performance gap’ and affects both non-residential and residential buildings. Research acknowledging the performance gap first appeared in the 1990s e.g. (Norford *et al.*, 1994) and research on this topic has continued to the present day. There are two common aims of research in this field:

- To identify the key sources of the uncertainty that cause the performance gap by comparing field-data measurements of energy consumption and related parameters with building performance simulations; and
- To reduce the performance gap by implementing new methods that address one or more of the key sources of uncertainty in the measured data or, more commonly, in the simulation inputs.

### **2.6.1 Available Data on the Performance Gap of Australian Dwellings**

The residential sector of Australia comprised 11% to 12% of Australia’s total energy consumption (IEA, 2018; Department of the Environment and Energy, 2019a). Space heating was the largest end-use of energy in residences in Australia, accounting for 37% of the total energy consumed, whereas space cooling accounted for 5% (EnergyConsult, 2015; IEA, 2018).

There have been a number of studies conducted over the past two decades that have compared the measured space-conditioning energy consumption of residential dwellings throughout Australia.

The majority of such studies evaluated the measured consumption relative to the simulated consumption determined via NatHERS. There have generally been two core research objectives within these studies:

- To determine whether a correlation exists between the measured energy consumption and the simulated energy consumption determined via NatHERS. In other words, is the rating system accurate and is it effective in reducing residential energy consumption?
- To evaluate the relevance of default assumptions used within NatHERS compared to characteristics observed in occupied dwellings.

#### 2.6.1.1 Detached/Mixed Dwellings

As detached dwellings are the predominate dwelling type in Australia (Coleman, 2017), studies that assessed the measured thermal performance of residential dwellings were based exclusively on data obtained from detached dwellings or included a only a small proportion of semi-detached or apartment dwellings that reflected the distribution of dwelling types amongst the broader population, e.g. (Ambrose *et al.*, 2013; Ding *et al.*, 2019).

The most consistent finding in these studies has been that cooling consumption is underestimated by NatHERS. The Residential Baseline Energy Efficiency (RBEE) study by CSIRO, for example, found higher cooling consumption in homes with higher star ratings (i.e. lower simulated annual combined energy consumption) relative to older homes with lower star ratings (Ambrose *et al.*, 2013). While O’Leary *et al.* (2016) demonstrated a stronger correlation between predicted star rating and measured space-conditioning loads than the RBEE study, annual measured cooling consumption still exceeded average simulated cooling loads by 22%. An earlier study of six detached dwellings in Adelaide found that average measured cooling loads exceeded the average simulated cooling loads by 86% (Saman *et al.*, 2008). Similarly, Ren *et al.* (2018) found that the average measured cooling energy consumption of 72 detached dwellings from Melbourne, Brisbane, and Adelaide exceeded the average simulated cooling consumption by approximately 90%. Finally, Ding *et al.* (2019) found that the average measured cooling consumption was 113% greater than the average simulated cooling consumption using NatHERS mandatory assumptions for dwellings in Sydney and surrounding areas. While Ding *et al.* (2019) included results from apartments, which comprised approximately one quarter of the study cohort, the published results were not reported by dwelling type.

In contrast, the difference between the measured and simulated heating consumption was significantly smaller than for cooling, although results were less consistent. O’Leary *et al.* (2016) and Saman *et al.* (2008) found that the average measured heating consumption was 6% and 9% less than the average predicted heating consumption, respectively, although Saman did exclude

one extreme user of heating as an outlier. On the other hand, Ding *et al.* (2019) found that the average measured heating consumption exceeded the average predicted heating consumption by 61%.

Willand, Ridley, and Pears (2016) postulated that the legislative focus on annual combined consumption thresholds within NatHERS led to dwelling designs in heating-dominated climates that improved heating performance to the detriment of cooling performance. This hypothesis was supported by findings from the RBEE study that cooling use increased with increasing star rating, while heating consumption decreased significantly (Ambrose *et al.*, 2013). A similar conclusion was reached by Hatvani-Kovacs *et al.* (2018), who demonstrated that several home designs with high star ratings could have similar predicted cooling loads to homes with low star ratings and often had comparable and in some cases worse heat-stress resistance, which was quantified in terms of free-running performance and annual and peak cooling consumption. The study by Willand, Ridley, and Pears (2016) led to the foundation of the separate heating and cooling maximum load limits for residential dwellings in the NCC, which are intended to ensure that buildings can perform sufficiently well in both heating and cooling. The large discrepancies between the NatHERS simulated and measured loads identified in previous studies are further explored in Section 2.7.

In the Australian context, many of the studies with the former aim have focussed on examining the performance gap related to NatHERS tools and the associated protocol. The most prominent of these studies have already been introduced in Section 2.5, where significant performance gaps were reported, particularly for cooling. Differences between NatHERS simulations and reality in regards to occupant thermal comfort preferences and their use of natural ventilation were the most commonly attributed sources of difference between measured and simulated energy consumption (Saman *et al.*, 2008; Ambrose *et al.*, 2013; Ambrose and James, 2014; O’Leary *et al.*, 2016; Willand, Ridley and Pears, 2016; Ren, Chen and James, 2018). However, only one of these studies (Ambrose and James, 2014) explicitly measured window use. Differences in climate conditions were the second most frequently attributed source of difference. While only Belusko *et al.* (2019) quantified the impact of the varied climate on the simulated energy consumption, O’Leary *et al.* (2016), Belusko *et al.* (2019), and Ding *et al.* (2019) each demonstrated that there were substantial differences between the NatHERS climate files and the weather observed during the monitoring periods. The most common observation was that average annual temperatures were higher in reality than in the simulation weather files; a situation that was more significant during summer months. The RBEE study also attributed the differences to poor building envelope construction practices that caused higher infiltration rates and lower total thermal resistances than assumed in NatHERS protocols (Ambrose *et al.*, 2013). These issues were examined further in a subsequent

CSIRO study of building envelope performance in recently constructed dwellings (Ambrose and Syme, 2015).

#### 2.6.1.2 Apartments

While Roberts *et al.* (2019), Fan *et al.* (2015), and Rickwood (2009) postulate that the significant difference in average daily electricity consumption between detached dwellings and apartments in Australia is associated with lesser thermal loads in apartments, to date, there appears to have been no studies that have exclusively measured and evaluated the thermal performance of Australian apartments. Current information about the thermal performance of Australian apartments therefore appears to be solely based upon simulated performance determined from NatHERS Certificate data.

The Australian Housing Data (AHD) Portal managed by CSIRO states that the average NatHERS rating of the 272,000 apartments across Australia assessed on record between May 2016 and March 2021 was 6.3 stars (CSIRO, 2021b). Approximately 208,000 of these apartments were located in NSW, where NatHERS assessments are mandatory for apartment dwellings to demonstrate compliance with the simulated heating and cooling load limits specified by BASIX. The average NatHERS rating in NSW was 6.2 stars and more recent assessments tended to have higher NatHERS ratings. A marked increase was observed after July 2017 when more stringent BASIX targets came into effect.

BASIX Certificate data obtained from the NSW Government Planning Portal indicated an average NatHERS rating of 5.4 stars based on almost 440,000 apartment dwellings assessed between Financial Year (FY) 2011/12 and FY 2018/19 (NSW Department of Planning and Environment, 2020). Despite a disparity between the two data sources, both indicated that NatHERS ratings of apartments are increasing over time.

While this data is based upon a large sample size, it is based exclusively on NatHERS Certificate data. There currently appears to be no data linking the NatHERS rating of apartments to their thermal performance in reality.

### **2.6.2 Performance Gap of Residential Dwellings in Other Countries Outside Australia**

Differences between building performance simulations and reality within the residential context are not specific to NatHERS and Australia. Performance gaps have been observed from policy-linked rating tools from UK (Kelly, 2011; Jones, Fuertes and De Wilde, 2015), Switzerland (Cozza *et al.*, 2020), Belgium (Delghust *et al.*, 2015), Netherlands (Majcen, Itard and Visscher, 2013), and USA (Stein and Meier, 2000).

Like the majority of Australian studies examined here, the main aim of the overseas studies was to explore the relationship between rating scores and the actual energy consumption of residential dwellings. Stein and Meier (2000) compared HERS ratings and actual utility billing data for approximately 500 houses across four states in the US. They found that while the predictions were reasonably accurate on average, large discrepancies were often present on an individual house basis. The most significant discrepancies were attributed to natural uncertainties regarding occupant behaviour. Delghust *et al.* (2015) similarly compared Energy Performance of Buildings (EPB) ratings with utility consumption data of 325 dwellings located in Belgium. Predicted heating consumption correlated strongly with actual heating consumption but predictive accuracy varied significantly, with a tendency for overestimation. Multiple linear regression models using several explanatory variables that included building envelope parameters and occupant behavioural parameters showed that while occupant behaviour was a significant variable, the building envelope parameters (in particular, air permeability) explained more of the variance. Majcen, Itard, and Visscher (2013) compared EPB ratings and measured energy consumption of 340,000 dwellings in the Netherlands. They found that low-rated dwellings consumed less energy than predicted whereas higher rated dwellings consumed more energy than predicted. Similar findings were observed by Cozza *et al.* (2020), who explored the relationship between the Cantonal Energy Certificate for Building (CECB) ratings and actual energy consumption of 1172 pre-retrofitted dwellings in Switzerland. Cozza *et al.* (2020) also explored how well the CECB rating and other relevant parameters correlated with the predicted and actual energy consumption using multiple regression analysis. They found the CECB rating was a strong predictor of both predicted and actual energy consumption but had a relatively weak correlation with actual energy consumption, which implied that the association between CECB rating and actual energy consumption was subject to high uncertainty. In the UK, Kelly (2011) assessed the statistical relationship between measured energy consumption in 2541 residential dwellings with various explanatory variables, including dwellings to the design stage Standard Assessment Procedure (SAP) ratings. Note that the SAP is the method used by the UK Government to assess and compare the energy and environmental performance of dwellings (Building Research Establishment, 2013). They concluded that SAP ratings explained very little of the variance in the multivariate analysis. However, using a structural equation model that included a reciprocal relationship between SAP rating and measured energy consumption, they showed that SAP rating moderately correlated to lower energy consumption despite higher rated dwellings tending to have higher energy consumption.

Studies of considerably smaller scope than those mentioned above have also been conducted to examine the causes of discrepancies in greater detail. For example, Jones, Fuertes and De Wilde (2015) compared the actual energy consumption of six identical apartment dwellings to the

theoretical consumption predicted from SAP ratings. The study found a wide range of actual annual measured gas and electricity consumption amongst the apartments despite identical designs and near-identical weather conditions. This suggested that occupant behaviour was the key source of uncertainty contributing to variance in the measured energy consumption. Comparisons of the annual mean measured gas and electricity consumption of the six apartments with the corresponding SAP simulation results revealed that the simulations over-predicted mean annual gas consumption by 70% and under-predicted mean annual energy consumption by 50%.

Metadata review studies have also been conducted to examine the causes of the performance gap. A comprehensive review concerning the performance gap by Mahdavi *et al.* (2021) examined 144 publications from 26 different countries. Of the 144 papers, 60% examined the performance gap in residential buildings, and occupant behaviour was stated as the primary cause of the performance gap in over 70% of the studies examined. Amongst these studies, the impact of occupant behaviour was classified into three categories: i) use of ventilation openings and shading; ii) occupant thermal comfort preferences; and iii) general appliance consumption (i.e. plug-in loads). However, the review concluded that most articles did not explore the causes of how occupant behaviour contributed to the performance gap sufficiently.

The review by Cozza *et al.* (2021) of the causes and solutions to the performance gap divided causes into two categories. The first was related to issues in calculating the theoretical consumption, which represents the limitations of using a theoretical model to describe real conditions of use of a building (e.g. inaccuracies of occupant behaviour modelling, inaccuracies of inputs and assumptions for the building model, and inaccuracies in assumed weather data). The second was related to deviations between the optimal and actual consumption of buildings caused by the quality of building construction, malfunctions and incorrect/sub-optimal use of a building by occupants, and measuring system limitations (Cozza *et al.*, 2021). Of the studies examined in this review, the majority attributed the performance gap to inaccuracy of initial standard assumptions of the building model (i.e. air permeability, thermal transmittance) followed by inaccuracy of occupant behaviour modelling, which included thermal comfort preferences, occupant use of the building, and occupancy rates.

## **2.7 Key Factors that Contribute to the Performance Gap**

As highlighted by previous studies, there are four key sources of uncertainty that most significantly lead to differences in the simulated and measured energy consumption for space-conditioning. These are:

- thermal comfort perceptions;
- occupant behaviour;

- weather variation; and
- building envelope performance.

The following sections provide an introduction, a review of assessment methods and the impact that each of these factors have on residential energy consumption, and methods to address these issues as reported in previous literature.

### **2.7.1 Thermal Comfort**

Thermal comfort has been defined as “*that condition of mind that expresses satisfaction with the thermal environment and is assessed by subjective evaluation*” (ANSI/ASHRAE, 2017). Thermal comfort is influenced by physical, physiological, and psychological processes and generally occurs when body temperature is held within a relatively narrow range, skin moisture is low, and the physiological effort of thermoregulation is minimised (ASHRAE, 2017). Comfort also depends on both conscious and subconscious behaviour guided by thermal and moisture sensations to reduce discomfort (ASHRAE, 2017).

#### **2.7.1.1 Assessment Methods**

Many studies have sought to develop models that adequately predict the thermal comfort experienced by individuals. However, there are currently two thermal comfort models that have become widely accepted. They are:

- the Predicted Mean Vote/Predicted Percentage Dissatisfied (PMV/PPD) model, developed by Fanger (1970); and
- the adaptive comfort model, developed by de Dear, Brager and Cooper (1998).

The PMV/PPD model was developed by examining the thermal comfort sensation responses of participants within climate-chamber controlled environments at the Technical University of Denmark and in the United States (Fanger, 1970). Fanger proposed that the following six indoor environmental parameters influenced the thermal comfort sensations of an individual:

- dry-bulb air temperature;
- relative humidity;
- mean-radiant temperature;
- air velocity;
- metabolic rate based on activity level; and
- insulation provided by clothing.



The first four parameters are attributable to the indoor physical environment, and the final two parameters are dependent on each individual. Fanger categorised thermal sensation to a seven-point scale, spanning from -3 to 3, which ranged from ‘cold’ through ‘neutral’ to ‘hot’. Through climate-chamber studies Fanger derived a relationship between these six parameters and the mean thermal sensation votes of the participants, known as the predicted mean vote (PMV). Due to a variety of voting tendencies of participants within all experiments, Fanger postulated that there was no single combination of the above six parameters that all occupants would consider to be an optimal thermal environment. Thus, he developed the predicted percentage dissatisfied (PPD) scale, which represented the predicted percentage of occupants who would find the thermal conditions uncomfortable. The minimum PPD is considered as 5% at the neutral PMV of 0, and increases symmetrically as the PMV diverges away from 0, as shown in Figure 2-3.

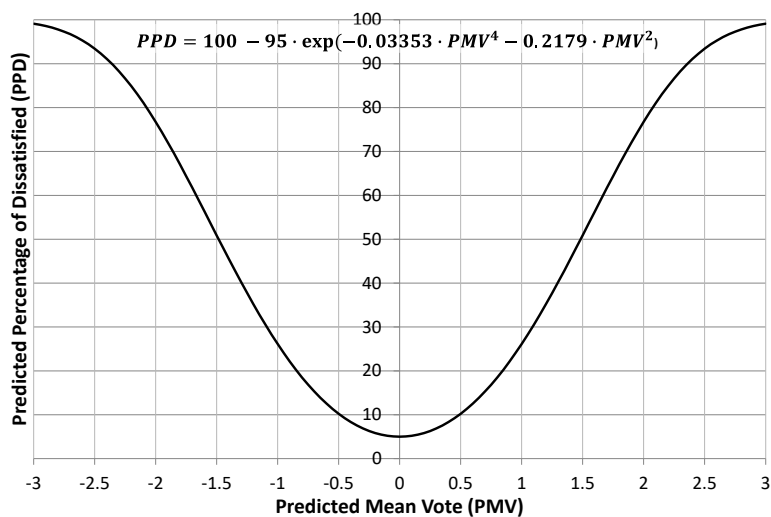


Figure 2-3 Predicted Percentage Dissatisfied (PPD) as a function of Predicted Mean Vote (PMV) (ANSI/ASHRAE, 2017).

The adaptive model originated from researchers who challenged the assumption of universal applicability of the ‘static’ PMV/PPD model, and sought to address concerns that global adoption of the PMV/PPD model had led to an increased reliance on mechanical cooling, causing unnecessary energy consumption (de Dear, Brager and Cooper, 1997). In contrast to the PMV/PPD model, which was developed under laboratory conditions, the adaptive model data was based on various field studies in which occupants provided thermal comfort sensation questionnaire responses whilst the thermal comfort parameters were monitored to various levels of fidelity (de Dear, Brager and Cooper, 1997).

Developers of the adaptive model postulated that in addition to behavioural adjustments, such as changes to clothing or activity levels, there are physiological and psychological adaptations, including acclimatisation and habituation, respectively, that affected an occupants thermal comfort sensation (de Dear, Brager and Cooper, 1997). The researchers found that while the

PMV/PPD model suitably predicted the thermal comfort sensations within air conditioned buildings, the responses of occupants within naturally ventilated buildings were shown to be more significantly influenced by and in accord with both indoor and outdoor prevailing conditions. This resulted in a range of neutral indoor temperatures that was about twice as large as that predicted by the PMV/PPD model (de Dear, Brager and Cooper, 1997).

From the study, an adaptive model was developed, which defined a comfortable indoor operative temperature range that was dependent on the outdoor effective temperature (ET\*), and was designated to be specifically applicable to naturally ventilated buildings in which occupants had access to operable windows and other adaptive opportunities (de Dear, Brager and Cooper, 1997). In 2002, the adaptive model was revised and the use of outdoor effective temperature (ET\*) was replaced by the theoretically less adequate, but simpler, prevailing mean outdoor temperature,  $T_{pma,out}$  to aid practising engineers to more easily implement the model (de Dear and Brager, 2002).

$$T_{neutral} = 0.31 \cdot T_{pma(out)} + 17.8^{\circ}C \quad (2-1)$$

The revised relationship is provided in Equation (2-1), in which  $T_{neutral}$  refers to the indoor operative temperature that corresponds to a predicted mean vote or thermal sensation vote of 0. The 80% and 90% upper and lower acceptability limits were derived from the thermal sensation votes according to the PMV-PPD relationship provided in Figure 2-3, wherein 90% and 80% acceptability correspond to a PMV of  $\pm 0.5$  and  $\pm 0.85$ , respectively (de Dear and Brager, 2002). The arithmetic averages of the indoor operative temperatures corresponding to 90% and 80% acceptability limits produced comfortable zone widths of  $5^{\circ}C$  and  $7^{\circ}C$ , respectively (de Dear and Brager, 2002). The current depiction of the adaptive model, including acceptability limits is provided in Figure 2-4.

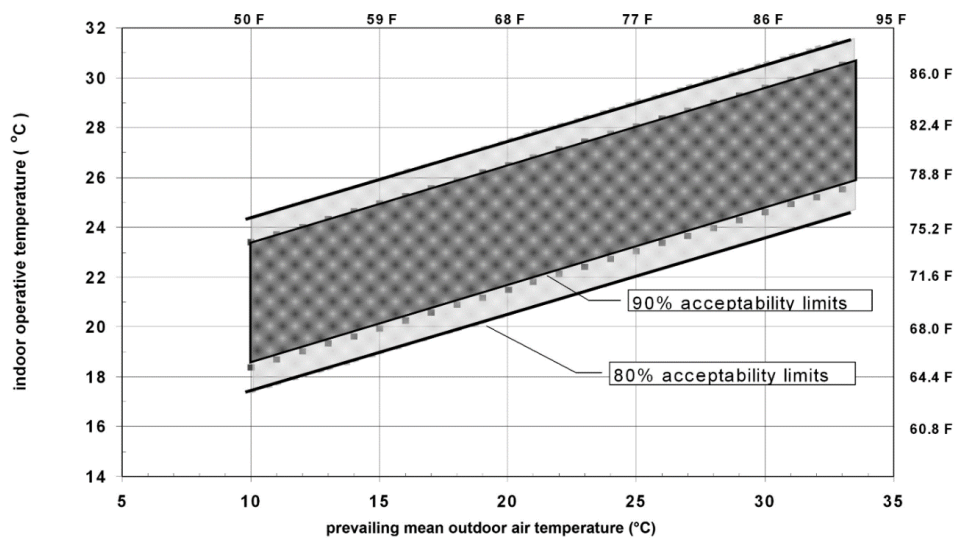


Figure 2-4 Acceptable indoor operative temperature ranges for naturally ventilated buildings as a function of prevailing mean outdoor air temperature as defined by the adaptive comfort model (ANSI/ASHRAE, 2017).

It has been argued that using just the outdoor temperature to derive indoor thermally comfortable temperatures ignores many other factors, including humidity and air movement (Nicol and Humphreys, 2002). However, it was acknowledged that people's clothing insulation and building controls, and potentially posture and activity levels are dependent on outdoor temperature (Nicol and Humphreys, 2002). In this way, through the use of the prevailing mean outdoor temperature, the feedback between the outdoor climate and the adaptive actions are empirically integrated into the adaptive model, despite not fully defining all the inter-relations between these factors (Nicol and Humphreys, 2002).

#### 2.7.1.2 Assessment of Thermal Comfort Models for Mixed-Mode Residential Dwellings

There exists a level of ambiguity/uncertainty as to which of the two established thermal comfort models is most applicable within mixed-mode ventilated buildings, i.e. buildings that use both natural ventilation and air conditioning to maintain comfort.

While ASHRAE Standard 55-2017 considers mixed-mode ventilated buildings as air conditioned buildings that consequently must be assessed exclusively using the PMV model, EN15251 permits use of the adaptive comfort model to assess thermal comfort during times when mechanical cooling is not in use (Deuble and de Dear, 2012). Recent thermal comfort studies within mixed-mode office buildings have deduced that occupant thermal comfort preferences were influenced by the operating mode of the building. When in natural ventilation mode occupant thermal sensation votes aligned better with the adaptive model than the PMV model (Deuble and de Dear, 2012; Kim *et al.*, 2019). In addition, when the air conditioning is on, occupant perceptions of the indoor thermal environment were somewhere between those of exclusively naturally ventilated and exclusively air conditioned buildings (Kim *et al.*, 2019), although a good correlation was still obtained by using the PMV model (Deuble and de Dear, 2012). Overall the predicted occupant perceptions of the thermal environment within mixed-mode buildings aligned better with the adaptive comfort model than the PMV model. However, the assessment methodology established by EN15251 provides a conservative balance between the use of the PMV and adaptive comfort models when assessing thermal comfort in mixed-mode buildings.

While the aforementioned literature suggests that the adaptive model is suitable to assess thermal comfort in mixed-mode buildings, the studies were conducted in commercial buildings and no specifications were made as to the applicability of the adaptive model for mixed-mode residential dwellings. However, the logic behind both the PMV and adaptive model are deterministic in that the comfort guidelines are intended to be applicable across all building typologies, given other criteria such as the availability of natural ventilation are satisfied (de Dear, Kim and Parkinson, 2018). Furthermore, the underlying hypothesis of the adaptive thermal comfort model suggests

that the perception of thermal comfort is influenced by the degree of control available to occupants to make comfort interventions in their pursuit of thermal comfort (de Dear, Kim and Parkinson, 2018). Therefore, the adaptive comfort model is expected to be more applicable in residential dwellings than office buildings due to the broader range of adaptive opportunities available in residential settings (de Dear, Kim and Parkinson, 2018).

de Dear, Kim, and Parkinson (2018) developed a revised adaptive comfort model using data collected exclusively from residential dwellings located in Sydney and Wollongong. The 80% acceptability limits of the revised model were 2°C wider than in the adaptive comfort model recognised by ASHRAE Standard 55-2017, which represented a 30% increase in the 80% acceptability limit range. The increased acceptability range was postulated to reflect the more extensive range of adaptive opportunities in the residential context. In addition, the neutral temperature of the revised model was 2.4°C cooler than the adaptive comfort model. This suggested that residential occupants were either more tolerant of, or better able to adapt to cooler indoor conditions compared with occupants in commercial buildings (de Dear, Kim and Parkinson, 2018). The adaptive hypothesis has also been demonstrated in other residential settings including in Japan (Rijal, Humphreys and Nicol, 2019).

For the reasons outlined above, the adaptive comfort model was therefore considered more suitable to assess thermal comfort within mixed-mode residential dwellings and was adopted for data analysis in the present study.

### 2.7.1.3 Impact of Thermal Comfort Criteria on Energy Consumption

The thermal performance of a residential dwelling is a quantitative measure of the energy required to maintain indoor conditions that satisfy the thermal sensation of its occupants. The thermal performance is therefore a function of the criteria used to define thermal comfort. For example, Attia and Carlucci (2015) demonstrated through building performance simulation that use of the adaptive thermal comfort model to define thermal comfort reduced the annual energy consumption by 21% compared to use of the PMV/PPD model for a case-study apartment building in a hot climate. The reduction was driven by the broader operative temperature range and increased opportunity for natural ventilation provided by the adaptive thermal comfort model relative to the PMV/PPD model. Similarly, energy consumption is also dependent on the specified range of acceptability limits, which is the proportion of occupants expected to be thermally satisfied with the indoor environment at any point in time. For example, Ren and Chen (2018) demonstrated cooling consumption reductions of up to 48% if the NatHERS cooling logic were to be modified to achieve 70% rather than 90% thermal acceptability. Similar effects have also been observed in reality (Daniel *et al.*, 2015).

## 2.7.2 Occupant Behaviour

Occupant behaviour in the present context is defined as the interactions between humans and buildings associated with energy usage. In IEA-EBC Annex 66: *Definition and Simulation of Occupancy in Buildings*, the relationship between occupant behaviour and energy consumption is attributed to the occupants' pursuit of environmental comfort (Balvedi, Ghisi and Lamberts, 2018).

In accordance with the adaptive model, if a change occurs that tends to produce discomfort, occupants react in ways which tend to restore their comfort, such as the utilisation of fans, blinds, heaters, or air conditioners; and in ways that vary between cultures (Nicol, Humphreys and Olesen, 2004). Adaptive behaviours are stated to take two forms: actions that help the occupant to become comfortable within the prevailing environmental conditions, such as changing clothing or activity levels; and actions that modify the environment to needs of the occupant, such as the operation of windows or air conditioning equipment (Nicol, Humphreys and Olesen, 2004).

### 2.7.2.1 Assessment Methods

There have been numerous studies conducted over the past two decades that have attempted to characterise occupant behaviour within various building environments, examining various specific occupant actions including window, lighting, shading, and air conditioning operation (Nicol, Humphreys and Olesen, 2004; Rijal *et al.*, 2007; Haldi and Robinson, 2009; D'Oca *et al.*, 2014; Kim *et al.*, 2017; Yan *et al.*, 2017; Yao and Zhao, 2017).

The majority of studies conducted have been *in situ* studies; however laboratory studies, in which human subjects are placed in highly monitored research environment designed to emulate a real indoor environment, have also been conducted (Haldi and Robinson, 2009; Yan and Hong, 2018). Data collection methods have included direct monitoring of occupant behaviours using specific instruments (e.g. reed switches) (Andersen *et al.*, 2009; D'Oca *et al.*, 2014; Ren, Chen and James, 2018) and the use of questionnaires for occupants to complete either at predetermined intervals, when prompted, or every time they interact with building components of interest (Rijal *et al.*, 2007; Daniel, Soebarto and Williamson, 2015; Kim *et al.*, 2017; Ding *et al.*, 2019; Park and Choi, 2019).

Simultaneously, various potential drivers of occupant behaviour have been monitored in previous studies (Fabi *et al.*, 2012; Peng *et al.*, 2012). These drivers can be categorised into environmental, contextual, psychological, physiological, and social factors (Fabi *et al.*, 2012). This enabled specific occupant actions to be characterised as a function of one or more of these potential drivers, which act as independent predictor variables (Balvedi, Ghisi and Lamberts, 2018). Indoor and outdoor air temperatures are the two most commonly reported independent variables and there has been some apparent contention as to which of the two predictors is most appropriate amongst

researchers (Nicol, Humphreys and Olesen, 2004; Haldi and Robinson, 2008, 2009). Indoor temperature was a more consistent predictor of window usage than outdoor temperature, but outdoor air temperature was more suitable heating usage, which was thought to be due to feedback between heater use and indoor temperature (Nicol, Humphreys and Olesen, 2004). Other studies found that indoor temperature was a better predictor for window opening events but outdoor temperature was a better predictor for window closing events (Haldi and Robinson, 2008, 2009; Park and Choi, 2019). In the majority of cases, the correlation with occupant behaviour was similar for indoor temperature and outdoor temperature (Nicol, Humphreys and Olesen, 2004; Rijal *et al.*, 2007; Haldi and Robinson, 2008). Other environmental parameters examined include indoor and outdoor humidity, indoor CO<sub>2</sub> concentration, wind speed, wind direction, rainfall, solar radiation, and outdoor PM10 concentration (Haldi and Robinson, 2009; Park and Choi, 2019).

#### Probabilistic Modelling Approaches

Due to inherent uncertainties in human behaviour, the majority of studies have used probabilistic modelling approaches to more accurately represent actual occupant behaviour. Such models consider the stochastic nature of occupants by predicting the likelihood of a specific occupant action occurring as a function of one or more independent variables (Nicol, 2001; Rijal *et al.*, 2007; Andersen *et al.*, 2009; D'Oca *et al.*, 2014; Balvedi, Ghisi and Lamberts, 2018). The uncertainty of occupant behaviour is expected to be accentuated in residential dwellings, where occupants are required to self-manage the indoor environment while conducting more diverse activities compared to office occupants (Kim *et al.*, 2017; Balvedi, Ghisi and Lamberts, 2018).

Stochastic modelling methods to characterise occupant behaviour first began to rise to prominence with the application of simple logistic regression model to study window, shading, lighting, fan, and heating usage as a function of outdoor air temperature using previously collected data from studies conducted in Europe, UK, and Pakistan (Nicol, 2001). Logistic regression models the probability of the state of a typically binomial dependent variable, with states generally denoted as 0 and 1, by expressing the log-odds (Logit Function) as a function of one or more independent variables, assumed to be linear, as shown in Equation (2-2)

$$\ln\left(\frac{p}{1-p}\right) = \beta_0 + x_1\beta_1 + \dots + x_n\beta_n \quad (2-2)$$

where  $p$  is the probability of the state of the binomial dependent variable being in the state considered "1",  $x_1$  to  $x_n$  represent each independent variable, and  $\beta_1$  to  $\beta_n$  represent the coefficients to the independent variables, including the intercept term  $\beta_0$ .

This can be rearranged to form the Logistic Function, presented in Equation (2-3), where the probability is expressed as a function of the independent variables. Logistic regression modelling is the process used to determine the values of the coefficients based on observed data.

$$p = \frac{1}{1 + e^{-(\beta_0 + x_1\beta_1 + \dots + x_n\beta_n)}} \quad (2-3)$$

While simple logistic regression has continued to be used, e.g. (Kim *et al.*, 2017), several more recent studies performed multiple logistic regression (i.e. included multiple independent variables) to better predict occupant behaviour (Rijal *et al.*, 2007; Haldi and Robinson, 2008, 2009; Park and Choi, 2019). Most commonly, this included the use of both indoor and outdoor temperature to predict occupant behaviour to avoid the drawbacks of using just one of these variables. Using both indoor and outdoor temperature demonstrated a better statistical fit than either alone, and observed variations were better accounted for by the model, which indicated independent contributions from the two variables (Haldi and Robinson, 2009). Kim *et al.* (2017) used multiple logistic regression to better reflect occupant responses and in the process challenged that previous characterisations of window use, in which the likelihood of windows being open monotonically increased with outdoor temperature, were inappropriate. Instead, they postulated that windows were likely to be open when outdoor temperatures were favourable, and were likely to be closed if outdoor temperatures were either too cold or too warm, which was reflected in their observed responses. A second-order polynomial term of outdoor temperature was added as an additional independent variable, which transformed their original simple logistic regression model into a multiple logistic regression model in order to produce the quadratic curve that more accurately depicted occupant behaviour. A similar approach had previously been used by Haldi and Robinson (2009).

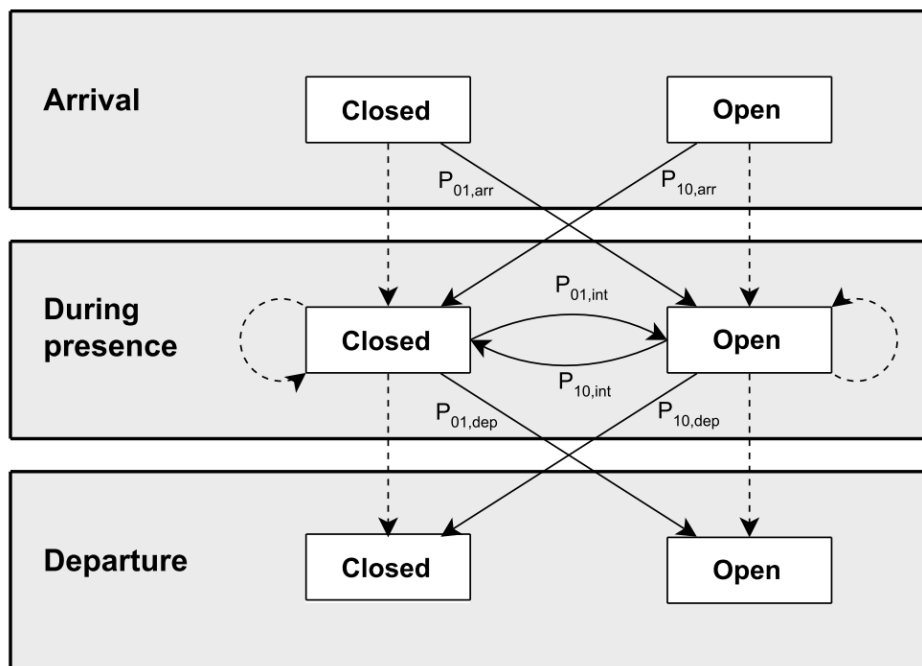


Figure 2-5 Scheme of the discrete-time Markov process model developed by Haldi and Robinson (2009) that highlights the three sub-models for arrival, during presence, and departure.

While logistic regression modelled the likely state of the windows as a function of one or more independent variables, Haldi and Robinson were interested in modelling the likelihood of a window being opened or closed (i.e. a transition of state) by occupants as a dynamic process. Thus, they opted to model the window state over time as a discrete-time Markov chain process. Based on observations from several studies that window interactions were most likely to occur on arrival or departure from the office, Haldi and Robinson devised a set of three sub-models to provide different transition probabilities as a function of the occupancy status of the office as shown in Figure 2-5. The transitional probabilities for each sub-model were determined by multiple logistic regression performed on filtered data that was relevant to the occupancy status. Haldi and Robinson also examined the viability of using Kaplan-Meier estimates of survival curves to predict the duration that windows would remain open or closed as a continuous-time stochastic-process based on both the initial indoor and outdoor temperature at the time the window was opened or closed.

While each of the above models account for stochastic effects, the combination of many individual occupant behaviours into a single aggregated model often results in high variance due to contrasting occupant behaviours. To account for this issue, several researchers categorised occupants by their likelihood to interact with the building, based on the number of observed interactions as a function of time and individually characterised each category. Examples of categorisations included passive/medium/active and low/average/high occupants (Haldi and Robinson, 2009; D'Oca *et al.*, 2014; Park and Choi, 2019).



### Non-Probabilistic Modelling Approaches

Occupant behaviour has also been studied without the application of stochastic modelling techniques. These studies typically represent the stochastic-nature of occupant behavioural patterns at a more general level of detail by examining probability distributions or via cumulative, average, or typical values. Examples of such characterisations, when applied to air-conditioning use, include: average thermostat set point, cumulative frequency of use, use while windows were open, average duration of use, average operational state as a function of the time of day, and the average temperature difference between indoors and outdoors during use (Ambrose and James, 2014; Daniel, Soebarto and Williamson, 2015; Ren, Chen and James, 2018).

Occupant behaviour has also been characterised graphically through the development of mind-maps that grouped and interlinked the most prominent anecdotal influences of cooling use given by occupants (Samaratunga *et al.*, 2017; Ding *et al.*, 2019). The responses were summarised into four primary categories: thermal perceptions/preferences, lifestyle choices, knowledge (or lack thereof) of building system operation, and external influences and limitations.

#### 2.7.2.2 Impact of Occupant Behaviour on Energy Consumption

The goal of occupant behavioural studies is to develop suitable models that represent observed trends in the occupant behaviour that can be used in building performance simulation (BPS) software to more realistically predict the energy consumption (Nicol, Humphreys and Olesen, 2004; Kim *et al.*, 2017). Occupant models currently utilised within BPS software, including NatHERS approved software, are completely deterministic (Nicol, Humphreys and Olesen, 2004; Rijal *et al.*, 2007). These models represent occupant operation of windows, thermostats, air conditioners, and shading devices as a deterministic consequence of indoor and outdoor climatic conditions or daily activity schedules based on generalised relationships (Nicol, 2001; Nicol, Humphreys and Olesen, 2004; Rijal *et al.*, 2007; Yan *et al.*, 2017). However, such methods do not consider natural uncertainties present in occupant behaviour, nor do they consider variation amongst occupants, which limits their applicability when used to predict the energy consumption of buildings in use (Nicol, 2001; Rijal *et al.*, 2007; D'Oca *et al.*, 2014).

Various studies have integrated probabilistic models derived from *in-situ* monitoring of occupant behaviour into BPS software to better account for natural uncertainties in occupant behaviour (Rijal *et al.*, 2007; D'Oca *et al.*, 2014). By running the simulations multiple times, the predicted energy consumption can be presented as a frequency distribution rather than as a single value (Nicol, 2001).

Rijal *et al.* (2007) integrated their logistic regression model of window usage behaviour into ESP-r to compare the impact of realistic occupant behaviour against several deterministic window usage cases, such as windows always closed or a constant, typical fresh air supply rate, in a simplified

model of an office building. In comparison to the deterministic models, even single iterations of simulations using stochastic models improved comfort, reduced unnecessary use of windows, and reduced simulated annual heated demand by 7% in the various cases examined. D'Oca *et al.* (2014) also integrated their logistic regression model of window use into BPS software, but also integrated probabilistic models for heating thermostat set-point adjustments. Separate models were developed for passive, medium, and active users. Rather than a single iteration, the researchers conducted ten simulations for each of the examined window and thermostat model combinations to generate a frequency distribution of annual energy consumption. Over the ten repeated simulations, the maximum variation in annual energy consumption was 32% for the “medium” interaction occupants and predicted energy consumption was found to be significantly influenced by the occupant model applied. The study concluded that the deterministic model sourced from EN 15251:2007 generally under-predicted heating consumption, relative to the stochastic models based on actual observations (D'Oca *et al.*, 2014).

It can also be said that modification of deterministic models to better align with observations of occupant behaviour from individual dwellings has led to significant improvements in the alignment between simulated and measured energy consumption. For example, Ren *et al.* (2018) derived thermostat settings for the NatHERS cooling logic from individual dwelling observations based on the average measured indoor temperatures at which the air conditioner was turned on and turned off. These significantly improved agreement between the measured and simulated cooling loads determined by NatHERS, increasing the coefficient of determination from 0.17 to 0.65. Similarly, while Saman *et al.* (2008) determined that average simulated cooling loads were 46% below the average measured cooling loads when using the default NatHERS thermostat settings, by modifying the NatHERS thermostat settings to better match reality, the average simulated cooling loads increased to just 7% below the measured cooling loads.

### **2.7.3 Weather Variations**

Uncertainty in the weather conditions ahead of time necessitates the use of historical or artificial weather conditions as a substitute to simulate the thermal performance of a building at the design stage. Such uncertainties can produce differences between the weather conditions used in simulation and the actual weather conditions, which contribute to differences between the simulated and actual energy consumption used for space conditioning.

In an attempt to minimise uncertainty in the simulated energy consumption caused by weather variations, building thermal performance is simulated using typical weather data most relevant to the specified building location (Wang, Mathew and Pang, 2012; Cuerda *et al.*, 2020). Such typical weather data is compiled from a concatenation of twelve typical meteorological months of actual, historical meteorological data taken from multiple years over a long period of time to represent a

typical meteorological year across the denoted time period (Wilcox and Marion, 2008; Belusko *et al.*, 2019). The most prominent of such data set types is the typical meteorological year (TMY) data produced for 1020 locations across USA and its territories by the National Renewable Energy Laboratory (NREL) (Wilcox and Marion, 2008). Similarly, NatHERS provides equivalent representative meteorological year (RMY) data for 69 distinct climate zones across Australia using a selection of weather data from 1976 to 2004 that was measured and provided by the Bureau of Meteorology (BOM) (Chen, 2016).

However, the use of TMY/RMY data nonetheless presents several uncertainties. With the aim to represent only typical weather, TMY data purposefully excludes unusual weather fluctuations such as heat waves and other extreme weather events. Thus, TMY/RMY data is not suitable for the assessment of building performance under extreme weather conditions (Wilcox and Marion, 2008), which are becoming more frequent and severe in many areas of the world as a result of climate change, including in Australia (de Wilde and Coley, 2012; Farah *et al.*, 2019). Climate change is also gradually changing what were previously considered typical weather conditions (de Wilde and Coley, 2012). Given the expected life of a building, TMY/RMY data is not likely to represent typical weather conditions over the life of the building, and may not necessarily depict typical weather conditions at the time of construction. Indeed, in Sydney and other parts of Australia, recent years have experienced consistently warmer temperatures than indicated in the corresponding RMY files (Bureau of Meteorology, 2019a; Ding *et al.*, 2019; Upadhyay, Munsami and Smith, 2019). Finally, uncertainty also arises from the use of the TMY/RMY data, which is provided at a limited spatial resolution, to represent the weather over a much larger geographical area (Eames, Kershaw and Coley, 2012). Thus, TMY/RMY data generated using measurements from the geographically nearest weather station may not correspond to local weather conditions at the building site (Taylor *et al.*, 2014). In the case of simulating existing buildings for the purposes of developing a calibrated model, it is imperative that real weather data files are used (U.S. Department of Energy, 2002).

#### 2.7.3.1 Impact on Energy Consumption

While studies that involved *in-situ* energy measurements and quantified the impact of climate variations on energy consumption have been rare, simulation-based studies that compared simulated energy consumption under historical/design (i.e. TMY), current/actual (i.e. measured), and future climate scenarios have been quite prevalent, including a few studies within the Australian context.

Upadhyay, Munsami, and Smith (2019) demonstrated that for the NatHERS Demonstration House, the simulated heating consumption was lower and cooling consumption was higher when using actual weather conditions compared with NatHERS default climate files. In their study, the

average simulated heating and cooling consumption was 15% less and 41% more, respectively, when actual weather data from 2013 to 2017 measured at the BOM weather station in Richmond was used than when the NatHERS default RMY climate file for Richmond were used. This finding was even more striking when actual weather data exclusively from 2017 was used, which resulted in an 89% higher simulated cooling consumption relative to the default RMY weather file. The annual average dry-bulb temperature measured at the BOM weather station in Richmond between 2016 and 2018 was 1.2 °C warmer than the corresponding RMY weather data file. The temperature difference was highest in summer, being on average 1.7 °C warmer between December and March, but was still 0.8 °C warmer in winter. Other discrepancies in the weather files were not reported in the paper, although the paper did postulate that high dry-bulb temperature, high relative humidity, and low wind speed will become a major cause of discomfort in the region based on a 2030 future climate scenario for Richmond generated using the CSIRO Mk3.5 Climate Model. Under this scenario Upadhyay, Munsami, and Smith (2019) predicted a 46% decrease and an 81% increase in the simulated heating and cooling consumption, respectively. Similarly, Ren and Chen (2018) calculated an 87% decrease in heating loads and a 71% increase in cooling loads in Sydney based on a future climate scenario with a 2°C average global temperature rise. The effects of climate change resulting in large discrepancies between historic weather data (i.e. TMY data) and real weather from recent years have also been demonstrated to impact simulated energy consumption for dwellings in the UK (Taylor *et al.*, 2014) and Italy (Erba, Causone and Armani, 2017).

While simulated heating and cooling loads changed significantly as a result of weather variations, simulated total annual space conditioning loads were less sensitive to weather fluctuations. For example, despite significant changes in simulated heating and cooling consumption, total simulated space conditioning loads determined under proposed future climate scenarios were only 10% higher and slightly less than those determined with RMY weather data in the two previously mentioned studies by Upadhyatay, Munsami, and Smith (2019) and Ren and Chen (2018), respectively. Furthermore, Wang, Mathew, and Pang (2012) demonstrated that using weather data from the past 10 to 15 years for four climate zones in USA only changed total annual space conditioning consumption by between -4% to 6% relative to using TMY weather data.

The change in the simulated energy consumption calculated by NatHERS as a result of using actual weather compared to using NatHERS RMY weather files appears to have only been examined in one previous study to date to the best of the present authors' knowledge. In this study of detached dwellings located in Lochiel Park in Adelaide, the average simulated heating and cooling loads using RMY weather data were 8% and 18% lower, respectively, than those measured (Belusko *et al.*, 2019). Simulating the same dwellings using weather data collected during the measurement periods significantly improved the level of agreement between the

heating loads although simulated cooling loads overshoot the measured data by 18%. Under both weather scenarios, the simulated heating and cooling loads corresponded relatively well to measured heating and cooling loads for these dwellings. The study also tested the correlation between the simulated and measured heating and cooling loads for a subset of 44 homes from the RBEE study by the CSIRO. These comparisons found very poor agreement between the simulated and measured heating and cooling loads despite the use of real weather data, which indicated that the performance gap observed in these comparisons was due to other factors. Unfortunately, specific differences between the RMY weather files and measured weather were not reported in this study.

Other climate factors that are seldom considered in conventional building performance simulation include the urban heat island (UHI) effect and effects of other local microclimates (Mirsadeghi *et al.*, 2013; Taylor *et al.*, 2014; Carter and Kosasih, 2018). Existing studies have demonstrated that including UHI and local microclimatic effects can increase energy consumption by up to 11% (Liu *et al.*, 2017) and can increase the dry-bulb temperature by between 1°C to 6°C (Liu *et al.*, 2017; Santamouris *et al.*, 2017; Tsoka *et al.*, 2018).

#### **2.7.4 Building Envelope**

There are also several uncertainties regarding building envelope characteristics when predicting building performance via simulation. Uncertainties arise from both defects and poor quality of the building envelope caused by deficient construction practices and from assumptions and simplifications regarding heat transfer and air flow through the envelope during simulation.

##### **2.7.4.1 Insulation**

Many studies have pointed towards poor construction quality as a cause of sub-optimal building envelope performance, that in turn contributes to excessive energy consumption for space conditioning compared to design calculations (Ambrose and Syme, 2015; Munsami, Prasad and Ding, 2017). Poorly installed insulation has been observed in detached dwellings across Australia. Ambrose and Syme (2015) identified that 10% of examined detached dwellings in the capital cities across Australia had poorly installed ceiling insulation with significant gaps and a further 39% had mediocre insulation coverage with some gaps. However, the resulting impact on energy consumption was not quantified.

In the case of apartments, at an individual unit level, the building envelope constitutes not just the building elements exposed to the outdoors, but also interior partition walls, floors, and ceilings shared by neighbouring apartments and abutting the corridor. Since these interior walls typically have less insulation than external walls, even small temperature differences can result in relatively substantial heat transfer. In rating tools, these interior partitions are often considered to be adiabatic. However, differences in occupant preferences and behaviour in adjacent apartments

can lead to inter-apartment heat transfer. This has been shown to be significant in previous studies (e.g. Moeller *et al.*, 2020), and contributes to the performance gap observed in apartment buildings.

#### 2.7.4.2 Infiltration

Uncertainty in the infiltration rate is the most significant cause of uncertainty in simulated annual heating energy (de Wilde and Tian, 2009; Hopfe and Hensen, 2011), and field studies have demonstrated a significant correlation between infiltration rate and space heating consumption (Scanada Consultants Limited, 1997; Jokisalo *et al.*, 2009; Khoury, Alameddine and Hollmuller, 2017; Feijó-muñoz, Pardal, *et al.*, 2019). For example, a field-study and simulation study of mid-rise apartment buildings in Canada demonstrated that air leakage and ventilation typically contributed to 39% of the heat losses during the heating season, with the remaining heat losses transferred directly through the building envelope (Scanada Consultants Limited, 1997). A similar study in Finnish detached houses demonstrated that infiltration accounted for between 15% to 30% of space heating consumption (Jokisalo *et al.*, 2009).

Significant differences between the measured airtightness and the airtightness resulting from normative assumptions used in rating tools have been observed for typical detached dwellings (Sinnott, 2016; Gupta and Kotopouleas, 2018; Cuerda *et al.*, 2020). These differences have been significantly smaller amongst dwellings aiming for the Passivhaus standard (Gupta and Kotopouleas, 2018; Kang *et al.*, 2021), which has fairly rigorous airtightness targets. Interestingly, inaccuracies of the assumed airtightness did not significantly account for differences between the measured and modelled space heating loads (Gupta and Kotopouleas, 2018; Cuerda *et al.*, 2020; Kang *et al.*, 2021), despite other studies observing correlations between the actual infiltration rate and actual space heating consumption. Poor installation was the most commonly stated reason why the measured airtightness differed from the modelled airtightness (de Wilde and Tian, 2009; Hopfe and Hensen, 2011; Sinnott, 2016; Gupta and Kotopouleas, 2018).

Typical infiltration rates determined using the infiltration model within the Chenath engine used by NatHERS simulation software align well with average infiltration rates measured in recently constructed detached dwellings across Australia (Ambrose and Syme, 2015, 2017; Ding *et al.*, 2019). However, there is currently very limited data nationally regarding typical infiltration rates of apartment buildings. The majority of international studies identified by the author found that on average apartment dwellings were significantly more airtight than detached dwellings, both when limited to the assessment of recently constructed dwellings (Korpi, Vinha and Kurnitski, 2008; Pan, 2010) and without constraining the comparison by year of construction (LBNL, 2020). A study into the air permeability of dwellings constructed in the UK between 2006 and 2010

found that the mean air permeability of 177 apartments was 5.25 m<sup>3</sup>/h/m<sup>2</sup> whilst the mean air permeability of 100 detached dwellings was considerably higher at 7.14 m<sup>3</sup>/h/m<sup>2</sup> (Pan, 2010). The study also identified that mid-floor apartments were the most airtight, followed by ground-floor apartments, whereas top-floor apartments were again found to be the least airtight (Pan, 2010). However, one such study based on dwellings in Spain constructed between 1960 and 2006 found apartments to be less airtight than detached dwellings (Feijó-muñoz, González-lezcano, *et al.*, 2019).

Studies that quantified airtightness of detached dwellings in Australia using the fan pressurisation method have adhered to the “building-in-use” method specified in AS/NZS ISO 9972:2015 *Thermal Performance of Buildings – Determination of air permeability of buildings – Fan Pressurisation Method*, in which air vents are not temporarily sealed (Ambrose and Syme, 2017). The reason was to assess the airtightness of the dwelling as a whole, rather than to quantify the airtightness of the building envelope, in order to characterise the typical conditions of the dwelling during operation (Ambrose and Syme, 2017). An additional concern presented when measuring airtightness of apartment units is how to distinguish between infiltration of exterior air and infiltration from adjacent interior partitions (e.g. neighbouring apartments, corridor, etc.), which may be less detrimental to the energy performance. Guarded-zone pressure can be established to equalise pressure between specific partitions (e.g. between neighbouring apartments) to eliminate flow in order to isolate building envelope elements of interest. It has been demonstrated through comparison of guarded and unguarded pressure testing in highly airtight apartments in Germany that air leakage through internal partitions accounted for 27% of the total air leakage (Kaschuba-holtgrave *et al.*, 2020).

#### 2.7.4.3 Thermal Bridging

The effects of thermal bridging in the building envelope are not conventionally considered when practitioners conduct building performance simulations. Instead, heat transfer through the building envelope is assumed to be one-dimensional despite two- or three-dimensional heat transfer in reality. This introduces uncertainty into the thermal resistance of the envelope, which is overestimated by excluding the effects of thermal bridging.

A more thorough description of thermal bridging and its impacts are provided in the following section.

## 2.8 Thermal Bridging in Apartment Buildings

One of the key properties of the building envelope is its thermal resistance, i.e. the degree to which a building envelope element impedes heat transfer between the indoor and outdoor environments. This property is influenced by the constituent materials of the building envelope and their configuration. Thermal bridges are localised areas of the building envelope that have a locally

lower heat transfer resistance and are caused by material or geometric non-uniformities. Material thermal bridges arise from differences in conductivity between dissimilar materials used in parallel, while geometric thermal bridges arise from differences in interior and exterior surface area at localised sections of the building envelope (e.g. at a corner) despite continuity of the envelope composition.

### **2.8.1 The Australian Context**

The 2019 edition of the National Construction Code (NCC) Volume One (relevant to all buildings except detached dwellings) introduced several changes to the calculation processes for the thermal resistance of the building envelope, including a new clause requiring that thermal bridges be taken into consideration when assessing whether a building assembly meets the minimum total thermal resistance DTS elemental provisions. However, these new requirements do not apply to sole-occupancy units (SOU) in Class 2 buildings (i.e. apartment dwellings) and Class 4 buildings (sole residences within buildings that are otherwise non-residential in nature), as no DTS elemental provisions currently exist for building envelopes of such building types. While DTS elemental provisions to address thermal bridges exist for detached buildings, these provisions are significantly less stringent than those introduced in NCC Volume One 2019. Please refer to Section 6.1.1 for more information.

The impacts of thermal bridges are not taken into account in formal NatHERS assessments (i.e. regulatory building performance simulations) as decreed by the NatHERS protocol. This omission represents a potentially significant source of uncertainty in the thermal performance of the building envelope that may significantly contribute to the performance gap. Given that the proportion of new detached dwellings constructed using steel frames is rising (Australian Construction Insights, 2018), and interior partition walls and non-loadbearing external walls of apartment buildings are typically constructed with steel frames (Peterman *et al.*, 2016; Gyprock, 2021), the issue of thermal bridging is also prevalent amongst new residential building stock, and is currently not being regulated.

### **2.8.2 Thermal bridges caused by Steel Framing**

One of the disadvantages of steel-framed construction is that the high thermal conductivity of steel may lead to significant thermal bridges (Gorgolewski, 2007; Soares *et al.*, 2017; Lawson, Way and Sansom, 2018). Thermal bridges caused by steel framing members are regarded as ‘repeating’ thermal bridges, as they occur at regular intervals throughout the building envelope. In regards to their thermal performance, steel-framed building envelope elements can be categorised, from the point of view of cold climate zones, as either: i) cold-framed, where insulation is positioned only between steel framing members; ii) hybrid-framed, where insulation is installed between steel framing members as well as on the exterior side of the framing; or iii)



warm-framed, where all insulation is installed on the exterior side of the framing (Gorgolewski, 2007; Soares *et al.*, 2017).

The large difference in thermal conductivity between the metal framing material (most commonly steel) and the adjacent insulation suggests that thermal bridges formed by metal framing can have a significant impact on the total thermal resistance of the building envelope. Finite-element modelling of typical cold-formed steel framed external wall assemblies found in Canada and the UK has indicated that the effects of steel framing can reduce the effective total thermal resistance of the wall by between 10% to 50% compared to unbridged elements (Gorgolewski, 2007; Finch, Wilson and Higgins, 2013). While such studies were based on warm-framed construction methods, similar levels of attenuation were measured experimentally for steel-framed wall assemblies (i.e. cold/hybrid-frame construction) commonly used in Australia (Trethowen, 2004).

Many strategies exist to mitigate or minimise the thermal bridging effects associated with steel-framed construction. These include: the installation of thermal breaks at the interface between metal and other components to provide a thermal barrier that reduces heat flow between the conductive components; modification of the stud geometry to reduce the transmission area and/or contact area; and substitution with alternative materials with a lower thermal conductivity (e.g. stainless-steel) (Way and Kendrick, 2008; Martins, Santos and Da Silva, 2016; Lawson, Way and Sansom, 2018).

### **2.8.3 Simple Calculation Methods**

The conventional approach to calculate the steady-state total thermal resistance of a building envelope element is to assume one-dimensional heat transfer through the building envelope, despite the occurrence of complex two- or three-dimensional heat transfer in reality. If each of the layers are homogeneous, the thermal resistances of each of the layers can be assumed to act in series. The total thermal resistance is thus the sum of the thermal resistances of each of the constituent layers and the film resistances of the exterior and interior surfaces of the envelope. However, non-homogeneous layers, i.e. those in which thermal bridges are present, require different treatment to account for thermal bridging effects.

There are currently two fundamental approaches to account for thermal bridging effects in non-homogeneous layers:

- The parallel planes method, which represents a theoretical upper bound on the total thermal resistance of the building envelope element (see Figure 2-6); and
- The isothermal planes method, which represents a theoretical lower bound on the total thermal resistance of the building envelope element (see Figure 2-7).

The parallel paths method shown in Figure 2-6 estimates the total thermal resistance of a thermally bridged building component by assuming heat flow occurs in multiple one-dimensional paths that are perpendicular to the surfaces of the component. Thus, the parallel paths method assumes that there is no lateral heat flow in the building component.

The calculation process involves the separation of the component into sections of homogeneous layers with one dimensional flow, for which the thermal resistance can be calculated in series. Then, the total thermal resistance is calculated as the area-weighted average of each of the one-dimensional flow paths, taken in parallel. The total thermal resistance is therefore given by Equation (2-4)

$$R_T = \frac{1}{\sum_{i=1}^n \frac{f_i}{R_i}} \quad (2-4)$$

where  $R_T$  is the total thermal resistance of the building component,  $n$  is the number of sections, or one-dimensional heat flow paths through the building component,  $f_i$  is the area-fraction of one-dimensional heat flow path  $i$ , and  $R_i$  is the total thermal resistance of the building component corresponding to heat flow path  $i$ .

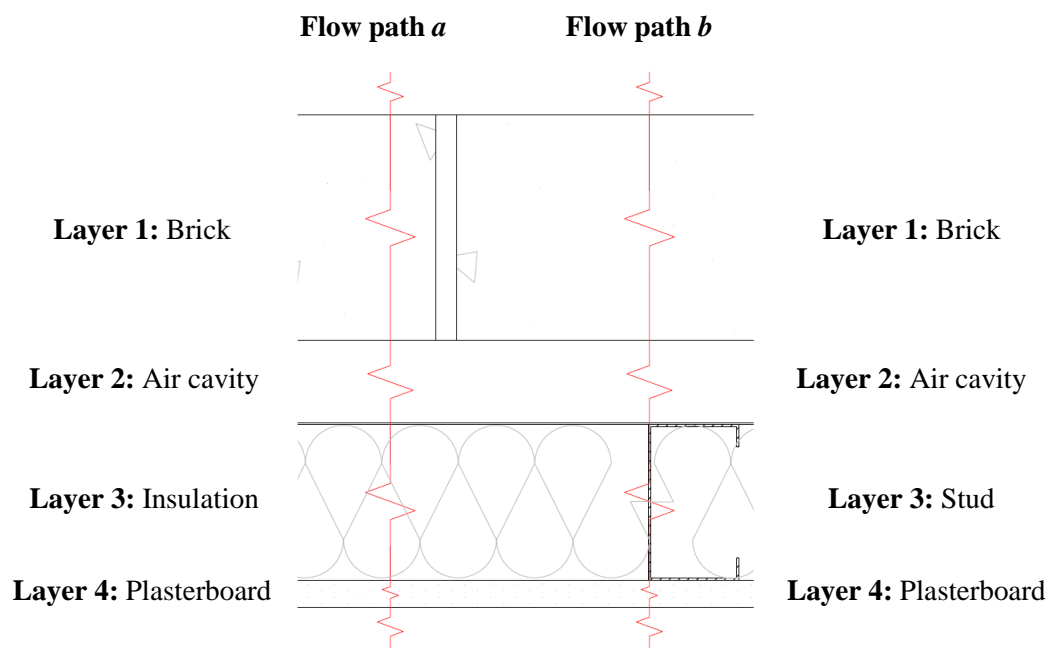


*Figure 2-6 Schematic representation using a resistance network to illustrate how the parallel paths method treats thermal bridges. The distribution of the heat flow amongst the heat flow paths is determined by area-weighting.*

The isothermal planes method illustrated in Figure 2-7 assumes unrestricted lateral heat flow at the planar interface between homogeneous and non-homogeneous layers. In effect, it considers heat flow through homogeneous layers in series and heat flow through non-homogeneous layers in parallel.

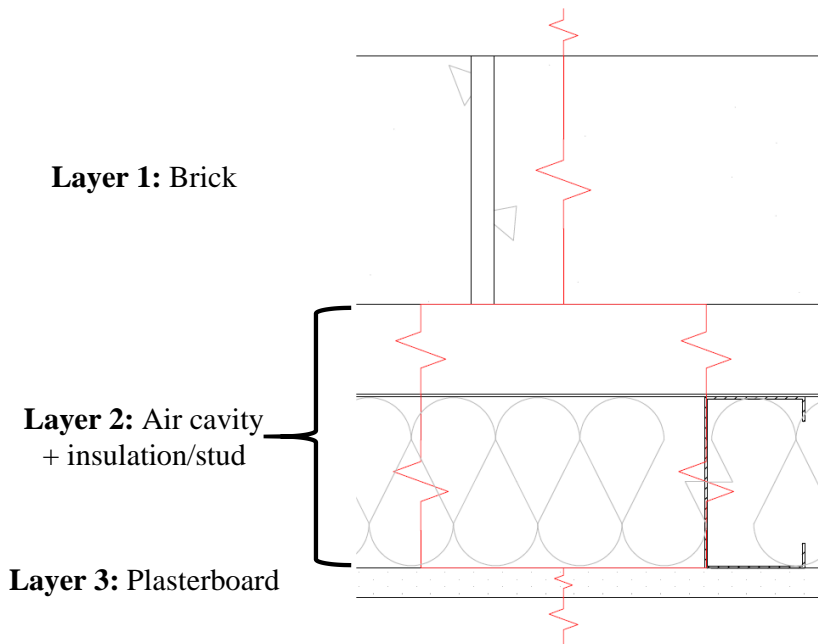


Figure 2-7 Schematic representation using a resistance network to illustrate how the isothermal planes method treats thermal bridges. The distribution of the heat flow amongst the heat flow paths is determined by area-weighting. Note that the isothermal planes in the figure have been positioned in accordance with NZS 4214.

The thermally bridged layers enclosed by the pairs of isothermal planes are subdivided into regions such that each region only has one set of thermally homogeneous sub-layers. The area-fraction and thermal resistance of each region are then combined in parallel to calculate the thermal resistance of the non-homogeneous layer, as shown in Equation (2-5)

$$R_b = \frac{1}{\sum_{i=1}^n \frac{f_i}{R_i}} \quad (2-5)$$

where  $R_b$  is the resistance of the thermally bridged layer,  $n$  is the number of one-dimensional regions within the thermally bridged layer,  $f_i$  is the area-fraction of the region,  $i$ , and  $R_i$  is the thermal resistance through the region corresponding to  $f_i$ . The total resistance is then the sum of the homogeneous and non-homogeneous layers, including the thermal resistances of the air films on the interior and exterior surfaces of the wall.

While these two fundamental approaches represent the upper and lower theoretical limits of the total thermal resistance of a building envelope element, the actual total thermal resistance of the building element is likely to be somewhere in between. Various methods, which are based on a combination or adaptation of these two fundamental approaches, have been developed to provide a more accurate estimate of the total thermal resistance.

### 2.8.3.1 NZS 4214

Currently, the NCC 2019 Volume One refers to AS/NZS 4859.2:2018 *Thermal insulation materials for buildings – Part 2: Design* for calculation of the total thermal resistance of building envelope elements, which specifies that thermal bridges are treated following the method outlined in NZS 4214:2006 *Methods of determining the thermal resistance of parts of buildings*.

NZS 4214 is based on the isothermal planes method, but specifies a number of modifications to improve the accuracy of the estimation.

Specification of where to locate the isothermal planes is not made abundantly clear in NZS 4214. However, it is stated in formative reports preceding finalisation of the standard that isothermal planes are to be positioned such that they enclose only the non-homogeneous layer, except where the non-homogeneous layer is adjacent to an air cavity, in which case the air cavity is also bound within the isothermal planes (Trethowen, 1998). Similarly, adjacent non-homogeneous layers should be fused into a single zone, i.e. bound by a single pair of isothermal planes.

For metallic thermal bridges, such as a C-section stud, rather than only considering heat flow along the web of the stud, NZS 4214 replaces the non-rectangular geometry with a notional rectangular shape that has a modified thermal conductivity which would result in the same heat flow. The thermal resistance of the equivalent rectangle, of dimensions  $a \times l$ , is given by Equation (2-6)

$$R_{eq} = \frac{l}{k} = \frac{a \cdot l}{d \cdot k} \quad (2-6)$$

where  $R_{eq}$  is the thermal resistance of the equivalent rectangle,  $l$  is web length,  $a$  is the flange width,  $d$  is the web thickness, and  $k$  is the thermal conductivity of the stud material.

NZS 4214 also specifies that contact resistances must be included where metal frames are in contact with adjacent layers. The standard specifies a nominal contact resistance of 0.03 m<sup>2</sup>K/W, which was informed by empirical testing of light steel-framed panels by BRANZ (Trethowen, 1989; Trethowen and Cox-Smith, 1996). While such resistances are small, they have been demonstrated to be significant in metal-framed construction (Trethowen and Cox-Smith, 1996) and typically provide much larger thermal resistances than that of the metal frame.

The method in NZS 4214 was validated against 84 test cases, which included metal-framed, timber-framed, and masonry walls, as well as timber-framed roofs, each containing a variety of real-world features such as furring strips, workmanship defects, edge gaps, and so on, that were not strictly considered in the calculation (Trethowen, 1995). Differences between the predicted and measured thermal resistances were within 0.1 m<sup>2</sup>K/W in 81% of the test cases considered, and 75% of the predictions were within 10% of the measured thermal resistance (Trethowen, 1995).

### 2.8.3.2 ISO 6946

ISO 6946:2017 *Building components and building elements – Thermal resistance and thermal transmittance – Calculation methods* specifies that the total thermal resistance of a building element can be estimated as the arithmetic mean of the total thermal resistance calculated using the parallel paths method and the isothermal planes method, as shown in (2-7)

$$R_T = \frac{R_{T,PP} + R_{T,IP}}{2} \quad (2-7)$$

where  $R_T$  is the total thermal resistance of the component,  $R_{T,PP}$  is the total thermal resistance using the parallel paths method, and  $R_{T,IP}$  is the total thermal resistance using the isothermal planes method.

However, ISO 6946 is not applicable in instances where the ratio of  $R_{T,PP}$  to  $R_{T,IP}$  exceeds 1.5, or where non-homogeneous elements are bridged by metal framing.

### 2.8.3.3 Gorgolewski Method

Gorgolewski (2007) sought to adapt the method provided in ISO 6946 to increase the accuracy and hence applicability of the method when applied on building envelope assemblies bridged by metal framing.

By acknowledging that the parallel planes and isothermal planes method represented the theoretical upper and lower bounds of the total thermal resistance, respectively, Gorgolewski postulated that rather than the arithmetic mean as used in ISO 6946, there must be some weighting value,  $p$ , between 0 and 1, such that the actual total thermal resistance is given by Equation (2-8).

$$R_T = p \cdot R_{T,PP} + (1 - p) \cdot R_{T,IP} \quad (2-8)$$

Gorgolewski evaluated several different methods to determine  $p$  by comparing the total thermal resistance calculated using his methods to two-dimensional finite element modelling solutions for 52 steel framed assemblies. The best level of agreement between the simple model and the finite-element models was achieved when  $p$  was defined by Equation (2-9), which is a function of the flange width,  $w$ , centre distance,  $s$ , and web length,  $d$ . This resulted in an average absolute error of 2.7%, with a maximum error of 8%.

$$p = 0.8 \frac{R_{T,IP}}{R_{T,PP}} + 0.44 - 0.1 \frac{w}{0.04} - 0.2 \frac{0.6}{s} - 0.04 \frac{d}{0.1} \quad (2-9)$$

This method has since been adopted in the UK for Building Regulations compliance, as described in detail in BRE Digest 465, and is also currently available in non-regulatory mode within

NatHERS-approved software, AccuRate Sustainability, to account for thermal bridges caused by metal framing.

## **2.8.4 Methods to Simulate Thermal Bridges**

Numerical simulation provides a means of solving two-dimensional and three-dimensional heat flow problems to determine the total thermal resistance of building envelope components more accurately. Numerical simulations of building envelope elements are even used as reference data in the development of simplified methods, as described above.

However, the limitations of the various numerical simulation methods should also be recognised before they are relied upon to provide realistic data. A brief overview of the relevant methods is provided below.

### **2.8.4.1 Finite-Element and Finite-Difference Conduction Analysis**

Finite-element and finite-difference thermal conduction analysis can be used to solve steady-state or transient two-dimensional or three-dimensional heat flow problems to quantify the impact of thermal bridges within building envelope elements. Various commercial software packages are available to perform such calculations and several standards such as ISO 10211:2017 *Thermal bridges in building construction – Heat flows and surface temperatures – Detailed calculations* are available to guide and standardise this process.

The primary limitation of such methods is that air cavities, which are common in building envelope assemblies, are often represented using simplified methods. Generally, air cavities are modelled as solid layers with an equivalent thermal conductivity to represent the convective and radiative heat flow (British Standards Institution, 2017a, 2017b). The convective and radiative resistances are typically derived using semi-analytical methods such as the method provided in ISO 6946 (British Standards Institution, 2017b), which considers the direction of heat flow, cavity width, temperature difference, and surface emissivity. The equivalent thermal conductivity is specified such that the thermal resistance of the solid layer matches the thermal resistance calculated using the semi-analytical method.

### **2.8.4.2 CFD**

Computational Fluid Dynamics (CFD) allows the full details of fluid flow (e.g. in building envelope cavities) to be modelled in two- or three-dimensions. CFD simulations are able to combine fluid motion and convective heat transfer with conductive heat transfer through solids to facilitate the integrated simulation of a building envelope element. Heat transfer that involves the interaction between heat conduction through solids and convection from the solid surface into fluids is referred to as conjugate heat transfer.

As direct numerical simulation (DNS) of the Navier-Stokes equations, which describe fluid flow, requires extremely large computational resources, various modelling techniques (e.g. turbulence models, near-wall treatment, etc.) have been developed to reduce the computational effort but maintain a reasonable level of accuracy (Versteeg and Malalasekera, 2007). The accuracy of such methods is dependent on the problem specification. Validation of appropriate modelling techniques for specific problems is conducted via comparison against DNS solutions or experimental data, and generally involves highly idealised versions of common engineering problems. Thus, it is imperative that the modelling techniques applied are appropriate to the problem at hand so as to ensure that simulation produces realistic results.

### Air Cavities in the Building Envelope

The fundamentals of natural convection within enclosed rectangular and parallelepiped cavities has been thoroughly characterised using both experimental and simulation based studies. However, such studies have examined idealised cases that featured isothermal vertical walls with the remaining walls typically treated as adiabatic. These studies sought to identify the flow regimes, i.e. the onset of turbulence, and the thermal characteristics of the cavities as a function of Rayleigh number ( $Ra$ ), Prandtl number ( $Pr$ ), and aspect ratio ( $A_H$ ) of the cavity (height relative to width) (Yin, Wung and Chen, 1978; Chenoweth and Paolucci, 1986; Paolucci and Chenoweth, 1989; Henkes and Quere, 1996; Manz, 2003). Typically, air cavities of external walls involve large aspect ratio geometries, relatively small temperature differences, and surface-to-surface radiation in addition to conduction and convection.

While relatively few studies included radiative heat transfer, Xamán *et al.* (2008) concluded that surface-to-surface radiation does not significantly influence flow behaviour within the cavity. Thus, studies that did not consider radiation are still valuable to identify the likely flow regime within air cavities of external walls. Several such studies indicated that the critical Rayleigh number required for the onset of turbulence rapidly decreases as the aspect ratio of the cavity increases (Yin, Wung and Chen, 1978; Paolucci and Chenoweth, 1989; Betts and Bokhari, 2000). Nonetheless, expected conditions within enclosed building envelope cavities do not meet the criteria required for the onset of turbulence. Thus, flow is likely to be laminar in such cavities. While several flow patterns exist within the laminar regime (Chenoweth and Paolucci, 1986), such as the transition to multicellular flow and return to unicellular flow within a certain range of Rayleigh number and aspect ratios, the existence of such phenomena do not require the use of different the modelling techniques.

While there have been many fundamental studies of natural ventilation within enclosed cavities, there appears to have been no studies that have investigated the effects of non-uniform surface

temperatures on the fluid dynamics within air cavities. This significant knowledge gap was the focus of CFD simulations described in Chapter 6.

## **2.9 Summary**

This literature review outlined in this chapter identified that the proportion of Australians opting to live in apartment buildings has increased significantly over the past decade and is continuing to increase. Dwelling type (i.e. detached or apartment) was also identified as a significant indicator of residential energy consumption, which has been postulated to be driven by differences in thermal performance.

While many previous studies were identified that measured the thermal performance of detached dwellings, there were no studies that provided results exclusively for apartment dwellings in Australia. The previous studies that examined detached dwellings identified that there were significant differences between heating and cooling consumption in reality compared to simulations conducted in accordance with the NatHERS protocol.

Various causes of uncertainty were examined in the studies of detached dwellings to explain the differences in the measured and simulated heating and cooling consumption. The most significant causes stemmed from differences in occupant behaviour and occupant thermal comfort preferences followed by differences in weather. These effects resulted in significantly greater cooling consumption in reality compared to NatHERS simulations. Differences in infiltration rates and insulation coverage were also regarded as contributing factors.

While the infiltration model used in NatHERS typically produced infiltration rates in alignment with those measured in detached dwellings in Australia, there was no available measurement data of the airtightness of apartment dwellings in Australia to facilitate a comparison. However, the majority of comparisons conducted internationally indicated that apartments are significantly more airtight than detached dwellings.

Previous studies have shown that the impact of thermal bridging caused by repeating frame elements can significantly reduce the total thermal resistance of the building envelope. However, the reported impacts varied considerably and were dependent on building envelope construction details. Furthermore, many simulation studies have used simplified treatments of air cavities that do not consider the impact of the thermal bridge on the fluid dynamics of the air within the cavity itself. It could therefore be stated that the impact of non-homogeneous or periodic variations in surface temperatures on natural convection in enclosed cavities is not well understood.



## Chapter 3

### 3 Thermal Performance Evaluation of Existing Apartment Buildings: Experimental Methodology

#### 3.1 Introduction

The aim of this component of the research was to quantify and compare the *in-situ* thermal performance of the occupied case-study Australian apartments against the relevant Australian building requirements including the Australian National Construction Code (NCC), the National House Energy Rating Scheme (NatHERS), BASIX, and other relevant standards or guidelines. The thermal performance was considered to be the dependence on external energy input to maintain thermally comfortable indoor conditions, which is predominantly a function of occupant preferences, building envelope characteristics, and the local climate.

This chapter focusses on the experimental methodology developed to recruit, monitor, and evaluate the thermal performance of a set of occupied case-study Australian apartments. It also describes the various methods employed or developed to characterise and evaluate the energy consumption, thermal conditions, occupant behavioural responses, building envelope performance, and the occupancy status of the apartments.

An outline of the key activities involved in monitoring each of the apartments is provided schematically in Figure 3-1.

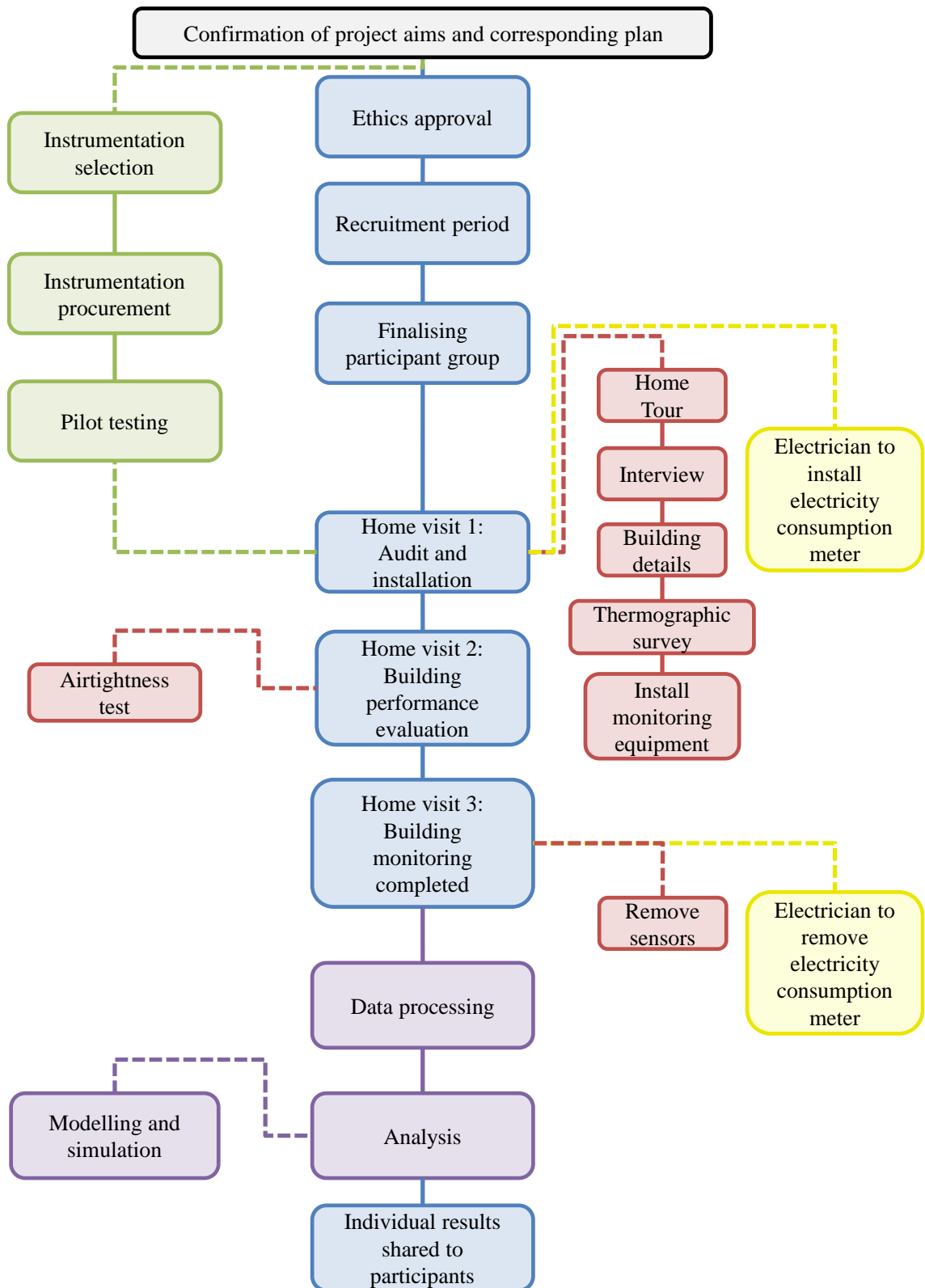


Figure 3-1 Flowchart indicating sequence of activities associated with apartment thermal performance monitoring. Blue rectangles indicate interactions with the participants, green indicates instrumentation preparation, red indicates research activities conducted within the apartments, yellow indicates work conducted by the electrical contractor, and purple indicates data processing.

## **3.2 Participant Recruitment and Apartment Selection Methodology**

### **3.2.1 Selection of Case-Study Buildings**

The apartment selection was limited to major growth areas in the nearby regions, which included Wollongong and Sydney in New South Wales (NSW), and Canberra in the Australian Capital Territory (ACT).

The size of the apartment development was the primary selection criterion. The study was focused on examining medium-to-high density apartment developments, and thus building size was constrained to Class 2 (*multi-unit residential*) buildings with a minimum of 3 floors, and a maximum height of 10 floors.

The year of construction was the secondary selection criterion. In NSW, apartments complying with the BASIX requirements for apartment units that were introduced in 2005 were preferred. Similarly, in the ACT, apartments that complied with the National Construction Code (NCC) thermal performance requirements for apartment units, which were most recently updated in 2010, were preferred.

Thus, the population size was determined by summing building approvals for apartment dwellings between January 2006 and June 2017 in NSW and between January 2010 and June 2016 in the ACT. This resulted in a population size of 226800 dwellings, based on Australian Bureau of Statistics (ABS) 8731.0 Building Approvals, Australia using Tables 22 and 29 (Australian Bureau of Statistics, 2019).

However, the project budget allowed for just 9 apartment units to be assessed. For a population size of 226800, a sample size of 9 indicated that findings generated within this study were 95% likely to be within 35% of the findings generated from observing the entire population. While this meant that the study would potentially have a relatively large margin of error in terms of a statistical match with the wider population of all apartments, a cohort of this size provided the opportunity for in-depth monitoring, analysis, and diagnostics of each individual dwelling. The methodology adopted to assess this small sample could then be refined to guide and streamline future monitoring and analysis methods in studies with larger, more representative sample sizes.

### **3.2.2 Recruitment Procedure**

An information package was developed to inform potential participants of the purpose of this study and how they could participate. The package included an invitation letter, which was a brief two-page document that provided an overview of the study. It also included a short questionnaire to obtain specific characteristics of the potential participant's apartment to ensure that the apartment met the selection criteria and was therefore suitable for this study. The second document was the Participant Information Sheet, which described the research context, the

specific research activities that were to be conducted, data management and confidentiality, and the potential impacts/risks of participating.

The recruitment package was electronically distributed to administration officers at the key company partners within the ARC Research Hub for Steel Manufacturing in Australia including BlueScope Steel, Cox Architecture, Stockland, and the University of Wollongong. The administration officers were then asked to distribute invitations containing the recruitment package content to their staff via email. The email and accompanying documents provided instructions and contact information to allow potential participants to express their interest in participating to the research team. Friends and family living in suitable apartments were also contacted personally and asked to participate; those interested were provided with the invitation email and associated documents.

These organisations and groups formed the initial recruitment pool. Had an insufficient number of participants were recruited from this subset of the population, calls for participation from a broader recruitment pool would have been necessary.

Each participant that expressed their interest in participating was contacted by the author over the phone to inform them whether there was interest in including their apartment in the research study, to discuss the Participant Information Sheet, and to arrange a suitable date and time to conduct the first home visit. The participants also had the opportunity to voice any questions or concerns they may have had regarding participation during the phone call.

### **3.2.3 Ethics**

The recruitment methodology, as well as the activities and procedures involved were assessed by the Human Research Ethics Committee (HREC) of the University of Wollongong prior to initiating the recruitment process. The research project was approved under HREC Protocol 2018/118.

## **3.3 Inspection of Apartment General Characteristics**

A walk-through audit inspection was conducted during the first home visit to obtain the general characteristics of each apartment.

The inspection involved measurements of the apartment dimensions for subsequent development of a detailed floor plan for each apartment, or, for checks of consistency and verification in the case of apartments where floor plans were made available. The inspection also involved obtaining external shading details of the apartments, including shading caused by nearby adjacent structures, and determining the types of spaces adjacent to the apartments within the building, such as common areas, lift cores, car parks, or neighbouring apartments. This data was used in the

development of building performance simulation models, as well as to determine key apartment characteristics including the floor area, envelope area, and window-to-wall ratio.

The inspection also involved thorough cataloguing of the primary energy consuming appliances within the apartment, included fixed appliances such as lighting. Details collected on the appliances included type, brand, model, and nameplate power consumption rating where available. The details of all HVAC appliances in the apartment, including portable and fixed systems were of primary interest in this study. Information gathered from portable equipment, such as pedestal fans and electric heaters that were connected to general power outlets, included the brand, model, nameplate power rating, and the location within the apartment that they were used. For fixed HVAC systems, which were exclusively reverse cycle air conditioners typically on dedicated electrical circuits, the details collected included the brand, model, thermostat settings, and location of the indoor and outdoor units. For ducted systems, the return air and diffuser locations were also recorded. Photographs of all significant appliances, their nameplates, and associated components were taken where possible. Additional information for each appliance, such as the coefficient of performance, was able to be determined off-site from photographs taken of the nameplate and from product details supplied on manufacturer websites, using the model identification code obtained from the nameplate.

The characteristics of various building elements were also obtained to the highest degree of detail possible from superficial observation. This included the floor covering in each room, glazing, shading, sealing, and framing details, and the construction system details of the internal walls, intertenancy walls, and external walls. Supplementary construction system details were obtained by an inspection of the ceiling cavity where possible. The ceiling cavity inspection also provided information of the insulation, ducting, and water piping systems.

The energy efficiency assessment section of the local government Development Application (DA) was successfully obtained for the majority of the apartments. This was primarily the BASIX Certificate for apartments in NSW, and the NatHERS Rating and associated report for apartments in the ACT, however, some apartments in NSW also had NatHERS assessment reports available. These reports were primarily used for the purposes of comparison of the predicted versus measured heating and cooling loads, but were also useful for facilitating data input into the thermal models of the apartments, particularly for obtaining non-superficial construction details.

The general characteristics were gathered mainly to inform building performance simulation modelling, but also to characterise the measured energy consumption within each apartment and inform causal influences on the thermal performance.

### **3.4 Electricity Consumption**

Apartment electricity consumption in this study was monitored primarily to measure the observed heating and cooling energy used in each of the apartments. The electricity consumption data was also used to infer the presence of occupants within the apartments and more generally assess the consumption of electricity in apartments.

#### **3.4.1 Electricity Monitoring Equipment**

Electricity consumption within each apartment was monitored using a Wattwatchers Auditor 6M. The Wattwatchers devices had six independent measurement channels, which enabled the electricity consumption to be differentiated at the sub-circuit level and into end-usage loads. Typically, electricity consumption was grouped by total power, lighting, air conditioning, wall-oven, and general power loads.

The Wattwatchers devices measured the minimum and maximum root mean square voltage and current, and the real and reactive energy over a short interval of 30 seconds, and a long interval of 5 minutes for each channel. While both the short-interval and long-interval were transmitted instantaneously to Wattwatchers' database over the 4G network, up to 27 days of long-interval data was also recorded on the device locally. Thus, the long-interval data was less susceptible to data loss in the case of network interruptions, and hence, long-interval data was used as the primary source of electricity consumption data in this study.

The accuracy of the Wattwatchers device was specified as 1% of the reading for voltage and current, and Class 1 and Class 2 as defined by IEC 62053-21 for active energy and reactive energy respectively.

The Wattwatchers devices were installed by a licensed electrician in accordance with the device specifications and installation instructions as a safety requirement. The electrician was typically organised to arrive whilst the author was conducting the initial apartment inspection to minimise disruption to the participants. A photograph of one of the Wattwatchers devices installed in one of the apartments is shown in Figure 3-2.



Figure 3-2 Wattwatchers Auditor 6M device installed within the circuit-breaker panel in an apartment.

### 3.4.2 Characterisation of Air Conditioning Energy Consumption

The measured air conditioning energy consumption in each apartment was characterised using the energy signature method to determine change in air conditioning consumption as a function of outdoor temperature.

Subsequently, various methods were applied to identify when the air conditioning systems were in standby operation and when they were actively conditioning; and whether, while conditioning, the air conditioning systems were supplying heating or cooling.

#### 3.4.2.1 Energy Signature Method

The energy signature (ES) method involves fitting a three-segment piecewise linear regression line of best fit to a scatter plot of the daily air conditioning electricity consumption as a function of the daily mean outdoor temperature (Kissock, Haberl and Claridge, 2003). The three segments of the line are intended to correspond with heating consumption for cooler temperatures, baseline consumption for moderate temperatures, and cooling consumption for warmer temperatures (Kissock, Haberl and Claridge, 2003). In this study, the baseline air conditioning consumption was assumed to be constant, in other words, the baseline consumption was not considered to vary with outdoor temperature between the balance points that formed the central segment. In addition, the baseline consumption was expected to align with the standby consumption, indicating close to no air conditioning use between the two balance points. Therefore, the slope of the central segment of the regression line was constrained to zero.

The resulting energy signature line-of best fit involved five unknown parameters:  $x_0$ ,  $x_1$ ,  $k_1$ ,  $k_2$ , and  $b$ , as shown in Equation (3-1)

$$f(x) = \begin{cases} k_1x + b & \text{if } x < x_0 \\ k_1x + b - k_1(x - x_0) & \text{if } x_0 \leq x < x_1 \\ k_1x + b - k_1(x - x_0) + k_2(x - x_1) & \text{if } x \geq x_1 \end{cases} \quad (3-1)$$

where  $x$  is the daily mean outdoor temperature,  $f(x)$  is the air conditioning energy consumption,  $x_0$  and  $x_1$  are the heating and cooling balance points, respectively, and  $k_1$  and  $k_2$  are the rate of change of the heating and cooling consumption as a function of temperature, respectively. While  $b$  is an arbitrary constant, it corresponds to the y-intercept of the heating curve (first segment) and also is required in the calculation of the remaining segments.

The piecewise regression model was defined in Python by the author using Python Library *NumPy*. The model was initialised and constraints were applied using Python library *Lmfit*. Finally, the line-of-best fit was determined using Python Library *SciPy* via least-squares using the Levenberg-Marquardt optimisation algorithm. This method was considered more robust than manual/visual determination of the balance points as it ensured the best fit.

For those apartments where the scatter plots did not have three well-established segments due to the absence of occupants using either heating or cooling, an equivalent reduced form of Equation (3-1) that contained two segments and three unknown parameters was used to generate the energy signature.

Under ideal conditions, the slopes of the heating and cooling segments of the energy signature curve are a function of: the COP and EER, respectively, of the air conditioner; the indoor temperature set-points; the total building thermal transmittance; and the building envelope area. However, in practice, day to day variations are observed due to variations in solar gains, changes in the wind velocity, and most significantly, changes in the internal heat gains, schedules, and desired internal conditions caused by differing occupancy behaviour, particularly in residential buildings (Kissock, Haberl and Claridge, 2003; Hitchin and Knight, 2016).

The ES method has been commonly used to assess: the impact of retrofits; compare thermal performance between design and as-built; fault-detection; and in some cases, the building envelope heat-transfer parameters (Kissock, Haberl and Claridge, 2003; Nordström, Lidelöw and Johnsson, 2012; Ferdyn-Grygierek *et al.*, 2018).

#### 3.4.2.2 Standby Air Conditioning Energy Consumption

The standby energy consumption of the air conditioning systems was examined relative to the active air conditioning energy consumption in the apartments. The term ‘active consumption’ is



used here to denote the energy consumed by the air conditioner while it was heating or cooling the indoor environment.

Standby energy consumption of the air conditioning systems was due to a combination of ancillary functions including the monitoring of remote control inputs and the thermostat. However, in some systems, a significant proportion of standby energy consumption was suspected to be due to intermittent operation of a crankcase heater, which maintained internal fluid temperatures within the operating range. This was deduced from periodic increases in the standby power consumption at regular time intervals in several of the monitored air conditioning systems. In one other system, the standby consumption increased whenever the ambient outdoor temperature dropped below approximately 10°C, which suggested that this crankcase heater was controlled by a thermostat. In each of these cases, the power consumption increased by between 25 and 75 W while the crankcase heater was considered to be operating.

The average daily air conditioning electricity consumption was separated into active and standby consumption by establishing a threshold energy consumption value that denoted the air conditioning system as being in active operation when exceeded, and in standby operation otherwise. The threshold energy consumption value was established by determining the baseline energy consumption of the air conditioning systems, which represented the regular standby consumption, and then accounting for minor and major fluctuations in the standby consumption, such as those caused by intermittent operation of the crankcase heater as discussed above.

The baseline consumption was identified by calculating the statistical mode of the energy consumption data (i.e. the most frequently occurring value in the dataset), which was resampled into 15-minute intervals to align with temperature data for other analyses. However, prior to calculating the statistical mode, the data was discretised into 1000 J intervals to account for minor fluctuations and measurement error in the baseline consumption. This process amplified the prominence of the mode amongst the discretised distribution of dataset. An additional 90000 J (equivalent to 100 W over the 15 minute interval) was added to account for major fluctuations in the standby consumption. The magnitude of this constant offset was determined by ensuring it exceeded the power required to operate the crankcase heater, which was quantified above, but was not considered high enough to power the compressor and fans to provide any heating or cooling.

This enabled the standby and active energy consumption of the air conditioning systems to be separately analysed, and enabled the proportion of standby consumption to be determined as a function of the total air conditioning consumption.

### 3.4.2.3 Heating and Cooling

The air conditioning energy consumption that was labelled as active consumption during the standby analysis was further classified as either heating or cooling operation. The intermittent periods of active air conditioning operation were individually analysed as separate air conditioning ‘use events’. The following single rule-based methods were tested to classify each ‘use event’ as being either a heating or cooling operation.

- If the date of an air conditioning use event was between 16<sup>th</sup> April and 15<sup>th</sup> October inclusive, then the event was considered heating; and if the date was between 16<sup>th</sup> October and 15<sup>th</sup> April inclusive, then the event was considered cooling. These date ranges approximately correspond with the Australian heating and cooling seasons, respectively. This method was adopted from Belusko *et al.* (2019).
- If the temperature difference in the conditioned zone between the time that the air conditioner was turned on and the temporal midpoint of the air conditioning use event was positive, then the event was classified as heating; and if the temperature difference was negative, then the event was classified as cooling. This method was adapted from the method used by de Dear, Kim and Parkinson (2016; 2018), who determined the temperature difference between the time that the air conditioner was first turned on with multiple subsequent measurements and evaluated the operation using a temperature threshold. This method assumed that the air conditioner always exchanged sufficient thermal energy to significantly influence the heat transfer processes in the zone.
- If the daily mean outdoor temperature on the day of an air conditioning use event was below the mean of the heating and cooling balance points obtained from the energy signature presented in Figure 4-8 for a specific apartment, then the event was classified as heating. Otherwise, if the daily mean outdoor temperature was above the mean of the heating and cooling balance points, then the event was classified as cooling. This method was considered similar to using heating and cooling degree-days to estimate and classify the air conditioning use, but enabled the use of base temperatures that were determined specifically from the observed air conditioning use of each particular apartment.

A complex rule-based method with multiple conditions was also developed to more accurately determine the most likely operating mode. This method used a score-based approach where conditions that corresponded with increased likelihood for heating were assigned positive scores and conditions that corresponded with increased likelihood for cooling were assigned negative scores. If the final tally was positive, then the event was classified as heating; and if the final tally was negative, then the event was classified as cooling. If the final tally was zero, then manual

intervention was used to discern the most likely operating mode. The list of rules used in this method are presented in Table 3-1.

*Table 3-1 List of rules used in the score-based classification method to determine whether an air conditioning event was providing heating or cooling.*

<b>Method</b>	<b>Condition during air conditioning use event</b>	<b>Score weighting</b>
Date range	If the date was between April 16 <sup>th</sup> and October 15 <sup>th</sup> inclusive	+1
	If the date was between October 16 <sup>th</sup> and April 15 <sup>th</sup> inclusive	-1
Indoor temperature comparison	If temperature difference of zone between turning air conditioner on and midpoint of use event was positive	+1
	If temperature difference of zone between turning air conditioner on and midpoint of use event was negative	-1
Energy Signature	If daily mean temperature was below heating balance point from the energy signature	+1
	If the daily mean temperature above the cooling balance point from the energy signature	-1
Outdoor temperature threshold	If the outdoor temperature exceeded 25°C	-2
Temperature comparisons with time constraints	If the use event: started between 12:00am and 9:00am and ceased before 10:00am; the maximum indoor temperature was greater than maximum outdoor temperature; and the maximum indoor temperature occurred after the minimum indoor temperature	+2

The complex rule-based system integrated modified versions of the rules used in the three simple methods. However, two additional rules were added to the algorithm to resolve classification errors that resulted from using the first six conditions alone under specific circumstances.

The first additional rule addressed classification errors that occurred during use events that were deduced to be cooling by the present author from manual observation of a more extensive and detailed dataset than that observed by the preliminary classification algorithm, but were misclassified as heating by the preliminary algorithm due to an increase in indoor temperature between the onset and mid-point of the use event caused by excessive heat gains and due to the date range suggesting heating operation. In such circumstances, if the outdoor temperature was above 25°C, the algorithm placed additional weighting towards the event most likely being cooling.

The second additional rule addressed classification errors that occurred during use events that were deduced to be heating from manual data observation, but were misclassified as cooling by the preliminary algorithm due to the date range suggesting cooling operation and due to the daily mean outdoor temperature exceeding the cooling balance point. These circumstances occurred during cool mornings of otherwise warm days, most often in mid to late spring. If the event occurred in the morning, the maximum indoor temperature was greater than the outdoor

temperature, and the minimum indoor temperature occurred earlier than the maximum indoor temperature, then the algorithm placed additional weighting towards the event most likely being heating.

These additional rules were developed and weighted by manual scrutiny of the datasets to ensure the algorithm remained robust. However, there was considerable slack in the threshold and time ranges associated with the first and second additional rules, respectively, which were not tuned to coincide with a critical value that altered the algorithm outputs.

During air conditioning use events in which the air conditioner was operated for a very brief period or otherwise had low power consumption, there was insufficient data on the impact of the air conditioner on the indoor temperature conditions to accurately classify the use event using the rule-based algorithm. Thus, classification of such events was deferred by the algorithm, which were eventually classified to match that of the most temporally proximal use-event. Such use events were deemed to have occurred when the average power consumption of the air conditioner was more than 500 W for fewer than two 15-minute intervals.

One limitation to the assessment of the overall heating use within the apartments was that the heating output provided by any appliances other than from the air conditioner were unable to be distinguished from the power consumption on the general power circuits. This concern was most significant for apartments in which the participants acknowledged that they occasionally utilised their oil heaters, despite having the reverse-cycle air conditioning available.

### **3.5 Indoor Thermal Conditions**

The primary objective of the study was to evaluate the actual energy performance of the apartments in terms of energy consumed for heating and cooling to achieve and maintain thermally comfortable conditions. Thus, in order to evaluate the energy performance of the apartments, it was necessary to also assess the thermal conditions in the apartments. This enabled the measured heating and cooling consumption to be contextualised with respect to thermal conditions in the apartments.

By acknowledging that heating and cooling are used to improve thermal conditions, it is clear that heating and cooling consumption and the performance gap are affected by: a) occupant thermal comfort preferences relative to what is deemed to be comfortable by conventional thermal comfort models (i.e. occupant preferences assumed by rating tools); and b) the methods sought by occupants to control their indoor environment (i.e. occupant behaviour, specifically, the use of heating, and natural ventilation versus air conditioning). In this regard, the adaptive thermal comfort model was considered a satisfactory representation of conventional thermal comfort preferences in the residential context for this study.

Characterisation of the thermal conditions in the apartments during occupied periods indicated whether occupant preferences varied from conventional thermal comfort models. In this case, occupant preferences were inferred from the measured occupant behaviour with respect to the thermal conditions. Thus, monitoring of thermal conditions primarily served to explain large differences in measured heating or cooling use than what would have been consumed if the indoor zones were maintained within the conventional thermal comfort boundaries.

Note that this study did not investigate the thermal sensations of the occupants in the apartments. This was considered to be beyond the scope of this study as it was considered that the specific sensation votes of the occupants were not required to assess the energy performance of the apartments with respect to the NatHERS rating tool.

### 3.5.1 Indoor Environment Monitoring Equipment

Two types of sensors were used to monitor the indoor thermal environment. A HOBO UX100-003 Temp/RH logger was deployed in the main bedroom and another in the bathroom to monitor the dry-bulb air temperature and relative humidity at 15 minute intervals, and an indoor environmental quality monitoring device developed by the Sustainable Buildings Research Centre (SBRC) at the University of Wollongong (UOW) was deployed in the living room to measure dry-bulb air temperature, relative humidity, globe temperature, and air speed at 5-minute intervals. Photographs of each sensor are provided in Figure 3-3 and Figure 3-4.

The temperature and humidity sensors used in this study were selected to conform to the minimum accuracy requirements specified for Class C (Comfort) measurements in ISO 7726 – *Ergonomics of the thermal environment – Instruments for measuring physical quantities* (ISO, 1998), which are specified in Table 3-2.

Table 3-2 Accuracy of indoor thermal environment monitoring equipment extracted from ISO 7726 (ISO, 1998)

Parameter	Accuracy	Measurement Range
Air temperature	Required: $\pm 0.5^{\circ}\text{C}$ Desired: $\pm 0.2^{\circ}\text{C}$	$10^{\circ}\text{C}$ to $40^{\circ}\text{C}$
Mean radiant temperature	Required: $\pm 2.0^{\circ}\text{C}$ Desired: $\pm 0.2^{\circ}\text{C}$	$10^{\circ}\text{C}$ to $40^{\circ}\text{C}$
Humidity	$\pm 0.15$ kPa	0.5 kPa to 3.0 kPa

The HOBO UX100-003 devices had a specified accuracy of  $\pm 0.21^{\circ}\text{C}$  within the range of  $0^{\circ}\text{C}$  to  $50^{\circ}\text{C}$  for air temperature and 3.5% within the range of 25% to 85% for relative humidity. For relative humidity measurements lower than 25% or higher than 85%, the stated accuracy decreased to 5%. The sensors were placed on a wall away from direct sunlight and generally placed on the faces of plastic power outlet coverings or on top of furniture to avoid any surface

damage to the walls. The height of the sensors was nominally 1.1 metres from the floor level, but a different height was used if there were no suitable surfaces present at this height.

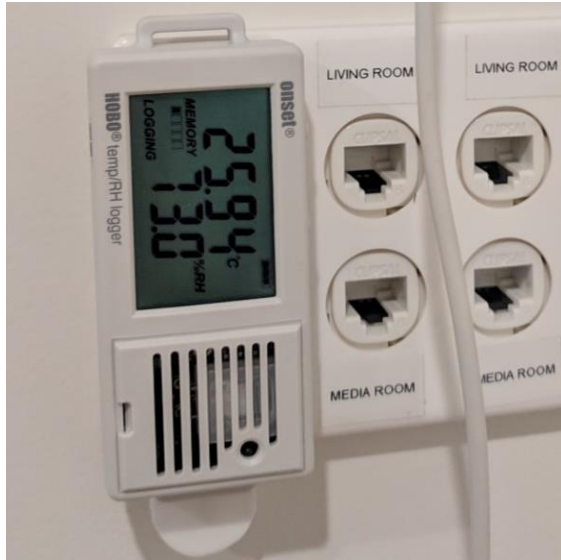


Figure 3-3 HOBO Temp/RH logger in a typical installation location within the apartment.



Figure 3-4 Close-up of the Raspberry Pi IEQ monitoring device.

The specific instrumentation on the IEQ monitoring device is detailed in Table 3-3, including the accuracy and measurement range of each of the sensors. The device ran on a Raspberry Pi 3 Model B+ and had a GrovePi+ add-on board to interface the various digital Grove and analogue sensors with the Raspberry Pi. The Raspberry Pi and GrovePi+ were contained within an enclosure separated from the thermal monitoring sensors to eliminate erroneous measurements caused by heat transfer from the processor to the sensors.

Table 3-3 Specific instruments installed on the IEQ monitoring device.

Parameter	Measurement Range	Accuracy	Sensor Type/Model
Dry-bulb air temperature	-20 to +80°C	±0.5°C	DHT22 / Grove Temperature and Humidity Sensor Pro
Relative humidity	0-99% RH	±2%	
Globe temperature	-40 to +125°C	±1.5°C	TTC3A103*39H Thermistor encased within a 40 mm (diameter) matte black plastic sphere.
Air speed	0-20m/s	Not specified	Hot-wire anemometer / Modern Device Wind Sensor Rev C
Occupancy	120° 0.5-6 metres	N/A	Grove PIR Motion Sensor

### 3.5.1.1 Calibration

A large number of these devices had already been developed previously by a researcher for an earlier project, however many were still deployed in ongoing research projects and there were not enough available units for this study. Thus, more units were assembled and all units were subsequently calibrated by the present author prior to deployment within the apartments.

The dry-bulb air temperature sensors of the Raspberry Pi IEQ Monitoring devices were calibrated relative to a Fisher Scientific Traceable platinum ultra-accurate thermometer with an accuracy of  $\pm 0.05^{\circ}\text{C}$  and the globe temperature sensors were calibrated relative to a globe thermometer with a diameter of 150mm and a K type thermocouple that had an accuracy of  $\pm 0.3^{\circ}\text{C}$ .

The Raspberry Pi IEQ Monitoring devices and the reference temperature sensors were placed within a climate-controlled chamber as pictured in Figure 3-5. Spot measurements within the climate-chamber were conducted at temperature set points of  $10^{\circ}\text{C}$ ,  $20^{\circ}\text{C}$ ,  $30^{\circ}\text{C}$  and  $40^{\circ}\text{C}$  to satisfy the measurement range requirements specified in ISO 7726:1998.



*Figure 3-5 Raspberry Pi IEQ monitoring devices and the reference temperature sensors within the climate chamber prior to calibration.*

The calibration offset for each of the sensors was determined using the sum of the least absolute difference between the temperature sensors and the calibration measurements over the measured data points.

It was not possible to individually calibrate the Modern Device Wind Sensor Rev C hot-wire anemometers due to lack of resources, however, the researcher who initially developed the in-house Raspberry Pi IEQ device calibrated a typical set of Wind Sensor Rev C units and fitted a 4<sup>th</sup> degree polynomial curve of the voltage output of the tested Rev C sensors to the measured velocity of a reference laboratory grade anemometer. This same correlation was used for the

present study and deemed to be of sufficient accuracy for estimation of the influence of air velocity on thermal conditions.

### **3.5.2 Assessment of Thermal Conditions**

#### **3.5.2.1 Adaptive Comfort Model**

The way in which thermal comfort would be perceived by typical occupants in each of the apartments was predicted using the Adaptive Thermal Comfort model in accordance with ASHRAE Standard 55-2017 for the evaluation of thermal comfort in existing spaces from longitudinal environmental measurements (ANSI/ASHRAE, 2017). The Adaptive Thermal Comfort model was used rather than the PMV model for various reasons outlined above in Section 2.7.1.2

According to Standard 55-2017, the adaptive model is applicable when each of the following conditions are met:

- No mechanical cooling system is present and no heating system is in operation;
- Occupants were engaged in sedentary activities with metabolic rates ranging between 1.0 and 1.3 met;
- Occupants were free to adapt their clothing within a range at least as wide as 0.5 to 1.0 clo; and
- The prevailing mean outdoor air temperature was between 10.0 °C to 33.5°C.

However, there were two significant deviations between the conditions permitted by ASHRAE Standard 55-2017 and those in the present study. It was concluded previously (Section Assessment of Thermal Comfort Models for Mixed-Mode Residential Dwellings) that the adaptive model better aligned with occupant thermal sensations than the Predicted Mean Vote (PMV) model in mixed-mode residential buildings. Thus, in the present study the adaptive model was used to predict thermal comfort despite the presence and intermittent use of mechanical heating and cooling systems. In addition, the prevailing daily mean temperature in Canberra was frequently below the 10°C lower limit permitted within Standard 55 during winter and reached a minimum of 3.3°C during the present study. Original analysis within RP-884 demonstrated that the data forming the basis of the adaptive model was suitable from prevailing mean outdoor temperatures as low as 5°C (de Dear and Brager, 2002). Therefore, it was considered acceptable to extrapolate the applicability of the adaptive comfort model beyond the lower limit specified within Standard 55 in order to assess thermal comfort in Canberra during winter.

The environmental parameters required to assess thermal comfort using the adaptive model were the indoor operative temperature, prevailing mean daily outdoor temperature, and indoor air



speed. While the indoor air speed was measured directly using the IEQ monitoring device, the indoor operative temperature and prevailing mean daily outdoor temperature were derived from measured quantities.

The indoor operative temperature,  $T_{op}$ , is defined in Appendix A of ASHRAE Standard 55-2017 as function of the indoor air temperature,  $T_a$ , mean radiant temperature,  $T_{mrt}$ , and  $A$ , which itself is a function of the indoor air speed,  $V_a$ . The expression for operative temperature is given by Equation (3-2) and the values for  $A$  are given below.

$$T_{op} = A \cdot T_a + (1 - A)T_{mrt} \quad (3-2)$$

$V_a$	<0.2 (m/s)	0.2 to 0.6 (m/s)	0.6 to 1.0 (m/s)
$A$	0.5	0.6	0.7

The mean radiant temperature,  $T_{mrt}$ , used in Equation (3-2) was calculated from indoor air temperature, globe temperature, and indoor air speed using the method specified in Annex B of ISO 7726:1998 *Ergonomics of the Thermal Environment – Instruments for Measuring Physical Quantities* (ISO, 1998). For the rooms monitored by the HOBO UX100-003 sensors, which did not incorporate a globe temperature sensor, the mean radiant temperature was assumed to be equal to the indoor air temperature when determining the operative temperature. However, it is acknowledged that although this method has been commonly used by many other researchers, it has been reported that it can result in average inaccuracies of 6.7% (Chaudhuri *et al.*, 2016).

The prevailing daily mean outdoor air temperature was calculated in accordance with Appendix J of ASHRAE Standard-55 2017, using the exponential series formula J-2, in which  $\alpha$  was set to 0.6 to better portray daily fluctuations in the weather (ANSI/ASHRAE, 2017). The outdoor temperature measurements were sourced from the nearest BOM weather station to each apartment as described in Section 3.8.1.

The thermal conditions experienced in the apartments were evaluated with respect to the 80% acceptability limits defined by the adaptive model. The thermal environment within these boundaries is considered thermally acceptable by a substantial majority (80%) of occupants. The upper and lower 80% acceptability limits are given by the equations listed below, where  $T_{op}$  is operative temperature and  $T_{pma(out)}$  is prevailing mean daily outdoor air temperature.

$$\text{Lower 80\% acceptability limit (}^\circ\text{C): } T_{op} = 0.31 \cdot T_{pma(out)} + 14.3$$

$$\text{Upper 80\% acceptability limit (}^\circ\text{C): } T_{op} = 0.31 \cdot T_{pma(out)} + 21.3$$

For operative temperatures above 25°C, the upper acceptability limits were increased in accordance with Table 5.4.2.4 from Standard 55-2017 to account for indoor air speeds above 0.3 m/s.

Finally, the thermal comfort was evaluated in terms of the number of occupied hours that were outside the 80% acceptability limits, expressed as fraction of the total number of occupied hours.

### **3.6 Occupant Behaviour**

It was important to not only examine the thermal conditions within the apartments, but also the comfort management behaviours that were utilised by occupants to help maintain an adequate level of comfort within the apartments. The two comfort management strategies to control the indoor environment of interest within this study were occupant use of: i) natural ventilation and ii) air conditioning.

The frequency and manner of use of natural ventilation and air conditioning has implications on the energy consumption in the apartments, and the corresponding occupant behaviours are regarded in literature as a major cause of the difference between the measured and simulated energy consumptions in building performance simulation studies, particularly in the residential context (DEWHA, 2008).

#### **3.6.1 Monitoring Occupant Behaviour**

##### **3.6.1.1 Natural Ventilation**

Natural ventilation was observed in each apartment by monitoring the opening states of two representative windows in each apartment using HOBO UX90-001 State Loggers, which functioned via an internal magnetic reed switch.

The windows were selected as representative of the usage of natural ventilation in the apartment, particularly if the two were generally/often operated simultaneously to generate cross-flow of air through the apartment. To identify which windows to monitor, the participants were asked which windows they operated most frequently to generate a draught through the living room and or bedroom. If the participants identified more than two windows that were frequently used, the researcher made a judgement as to which windows to monitor based on the layout of the apartment. Typically, the primary living room window and primary bedroom window were monitored.

The installation procedure was dependent on the opening mechanism of the window or sliding door of interest. Examples of installations on sliding mechanisms and hinge mechanisms are shown in Figure 3-6 and Figure 3-7, respectively. Both were positioned such that the sensor appropriately detected the presence of the magnet when the window or door was closed without obstructing the full range of motion of the window or door.



*Figure 3-6 HOBO state logger installed on a sliding door in closed position*



*Figure 3-7 HOBO state logger installed on an awning window in opened position*

The HOBO state logger detected when the window or door was opened or closed and logged the time of the change and retained information of the current position. The data as before stored locally and was transferred to a PC following the completion of the monitoring period.

One limitation to using reed switches to monitor the openable windows/doors of a building was that the size of the opening at a particular time was not captured, which meant that the difference between the window being somewhat ajar or wide open was not captured. However an alternative more comprehensive, but cost-effective and reliable, window position monitoring system was not available on the market, and development of a bespoke system was beyond the resources available to the author. Moreover, the primary objective of monitoring the windows was simply to indicate when the participants were using natural ventilation, rather than air conditioning or taking no action. Thus, while the magnitude of the natural ventilation air flow rate could not be assessed, the corresponding changes to indoor conditions relative to outdoor conditions while the windows were open was a satisfactory indication of occupant utilisation of natural ventilation.

The data captured by the HOBO state loggers was event based, rather than being taken at a particular sampling rate. To integrate information of the window state into the dataset for analysis, the window data was resampled at two second intervals and the final state within each two-second interval was labelled as the position of the window at that timestamp. The resampled window data was then again resampled at 15-minute intervals to align with the remaining dataset. The window state within the 15-minute interval was assigned as the mean state indicated from the subset of 2-second interval measurement data. This enabled the data to accurately reflect the proportion of time that the window was open across a 15-minute interval rather than portray a simple binary output of the window status at each timestamp.

### 3.6.1.2 Air Conditioning

Air conditioning use was monitored using sub-circuit electricity metering as previously described in Section 3.4.1. The periods when heating or cooling were in use were individually determined via the methodology previously described in Section 3.4.2.3.

## 3.6.2 Assessment of Occupant Behaviour

### 3.6.2.1 Air Conditioning and Natural Ventilation Use

Occupant use of heating, cooling, and natural ventilation were characterised using binary logistic regression. Each of the aforementioned dependent variables were categorised into binary states (off and on) using the following methods:

- Air conditioning was considered “on” when the air conditioning consumption was above the standby operation threshold for energy consumption as described in Section 3.4.2.2 and labelled as either heating or cooling using the score-based method discussed in Section 3.4.2.3.
- Natural ventilation was considered “on” when at least one of the two monitored windows was open and was considered “off” if both of the monitored windows were closed.

The function for the log of the odds (log-odds) of a linear logistic model is expressed in Equation (3-5), where  $x$  is the independent variable, and  $\beta_0$  and  $\beta_1$  are the regression coefficients. Rearranged, the probability of the dependent variable being “on” as a function of  $x$  is given in Equation (3-4).

$$\text{Ln}\left(\frac{p}{1-p}\right) = \beta_0 + \beta_1 x \quad (3-3)$$

$$p = \frac{1}{1 + e^{-(\beta_0 + \beta_1 x)}} \quad (3-4)$$

Outdoor temperature was selected as the independent variable to predict the status of each of the applied adaptive strategies in lieu of indoor temperature to avoid feedback between the independent variable and the dependent variables as discussed in Section 2.7.2 of the literature review.

As evidenced by Kim *et al.* (2017), it was postulated that occupants open the windows when the outdoor conditions were comfortable and close the windows when the outdoor conditions were either too cool or too warm. Thus, a quadratic term was added to the regression analysis for natural ventilation to account the hypothesised non-monotonic interactions between the outdoor temperature and the window operating behaviour. The modified log-odds of the logistic regression function for natural ventilation is expressed in Equation (3-5).

$$\text{Ln}\left(\frac{p}{1-p}\right) = \beta_0 + \beta_1x + \beta_2x^2 \quad (3-5)$$

The logistic regression models were fitted using Maximum Likelihood Estimation (MLE) with the statistical Python module *Statsmodels*. The Newton-Raphson optimisation algorithm was used to iteratively determine the maximum likelihood. Finally, the 95% confidence intervals for each model were determined using the endpoint transformation method.

The key metrics used to assess the logistic regression models were likelihood ratio test, McFadden's pseudo-R<sup>2</sup>, and the area under the curve (AUC) of the Receiver-Operator Curve (ROC).

In this study, the likelihood ratio test was used to determine whether all the predictor variables ( $x$  and  $x^2$ ) were statistically significant by comparing the likelihood between the fitted model and the null model without predictor variables, which is the mean probability of the dependent variable being “on”.

The McFadden's pseudo R<sup>2</sup> value, denoted  $\rho^2$ , similarly contrasts the log-likelihood of the fitted model to the log-likelihood of the null model and is analogous to the sum of squared errors to the mean (Allison, 2013). Values for McFadden's pseudo R<sup>2</sup> are often considerably lower those presented for the coefficient of determination used in linear regression (Louviere *et al.*, 2000).

The ROC expresses the classification capability of the fitted model by examining the degree of overlap between the probability distributions of the positive and negative classes of the resulting model (Narkhede, 2018). This is quantified by plotting the true positive rate (TPR) against the false positive rate (FPR) as a function of the classification threshold. The threshold denotes the probability at and above which the model outputs are classified as positive and below which the model outputs are classified as negative. This determines the number of true positives, true negatives, false positives, and false negatives amongst the classification distributions.

### 3.6.2.2 Air Conditioning On and Off Temperatures

Determination of the indoor temperatures at which occupants turned heating and cooling on and off are extremely important for many reasons, not least because they have a very significant influence on energy consumption and thermal comfort predicted by Building Performance Simulation software. This study is one of very few to identify such temperature thresholds. The heating and cooling switch on temperatures indicated the temperatures at which occupants were uncomfortable and sought to improve the indoor conditions and the heating and cooling switch off temperatures indicated that the occupants were thermally satisfied with the indoor conditions. These temperatures were compared to the NatHERS heating and cooling set-point temperatures and were also evaluated with respect to the adaptive comfort thermal acceptability limits to

examine whether the switch points identified in the study corresponded to the most widely-accepted definition of thermal comfort in occupant controlled spaces.

Heating and cooling were considered to have been turned on when the air conditioning system energy consumption shifted from standby mode into active operation, which was determined using the method described in Section 3.4.2.2. It was considered to have been turned off by the occupant or reached the set-point when the air conditioning system energy consumption returned to standby operation.

### **3.6.3 Semi-Structured Interview**

During the first home visit to each apartment, the researchers carried out a semi-structured interview with the participant, often accompanied by their partner, to discuss the activities that comprised a typical day within their homes, and their strategies used to remain thermally comfortable (e.g. use of heating, cooling, natural ventilation, etc.)

The purpose of the semi-structured interviews was to collect qualitative, anecdotal evidence directly from the occupants to complement the quantitative findings generated by the measurements. These anecdotal statements offered potential explanations for observed thermal conditions and have been included in relevant discussions within Chapter 4. Information gathered from the interviews also aided in selecting the most appropriate sensor deployment locations within each apartment.

## **3.7 Building Envelope**

Aspects of the building envelope were examined for each of the apartments to assess the quality of construction and to inform subsequent building performance simulation analyses to determine the significance of the differences between the building envelope performance in reality and the performance assumed by NatHERS during thermal performance assessments.

### **3.7.1 Air Permeability Test**

The air permeability of each apartment was tested in accordance with AS/NZS ISO 9972:2015 *Thermal Performance of Buildings – Determination of air permeability of buildings – Fan Pressurisation Method* (Standards Australia and Standards New Zealand, 2015). The air permeability was assessed using the building in use method, which was considered to be most appropriate for evaluating for the overall energy performance of occupied buildings. The building-in-use method has been applied in significant bodies of existing literature concerning airtightness of residential buildings in Australia e.g. (Ambrose and Syme, 2017).

The building in use method required natural ventilation openings to be closed, internal partitions to be open, and continuously operating air conditioning or mechanical ventilation inlets/outlets to

be sealed. Intermittently operating air conditioning or mechanical ventilation systems were to be closed if the unit featured a closing mechanism, otherwise, they were to remain open.

The blower door was temporarily installed within the apartment entrance from the common area corridor, as shown in Figure 3-8. This opening was selected as opposed to an external door as the glass sliding doors leading to the balcony were generally too tall and occasionally too wide to seal using the blower door panels. Another factor was that the balcony sliding doors often contribute significantly to the leakage of the external envelope of an apartment. To ensure that the apartment was pressurised adequately relative to the ambient atmospheric pressure (rather than the pressure in the corridor), external windows and doors were opened where possible in the corridor to minimise flow restrictions between the outdoors and the corridor so as to minimise the pressure differential.



*Figure 3-8 Typical blower door setup.*

The apartments were tested without guarded-zone pressure arrangements. That is, the adjacent apartments and corridor were not equalised relative to the apartment of interest, and thus the total leakage measured included both internal leakage between apartments as well as the external leakage through the building envelope. This was selected as it aligned with the intended goals of the “building-in-use” method, in which the whole dwelling envelope airtightness was assessed. In addition, guarded-zone pressure testing presented significant additional logistical challenges, including additional test equipment, additional research assistants, and significant level of coordination from each of the neighbours (e.g. obtaining unanimous consent and a suitable time). This meant that the air leakage tests did not measure the proportion of leakage that was through the external envelope versus internal partitions. However, the leakage paths were qualitatively

located and assessed using a smoke puffer device to indicate air movement while the apartment was pressurised.

The overall uncertainty of the results are affected by many factors, environmental conditions being the most significant source of uncertainty. It is stated within AS/NZS ISO 9972:2015 (2015) that the typical uncertainty under calm environmental conditions is below 10%, but can reach up to  $\pm 20\%$  during windy conditions.

### **3.7.2 Thermographic Survey**

A thermographic survey of the building envelope, which included all exterior walls for each apartment and the ceiling for top floor apartments, was conducted during the first home visit to detect the presence and spatial variation in insulation and the influence of thermal bridges that may have been caused by framing, infiltration points, or the envelope geometry. The present author utilised the thermographic images in conjunction with the visual inspection of the ceiling cavity to qualitatively determine the quality of insulation in each of the apartments. It was not physically possible to enter the ceiling cavities, which were generally suspended ceilings around 300-400 mm high. Thus, the visual inspections were limited to what was visible from the ceiling cavity hatch.

Thermography allows the temperatures of the surfaces seen through the camera lens to be observed by examining the infrared radiation emitted from those surfaces. A thermographic camera requires certain input parameters to determine the temperature of the surfaces based on the incoming radiation. These parameters include the emissivity of the surface observed, the temperature and humidity of the ambient air in-between the surface and the camera, and the temperatures of any objects that are potentially being reflected from the surface of interest. The air temperature and humidity were measured using a hand-held sensor and the interior surfaces of the sections of the building envelope of interest consisted solely of painted plasterboard, which was regarded as a highly emissive surface. This allowed a satisfactory level of accuracy to be achieved that was sufficient for a qualitative assessment, as is common for building thermographic inspection.

## **3.8 Climate**

Climate data was collected to contextualise the observed occupant behaviours and corresponding thermal performance of each apartment and also to act as input information for building performance simulation modelling based on observed weather data.

### **3.8.1 BOM Weather Station**

The primary source of weather data was gathered from the nearest, or next nearest possible, Bureau of Meteorology (BOM) weather station to each apartment. The weather data included



quantitative air temperature and relative humidity, wind speed and direction measurements, as well as qualitative observations of the cloud cover.

### **3.9 Occupant Detection**

A method to deduce when occupants were present in the apartments was developed by the present author to confine the evaluation of thermal comfort and occupant behaviour to periods when the apartments were considered to be occupied. This was a significant refinement of the assessment of thermal comfort and occupant behaviour by disregarding the times in which the indoor conditions were not experienced by occupants and therefore did not depict occupant thermal preferences or reflect occupant comfort management strategies.

The originally intended method for occupant detection was to use the passive infrared sensors installed on the Raspberry Pi IEQ monitors described in Section 3.5.1. However, while these sensors demonstrated reliable performance during calibration, they demonstrated very poor signal-to-noise ratios when deployed in the apartments. This meant that the sensors could not be used to indicate the occupancy status of the apartments, which led to the need to develop an alternative method.

The alternative method used to detect the presence of occupants in the apartments was a combination of rule-based and machine-learning-based methods, as described below.

#### **3.9.1 Rule-Based Classification**

Rule-based classifiers use a series of conditional checks (i.e. IF-THEN) to distinguish between classifications, in this case, whether the apartments were occupied or unoccupied. Conditional checks in a rule-based system are manually determined by the model designer, and are used to represent the modeller's knowledge or judgement in assigning a classification.

##### **3.9.1.1 Ground Truth Conditions**

The rules primarily comprised of ground truths that indicated definitive presence or absence of occupants. The following conditions were considered to indicate the presence of occupants when satisfied:

- If any lights were switched on or off in the apartment. This was indicated by an increase or decrease of more than 10 W in the mean power consumption on the lighting circuit between the current and previous time-step.
- If the state (open or closed) of either of the two monitored windows changed during the time-step.
- If air conditioning was actively conditioning the apartment. This was determined using the same method described in Section 3.4.2.2 in which the air conditioner was considered

‘active’ if the mean power consumption of the air conditioning circuit over the time-step was more than 100 W greater than the statistical mode consumption of the air conditioner;

- If electric cooking equipment was in active operation. This was determined using exactly the same method described for the air conditioner;

It was assumed that the lighting and window state ‘switching’ events were necessarily performed by an occupant. Furthermore it was assumed that cooking appliances were very rarely used while the apartment was unoccupied, and thus, the use of cooking appliances also indicated the presence of occupants. Finally, although it was plausible that the air conditioner was left to condition the apartment while it was unoccupied, the use of air conditioning was the primary focus of this study; thus, the apartment was considered occupied while the air conditioner was active so that all air conditioning events were retained for further analysis.

Despite the poor signal-to-noise ratio observed for the PIR sensors, the data generated by the PIR sensors still appeared to provide some degree of correlation with the aforementioned ground truth occurrences. Thus, while the PIR sensor data itself could not be used as ground truth, it was still used as one of the features of the machine-learning classifier, which is discussed in Section 3.9.2.2.

#### 3.9.1.2 Holiday Periods

Holiday periods were regarded as long, continuous unoccupied periods within the apartments. Holiday periods were identified via manual observation of the data and were marked by at least two consecutive days in which the energy consumption on all circuits in the dwelling remained at or below baseload consumption and the state of the windows remained unchanged. Holiday periods that lasted more than one week were verified by the participants.

#### 3.9.1.3 Baseload Conditions

Extending the logic used to manually identify holiday periods, the apartments were also considered to be unoccupied if the apartment energy consumption was at or below the baseload consumption level, and there were no other signs of occupant activity. The baseload consumption threshold was determined manually by examining the subset of data during the verified holiday periods. The average baseline power consumption threshold of the apartment cohort was 120 W and ranged from 30 W up to 170 W.

#### 3.9.1.4 Finalising the Rule-Based Classifier

The datasets for each apartment contained data collected at 5-minute intervals. Consequently, each of the aforementioned rule-based conditions were examined on a 5-minute basis. However, the occupancy status of the apartments was evaluated in 30-minute intervals using the following logic:

- If any of the ground-truth conditions were triggered within any of the 5-minute intervals contained within a 30-minute period, the apartment was considered occupied during the 30-minute period.
- Conversely, if all six of the 5-minute intervals met the holiday period condition or met the baseload consumption condition then the 30-minute period was considered to be unoccupied.

### 3.9.2 k-Nearest Neighbours Classification

A k-nearest neighbours (KNN) classification algorithm was developed to classify data that was yet to be classified by the rule-based classification method. The KNN model used the data classified by the rule-based method as training data, but had access to a broader array of data features (i.e. independent variables) that were anticipated to correlate with occupancy, but did not explicitly indicate the presence of occupants and thus were not used in the rule-based model.

The KNN method was selected as it is a non-parametric, non-linear model that is considered to be relatively simple to implement and robust to measurement noise. KNN has been demonstrated to be effective in predicting occupancy in both residential and commercial environments using electricity consumption data, network connectivity data, and/or other environmental measurement variables (Yang *et al.*, 2014; Kleiminger, Beckel and Santini, 2015; Fiebig *et al.*, 2017; Wang, Chen and Hong, 2018; Vela *et al.*, 2020).

The study by Kleiminger, Beckel, and Santini (2015), which used electricity consumption data as the primary features of their occupancy detection modelling, was used for guidance during the development of this model.

#### 3.9.2.1 Labelling Data

The KNN classifier required a set of supervised training data in which the occupancy state was previously labelled in order to form associations between the features examined by the classifier and the classification states. The data labelled using the rule-based classification method were used to train the KNN model.

#### 3.9.2.2 Feature Selection

The following parameters measured in the apartments were used to derive the features for the KNN model:

- Energy consumption on the general power circuit;
- Energy consumption on the lighting circuit;
- Energy consumption on the air conditioning circuit;

- Energy consumption on the oven and/or stove circuits; and
- Number of movements detected from the passive infrared (PIR) sensor on the Raspberry Pi IEQ monitoring sensor.

It was assumed that occupancy would correlate with increased energy consumption and also with rapid fluctuations in the energy consumption and movement patterns observed in the respective aforementioned parameters. Therefore, similarly to the method used by Kleiminger, Beckel, and Santini (2015), the sum, mean, standard deviation, and sum of absolute difference of each of the above parameters were used as features within the KNN model. The sum, mean, standard deviation, and sum of absolute difference for each of the parameters were calculated over 30-minute intervals using six 5-minute data samples, thereby aligning with the 30-minute labelling intervals determined using the rule-based classification model. An example of the features derived from ‘general power’ is presented in Figure 3-9.

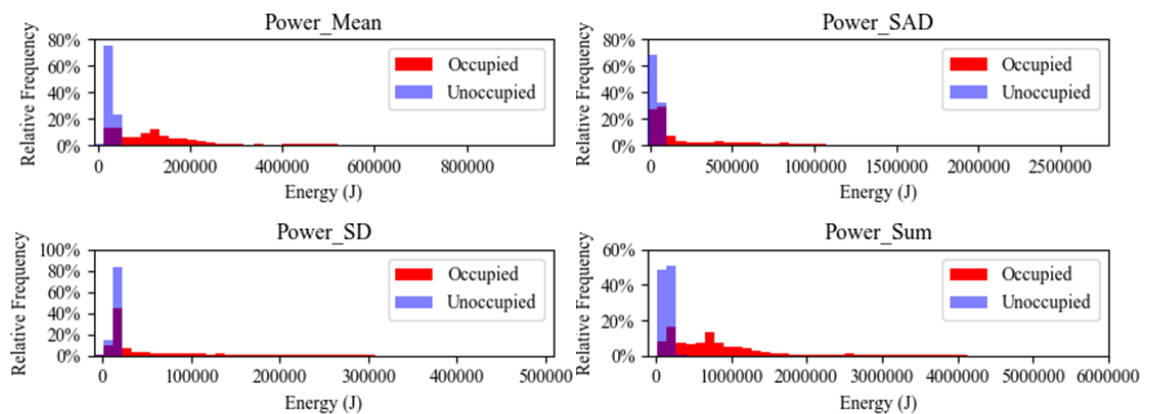


*Figure 3-9 Relative frequency distribution of the labelled unoccupied and occupied states for the features derived from the ‘general power’ circuit energy consumption in Apartment #1.*

Overall, up to 20 features were used in the KNN models, although fewer features were used in apartments where individual monitoring of air conditioning consumption, cooking energy consumption, or motion sensing was not possible.

### 3.9.2.3 Model Selection and Evaluation

The model selection phase involved determining the optimal hyper parameters to be used in the KNN models for each apartment. These parameters and the model performance were selected and evaluated using a stratified k-fold cross-validation method that is described below.

#### Hyper-Parameters

The two hyper parameters that were tuned in this study were:

- $k$ , the number of nearest neighbours used to classify an unclassified data-point; and
- the weighting assigned to each nearest neighbour.

All odd numbers between 5 and 25 inclusive were examined for  $k$  and the weighting metrics evaluated were ‘uniform’, in which all  $k$  neighbours were equally weighted; and ‘distance’, in which the weighting of each neighbour was inversely proportional to the Euclidean distance from the test point. The exclusive use of odd values of  $k$  was to ensure a majority vote could always be attained when using equal weighting. In total, 22 unique model hyper parameter combinations were evaluated.

### Cross-Validation

Each of the 22 unique model hyper parameter combinations were evaluated using the stratified  $k$ -fold cross-validation method with 4 folds. This means that for each of the 22 models, the labelled data was randomly separated into 4 groups of data, each with a similar distribution of ‘occupied’ and ‘unoccupied’ labels to that of the entire labelled dataset.

The cross-validation loop involved:

1. Assigning 1 of the 4 groups as the test data set and assigning the remaining 3 groups as the training data set.
2. Pre-processing using the training data set to derive the pre-processing function parameters and applying the pre-processing methods onto both the training and test data sets.
3. Fitting the model on the pre-processed training data set and evaluating the trained model by comparing the classes predicted by the model to the actual classes of the test data.
4. Retaining the selected model performance scoring metric and discarding the fitted model.
5. Repeating steps 1 to 6 until all 4 groups had been used as the test data set.
6. Calculating the average of the 4 model performance scores.

This process was then repeated for the next unique combination of hyper parameters. A diagram of the entire process is depicted in Figure 3-10.

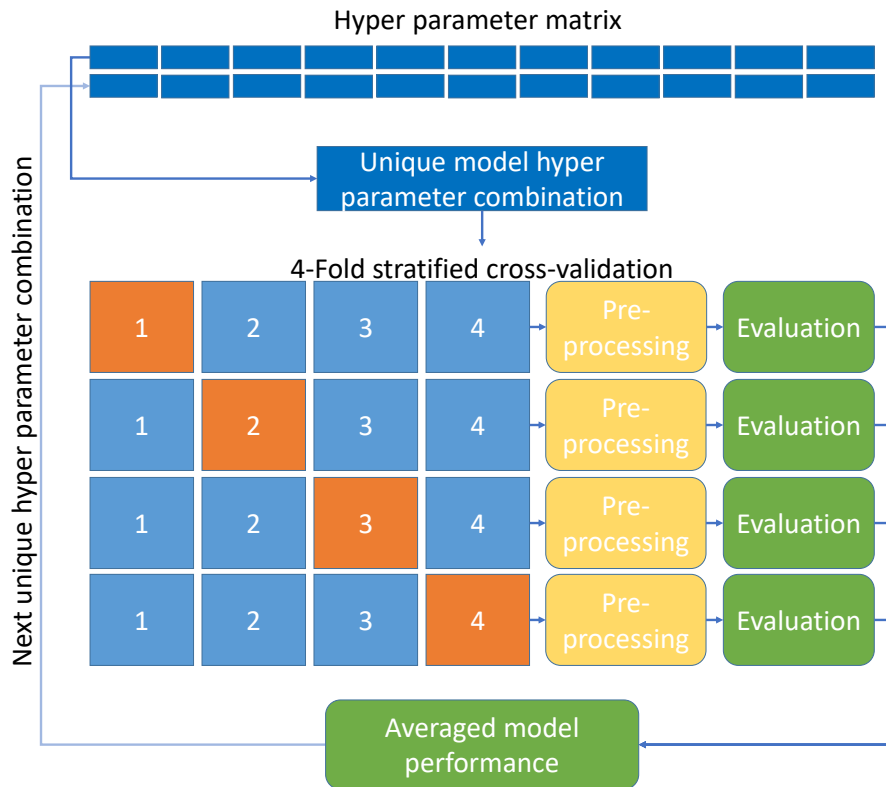


Figure 3-10 Diagram depicting the model selection and evaluation process.

As evident from Figure 3-10, the two major processes that occurred in the cross-validation loop were pre-processing and evaluation.

### Pre-Processing

Various pre-processing techniques were required to ensure the feature data was appropriately formatted for use by a KNN algorithm. Pre-processing involved the following steps.

- Imputing missing data. The mean was used in place of missing data in the training and test sets. KNN cannot function with missing data as the classification process involves calculating the distance from the test data point to all points within the training data. While improved imputation techniques are available, the mean was considered satisfactory given the low occurrence of missing data, which was only present in the PIR sensor data.
- Scaling the data. The KNN algorithm employed in this study used Euclidean distance to evaluate the proximity of a test point to its  $k$  nearest neighbours. Therefore, its performance was particularly sensitive to varying order of magnitudes amongst features. Min-Max scaling was used to rescale each of the features, such that the new range of each of the features in the training set was between 0 and 1. The same Min-Max transform function for each features derived from the training data set was then applied onto the test data set.

- Balancing class distribution. The performance of KNN algorithm is also sensitive to skew in the class distribution. This occurs as the majority class may saturate the feature space and therefore produce bias towards classifying a data-point as the majority class. The Random Over-Sampling technique was used to balance the class distribution. Random Over-Sampling randomly replicates data points within the minority class to ensure an equal number of data points for each class.

### Evaluation

The model performance within each cross-validation loop was examined using the confusion matrix, which expresses the predicted classifications in terms of the actual classifications by denoting the number of true positive (TP), true negative (TN), false positive (FP), and false negative (FN) classifications generated by the fitted model.

‘Precision’, which evaluates the number of true positive (TP) classifications as a fraction of the sum of the true positive (TP) and false positive (FP) classifications, as shown in Equation (3-6), was selected as the scoring metric to rate and contrast the KNN models. ‘Precision’ was considered the most appropriate scoring metric to use in this study as it minimises the number of ‘unoccupied’ periods incorrectly classified as ‘occupied’, and hence, minimises the potential bias within the thermal comfort and occupant behaviour analyses caused by including unoccupied periods.

$$Precision = \frac{TP}{TP + FP} \quad (3-6)$$

The unique hyper parameter combination with the highest precision, which was calculated as the average precision score over the 4 test/train folds, was considered to be the best performing model.

#### 3.9.2.4 Finalising Model

The KNN models with the best performing model hyper parameters for each apartment were refit using the entire labelled dataset for each apartment to improve predictive performance. The refitted KNN models were used as to predict the occupancy state of the unlabelled data.

The average precision amongst the refitted models for each apartment exceeded 0.99 and the average accuracy was 0.98. This indicated that the classifications made by the KNN algorithms closely matched those made by the rule-based method, which was effectively used to train the KNN models.

### **3.9.3 Combining and Applying the Occupancy Detection Models**

The rule-based and KNN models were combined into a single data series that indicated the occupancy status of each apartment over time by first assigning the class identified using the rule-

based method and then applying the KNN classification model to predict the occupancy state during periods that were unclassified by the rule-based model.

One remaining issue was the labelling of sleeping periods, in which feature characteristics mimicked those occurring during unoccupied states and were therefore frequently incorrectly labelled as ‘unoccupied’. To rectify this issue, it was assumed that occupants were at home and sleeping during periods that were initially labelled as ‘unoccupied’ if such periods were bounded by two periods of occupancy that last occurred after 9:00pm and recommenced between 5:00am and 10:00am the following morning.

After applying the assumption pertaining to suspected sleeping periods, there was finally a complete time-series for each apartment that indicated when the apartment was unoccupied, occupied by sleeping occupants, and occupied by active occupants. The data series produced for Apartment #6 is presented in Figure 3-11. The data series aligned with the monitoring periods of each apartment; hence, they could be used as a selection mask during subsequent analyses to filter out unoccupied periods.

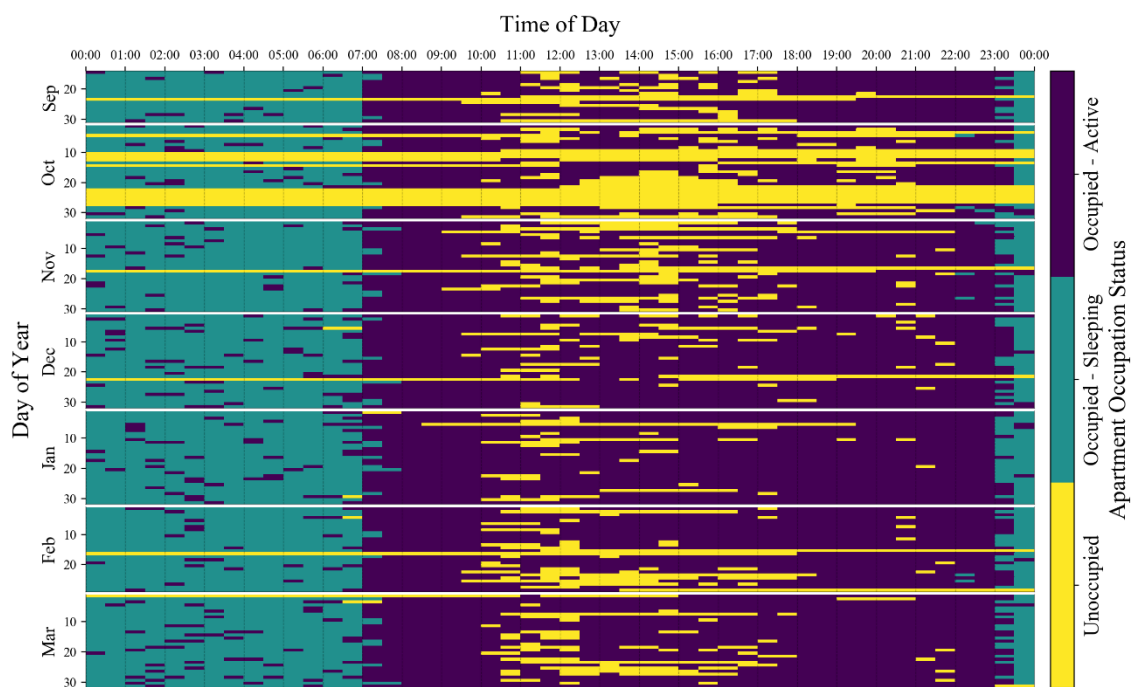


Figure 3-11 Plot of the occupancy status of Apartment #6 that resulted from the combination of the rule-based and KNN models, including the assumption of sleeping periods.



### 3.10 Summary

This chapter describes the methods used during recruitment, data collection, and analysis used to characterise and evaluate the thermal performance of a set of case-study Australian apartments.

Recruitment of participants was via invitational letters and participant information sheets shared throughout the University of Wollongong mailing lists and mailing lists of other organisations associated with the project as well as to interested associates of the author. Eligible participants were to be living in an apartment from a development site of between 3 to 10 stories high that was built after thermal performance requirements for apartments were introduced.

The chapter also describes the data collection and analysis methods developed for the following major tasks.

- Obtaining the key dwelling characteristics known to influence thermal performance in each apartment, including a thorough floor plan and major electrical appliances;
- monitoring and characterising the electricity consumption, in particular, the air conditioning electricity consumption;
- monitoring and evaluating the indoor thermal conditions in terms of a widely-accepted thermal comfort model;
- monitoring and evaluating occupant use of air conditioning and natural ventilation in terms of the indoor and outdoor air temperature;
- inferring the presence of occupants from a combination of rule-based and machine-learning methods;
- measuring the *in-situ* building envelope performance; and
- monitoring and characterising the local climate at each apartment.

A brief description of the specific measurements collected during the monitoring period is provided in Table 3-4 and a summary of the high-level parameters of interest and some of the key assessment methods are listed in Table 3-5.

*Table 3-4 Summary of measurements collected within the case study apartments over the duration of the monitoring period.*

<b>Parameter</b>	<b>Sample Interval</b>	<b>Sensor Location</b>	<b>Sensor Type/Model</b>
Dry-bulb air temperature, Relative humidity	15 minutes	Bathroom, Bedroom	HOBO Temp/RH Sensor UX100-003
Dry-bulb air temperature, Relative humidity, Air speed, Globe temperature Motion	5 minutes	Living room	SBRC IEQ monitoring device
Electricity consumption	5 Minutes	Circuit-level	Wattwatchers Auditor 6M
Window state	Event dependent	Two main windows	HOBO State logger UX90-001
Dry-bulb air temperature, Relative humidity	15 minutes	Balcony	HOBO Temp/RH Sensor UX100-003

*Table 3-5 Summary of the parameters of interest and assessment methods used within the experimental case-study.*

<b>Parameter of Interest</b>	<b>Assessments</b>
General apartment dwelling characteristics	<ul style="list-style-type: none"> <li>• Detailed floor plan</li> <li>• Cataloguing of major electric appliances</li> </ul>
Air conditioning consumption	<ul style="list-style-type: none"> <li>• Energy signature method</li> <li>• Standby and active consumption</li> <li>• Identification of heating and cooling operation</li> </ul>
Thermal comfort	<ul style="list-style-type: none"> <li>• Exceedance hours determined using the adaptive thermal comfort model</li> </ul>
Occupant behaviour	<ul style="list-style-type: none"> <li>• Air conditioning and natural ventilation use as a function of outdoor temperature using logistic regression</li> <li>• Air conditioning on and off temperature</li> <li>• Semi-structured interview</li> </ul>
Occupant detection	<ul style="list-style-type: none"> <li>• Rule-based methods</li> <li>• <i>k</i>-nearest neighbours algorithm</li> </ul>
Building envelope	<ul style="list-style-type: none"> <li>• Air permeability test using fan pressurisation method</li> <li>• Thermographic analysis</li> </ul>

## Chapter 4

### 4 Thermal Performance Evaluation of Existing Apartment Buildings: Results and Discussion

#### 4.1 Introduction

This chapter presents the results from the apartment monitoring described in Chapter 3. Firstly, it provides an overview of the apartment cohort characteristics followed by presentation and discussion of the energy consumption, thermal comfort, occupant behaviour, building envelope performance, and climate conditions informed by the longitudinal monitoring and energy performance inspections conducted in the apartments.

The electricity consumption in the apartments is quantified and compared with several Australian benchmark studies, with particular focus on heating and cooling consumption. The thermal conditions experienced in each of the apartments is presented and evaluated using the adaptive thermal comfort model. Occupant use of natural ventilation and air conditioning is characterised as a function of indoor and outdoor temperature using logistic regression modelling amongst other methods. Finally, building envelope performance is characterised from blower door test results and findings from the thermographic surveys.

#### 4.2 Description of Case-study Apartments

Monitoring was conducted in nine occupied apartments; two located in Canberra, two in Sydney, and five in Wollongong. The following characteristics were observed amongst the cohort.

- The average floor area was 94.7 m<sup>2</sup>. The average floor area for single, double, and triple bedroom apartments were 59.0 m<sup>2</sup>, 92.8 m<sup>2</sup>, and 121.0 m<sup>2</sup>, respectively, increasing by approximately 30 m<sup>2</sup> for each additional bedroom in the apartment.
- On average, there were 2.2 occupants per apartment, slightly above the national average of 1.9 occupants per apartment according to the 2016 Census (Australian Bureau of Statistics, 2017). For comparison, the national average number of occupants per detached dwelling was 2.8 from census data. Six of the apartments were occupied by two people; the remaining three apartments were occupied by one, three, and four people.
- The average year of construction amongst the cohort was 2012. Seven of the apartments were constructed after 2010. This included the two Canberra apartments that were therefore designed to meet more stringent NatHERS energy efficiency requirements that were introduced in 2010 and five of the apartments in NSW. Of the remaining two

apartments, one had been built in 2004, just prior to the introduction of BASIX requirements for apartments in 2005. The other apartment had been converted from a warehouse to a multi-unit residential building in 2000 (the year of the original construction of this warehouse was unknown).

- All the apartments were constructed using typical reinforced concrete structural systems.
- While plasterboard obscured direct visibility of the internal structural and material configurations of the external and internal walls, in every apartment walls were in all likelihood based on cold-formed steel framing as this also formed the ceiling framing in every apartment. The external and intertenancy walls also featured a masonry layer that consisted of either concrete blockwork, generic brick, or autoclaved aerated concrete (AAC) panels. Brick formed the external cladding of façades of two of the apartments, while the façades of the remaining seven apartments were rendered and the outer-masonry layer was not directly visible.
- Only a single apartment featured double-glazed windows; the remaining apartments had single-glazed windows. All windows were aluminium framed.
- Seven of the apartments had reverse-cycle air conditioning, whilst two apartments, which were located in same apartment building, were naturally ventilated.

An image of the exterior of each of the monitored apartments is shown in Figure 4-1 and a summary of key details is provided in Table 4-2. Floor plans of each of the apartments that include the locations of monitoring sensors is provided in Appendix A.



*Figure 4-1 Images of each of the monitored apartment blocks. The specific apartments monitored are outlined in red.*

The monitoring periods for each of the apartments are shown in grey shading in Figure 4-2. Also shown in Figure 4-2 are the daily Heating Degree Days (HDD) and Cooling Degree Days (CDD) measured at the BOM weather station nearest to each apartment over the period from April 2018 to March 2019. The HDD and CDD were calculated with a base temperature of 18°C, which is one of two base temperatures commonly used by the BOM (Bureau of Meteorology, 2020).

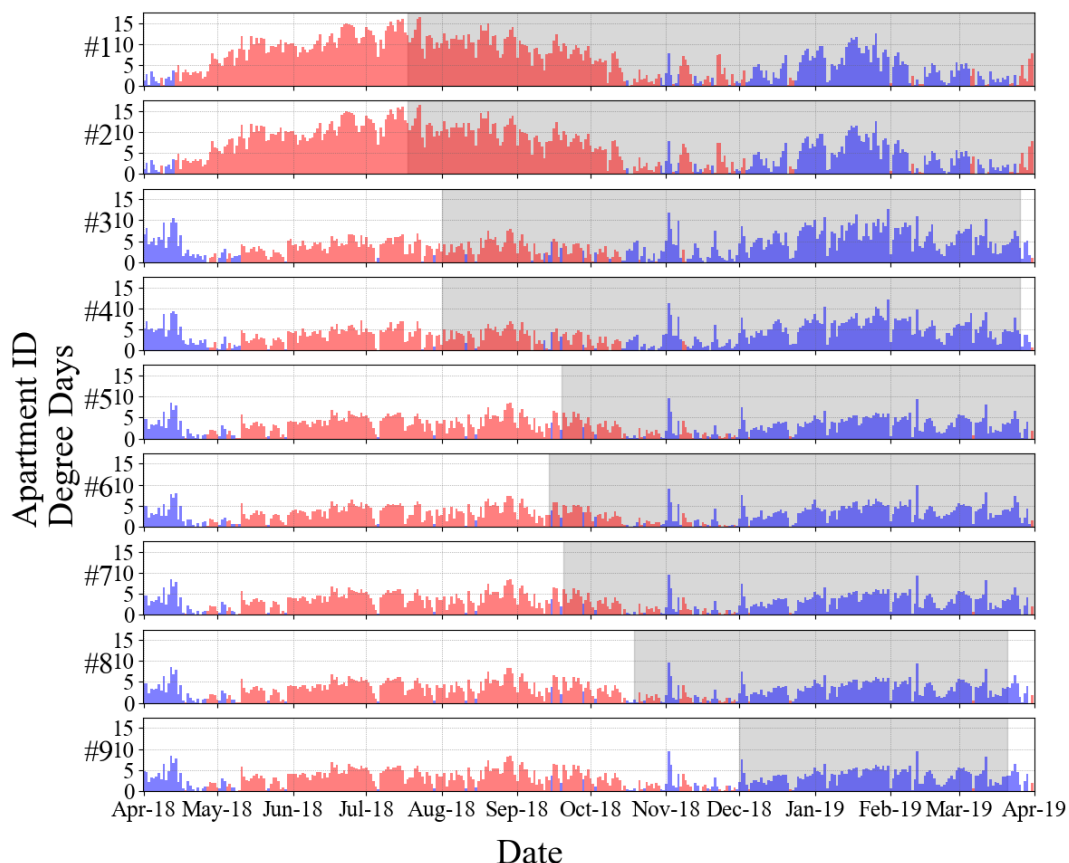


Figure 4-2 Monitoring periods for each of the nine participating apartments, indicated by the area shaded in grey. Daily HDDs and CDDs are shown in red and blue, respectively, as calculated using data from the nearest BOM weather station.

The fraction of the annual heating and cooling degree days within the monitoring period and the total length of the monitoring period for each apartment are presented in Table 4-1.

Table 4-1 Fraction of annual HDD and CDDs within each apartment's monitoring period.

Apartment ID	#1	#2	#3	#4	#5	#6	#7	#8	#9
Heating	64%	64%	43%	43%	17%	20%	17%	6%	1%
Cooling	96%	96%	86%	86%	83%	83%	83%	82%	76%
Monitoring Period Duration (days)	257	257	237	237	194	199	193	153	110

Table 4-2 Summary of the key characteristics for each of the case-study apartments.

Apartment ID	Location	NCC Climate Zone	Year of Construction	Gross Floor Area	Number of Bedrooms and Occupants	External Walls	Window-to-Wall Ratio	Window Type	Orientation	Air Conditioning System
#1	Franklin, ACT	Zone 7	2013	52 m <sup>2</sup>	Single (2)	Masonry Veneer	41.8%	Single-glazed; aluminium frame	North and South	Split-system in living
#2	Philip, ACT	Zone 7	2014	92 m <sup>2</sup>	Double (3)	Masonry Veneer	40.0%	Single-glazed; aluminium frame	North East	Split-systems in living and bedroom
#3	Rosebery, NSW	Zone 5	2017	94 m <sup>2</sup>	Double (2)	Brick Veneer	41.4%	Double-glazed; aluminium frame	East	Ducted; two zones
#4	Surry Hills, NSW	Zone 5	2000 (conversion)	95 m <sup>2</sup>	Double (2)	Brick Veneer	31.3%	Single-glazed; aluminium frame	North East	Split-system in living
#5	North Wollongong, NSW	Zone 5	2016	120 m <sup>2</sup>	Triple (4)	Masonry Veneer	60.1%	Single-glazed; aluminium frame	West	Ducted; two zones
#6	Wollongong, NSW	Zone 5	2014	124 m <sup>2</sup>	Triple (2)	Masonry Veneer	49.1%	Single-glazed; aluminium frame	South West	Split-system in living
#7	North Wollongong, NSW	Zone 5	2004	119 m <sup>2</sup>	Triple (1)	Masonry Veneer	63.1%	Single-glazed; aluminium frame	North East	Ducted; two zones
#8	North Wollongong, NSW	Zone 5	2015	90 m <sup>2</sup>	Double (2)	Masonry Veneer	54.2%	Single-glazed; aluminium frame	West	None
#9	North Wollongong, NSW	Zone 5	2015	66 m <sup>2</sup>	Single (2)	Masonry Veneer	33.4%	Single-glazed; aluminium frame	South East	None

### 4.3 Energy Consumption

#### 4.3.1 Overall Electricity Consumption

The average daily electricity consumption during summer for each apartment is presented in Figure 4-3.

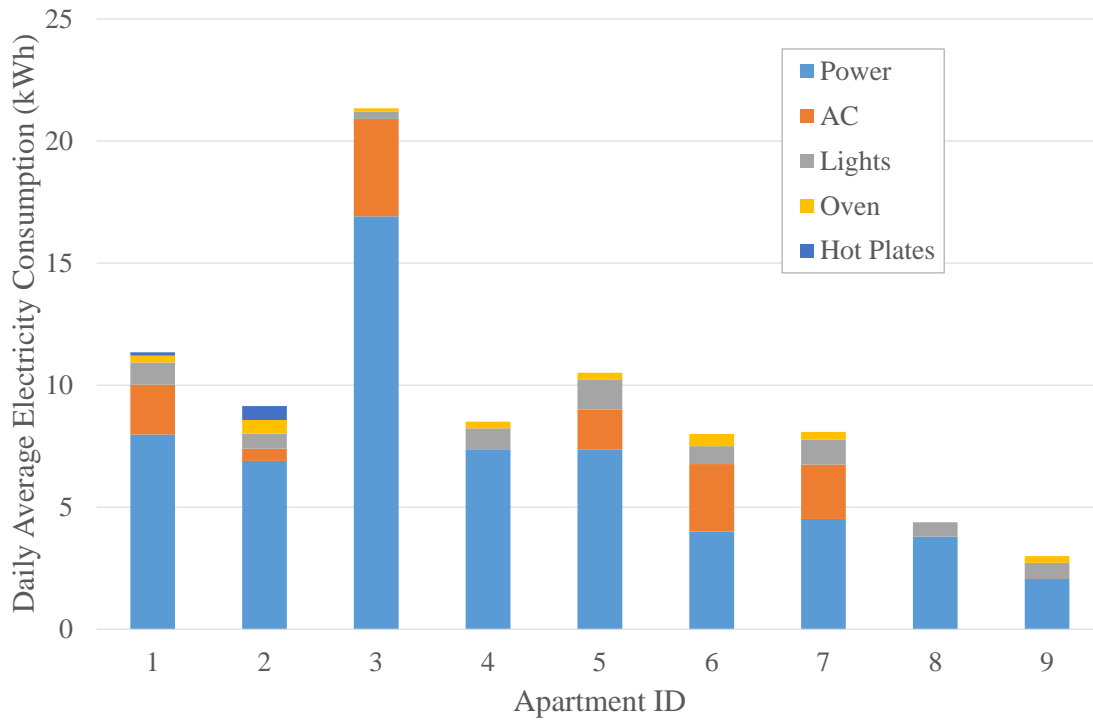


Figure 4-3 Average daily electricity consumption for each apartment in summer.

The mean daily electricity consumption of the apartments, both during summer and the entire monitoring period was 9.4 kWh ( $\sigma = 5.0$  kWh). This was slightly less than the mean daily electricity consumption of 10 kWh ( $\sigma = 6.0$  kWh) measured in 2000 apartments monitored in Sydney and nearby regions in 2013 as part of the Smart Grid Smart Cities (SGSC) project (Roberts *et al.*, 2019). This relatively close agreement with previous research indicates that the present study likely captured typical consumption patterns of apartments in Sydney and surrounding areas despite the comparatively small sample size of the current study. The relatively high standard deviation of both the present study and previous research suggests that there is substantial variance in the daily electricity consumption amongst apartments in Sydney and surrounding regions.

The mean daily electricity consumption in summer per capita was 4.7 kWh ( $\sigma = 2.8$  kWh) in the present study, which was around 30% lower than the value of 6.4 kWh ( $\sigma = 3.8$  kWh) measured by Roberts (2019).

The Australian Electricity Regulator (AER) requires that electricity consumption benchmark figures are included on electricity bills issued to residential customers by retail suppliers (Australian Energy Regulator, 2020). The benchmarks are updated every three years to remain

relevant and are based on the season, climate zone, number of occupants, and variables such as the presence of a swimming pool or under-floor heating. The mean daily electricity consumption for each of the case-study apartments was compared to the most appropriate AER benchmark for each season. The comparison revealed how well the electricity consumption patterns of the case-study apartments aligned with the prevailing electricity consumption patterns of comparable residential dwellings.

Averaged across the cohort of nine, the apartment consumptions were below the AER benchmarks in each season; on average being 76.0%, 73.8%, 68.5%, and 69.1% of the AER benchmarks for winter, spring, summer, and autumn respectively. The disparity between the apartment consumption and the AER benchmarks was most likely due to the benchmarks being based primarily upon detached homes (Acil Allen Consulting, 2017), with no consideration for the type of dwelling, which has been shown to be significant by Rickwood (2009), Fan *et al.* (2015), and Roberts *et al.* (2019) as discussed in the literature review.

One particular outlier was Apartment #3, where the total electricity consumption exceeded the associated annual AER benchmark by 55%. Apartment #3 had the largest AC consumption amongst the cohort, but AC consumption only made up 19% of the total electrical energy consumption, while 79% (17 kWh/day) of the electrical energy consumed was through “general power” use. The primary reason for the high “general power” consumption in Apartment #3 was thought to be the presence of the rooftop spa, which used a 3 kW electric heater to maintain a water set-point of 40°C throughout the year. This is supported by time-series data of the “general power” consumption channel during unoccupied periods where an intermittent load of approximately 3150 W was observed. This apartment also had several other major appliances (two wine coolers and two refrigerators) in operation that further contributed to high general power consumption. The presence of pools, of which the rooftop spa could be considered a small one, have been shown to be significant contributors/predictors of high end use energy consumption in both the AER Benchmark Study (Acil Allen Consulting, 2017) and at least one other Australian study into drivers of residential energy consumption (Fan, Macgill and Sproul, 2015).

### **4.3.2 Electricity End-Use Patterns**

Electricity consumption by end-use for summer for all apartments is presented in Figure 4-4.



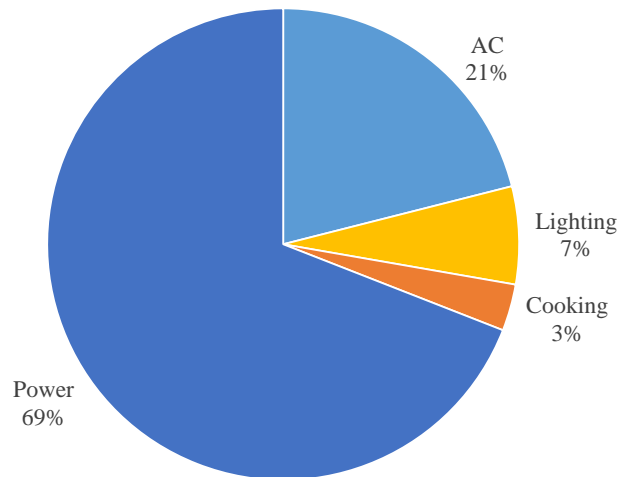


*Figure 4-4 Electricity consumption by end-use in summer for all apartments, expressed as a fraction of total consumption. Power includes all other electrical appliances not individually monitored, e.g. refrigeration, washing and drying appliances, television, entertainment devices, etc.*

General power, or plug-loads, which consists of all electric appliances connected to a shared ‘Power’ sub-circuit such as refrigerators, washing and drying appliances, televisions, entertainment devices, and so on, represented 69% of the total electricity consumption. Air conditioning accounted for 21% of consumption, which included both standby and provision of heating and/or cooling. Lighting consumed 7% and electric-powered cooking appliances accounted for 3% of the electricity consumption. However, only two of the nine apartments had electric hot plates, whereas the remainder had gas stoves.

Hot water system energy consumption was not metered in this study as the hot water system in each of the monitored apartments was independent from the apartment’s electricity supply, and was determined to be gas heated in eight of the nine apartments, and could not be determined in one apartment.

Figure 4-5 presents the proportion of electricity end-usage based on a typical three-person detached home in Western Sydney that exclusively used electrical appliances published by Ausgrid (2019), whilst Figure 4-6 presents the average proportion of electrical consumption by end-usage from a sample of detached dwellings and apartments across the Sydney Metropolitan area monitored between 2015 and 2018, sourced from the project entitled RP1017 ‘Validating and Improving the BASIX Energy Assessment Tool for Low-Carbon Dwellings’ (Ding *et al.*, 2019).

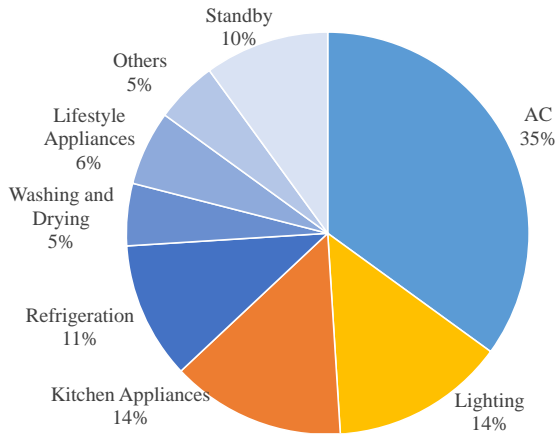


Figure 4-5 Proportion of household energy consumption end-use based on a typical three-person home in Sydney with all electric powered appliances (i.e. No gas or other energy sources) (Ausgrid, 2020). Note that the hot-water consumption has been removed from the chart for the purposes of comparison.

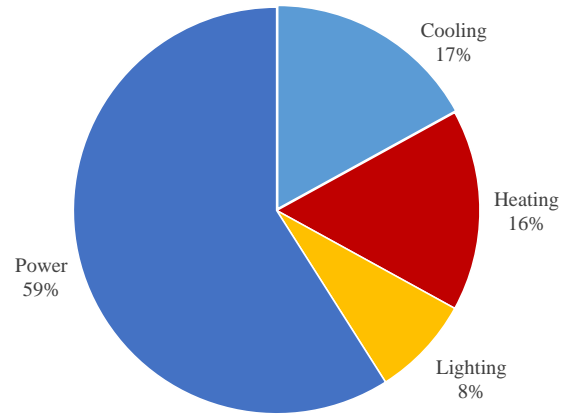


Figure 4-6 Average proportion of household electricity consumption end-use from a mixed cohort of detached and attached dwellings across the Sydney Metropolitan area monitored from September 2015 until June 2018 (Ding et al., 2019). Note that hot-water system consumption was not monitored within this study.

Air conditioning accounted for a smaller proportion of electricity use in the present study. This may support findings by Rickwood (2009), suggesting that reduced exposed envelope area and dwelling size (for the same number of bedrooms) of apartments compared with detached dwellings results in lower air conditioning consumption. The fraction of electricity consumption used for air conditioning during summer in the present study was also lower than the 24 to 28% measured by Saman *et al.* (2013) in six detached dwellings in Adelaide with NatHERS ratings at or above 7.5 stars. The fraction of energy used for lighting in the present study aligned well with that observed in RP1017, but was approximately half of the fraction accounted for lighting in the Ausgrid model dwelling. The remaining electricity consumption accounted for 72%, 59%, and 51% in the present study, RP1017, and the Ausgrid typical model dwelling, respectively.

### 4.3.3 Air Conditioning Consumption

The reverse-cycle air conditioning electricity consumption was independently monitored in six of the seven apartments that had air conditioning. This enabled detailed analysis of the space-conditioning energy consumption and enabled inferences to be made about the comfort management strategies adopted by occupants. The average and the area-normalised average daily air conditioning consumption are presented in Table 4-3.

Table 4-3 Average total daily air conditioning energy consumption in each air conditioned apartment and consumption intensity, i.e. normalised by floor area.

Apartment ID	Average daily air conditioning consumption (kWh/day)				
	Overall	Winter	Spring	Summer	Autumn
1	2.03	3.00	0.46	3.35	1.43
2	0.50	0.47	0.31	0.79	0.30
3	3.98	5.52	3.11	5.01	1.51

5	1.64		1.44	1.95	1.19
6	2.75		0.59	4.61	2.80
7	2.22		2.70	2.04	1.64
Apartment ID	Area-normalised average daily air conditioning consumption (Wh/day/m <sup>2</sup> )				
	Overall	Winter	Spring	Summer	Autumn
1	43.7	57.6	8.8	64.5	27.4
2	6.0	5.1	3.4	8.6	3.3
3	45.7	58.8	33.1	53.3	16.1
5	16.1		12.0	16.3	9.9
6	24.5		4.7	37.2	22.6
7	20.8		22.7	17.2	13.8

This analysis indicated that, on average, the apartments consumed 2.2 kWh/day for air conditioning, which was almost half that of the 4.0 kWh/day reported by Ding *et al.* (2019) from a mixed cohort of recently constructed detached and multi-unit dwellings in Sydney.

Apartments #1, #3, and #6 consumed the most electricity for air conditioning overall, with marked increases of energy consumption during summer and winter, whereas Apartments #2 and #5 consumed the least overall, independent of the season. Apartment #7 was a moderate user in each season. It should be noted however that the participant in Apartment #5 reported occasionally using a portable heater for localised heating effects.

Figure 4-7 presents the average daily air conditioning usage profile in terms of average hourly energy consumption amongst the six air conditioned apartments for each month within the monitoring period.

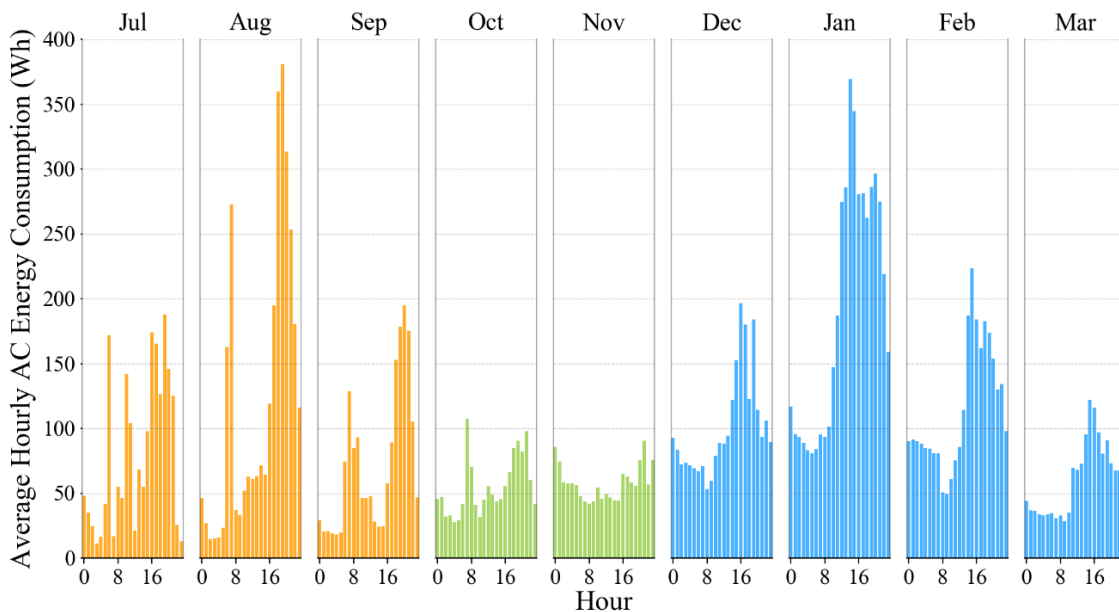


Figure 4-7 Average daily air conditioning usage profile in terms of average hourly energy consumption amongst the six air conditioned apartments for each month within the monitoring period. The colours indicate the predominant air conditioning operation for each month i.e. orange for heating only, green for mixed, and blue for cooling only.

Figure 4-7 indicates that heating dominated between July and September, cooling was dominant between December and March, and was highest in January. This figure also shows that there were both morning and evening peaks in consumption during the heating months, whilst there was a single large peak that began around midday and continued into the evening in summer. During the transitional months, the air conditioner was typically rarely operated. (It should be noted that due to the staggered commencement of the monitoring, the heating months of July, August, and September include fewer apartments than the other months.)

#### 4.3.3.1 Energy Signatures

The energy signatures for each of the air conditioned apartments are shown graphically in Figure 4-8 and the key parameter values from each of the energy signatures are presented in Table 4-4. The daily mean temperature was sourced from the nearest BOM weather station to each apartment. The solver algorithm successfully converged in each scenario, provided that the initial conditions for the balance points were within the domain of the dataset and were appropriately ordered. As Apartment #5 did not appear to use the air conditioner for heating, the energy signature regression curve was modified to have only two segments that corresponded to baseline and cooling consumption.

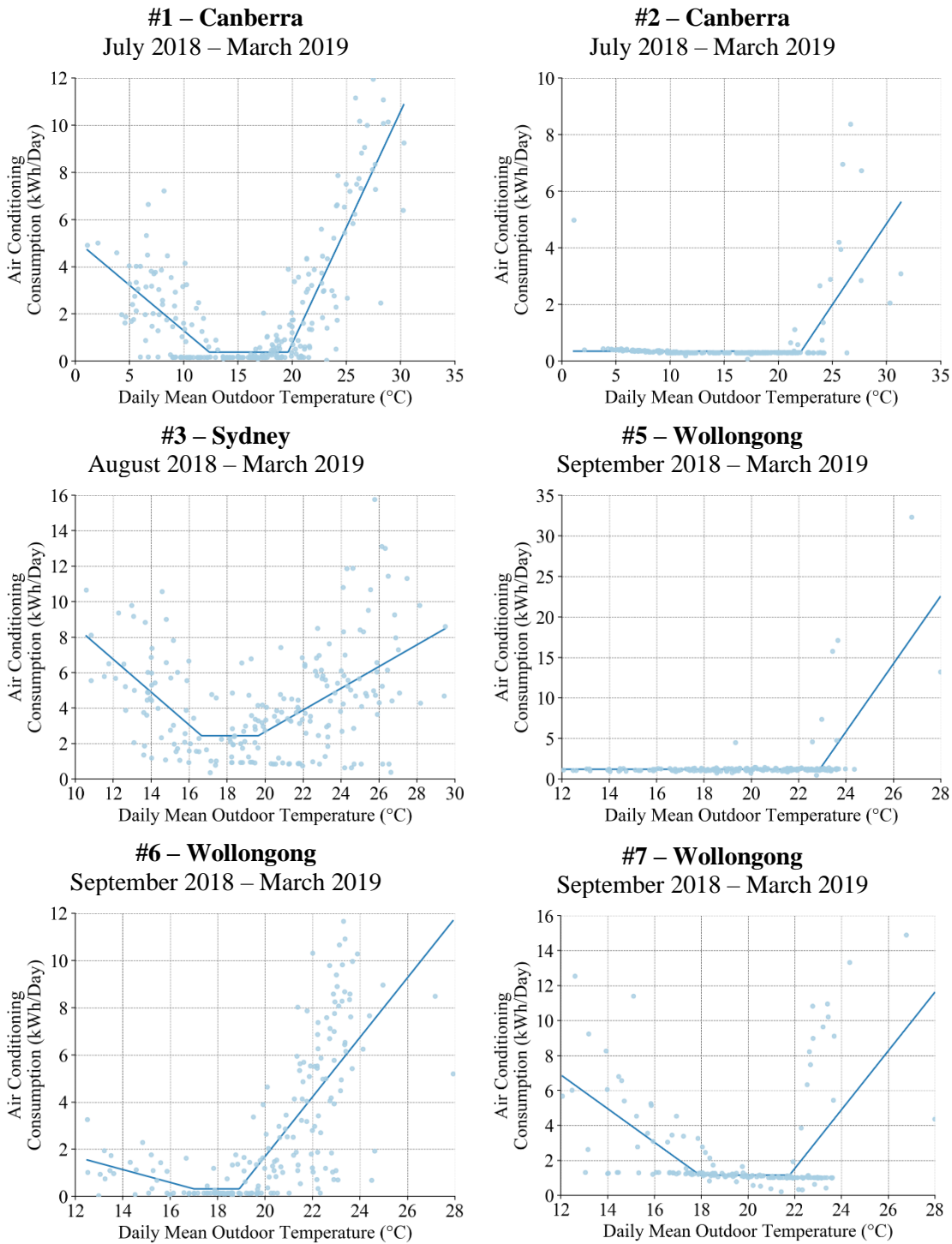


Figure 4-8 Energy Signatures for each of the monitored apartments in which air conditioning was separately monitored. Each data-point represents a day within the monitoring period and the line of best fit was determined via piecewise regression using the methodology outlined in Section 3.4.2.1.

Table 4-4 Key parameters of the energy signatures for each of the air conditioned apartments as determined using the methodology outlined in Section 3.4.2.1.

Apartment ID	Heating balance point (°C)	Cooling balance point (°C)	Baseline energy (kWh/day)	Heating curve gradient (kWh/day/°C)	Cooling curve gradient (kWh/day/°C)	Coefficient of determination (R <sup>2</sup> )
1	12.4	19.6	0.38	-0.39	0.98	0.72
2		22.1	0.35		0.57	0.45
3	16.7	19.6	2.44	-0.93	0.61	0.28
5		22.9	1.20		4.18	0.51
6	17.0	18.9	0.32	-0.27	1.26	0.56
7	17.9	21.8	1.16	-0.96	1.68	0.35
<b>Average</b>	<b>16.0</b>	<b>20.8</b>	<b>0.974</b>	<b>-0.64</b>	<b>1.55</b>	<b>0.48</b>
<b>Std. Deviation (σ)</b>	<b>2.1</b>	<b>1.5</b>	<b>0.75</b>	<b>0.3</b>	<b>1.2</b>	<b>0.15</b>

Note: Apartment #2 only once used the air conditioning for heating and Apartment #5 did not use air conditioning for heating.

Daily heating and cooling consumption correlated strongly with outdoor temperature in some apartments and moderately in others. This indicated that occupant operation of air conditioning was significantly influenced by outdoor temperature and that air conditioning use adhered to the general structure of the three-segment (or two-segment for #2 and #5) energy signatures.

#### Other Factors Influencing the Energy Signatures

Occupant thermal comfort perceptions and the number of conditioned hours were suspected to be the leading factors contributing to the unexplained variance of the energy signatures. Air conditioning operation in residential dwellings, such as the case-study apartments, are generally controlled by dwelling occupants. Thus, day to day consumption patterns and the resulting energy signatures are less consistent than those of commercial buildings, where occupants generally do not have control of the HVAC system. Fluctuations in wind and solar gains (due to cloud cover) were other potential sources of variance.

The temperature sensitivity of daily heating and cooling consumption was anticipated to be a function of total thermal transmittance of the building envelope, infiltration rate, and heat pump performance. However, due to occupant control of the HVAC system, the temperature sensitivity of daily heating and cooling consumption was also likely affected by occupant thermal perceptions, which are known to vary as a function of prevailing outdoor temperature in occupant controlled spaces (de Dear, Brager and Cooper, 1997).

The rate of increase of daily cooling consumption (i.e. the slope of the cooling segment) mildly to moderately correlated with external building envelope area, with a coefficient of determination of 0.28. While the sample size was insufficient to confirm this correlation as being more than coincidental, this finding suggests that increased cooling consumption was partially a result of

factors scaling with building envelope area. Interestingly, there was no such correlation observed for heating.

### Heating and Cooling Balance Points

The heating balance points were noticeably lower for the Apartments in Canberra relative to those in Sydney and Wollongong, which suggested some level of occupant thermal adaptation to the local climate. However, it should also be noted that the apartments in Canberra were monitored from July onwards whereas the apartments in Sydney and Wollongong were monitored from August and September, respectively.

The cooling balance points were lowest in the three apartments with the greatest total air conditioning consumption, i.e. #1, #3, and #6, as shown in Table 4-3. This suggests that heavy users of air conditioning have a propensity to use air conditioning at cooler daily mean outdoor temperatures than light and moderate users or air conditioning rather than explicitly using air conditioning more frequently above temperatures at which air conditioning is more commonly operated.

### Baseline Segment

One would expect that daily air conditioning consumption between the two balance points would: a) effectively only be standby consumption; and b) be relatively independent of the daily mean outdoor temperature.

The first expectation was met in Apartments #2, #5, and #7, in which the baseline energy consumption indicated from the energy signature was within 4% of the daily average standby consumption. On the other hand, the baseline energy consumptions from the energy signatures of Apartments #1, #3, and #6 were 170%, 408%, and 375% greater than their corresponding daily average standby consumptions. This indicated that air conditioning was still used between the two balance points, albeit to a lesser extent than in the temperature ranges outside the balance points.

However, despite air conditioning being used between the two balance points in half of the apartments, daily air conditioning consumption between the balance points nonetheless remained relatively independent of the daily mean outdoor temperature. The impact of constraining the gradient of the central, baseline segment to zero only reduced the average coefficient of determination between daily air conditioning consumption and daily outdoor temperature relative to the unconstrained piecewise linear regression line of best fit by 0.9%. The largest change occurred in Apartment #6, in which the correlation reduced by 4.7%, whereas the average reduction in correlation of the remaining apartments was less than 0.5%.

### 4.3.3.2 Standby Air Conditioning Energy Consumption

The air conditioning energy consumption was separated into standby and active consumption using an energy consumption threshold method, which is described in Section 3.4.2.2. The active and standby consumption in each air conditioned apartment for each season is presented in Figure 4-9.

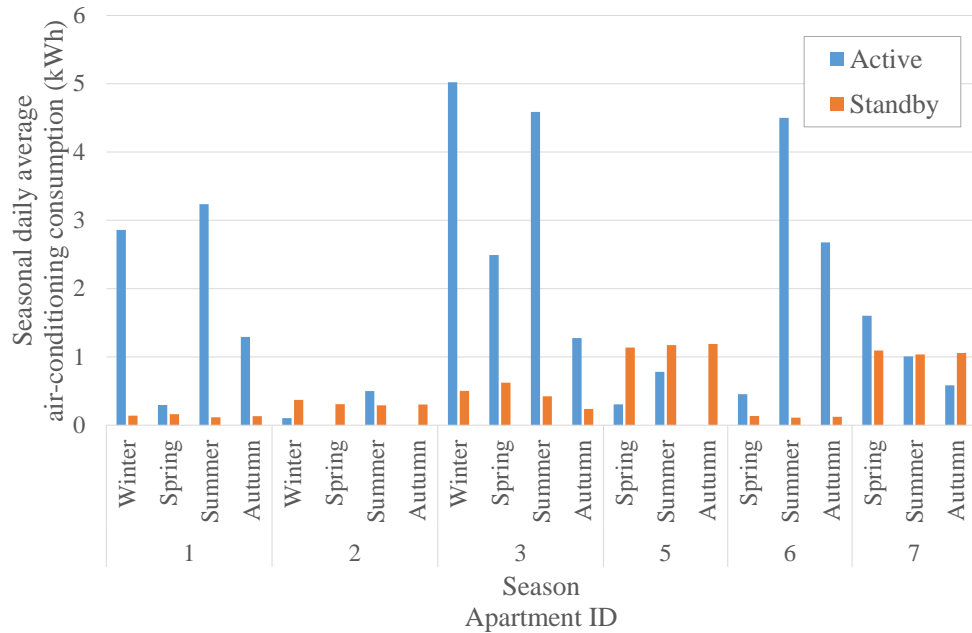


*Figure 4-9 Seasonal daily average air conditioning consumption for standby and active consumption in each of the monitored apartments with independently monitored reverse-cycle air conditioning.*

The average energy consumption in standby operation was 0.55 kWh/day. On average, wall-mounted split systems consumed 0.14 kWh/day, whereas larger, ducted split systems consumed 0.90 kWh/day in standby operation. Standby consumption was generally independent of the season for each apartment. However, in Apartment #2 it was observed that standby power consumption was greater in winter, which was likely due to thermostatic actuation of the crankcase heater. Initially, it appeared that standby consumption of the air conditioning system of Apartment #3 decreased in autumn, however, this apparent decrease was due to an air conditioning system malfunction/disconnection from the 12<sup>th</sup> March 2018 until after the cessation of monitoring, as reported by the participant.



*Table 4-5 Proportion of time that the air conditioner was actively conditioning each apartment in each season, and overall throughout the monitoring period.*

<b>Apartment ID</b>	<b>Winter</b>	<b>Spring</b>	<b>Summer</b>	<b>Autumn</b>	<b>Overall</b>
1	19.9%	2.8%	30.6%	19.8%	17.6%
2	0.5%	0.0%	3.8%	0.0%	1.4%
3	23.5%	22.3%	43.5%	14.7%	29.7%
5		0.6%	1.1%	0.0%	0.7%
6		3.7%	26.7%	20.1%	16.7%
7		13.1%	2.4%	1.3%	6.2%
Overall	13.6%	7.2%	18.0%	9.1%	12.4%

The standby consumption was below 10% of the total consumption in winter and summer and was, on average, 26% of the total consumption in spring in Apartments #1, #3, and #6. For Apartments #2, #5, and #7, which used air conditioning more sparingly, the standby consumption was more significant. The standby consumption accounted for 100% and 79% of the air conditioning consumption in spring for Apartments #2 and #5, respectively, and accounted for 100% of the air conditioning consumption in autumn for both of the aforementioned apartments. This indicated significant potential for reduced energy consumption by switching the air conditioner off completely in the shoulder seasons. However, doing so could lead to lubrication issues or damage to the compressor if the air conditioner is actively operated without allowing adequate time in standby operation to reverse any refrigerant migration that may have occurred while the system was switched off (Marchese, 2005; Tomczyk, 2018; Han, Yan and Yu, 2019).

#### 4.3.3.3 Heating and Cooling Classification Algorithms

The classification of air conditioning energy consumption as active vs standby consumption was further refined by using several different rule-based methods and algorithms that classified most likely air conditioning operating modes against particular observed parameters, as described in Section 3.4.2.3. Comparisons of the distribution of heating and cooling use determined using the score-based method and the three single rule-based methods are presented in Figure 4-11.

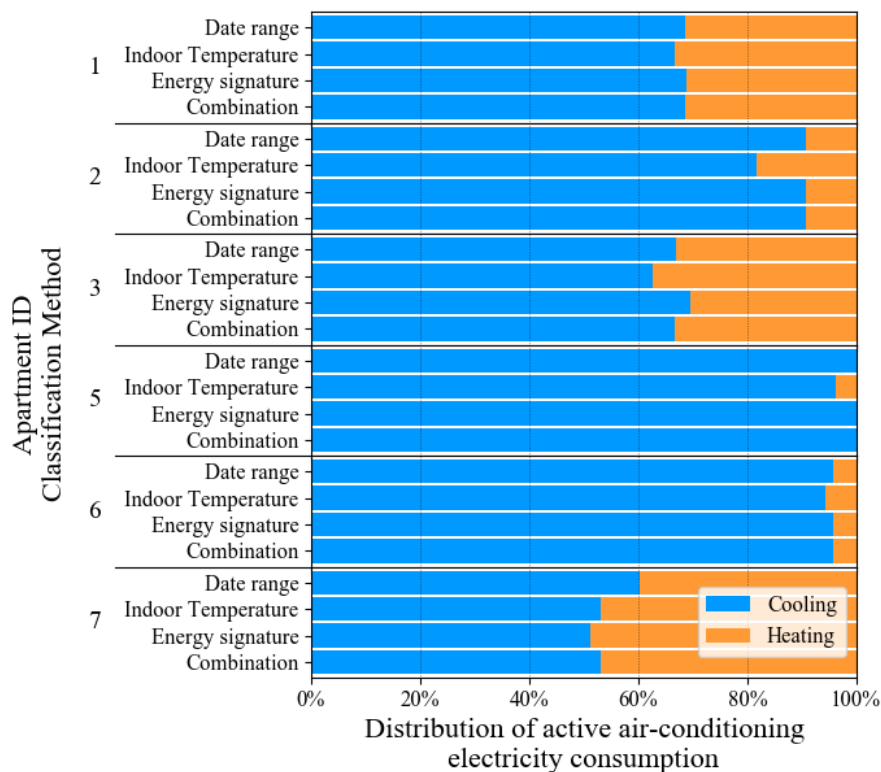


Figure 4-10 Distribution of air conditioning operating modes in terms of electricity consumption using four different classification methods/algorithms.

The score-based classification method (presented as “Combination” in Figure 4-10) was considered to be the most accurate method as it addressed the limitations of the three rule-based methods described in Section 3.4.2.3.

Using the score-based method, on average 25.8% of the air conditioning energy consumption while active was used for heating and 74.2% was used for cooling. In comparison, the date range and energy signature modes allocated an additional 1.2% and 0.9% towards cooling, respectively, whereas the indoor temperature method allocated an additional 1.4% towards heating. Thus, the energy signature date range method most closely aligned with the score-based classification method, followed closely by the date range method.

As mentioned in the methodology in Section 3.4.2.3, the overestimation of heating consumption using the indoor temperature method was caused by adopting the assumption that the thermal output of the air conditioner always dominated the heat-transfer processes in the zone. In reality, there were multiple occasions when the indoor temperature increased slightly during use events in which the air conditioner was operating at moderate output on hot days with outdoor temperatures above 25°C. Examination of environmental parameters indicated that heating was very unlikely to be in use during such periods. Alternatively, it was considered to be likely that cooling was in use, but was not providing sufficient cooling to counteract excessive thermal gains. On the other hand, the heating consumption was underestimated from the date range and energy

signature methods by not considering the use of heating during cool mornings of otherwise warm days during mid-to-late spring.

The score-based method has been used on all subsequent analyses involving air conditioning use that has been classified as either heating or cooling.

#### 4.3.4 Summary of Air-Conditioning Energy Consumption Findings

Using the methods described above, the energy consumption of the reverse-cycle air conditioners was able to be classified into periods of standby operation, heating operation, and cooling operation. The resulting distribution and daily average air conditioning consumption in each operating mode is presented in Figure 4-11.

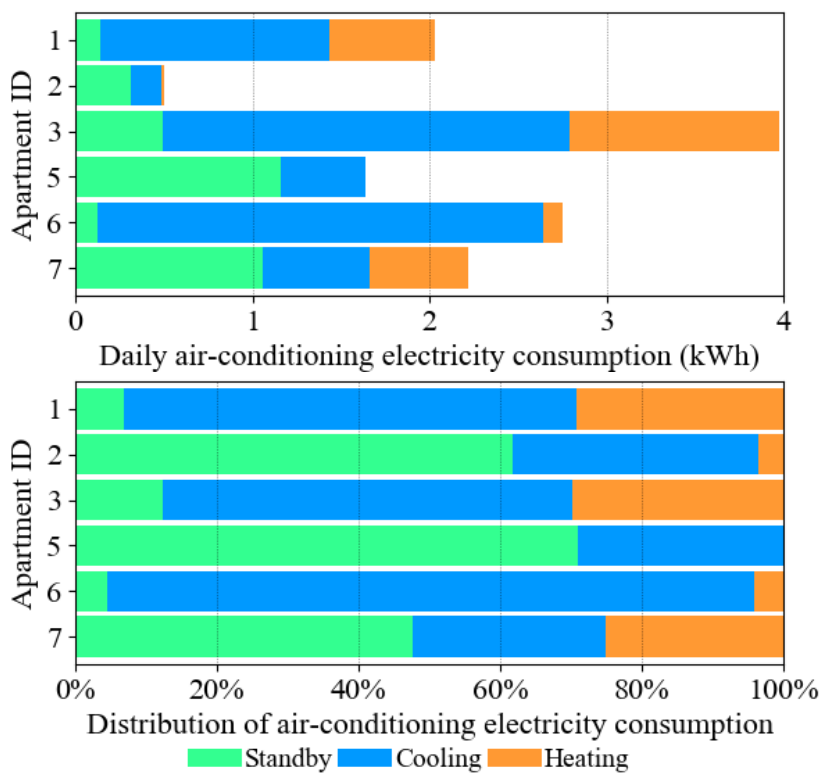


*Figure 4-11 Daily average air conditioning energy consumption for each apartment as a function of operating mode, and the proportion of the air conditioning energy consumption used in each operating mode.*

In addition, the energy signatures generated for each apartment using piecewise linear regression revealed values of the statistically significant daily mean outdoor temperatures below and above that heating and cooling were typically in operation. Furthermore, the energy signatures expressed the rate of change of energy consumption with respect to outdoor temperature beyond these temperature thresholds.

This classification enabled further analysis into occupant behavioural responses to various indoor and outdoor parameters, examined in Section 4.5 and enabled comparison of the thermal energy

consumption, when calculated using the coefficient of performance (COP) and energy efficiency ratio (EER), with the simulated energy consumption of the apartments, examined in Chapter 5.

## 4.4 Thermal Conditions

The measured indoor thermal conditions and the resulting thermal comfort perceptions predicted from widely used thermal comfort models have been assessed for the periods when the apartments were occupied. Only occupied periods during the monitoring periods were included in the thermal comfort analysis. The occupancy status of each apartment was determined using the methods presented in Section 3.9.

### 4.4.1 Indoor Air Temperature

A summary of the average hourly indoor air temperatures during occupied periods in the living rooms and bedrooms of each of the monitored apartments over summer, between 1<sup>st</sup> December 2018 and 28<sup>th</sup> February 2019, is shown in Figure 4-12.

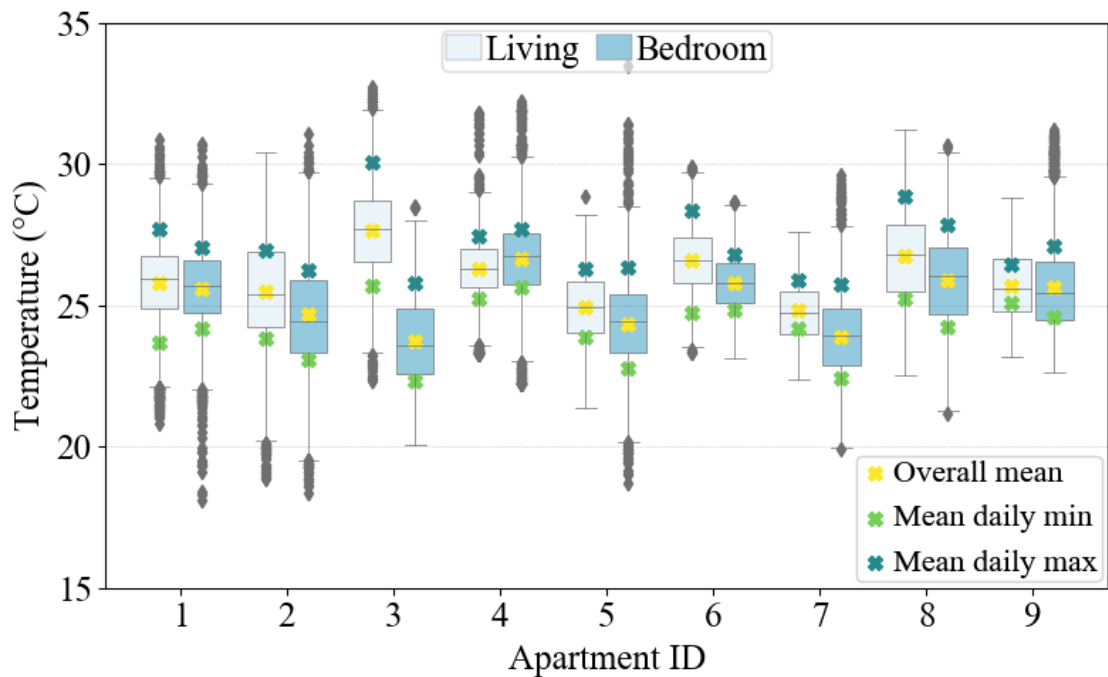


Figure 4-12 Box plot of the average hourly indoor air temperature data measured in the living rooms (left) and bedrooms (right) of the nine case study apartments in summer (01/12/2018 – 28/02/2019) during occupied periods. The chart also shows the overall mean, mean daily minimum, and mean daily maximum temperatures measured in each apartment.

Overall, there were only slight differences between the living room and bedroom temperatures during summer. Generally, the living rooms were slightly warmer than the bedrooms. The mean temperatures of the living rooms and bedrooms in summer were 26.0°C and 25.1°C, respectively.

The interquartile temperatures ranges spanned from 25.1°C to 27.0°C in the living rooms, and 24.1 to 26.1°C in the bedrooms.

However, the total temperature range experienced in the apartments was considerably broader; the average temperature range in the living rooms and bedrooms were 8.3°C and 10.2°C, respectively, i.e. 4.3 and 5.0 times broader than the interquartile ranges. The average maximum temperature in the bedrooms was 0.5°C warmer than in the living rooms, whereas the average minimum temperature in the bedrooms was 0.5°C cooler than in the living rooms, indicating that the indoor temperature in the bedroom varied over a broader range than the living room. Generally, the living rooms were more likely to be occupied during the warmest part of the day, and there was therefore likely to be less consideration about the indoor thermal conditions of the bedroom at these times of the day. Conversely, near the coolest times of the day, the bedroom was more likely to be occupied, and the bedrooms would be more likely to be cooled than the living room by using either natural ventilation or zoned air conditioning if available.

The most substantial difference between the living room and bedrooms in summer was observed in Apartment #3, in which the mean temperature of the bedroom was 4.0°C cooler than in the living room. This was hypothesised to be due to frequent use of zoned air conditioning and cooler thermostat settings in the bedroom compared to the living room. This hypothesis is supported by data presented in Section 4.5.2, in which heating and cooling on and off events in the living room and bedroom are presented. The temperature difference between the bedroom and living was also likely enhanced by thermal stratification and additional thermal gains through the ceiling due to the living room being located on the top floor and the bedroom on the bottom floor of the two-storey apartment.

A summary of the average hourly indoor air temperatures during occupied periods in the living rooms and bedrooms of each of the apartments in winter, is shown in Figure 4-13.

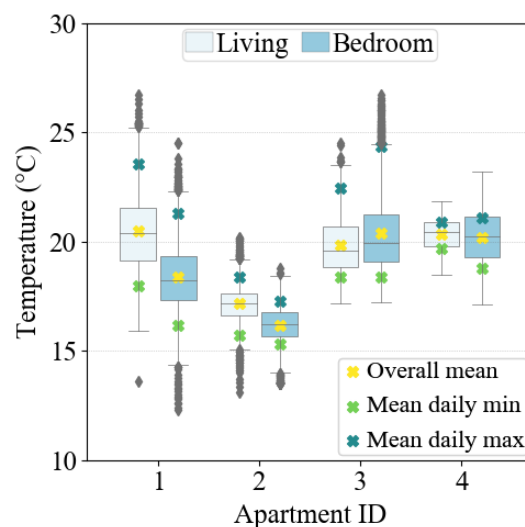


Figure 4-13 Box plots of the average hourly indoor air temperatures measured in the living rooms (left) and bedrooms (right) of the four case-study apartments that were monitored during winter. The chart also shows the overall mean, mean daily minimum, and mean daily maximum temperatures measured in each apartment.

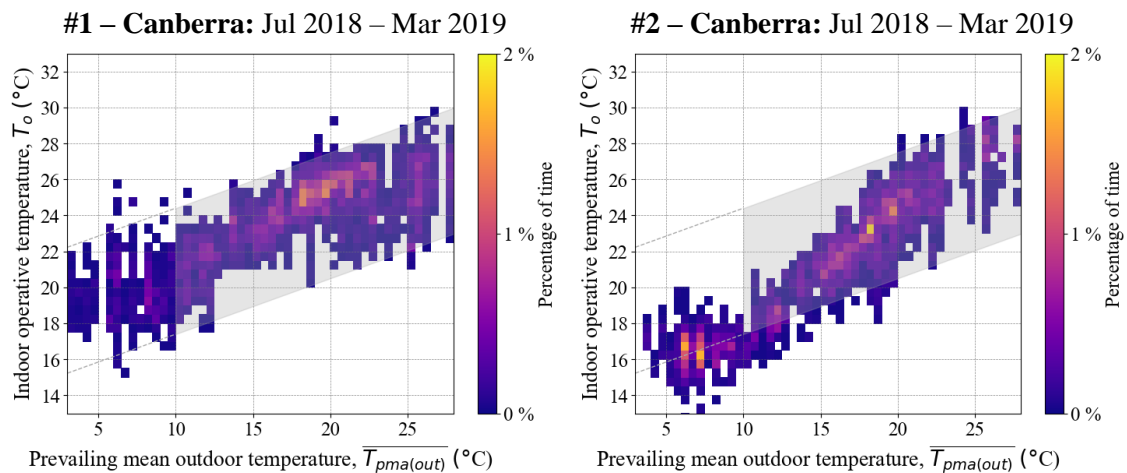
The average mean living room and bedroom temperatures during winter were 19.5°C and 18.8°C, respectively. The living rooms were thought to be warmer than the bedrooms for multiple reasons:

- The air conditioning system outlets in Apartments #1 and #4 were exclusively located in the living room;
- The window orientations in Apartments #1 and #2 led to higher solar gains in the living room than in the bedroom; and
- There were more appliances including heat generating kitchen appliances (kettles, ovens, and stoves) located in the living rooms than in the bedrooms.

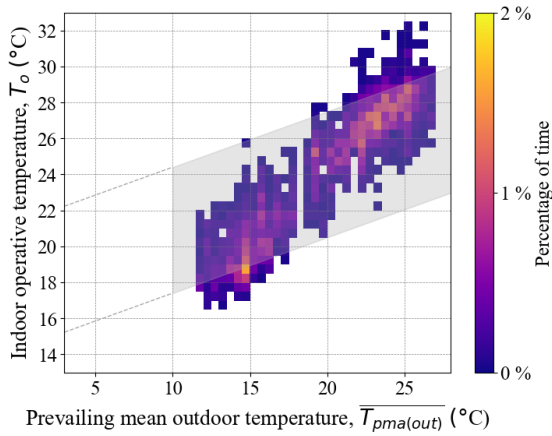
One significant observation was that Apartment #2 was below 18°C for more than 75% of the occupied periods during winter. The World Health Organisation (WHO) suggests that indoor temperatures below 18°C introduce health risks to individuals, particularly infants and the elderly (World Health Organization, 1987), although none of the regular occupants of Apartment #2 belonged to either of these vulnerable groups. Nevertheless, the indoor temperatures in Apartment #2 remained above 13°C without the use of heating despite numerous days where mean outdoor temperatures were below 5°C. It is possible that Apartment #2 was being heated by neighbouring apartments indirectly. Previous studies (e.g. Moeller *et al.* (2020)) have shown that internal heat transfers triggered by temperature differences between neighbouring apartments can be significant.

#### 4.4.2 Adaptive Thermal Comfort Model

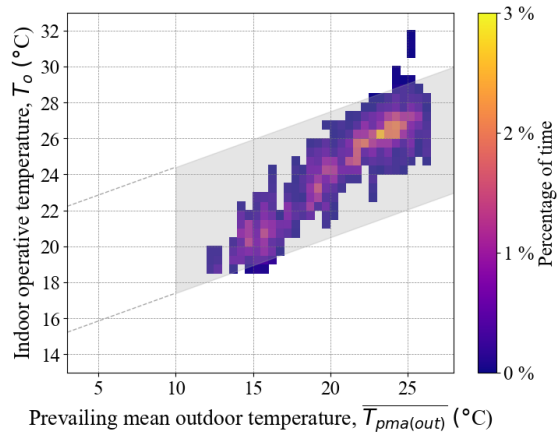
Figure 4-14 presents the indoor operative temperatures measured in the living room of each apartment during occupied hours as a function of the prevailing daily mean outdoor temperature. The 80% acceptability limits of the adaptive model from ASHRAE Standard 55-2017 have also been indicated on each chart.



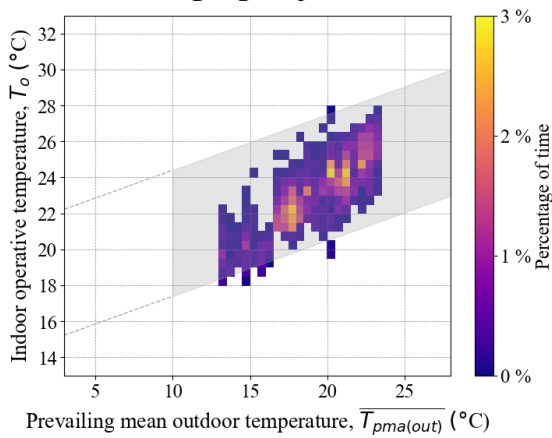
**#3 – Sydney: Aug 2018 – Mar 2019**



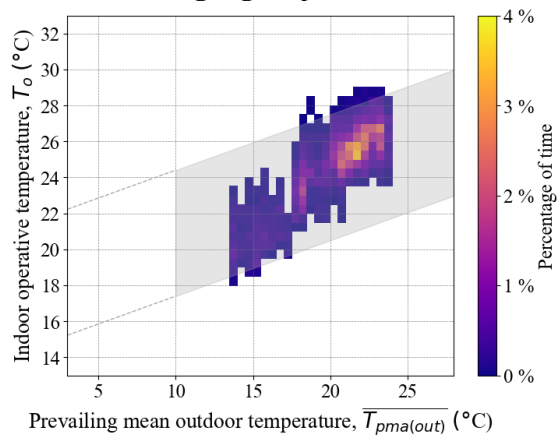
**#4 – Sydney: Aug 2018 – Mar 2019**



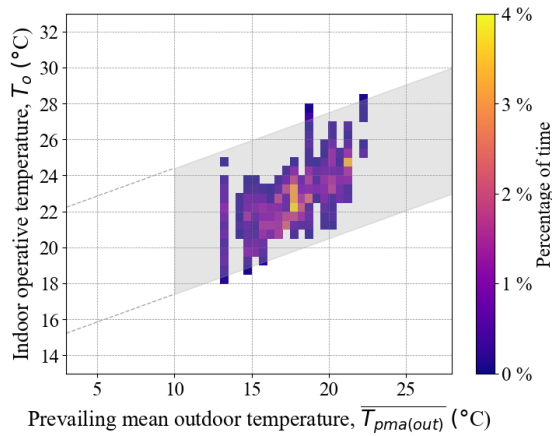
**#5 – Wollongong: Sep 2018 – Mar 2019**



**#6 – Wollongong: Sep 2018 – Mar 2019**



**#7 – Wollongong: Sep 2018 – Mar 2019**



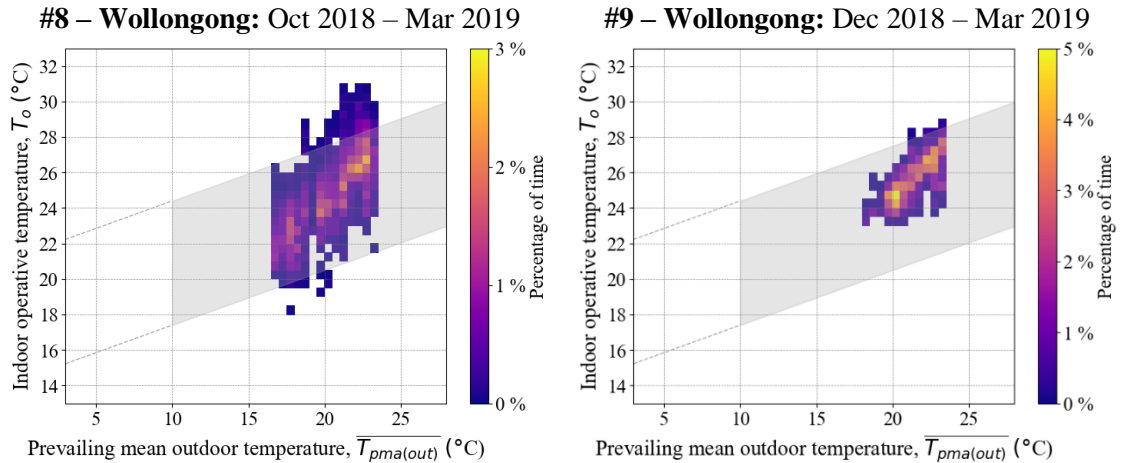


Figure 4-14 Hourly indoor operative temperature measured in the living room during occupied hours against the prevailing daily mean outdoor temperature. The 80% acceptability limits defined by the adaptive model from ASHRAE Standard 55-2017 is shown in grey.

The exceedance rates during occupied periods determined using the adaptive thermal comfort model from ASHRAE Standard 55-2017 are presented in Table 4-6.

Table 4-6 Seasonal exceedance hours determined using the adaptive model and expressed as a fraction of the total occupied hours.

Season	Apartment ID	Living		Bedroom	
		80% Acceptability Limits		80% Acceptability Limits	
		Below	Above	Below	Above
Winter	1	1.52%	4.26%	8.26%	0.11%
	2	47.76%	0.00%	58.82%	0.00%
	3	37.85%	0.00%	9.56%	0.6%
	4	0.00%	0.00%	11.14%	0.00%
	<b>Average</b>	<b>21.78%</b>	<b>1.06%</b>	<b>21.94%</b>	<b>0.18%</b>
Spring	1	0.38%	0.31%	8.53%	0.00%
	2	19.02%	0.00%	42.69%	0.00%
	3	4.72%	0.47%	4.26%	0.00%
	4	1.25%	0.00%	15.64%	0.28%
	5	1.78%	0.00%	11.15%	0.07%
	6	1.59%	0.18%	0.21%	0.21%
	7	0.21%	0.53%	11.27%	1.11%
	8	1.28%	1.05%	0.12%	0.82%
<b>Average</b>	<b>3.78%</b>	<b>0.32%</b>	<b>11.73%</b>	<b>0.31%</b>	
Summer	1	0.66%	0.66%	0.17%	0.46%
	2	0.97%	0.88%	1.19%	1.66%
	3	0.00%	11.24%	5.04%	0.00%
	4	0.00%	0.5%	0.00%	3.81%
	5	0.00%	0.08%	1.18%	0.75%
	6	0.00%	1.7%	0.00%	0.2%
	7	0.00%	0.00%	1.94%	0.62%
	8	0.00%	11.97%	0.00%	8.34%
	9	0.00%	0.8%	0.00%	5.53%
<b>Average</b>	<b>0.18%</b>	<b>3.09%</b>	<b>1.06%</b>	<b>2.37%</b>	



Using the adaptive model criteria, the thermal conditions in the apartments were thermally satisfactory for the majority of the monitoring period. The average fraction of occupied hours within the 80% acceptability limits amongst the cohort were 77.5% and 96.6%, in winter and summer, respectively. However, there were several notable exceedances that occurred in apartments #2, #3, and #8.

Apartment #2 had the highest exceedance rate in winter and spring. This was attributed to Apartment #2 having the least mechanical heating in winter amongst the cohort, in combination with being located in Canberra, which was the coldest climate zone within this study. By way of comparison, living room temperatures in Apartment #1 (also located in Canberra) were maintained above the lower 80% acceptability limits for 98.5% of the occupied hours in winter, but Apartment #1 used 36 times the area-normalised heating consumption in winter compared to Apartment #2. This highlights that significant heating energy is likely to be required to maintain thermal comfort in apartments such as these, i.e. built to NCC standards in Canberra. Despite the high exceedance rates measured during occupied periods in Apartment #2, it should be noted that clothing levels were not monitored in this study. While the adaptive thermal comfort model assessments are valid for occupant clothing level adaptations between a range at least as wide as 0.5 to 1.0 clo, it is possible that occupants wore clothing ensembles above this range, which would attenuate the exceedance rates to some extent. For reference 1.0 clo is approximately equivalent to long-sleeve pyjama tops, long pyjama trousers, a short ¾-length robe, and slippers without socks.

Apartment #8 had the largest exceedance rate in summer, where air conditioning was not present. However, similar exceedance rates were not observed in Apartment #9, which was also exclusively naturally ventilated and located in the same apartment building. The difference in exceedance rates between the two apartments was thought to be caused by the different orientations of the apartments; #8 was oriented towards the west and therefore received excessive solar gains during the afternoon, whereas #9 was oriented towards the south-east and was shaded for a much greater proportion of the day.

Large exceedance rates also occurred in the living room of Apartment #3 during winter and summer. However, similar exceedance rates were not reproduced in the bedroom. This was thought to have been caused by the use of zoned air conditioning to maintain a stringent range of comfortable conditions in the bedroom, as indicated by the highest use of both heating and cooling amongst the cohort. This is explored further in Section 4.5.2.

Occupants in this study generally, and in Apartments #2 and #3 in particular, frequently experienced indoor conditions that were cooler than the 80% acceptability limits defined by the adaptive comfort model in ASHRAE Standard 55-2017. However, a revised adaptive comfort

model developed by De Dear, Kim, and Parkinson (2018) from observations within residential dwellings in Sydney and Wollongong suggests that residential occupants are more tolerant of cooler temperatures than predicted using conventional comfort standards developed from studies of commercial buildings. Assessing the thermal conditions using the revised adaptive comfort model reduced the average exceedance rate in winter from 22.5% to 1.26%, but increased the average exceedance rate in summer from 3.35% to 13.0%.

ASHRAE Standard-55 2017 stipulates that both the adaptive model and PMV model are unable to evaluate thermal comfort from indoor conditions for occupants who were using blankets or otherwise in contact with bedding. To ensure the exceedances of the 80% acceptability limits reported in Table 4-6 were not disproportionately affected by periods when occupants were in contact with bedding, the exceedances were recalculated for occupied hours between 07:00am and 10:00pm, i.e. when occupants were significantly less likely to be in contact with bedding. The average difference in the exceedance rates calculated for occupied hours between 07:00am to 10:00pm and those calculated for all occupied hours across all monitored apartments was less than 2.5% in each season. Therefore, exceedance hours presented in this study were not disproportionately comprised of periods when occupants were in contact with bedding.

## 4.5 Occupant Behaviour

### 4.5.1 Air Conditioning and Natural Ventilation use

The logistic regression curves for the combined dataset from all the monitored mixed-mode apartments is presented in Figure 4-15 and the individual logistic regression curves for each apartment are presented in Figure 4-16. The parameter coefficients and key metrics for each of the logistic regression models for natural ventilation, cooling, and heating are shown in Table 4-7, Table 4-8, and Table 4-9, respectively. Note that natural ventilation use includes windows and sliding doors i.e. openings to the balcony. The two ventilation openings monitored in each apartment are shown on the floor plans presented in Appendix A.

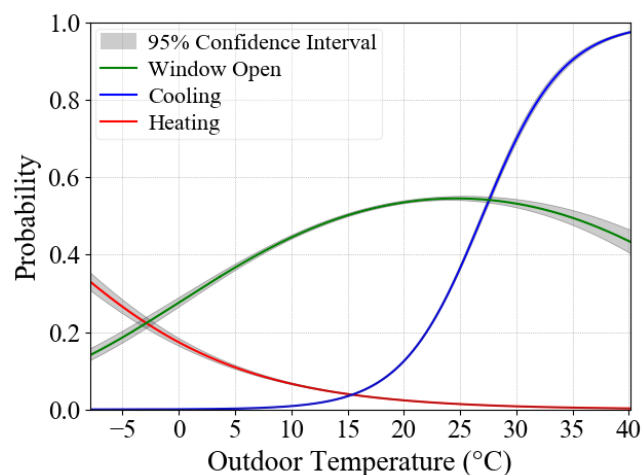
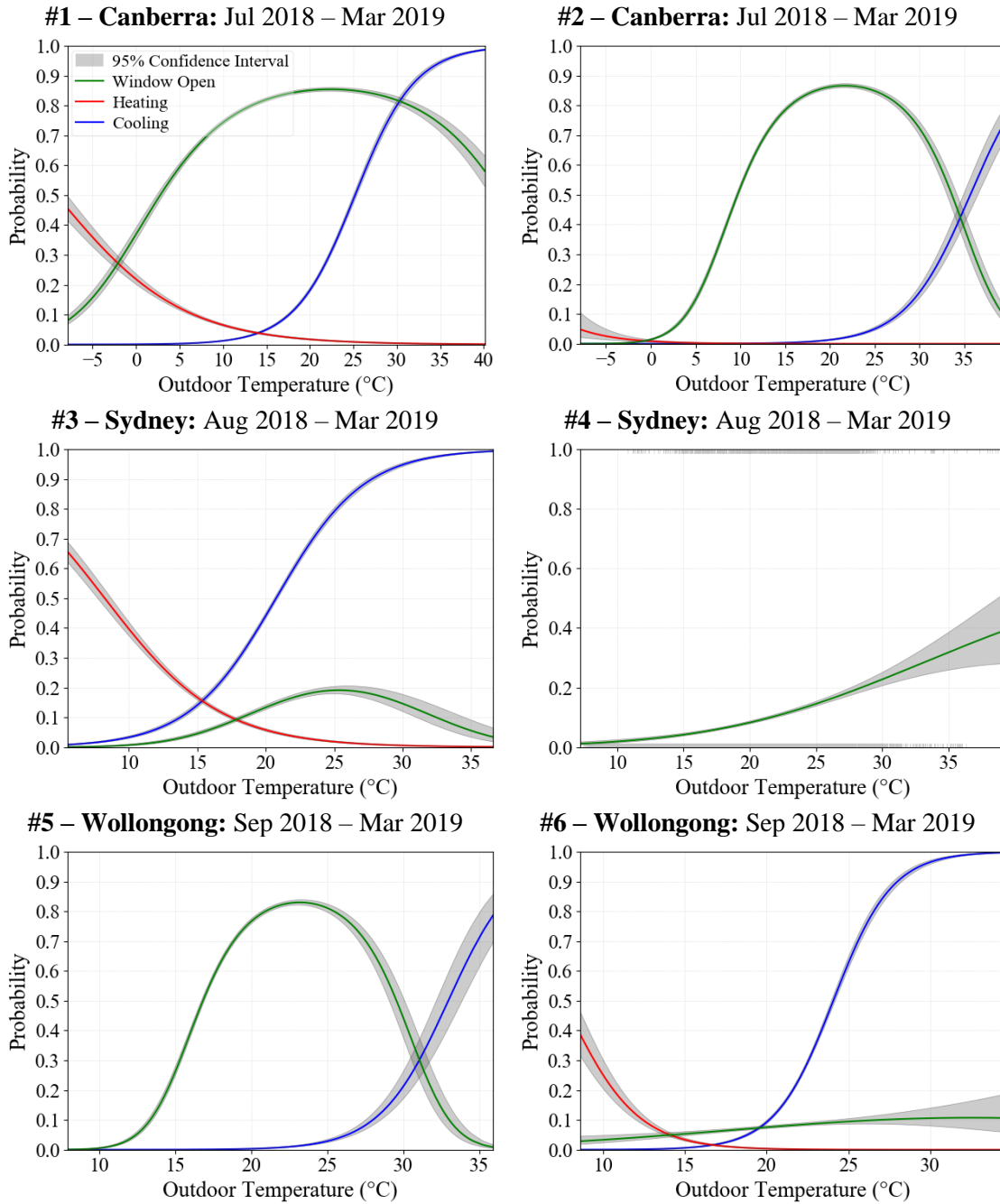
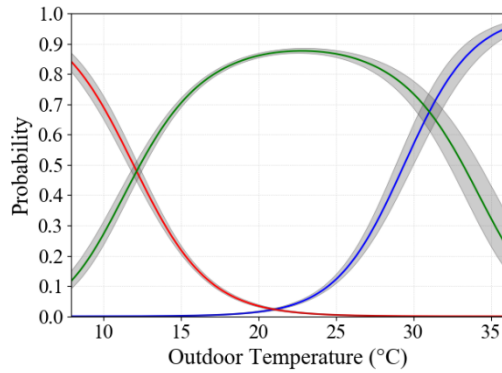


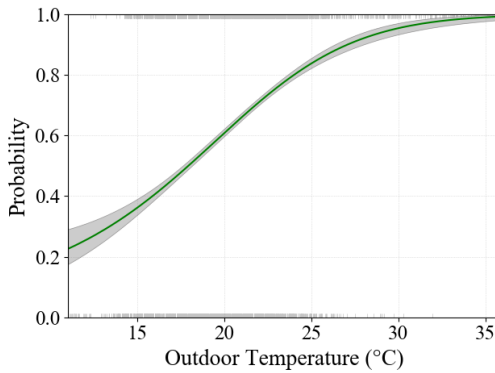
Figure 4-15 Probability of heating, cooling, and window operation as a function of outdoor temperature, determined using logistic regression. The data used in the above plots included all occupied hours within the monitoring periods for the six mixed-mode conditioned apartments.



#7 – Wollongong: Sep 2018 – Mar 2019



#8 – Wollongong: Oct 2018 – Mar 2019



#9 – Wollongong: Dec 2018 – Mar 2019

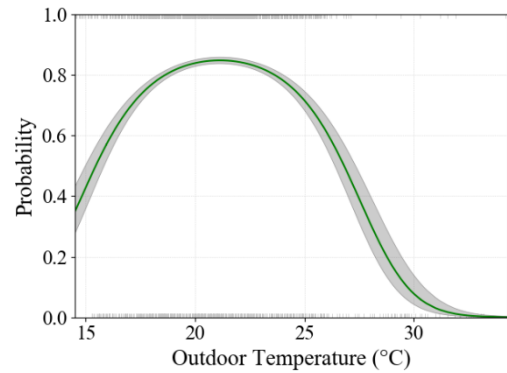


Figure 4-16 Probabilities of heating, cooling, and window operation during occupied hours as a function of outdoor temperature, determined using logistic regression. Note that Apartments #8 and #9 did not have air conditioning. While Apartment #4 did have air conditioning this was not individually monitored.

Table 4-7 Logistic regression modelling results for natural ventilation using outdoor temperature as the independent variable.

Apartment ID	$\beta_0$ Constant term (Intercept)	$\beta_1$ Coefficient ( $T_{out}$ )	$\beta_2$ Coefficient ( $T_{out}^2$ )	Likelihood Ratio Test ( $\chi^2$ )	McFadden's pseudo $R^2$ ( $\rho^2$ )	Area Under ROC (AUC)
1	-0.536*	0.206*	-0.0046*	1600*	0.075	0.67
2	-4.25*	0.565*	-0.0131*	6300*	0.270	0.83
3	-11.1*	0.759*	-0.0150*	592*	0.066	0.67
4	-5.84*	0.207*	-0.00180***	495*	0.046	0.66
5	-19.5*	1.81*	-0.0391*	3600*	0.190	0.77
6	-4.74*	0.161***	-0.0025	45*	0.0053	0.53
7	-7.41*	0.823*	-0.0181*	649*	0.071	0.76
8	-2.43**	0.0656	0.0039	848*	0.069	0.67
8 (linear)	-3.96*	0.221*		844*	0.069	0.67
9	-22.1*	2.26*	-0.0534*	268*	0.047	0.62
All mixed-mode apartments	-0.963***	0.0929**	-0.00190*	1260*	0.010	0.54

\*  $p$ -value < 0.001; \*\*  $p$ -value < 0.01; \*\*\*  $p$ -value < 0.05

Table 4-8 Logistic regression modelling results for cooling using outdoor temperature as the independent variable.

Apartment ID	$\beta_0$ Constant term (Intercept)	$\beta_1$ Coefficient ( $T_{out}$ )	Likelihood Ratio Test ( $\chi^2$ )	McFadden's pseudo $R^2$ ( $\rho^2$ )	Area Under ROC (AUC)
1	-7.29*	0.289*	7340*	0.417	0.909
2	-9.87*	0.277*	1100*	0.345	0.933
3	-6.51*	0.314*	4170*	0.242	0.815
5	-14.6*	0.443*	473*	0.303	0.863
6	-13.5*	0.561*	3700*	0.242	0.851
7	-13.2*	0.45*	822*	0.29	0.863
All mixed-mode apartments	-7.53*	0.279*	16400*	0.228	0.830

\*  $p$ -value < 0.001; \*\*  $p$ -value < 0.01; \*\*\* $p$ -value < 0.05

Table 4-9 Logistic regression modelling results for heating using outdoor temperature as the independent variable.

Apartment ID	$\beta_0$ Constant term (Intercept)	$\beta_1$ Coefficient ( $T_{out}$ )	Likelihood Ratio Test ( $\chi^2$ )	McFadden's pseudo $R^2$ ( $\rho^2$ )	Area Under ROC (AUC)
1	-1.27*	-0.139*	1020*	0.128	0.806
2	-4.78*	-0.229*	54.8*	0.156	0.912
3	1.96*	-0.238*	1390*	0.161	0.811
6	3.46*	-0.455*	475*	0.24	0.927
7	4.95*	-0.415*	1350*	0.244	0.891
All mixed-mode apartments	-1.56*	-0.108*	1950*	0.0677	0.773

\*  $p$ -value < 0.001; \*\*  $p$ -value < 0.01; \*\*\* $p$ -value < 0.05

#### 4.5.1.1 Model Efficacy

While both air conditioning use and natural ventilation use exhibited stochastic variations resulting from different occupant behaviours, the logistic regression models developed for heating and cooling correlated occupant behaviours more successfully than those for natural ventilation. This was indicated by the larger average McFadden's  $R^2$  values of 0.28 and 0.19 for cooling and heating, respectively, compared with 0.09 for natural ventilation. This demonstrated that there was less variance in occupant use of air conditioning than use of natural ventilation as a function of outdoor temperature. This may be because, unlike air conditioning, windows are operated for many functions besides just thermal comfort such as to regulate fresh air, sound, odour, or moisture transfer through the envelope and for security, privacy, or accessibility, such as in the case of balcony sliding doors (Nicol, Humphreys and Olesen, 2004; Haldi and Robinson, 2008; Kim *et al.*, 2017; Park and Choi, 2019). In addition, the area under of the curve (AUC) of the Receiver-Operator Curve (ROC) of 0.87 for both heating and cooling and 0.69 for natural ventilation indicated that air conditioning “on” and “off” states occurred at more distinct

temperature ranges with a higher degree of separation than the “open” and “closed” states for windows.

The logistic regression models for heating, cooling, and natural ventilation based on the aggregated occupant responses across all mixed-mode ventilated apartments, are shown graphically in Figure 4-15. These were less useful predictors of occupant behaviour than the models developed from observations within individual apartments. This was particularly apparent for the model developed for natural ventilation, which had very low predictive accuracy, with a  $\rho^2$  of 0.01 and an AUC of 0.54. This was primarily due to conflicting individual natural ventilation usage patterns amongst the cohort, which can be observed from the individual charts in Figure 4-16, indicating that occupant use of natural ventilation was not consistent throughout the cohort. This is examined further in Section 4.5.1.2. In comparison, heating and cooling use was more consistent across the cohort, although there were still noticeable variations between apartments. Nonetheless, the fits of all three aggregated models were still statistically significantly better than those of the null model (i.e. the model without any independent predictor variables).

#### 4.5.1.2 Natural Ventilation

For the majority of apartments (#1, #2, #5, #7, and #9), natural ventilation use patterns followed the expected second-order polynomial relationship with outdoor temperature postulated and observed by Kim *et al.* (2017), in which windows were highly likely open at moderate outdoor temperature ranges and were closed as outdoor temperatures deviated towards less comfortable weather conditions. In such apartments, the maximum likelihood of at least one of the windows being open was 86%, which occurred at 22.2°C, and at least one window was more than 50% likely to be open between 11.4°C and 33.0°C. The widest operating range of natural ventilation was observed in Apartments #1 and #2 in Canberra, which, like the energy signatures in Section 4.3.3.1, was postulated to indicate occupant adaption to the more extreme local climate in Canberra relative to Sydney or Wollongong.

However, very low usage of natural ventilation was observed in three of the apartments with air conditioning (i.e. #3, #4, and #6). It was clear that occupants in Apartment #3 and Apartment #6 preferred to use air conditioning rather than natural ventilation to cool their apartments. In these two apartments the monitored windows were never more than 20% likely to be open regardless of outdoor temperature and cooling was more likely to be in operation than windows to be open above outdoor temperatures of 20°C. Reasons for low use of natural ventilation in Apartment #4 could not be determined as air conditioning was not independently monitored.

The most unusual window usage pattern was observed in Apartment #8, which was one of the two apartments without air conditioning. The likelihood of at least one window being open in Apartment #8 significantly increased monotonically with increasing outdoor temperature. While

both the linear and quadratic outdoor temperature coefficients were statistically insignificant in the second-order model, in particular the quadratic coefficient, a linear model with the quadratic term removed confirmed that outdoor temperature was a significant predictor of window use in Apartment #8. As discussed in Section 4.4, Apartment #8 was the least comfortable apartment during summer. Thus, it is thought that despite the high outdoor air temperatures, occupant(s) of Apartment #8 were attempting to generate cross-flow ventilation in an attempt to attain some level of thermal comfort in the apartment. (Increased air velocity from cross flow would of course lead to increased comfort, but potentially increase outdoor air temperature). This is supported by an anecdote provided by one of the occupants of Apartment #8 who stated that they often left the apartment entrance door to the corridor open to aid in generating cross-flow ventilation. This behaviour directly contrasts with Apartment #9, the other apartment without air conditioning, in which occupants preferred to minimise natural ventilation when outdoor temperatures were above thermally acceptable thresholds.

Another observation of window use during the home visits was that bathrooms with external windows were often left ajar by occupants; most likely because of their desire to remove excess moisture (although bathroom windows were not monitored by sensors).

#### 4.5.1.3 Cooling

As expected, the logistic regression model fits indicate that cooling use increased with outdoor temperature. On average, within mixed-mode apartments cooling was more than 50% likely to be in use above 28.0°C ( $T_{50} = 28.0$  °C). This was substantially lower than the logistic regression model developed by Kim *et al.* (2017), based on residential detached dwellings in Sydney and Wollongong, in which cooling was more than 50% likely to be in use above 35.0°C.

While cooling use was more consistent than use of natural ventilation, there were three distinct participant cooling use profiles amongst the cohort. Cooling use in apartments with high cooling energy consumption, as determined in Section 4.3.3, increased at lower temperatures ( $T_{25} = 20.3$ °C for Apartments #1, #3, and #6) than apartments with moderate ( $T_{25} = 27.0$ °C for Apartment #7) and low cooling energy consumption ( $T_{25} = 31.1$ °C for Apartments #2 and #5). This confirms the hypothesis, originally inferred from energy signature profiles in Section 4.3.3.1, that in dwellings with high cooling consumption participants are more likely to use cooling at cooler outdoor temperatures than light or moderate users of cooling. That is, rather than having similar cooling temperature comfort thresholds as moderate users and simply using air conditioning more often at temperatures above these thresholds, high cooling consumption participants appear to have lower comfort temperature thresholds.

While participants in Apartments #3 and #6 preferred to use air conditioning rather than natural ventilation to cool their apartments, Apartment #1 demonstrated high usage rates of both natural

ventilation and air conditioning. As shown in Table 4-10, the bedroom window was open for 75% of the periods when cooling was active, whilst the window in the living room (where the air conditioner was located) was open for just 8.1% of the periods when cooling was active. The participant explained that the bedroom window was almost always left open to allow their pet dog access into and out of the apartment. However, it was evidently closed when outdoor temperatures became intolerable.

*Table 4-10 Proportion of time that at least one of the windows was open while cooling was in operation.*

<b>Apartment ID</b>	<b>1</b>	<b>2</b>	<b>3</b>	<b>5</b>	<b>6</b>	<b>7</b>
Living room window open	8.1%	14.6%	6.6%	8.0%	3.1%; 1.7%	29.1%
Bedroom window open	74.6%	20.9%	1.6%			24.8%
Either monitored window open	77.0%	30.8%	7.6%	8.0%	4.8%	37.9%
Both monitored windows open	5.8%	4.7%	0.6%		0.0%	15.9%

On average, at least one of the two windows was open for 27.7% of the time that cooling was active. However, it may have been possible for occupants to separate the conditioned zones from the naturally ventilated areas of the apartment using internal partitioning. Of the apartments in which the monitored windows were located in separate rooms, both windows were simultaneously open for just 7.0% of the periods that cooling was in use. Only in Apartment #7 were both windows simultaneously open for more than 10% of the periods when cooling was in use.

#### 4.5.1.4 Heating

As expected, the likelihood of heating being in use increased as outdoor temperature decreased. However, occupants appeared to be less dependent on heating than cooling during the monitoring period. For each apartment, if a neutral outdoor temperature is defined as the temperature at which heating and cooling were both equally likely to be in operation, then it was observed that the likelihood of heating being in use increased less rapidly than cooling as outdoor temperatures deviated below and above the neutral temperature, respectively, in every apartment.

The average probability of heating being in use at the minimum outdoor temperature measured during the study was considerably lower in Canberra (25.2%) than in Sydney and Wollongong (63.0%), despite average minimum measured temperatures of -7.9°C and 7.3°C, respectively. This indicated that occupants in Sydney and Wollongong were more dependent on heating than occupants in Canberra, despite experiencing significantly fewer heating degree days. This may provide further evidence of occupants developing adaptations to the local conditions.

However, even for the apartments in Sydney and Wollongong, heating was much less likely to be in use at outdoor temperatures measured during the monitoring period compared to the heating

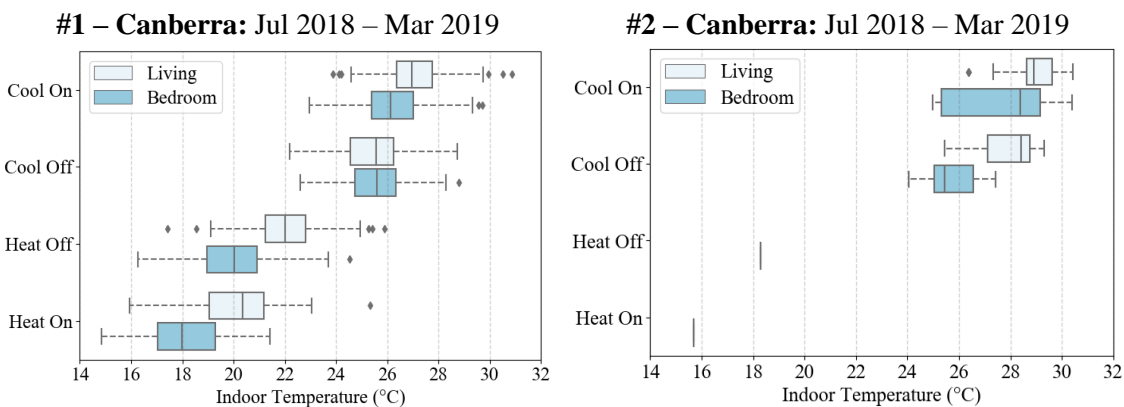


use patterns of occupants living in detached dwellings in and around Wollongong as observed by Kim *et al.* (2017), where heating use was reported to have increased sharply as outdoor temperatures decreased below 25°C, and was more than 50% likely to be in use below outdoor temperatures of 15°C ( $T_{50} = 15^{\circ}\text{C}$ ). In comparison, the average  $T_{50}$  of the apartments #3 and #7 was 10°C; heating was never more than 50% likely to be in operation in the remaining apartments.

As a caveat to the above assessment of heating use, only part of the winter period was monitored at Apartments #1, #2, and #3, and monitoring began in early spring for Apartments #5, #6, and #7. Since occupant heating over a full year was not monitored in this study, overall heating consumption should not be compared with annual figures from other studies. Nevertheless, the individual heating patterns determined within this study are valid over the temperature range experienced over the monitoring periods.

#### 4.5.2 Air Conditioning On and Off Events

Figure 4-17 presents box-plots of the indoor temperatures at which heating and cooling was turned on and off for each apartment. For the apartments with zoned air conditioning systems or multiple split-systems (#2, #3, #5, and #7), the indoor temperature measured at a heating or cooling on or off event was only included in the box-plots for the zone being conditioned by occupants, which was inferred by comparing the changes in temperature between zones. For the remaining apartments (#1 and #6), which had wall-mounted indoor units of split-system air conditioners in the living room, the indoor temperature measured at a heating or cooling on and off event was included for both the living room and bedroom in the respective box-plots as occupants had no way to heat or cool the bedroom without also conditioning the living room.



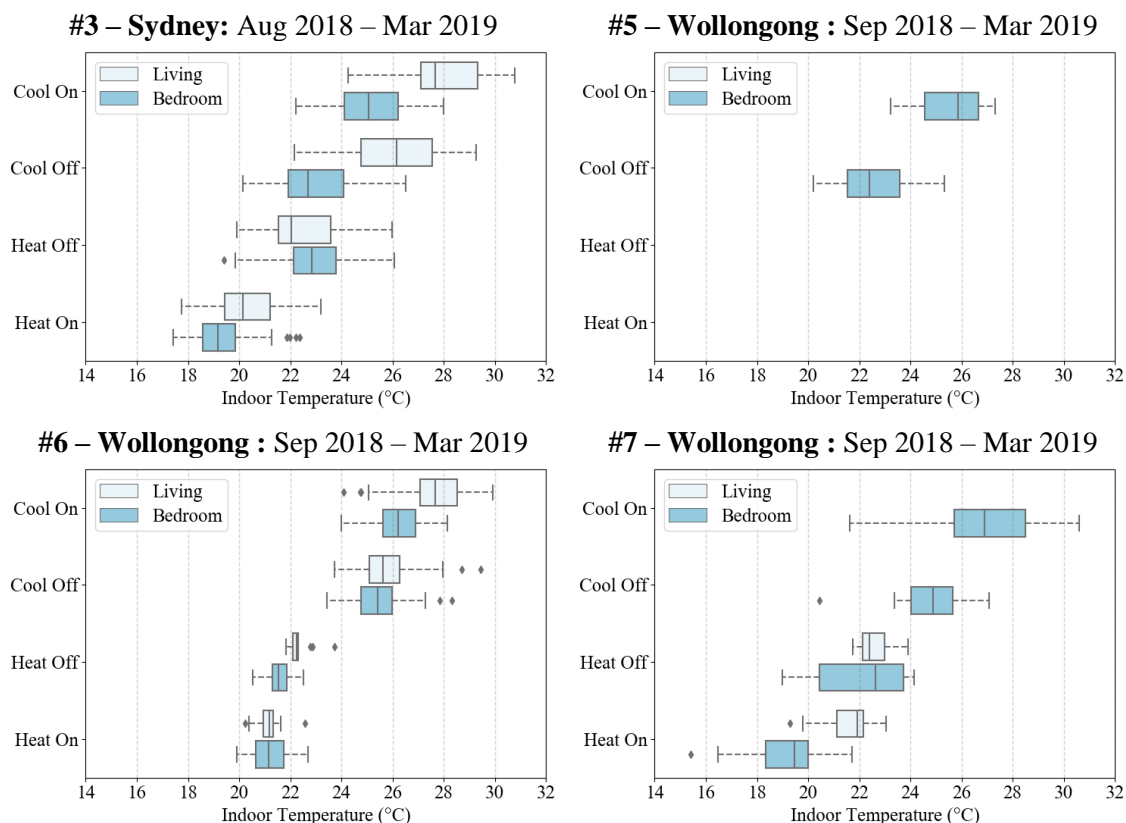


Figure 4-17 Box-plot distribution of indoor temperatures at which reverse-cycle heating and cooling was turned on and off in each apartment.

### Heating

The average indoor temperature on a per-dwelling basis at which heating was turned off was 22.4°C in the zone being heated, excluding Apartment #2, which only had one instance of heating use throughout the monitoring period. This temperature is very close to the outdoor temperature noted as having the maximum likelihood of natural ventilation being active (i.e. 22.2°C).

It is important to note that this heating switch-off indoor temperature of 22.4°C was fully 2.4°C above the heating thermostat setting prescribed for the living room by NatHERS (20.0°C), which suggests that the heating thermostat settings specified in NatHERS may be too low and not representative of occupant preferences/practices.

Similarly, the indoor temperature at which heating was turned on was also greater than the NatHERS thermostat settings. The average living room switch-on temperature was 20.8°C, i.e. 0.8°C higher than the thermostat settings for living rooms; and the average bedroom temperature at which heating was turned on was 19.4°C, 1.4°C higher than the NatHERS thermostat settings for bedrooms. Thus, while the heating switch-off temperature did not appear to change as a function of the zone being conditioned (where controllable by the occupant), the average heating switch-on temperature was lower in the bedroom than in the living room.

The primary zone being heated was the living room in all apartments except Apartment #3, in which the bedroom was heated in approximately 75% of the heating use events. Apartments #1 and #6, which had wall-mounted split-system air conditioners in their living rooms, had no means to directly heat their bedrooms. Therefore, the living room was always the primary zone being heated, regardless of occupant intentions.

### Cooling

The average temperature on a per-dwelling basis at which cooling was turned off was 25.1°C. However, the average indoor temperature at which cooling was turned off was 24.0°C when the bedroom was prioritised for cooling compared with 26.3°C when the living room was prioritised for cooling. In addition, the indoor temperature at which cooling was turned on was 27.1°C overall, but was again warmer in the living room (27.9°C) than in the bedroom (26.3°C). This suggests that occupants preferred cooler temperatures in the bedroom than in the living room. This may be caused by the cooler temperatures desired by occupants in bedrooms due to the insulating effect of bedding, but could also be attributed to the higher likelihood that bedrooms were cooled overnight when ambient temperatures, and thus indoor temperatures, were generally lower than during the day.

The NatHERS cooling thermostat settings at the time of writing were 24.0°C in Canberra and 24.5°C in Sydney and Wollongong, irrespective of the zone being conditioned. By comparison, occupants in the present study turned cooling off, on average, 0.9°C warmer than the NatHERS protocol. However, excluding the bedrooms in Apartments #3 and #5, which were cooled to temperatures that were on average 1.8°C cooler than the NatHERS thermostat settings, the average indoor temperature at which cooling was turned off was 1.6°C warmer than the NatHERS cooling thermostat settings. Ren, Chen, and James (2018) identified similar offsets between actual cooling off temperatures and the NatHERS cooling thermostat settings in residential dwellings in Brisbane, Adelaide, and Melbourne as part of the Residential Baseline Energy Efficiency (RBEE) project. These findings indicate that the majority of occupants cooled their dwellings less stringently during cooling events than anticipated by NatHERS, although occupants may have differing thermal preferences between the living room and bedroom.

### Alignment of Air Conditioning On and Off Events with the NatHERS Protocol

NatHERS uses complex logic for the application of cooling as it attempts to maximise the use of natural ventilation to maintain thermal comfort and uses dynamic thermal comfort boundaries that vary as a function of air speed and climate zone. The heating and cooling algorithm used in NatHERS is thoroughly described in Section 5.2.8.

Comparing the cooling switch-on events with the logic used to invoke cooling in NatHERS protocol resulted in the following observations.

- Only 9% of the cooling switch-on events (on a dwelling-averaged basis) satisfied all the indoor and outdoor conditions defined in the NatHERS protocol to invoke cooling i.e. that indoor conditions were considered unsatisfactory and outdoor conditions were not suitable to provide cooling via natural ventilation.
- An additional 56% of the cooling switch-on events partially met such conditions. In these instances, indoor conditions were considered unsatisfactory although environmental conditions satisfied the requirements defined in the NatHERS protocol to use natural ventilation to provide cooling.
- The remaining 35% of the cooling switch-on events did not meet any of the requirements defined in NatHERS to invoke cooling. In such instances, indoor conditions were within the thermal comfort boundaries defined by NatHERS. The largest proportions of these cooling switch-on events occurred in Apartments #3 and #5, which were observed to frequently cool their bedrooms to below the NatHERS cooling set-point.

Thus, it appears that NatHERS overestimates occupant perceptions of the potential for natural ventilation to provide thermal comfort. In addition, that 35% of the switch-on events occurred within the NatHERS thermal comfort region suggests that the thermal comfort region defined by NatHERS may not accurately represent occupant preferences. This value increases to 70% when considering the effects of indoor air movement (assumed to be 0.5 m/s) on extending the NatHERS upper thermal comfort boundary (see Section 5.2.8).

Therefore, it is postulated that the acceptable thermal comfort boundaries in NatHERS may go beyond occupant thermal perceptions in reality, which may lead to increased application of natural ventilation and reduced utilisation of air conditioning in building performance modelling.

However, the upper thermal comfort boundary defined by NatHERS corresponds approximately to the 90% acceptability limits for January of each climate zone as defined within the adaptive comfort model (Delsante, 2005; Ren and Chen, 2018). Thus, the heating and cooling on and off events were compared to the adaptive comfort model 80% and 90% acceptability limits as depicted in Figure 4-18.

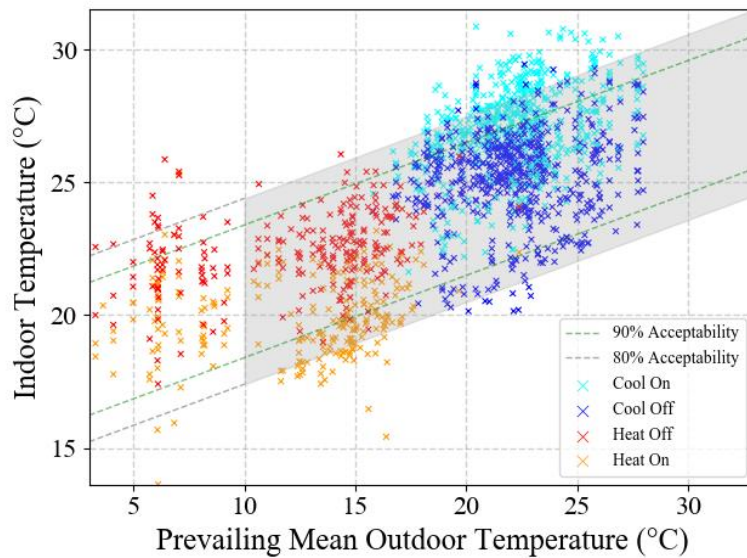


Figure 4-18 Indoor temperatures at which heating and cooling was turned on and off with respect to the adaptive comfort model 80% and 90% acceptability boundaries as a function of prevailing mean outdoor temperature.

Ninety four percent (94%) of the heating switch-off and cooling switch-off events occurred within the 90% acceptability limits, indicating that occupant preferences were well aligned with the thermal acceptability limits defined by the adaptive comfort model. On the other hand, 49% of the heating and cooling on events were outside of the Adaptive comfort 90% acceptability limits. Therefore, the adaptive comfort 90% acceptability limits can be seen to be a reasonable threshold to separate heating and cooling on and off behaviour.

However, the remaining 51% of the heating and cooling events were within the 90% acceptability limits, which suggests that occupant preferences differed from the adaptive comfort model to a certain extent. This may be due the use of mixed-mode ventilation, which influences occupant adaptation (Kim *et al.*, 2019), or may be due to cooler thermal comfort preferences of residential occupants living in this area as noted by de Dear, Kim, and Parkinson (2018).

## 4.6 Building Envelope

### 4.6.1 Airtightness

The air change rates (n50) for each of the apartments are shown in Figure 4-19 and the air permeability rates (q50) through the apartment envelopes are shown in Figure 4-20. The results were determined by averaging the depressurisation and pressurisation tests in accordance with ISO 9972, unless one test was invalidated in which case the results were based on just a single flow direction.

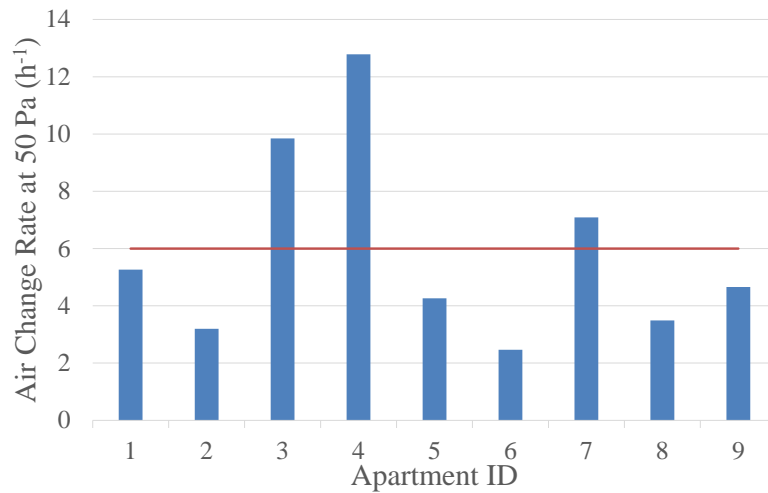


Figure 4-19 Air change rates ( $n_{50}$ ) of each apartment using the Fan Pressurisation Method from ISO 9972. The average air change rate of 5.9 ACH@50 Pa is indicated by the red line.

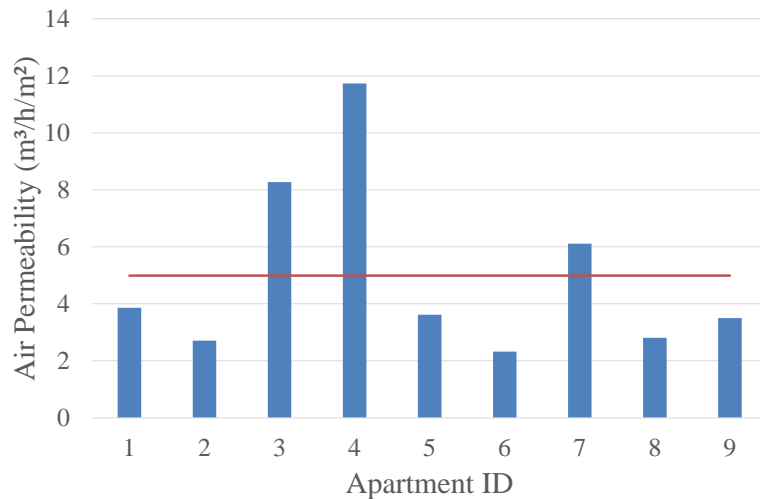


Figure 4-20 Air permeability rates ( $q_{50}$ ) through the envelope within each of the apartments using the Fan Pressurisation Method from ISO 9972. The envelope area is measured as the entire boundary of the apartment including external, intertenancy, and corridor walls, floors, and ceilings. The average air permeability rate, indicated by the red line, was 5 m<sup>3</sup>/h/m<sup>2</sup>.

The average air change rate at 50 Pa was 5.9 h<sup>-1</sup> and ranged from 2.5 to 12.8 h<sup>-1</sup>. Apartment #4 was the least airtight apartment, which was perhaps unsurprising given that it was previously an inner-city warehouse that was converted into a residential apartment around 2000. A photograph of the view within the ceiling cavity is shown in Figure 4-21. Apartment #6 had the lowest air change rate despite having the largest fraction of external wall area relative to total wall area. Overall, there was no apparent relationship between external envelope area and air flow rate, which is in agreement with the results presented by Kaschuba-Holtgrave *et al.* (2020). While the internal partition leakage was not quantified, the lack of an observed relationship between external envelope area and air flow rate implies that internal partition leakage may have been significant.



*Figure 4-21 Condition of the ceiling cavity of Apartment #4, which was the least airtight apartment amongst the cohort. This building had been converted from an inner-city warehouse to a multi-unit residential building around 2000.*

The primary leakage paths identified in the apartments by qualitative visualisation techniques were the exhaust fan ducting, air conditioning ducting, along the tracks of glass sliding doors, and ceiling cavity openings such as the access hatch and bathroom heat lamps. A photograph of the prominent leakage path along the door tracks is shown in Figure 4-22.



*Figure 4-22 Smoke puffer testing used to visualise the air leakage paths between the sliding door and the door tracks. This was the most common leakage path witnessed amongst the tested apartments along with the exhaust fan ducting.*

A CSIRO study into the airtightness of newly constructed dwellings across Australia concluded that the national average air change rate at 50 Pa was  $15.5 \text{ h}^{-1}$ , whereas the averages in Sydney and Canberra were  $20.8$  and  $14.1 \text{ h}^{-1}$ , respectively (Ambrose and Syme, 2017). A study examining the post-occupancy performance of BASIX affected dwellings in Western Sydney measured an average air change rate at 50 Pa of  $14.8 \text{ h}^{-1}$  amongst a cohort of six detached dwellings and two

apartments (of which one detached dwelling and one apartment dwelling were constructed prior to the introduction of BASIX energy efficiency requirements) (Ding *et al.*, 2019), however, results in this publication were not categorised by dwelling type. The results obtained in the present study appear to indicate that modern apartments are considerably more airtight than modern detached dwellings in Australia. However none of these three datasets could be said to be large enough to be statistically representative of Australia's residential building stock. The findings in this study also align with the majority of comparisons of airtightness measured in apartments and detached dwellings conducted internationally as stated in Section 2.7.4 of the literature review.

Overall, the evidence base of airtightness testing of apartments is relatively limited in comparison to detached dwellings, yet the literature indicates that recently constructed apartments are considerably more airtight than recently constructed detached dwellings. While Australian detached dwellings are considerably less airtight than detached dwellings in many developed countries, the small dataset gathered within this study suggests that the airtightness of modern apartments in Australia may be comparable to those in temperate areas of Europe.

#### **4.6.2 Building Envelope Thermal Characteristics**

Assessment of the thermal characteristics of the apartment building envelopes revealed insulation installation issues, the prevalence of thermal bridging, and interesting impacts of thermal mass attributed to the concrete structure, amongst other issues.

The majority of the apartments monitored were mid-level apartments, and thus, only a small portion of the apartment envelope was exposed to outdoor conditions and required insulation. The thermographic inspection of the external walls in every apartment revealed that the insulation within the walls appeared to be homogeneous and well installed. However, in every apartment the thermal bridging effects due to the steel framing were clearly visible, even during apartment inspections conducted when the internal to external temperature difference was very small. A typical example of such effects is presented in Figure 4-23. Please note that each of the thermographic images shown within this section have been processed assuming surfaces have an emissivity of 0.95 (equivalent to that of a typical painted drywall).

Figure 4-23 shows an approximate 0.5°C temperature difference between the drywall adjacent to the studs and the drywall between the studs. The effect was noticeably amplified in proximity to the screw fixtures due to improved thermal contact, and near the ceiling due to geometric bridging effects. While it is not possible to quantify the impact of the thermal bridges on the overall thermal performance of the apartments from this series of images/inspections, the observed ubiquity of such thermal bridges indicates that they may well have significant impacts on overall thermal performance. This is explored further in Chapter 6.



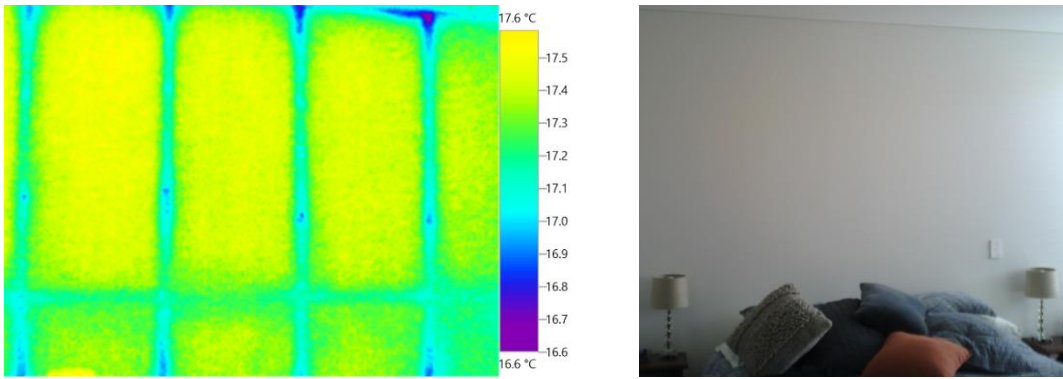


Figure 4-23 Thermographic and visual images of an external wall in Apartment #5. The thermographic image highlights the thermal bridging caused by steel framing. This image was taken on 12/09/2018 at 10:10 am.

In addition to external walling, ground floor apartments, particularly those above ventilated carparks were also exposed to outdoor conditions underneath the flooring. While the floor insulation was not visible from within the apartment, the presence of insulation of the underground carparks was observed in some cases, and insulation was noted as being present in the NatHERS Certificate for Apartment #5.

Apartment #3 was the only monitored top-floor apartment i.e. had a ceiling/roof structure that was exposed to outdoor conditions. A thermographic inspection of the ceiling revealed that the insulation batts had been poorly distributed and there were significant gaps across the ceiling, despite apparent satisfactory installation quality of the wall insulation. A thermographic image of a portion of the ceiling and external wall of Apartment #3 is shown in Figure 4-24. The issue of missing or poorly laid ceiling insulation has been observed in numerous cases within detached homes in Australia, such as reported in the CSIRO Energy Efficiency Inspections Report (Ambrose and Syme, 2015), the report entitled RP1041 ‘Improving the thermal performance of dwellings for carbon positive and healthy homes’ (Upadhyay, Munsami and Smith, 2019), and the report entitled RP1017 ‘Validating and Improving the BASIX Energy Assessment Tool for Low-Carbon Dwellings’ (Ding *et al.*, 2019)

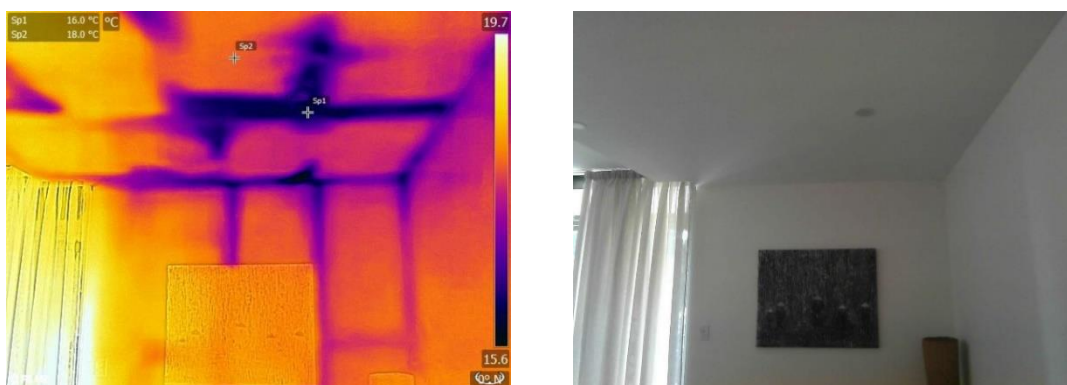
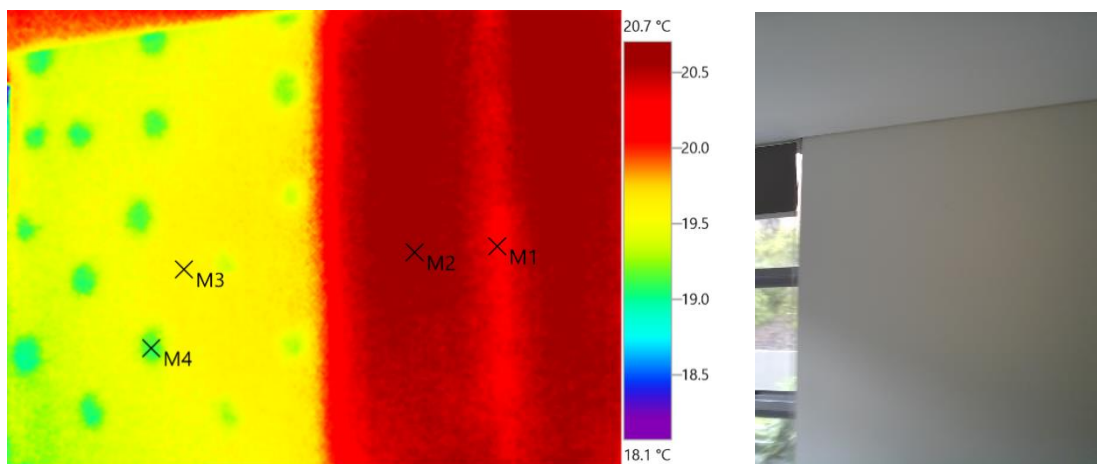


Figure 4-24 Thermographic image of the top floor of Apartment #3, indicating unsatisfactory ceiling insulation above the living room. The visual image is presented on the right for comparison. This image was taken on 23/07/2018 at 09:01am.

Another interesting observation that became apparent using the thermographic camera was the effects of thermally massive building elements, such as concrete columns, at various locations within the wall structure. As shown in Figure 4-25, the infrared image reveals the presence of a concrete column at the lateral edge of the internal wall within Apartment #2. The drywall in direct contact with the column appears to be  $0.9^{\circ}\text{C}$  cooler than the drywall further from the column. In Figure 4-26, the infrared image of an external wall in Apartment #9 highlights the presence of a concrete column, a steel stud, insulation, and the locations of the adhesive dabs used to bond the drywall to the column, which have formed small areas of improved thermal contact between the drywall and the concrete column. A similar column was witnessed within the ceiling cavity, which shows the blue adhesive used on the column and also shows the steel framing and insulation in the visual spectrum.



*Figure 4-25 Thermographic and visual images of an internal wall in Apartment #2. The thermographic image highlights the thermal mass of a concrete column at the confluence of the living room and the bedrooms. This image was taken on 12/07/2018 at 02:10pm.*



*Figure 4-26 Thermographic and visual images of an external wall in Apartment #9. The thermographic image highlights the presence of thermal bridging from steel framing effects and the influence of a concrete column. The green spots are caused by small thermal bridges of plasterboard adhesive. This image was taken on 28/11/2018 at 03:15pm.*

## 4.7 Summary

This chapter presents the findings from the field study on electricity consumption, air conditioning use, thermal comfort, occupant comfort management strategies, and building envelope performance of nine occupied apartments across Canberra, Sydney, and Wollongong, all of which were constructed in 2000 or thereafter.

The average daily electricity consumption of the nine apartments was slightly lower than the average daily electricity consumption of apartments monitored in Sydney as part of the Smart Grid Smart City (SGSC) project. However, the per capita consumption of the case-study apartments in the present study was 30% less than that of the apartments in the SGSC project. Similarly, on average, the electricity consumption in the apartments was approximately 30% less than the Australian Energy Regulator (AER) consumption benchmarks, which were based on detached dwellings with the same number of occupants within the same NCC climate zone classification.

Throughout the monitoring period, the average daily air conditioning electricity consumption was 2.2 kWh, which is slightly over half the average daily electricity consumption of air conditioning systems previously measured in predominantly detached homes in across Sydney. On average 25% of the electricity drawn by the air conditioning systems was consumed in standby operation. Of the air conditioning electricity consumed in active operation, an average of 74% was used for cooling and 26% was used for heating.

The temperatures of the interior of the majority of apartments were found to be outside the 80% acceptability limits defined by the adaptive comfort model in winter, spring, and summer for less than 10% of occupied hours. However, the temperatures in one apartment was below the 80% acceptability limits for up to 50% of occupied hours in winter. On the other hand, the greatest exceedance rates in summer occurred within the two apartments without air conditioning and in the only top-floor apartment, which was a two-storey apartment where the upper level was not thought to be conditioned frequently. Interestingly, mixed-mode apartments that prioritised natural ventilations and had lower cooling use over the monitoring period were not significantly less comfortable than apartments with a higher propensity to use cooling.

There were two distinct usage patterns of natural ventilation and cooling in mixed mode apartments:

- Occupants of the majority of apartments prioritised natural ventilation, and only deferred to the use of cooling when natural ventilation was considered insufficiently effective to maintain comfort. In these apartments, windows were most frequently (86% of the time) in an open state when outdoor temperatures were 22.2°C.

- The remaining apartments forewent natural ventilation opportunities, preferring to cool their apartments with air conditioning irrespective of outdoor conditions. In these apartments, windows were never more than 20% likely to be open regardless of outdoor temperature.

Overall, cooling was more than 50% likely to be in use above outdoor temperatures of 28°C. However, apartments with higher cooling consumption demonstrated significant use of cooling at temperatures below this threshold.

The average indoor temperature that cooling was turned on was 27.9°C and 26.3°C in the living rooms and bedrooms respectively. In addition, the average temperature that cooling was turned off was 26.3°C and 24.0°C in the living rooms, and bedrooms, respectively. Together, these indicated that occupants preferred to maintain cooler conditions in their bedrooms than their living rooms. Notwithstanding the relatively small sample size of the present study, this finding is at odds with the NatHERS assumption that occupant cooling thermostat settings do not vary across different room/zone types.

In addition, while NatHERS cooling thermostat settings were generally cooler than occupant cooling preferences, less than 10% of the cooling on events met all the necessary conditions required in the NatHERS protocol to activate cooling. This suggested that the definition of thermal comfort in NatHERS may differ from the thermal perceptions of actual occupants. Furthermore, occupants also heated their homes by between 2°C to 4°C above the NatHERS heating thermostat settings, which again indicated that NatHERS thermal comfort preferences differed from those of actual occupants. By comparison, the 90% acceptability limits defined by the adaptive comfort model separated cooling and heating on and off events with reasonable accuracy.

The average air change rate of the apartments at 50 Pa was 5.9 h<sup>-1</sup>, which was significantly less than the national average measured by Ambrose and Syme (2017) of 15.5 h<sup>-1</sup>, however, the latter figure was based on measurement of predominately detached dwellings. This suggests that recently constructed apartments are much more airtight than recently constructed detached homes in NSW and the ACT. In addition, thermographic inspections of the building envelope revealed that wall insulation appeared to be installed relatively well, despite minor thermal bridging effects caused by steel framing. However, the ceiling insulation was poorly laid and sparsely distributed in the sole top-floor apartment that participated in the study.

## Chapter 5

# 5 Thermal Performance Comparison of the Case-Study Apartments with Building Performance Simulation

## 5.1 Introduction

This chapter describes a numerical investigation of the thermal performance of each of the case-study apartments examined in Chapters 3 and 4 using National House Energy Rating Scheme (NatHERS) accredited building performance simulation software AccuRate Sustainability.

The main purpose of this work was to quantify the degree to which the actual thermal performance of occupied apartments met, or exceeded, legislative requirements.

The simulated thermal performance of the apartments, determined using assumptions and settings mandated within the NatHERS assessment protocol, was compared against the actual, measured thermal performance of the apartments. The primary comparison metric was the energy consumed for heating and cooling.

Differences between the actual and simulated thermal performance were interpreted by comparing differences in the indoor conditions, occupant behaviours, weather conditions, and building envelope characteristics measured in the apartments with those specified by the assumptions and settings mandated in the NatHERS protocol and the NCC. Understanding the major causes of the differences between the actual and simulated thermal performance was expected to aid in identifying where beneficial changes to the energy efficiency assessment framework could be made.

The simulated heating, cooling, and combined loads of the apartments derived from the modelling conducted within this study were also compared to the respective loads from the NatHERS assessments obtained from the original Development Applications of the apartments.

The simulated heating, cooling, and combined loads of the apartments were evaluated with respect to the maximum NatHERS heating/cooling intensity limits in effect: i) at the time of development, and ii) at the time of writing, to identify to what extent the apartments exceeded minimum performance requirements and whether some apartments might not meet the more stringent present day performance standards.

Thus, the five primary aims of the modelling study were as follows.

- a) Compare heating and cooling use in the apartments in reality with heating and cooling loads determined by building performance simulations of the apartments performed in accordance with NatHERS.
- b) Compare the default values for uncertain parameters assumed in the NatHERS protocol with the actual values for such parameters measured in the apartments.
- c) Assess the uncertainty in the simulated heating and cooling loads that can be attributed to default values for uncertain parameters specified by the NatHERS protocol.
- d) Assess the level of alignment between the simulated thermal performance of the case-study apartments determined within this study and those obtained from the original Development Applications.
- e) Evaluate whether the simulated thermal performance of the case-study apartments exceeded the minimum thermal performance requirements specified by the relevant jurisdictions and evaluate whether recent changes to minimum thermal performance requirements have had a substantial impact on dwelling designs.

## **5.2 Building Performance Simulation Methodology**

This section describes the methodology used to develop numerical models of each of the apartments using software tools and building performance simulation assessment protocols prescribed by NatHERS in accordance with the building regulations in NSW and ACT for National Construction Code (NCC) Class 2 buildings.

The numerical models of the apartments were designed to closely represent their physical characteristics deduced through the energy performance inspections of the apartments described in Chapter 4.

### **5.2.1 Software Tools**

The thermal performance of each of the apartments were examined using the building simulation software AccuRate Sustainability V2.3.3.13 SP3 running the Chenath Engine Version 3.13 as the numerical modelling tool, or ‘simulation engine’. At the time of writing AccuRate Sustainability is one of the three NatHERS approved software tools for thermal analysis and Chenath Engine 3.13 was the mandatory simulation engine used for NatHERS assessments between 2014 and 2020. Thus, the outputs produced by the modelling were suitable to be evaluated with respect to the regulatory requirements specified by the NCC and BASIX.

The assumptions and settings used within the building models were sourced directly from the NatHERS specifications, which were mandatory to produce a valid assessment as part of a

Development Application at the time of writing. These specifications were accessed through the Chenath Repository within the HERS Portal (Chen, 2016) and also through the default libraries included in AccuRate Sustainability.

### **5.2.2 Building Configuration, Boundary Conditions, and Zoning**

The geometric layouts of the apartment models were developed from the floor plans obtained during the energy performance inspections of the apartments described in Section 3.3.

The types of spaces adjacent to each of the apartment dwellings were also recorded during the energy performance inspections as the boundary conditions of the dwelling model at a particular building envelope interface were dependent on the type of space adjacent to the dwelling. The boundary conditions were specified in accordance with the NatHERS Technical Notes pertaining to Chenath Engine V3.13 (Department of the Environment and Energy, 2019c). Therefore, neighbouring apartments were considered to be at the same internal temperature as the modelled dwelling, as were mechanically conditioned corridors, lift cores and enclosed stairwells. Sections of the building envelope adjacent to unconditioned corridors were considered as external walls that were well shaded and shielded from wind effects. Floors above underground car parks were considered as being located above outdoor air.

Balconies and external living areas (of ground-floor apartments) were considered as shading elements in accordance with the NatHERS Technical Notes. This included smaller eaves, fencing and opaque balustrade elements where present. Neighbouring structures that were single-storey and within 10 metres of the dwelling or were two storeys or greater and within 20 metres of the dwelling were also included in the models as shading elements. Protruding external walls and upper floors of the apartment building that obstructed the sun or provided a wind shield were also included as shading elements within the building model.

Within NatHERS, the zone type governs the heating and cooling thermostat settings as well as the internal heat loads as a function of time of day. Generally, zones are considered active during either the daytime or night-time. The primary zone in each of the apartments modelled was an open-plan kitchen and living area, which constituted the main daytime zone. None of the apartments contained multiple kitchens or living spaces. The remaining zones consisted of bedrooms, bathrooms (both separate and ensuites), laundries, and other non-specific daytime-zones such as hallways.

### **5.2.3 Building Envelope Structure**

The apartment building external wall, intertenancy wall, internal partition wall, floor, ceiling, and roof specifications were determined from a combination of details observed during the energy performance inspections, details witnessed within the Development Application where available,

and inferences from the minimum building envelope thermal performance requirements specified in Section J1 of the National Construction Code (NCC) 2016 Volume One. The building envelope specifications are presented in Table 5-1, which were determined using a parametric analysis as part of the model calibration process. This process and the results are presented in Section 5.4.

*Table 5-1 Summary of the building envelope structural details used to model the thermal performance of the apartments in AccuRate Sustainability. Total thermal resistance values are calculated without the effects of thermal bridging nor the air-film resistances on the superficial surfaces. Air gaps have been specified using default nominal widths provided by AccuRate.*

<p align="center"><u>Brickwork External Wall</u></p> <ul style="list-style-type: none"> <li>• 110 mm Extruded Clay brickwork</li> <li>• 40 mm air gap with high emissivity surfaces</li> <li>• 32 to 102 mm bulk insulation</li> <li>• 13 mm plasterboard</li> </ul> <p>Total R-Value: 0.99-3.31 m<sup>2</sup>k/W</p>	
<p align="center"><u>Concrete Block External Wall</u></p> <ul style="list-style-type: none"> <li>• 140 mm concrete block (core-filled)</li> <li>• 40 mm air gap with high emissivity surfaces</li> <li>• 32 to 102 mm bulk insulation</li> <li>• 13 mm plasterboard</li> </ul> <p>Total R-Value: 0.97-3.29 m<sup>2</sup>k/W</p>	
<p align="center"><u>AAC External Wall</u></p> <ul style="list-style-type: none"> <li>• 50 mm or 75 mm autoclaved aerated concrete (AAC) panel</li> <li>• 40 mm air gap with high emissivity surfaces</li> <li>• 32 to 102 mm bulk insulation</li> <li>• 13 mm plasterboard</li> </ul> <p>Total R-Value: 1.20-3.52 m<sup>2</sup>k/W</p>	
<p align="center"><u>Intertenancy Wall</u></p> <ul style="list-style-type: none"> <li>• 13 mm plasterboard</li> <li>• 75-140 mm masonry layer</li> <li>• 20 mm air gap with high emissivity surfaces</li> <li>• 25 to 50 mm bulk insulation</li> <li>• 13 mm plasterboard</li> </ul> <p>Total R-Value: 1.63-2.03 m<sup>2</sup>K/W</p>	
<p align="center"><u>Internal Partition Wall</u></p> <ul style="list-style-type: none"> <li>• 13 mm plasterboard</li> <li>• 40 mm air gap with high emissivity surfaces</li> <li>• 13 mm plasterboard</li> </ul> <p>Total R-Value: 0.32 m<sup>2</sup>k/W</p>	
<p align="center"><u>Suspended flooring between two apartments</u></p> <ul style="list-style-type: none"> <li>• 100 mm, 150 mm, or 200 mm concrete</li> <li>• 90 mm air gap with high emissivity surfaces</li> <li>• 13 mm plasterboard</li> </ul> <p>Total R-value (up): 0.31-0.38 m<sup>2</sup>K/W</p>	



<p><u>Suspended flooring above underground carpark</u></p> <ul style="list-style-type: none"> <li>• 100 mm, 150 mm, or 200 mm concrete</li> <li>• 90 mm air gap with high emissivity surfaces</li> <li>• 66 mm bulk insulation</li> <li>• 13 mm plasterboard</li> </ul> <p>Total R-value (up): 1.81-1.88 m<sup>2</sup>K/W</p>	
<p><u>Floor Surfaces</u></p> <ul style="list-style-type: none"> <li>• Carpet: <ul style="list-style-type: none"> <li>○ 10 mm carpet</li> <li>○ 8 mm rubber underlay</li> </ul> </li> </ul> <p>Total R-value: 0.28 m<sup>2</sup>K/W</p>	
<ul style="list-style-type: none"> <li>• Tiles: <ul style="list-style-type: none"> <li>○ 8 mm ceramic tiles</li> <li>○ 6 mm fibre-cement underlay</li> </ul> </li> </ul> <p>Total R-value: 0.02 m<sup>2</sup>K/W</p>	
<ul style="list-style-type: none"> <li>• Laminate Flooring: <ul style="list-style-type: none"> <li>○ 12 mm timber</li> <li>○ 2 mm felt underlay</li> </ul> </li> </ul> <p>Total R-value: 0.12 m<sup>2</sup>K/W</p>	
<p><u>Stairway Rooftop</u></p> <ul style="list-style-type: none"> <li>• 2 mm steel sheeting</li> <li>• 20 mm air gap with high emissivity surfaces</li> <li>• 90 mm air gap with high emissivity surfaces</li> <li>• 120 mm bulk insulation</li> <li>• 13 mm plasterboard</li> </ul> <p>Total R-value (up): 4.18 m<sup>2</sup>K/W</p>	
<p><u>Accessible Rooftop area</u></p> <ul style="list-style-type: none"> <li>• 100 mm, 150 mm, or 200 mm concrete</li> <li>• 90 mm air gap with high emissivity surfaces</li> <li>• 120 mm bulk insulation</li> <li>• 13 mm plasterboard</li> </ul> <p>Total R-value (up): 3.91-4.00 m<sup>2</sup>K/W</p>	

## Wall Specifications

Thermographic inspections in conjunction with visual inspections of the ceiling cavities indicated that the wall systems were typically framed using cold-formed steel (CFS), with insulation infill between the voids in external and intertenancy walls. Internal partition walls also contained steel studs, however, internal partition walls were assumed to be uninsulated. The estimated stud widths were either 64 mm, 76 mm, 92 mm or 150 mm, which were standard CFS stud width dimensions available in Australia.

The detailed composition of each of the wall systems is described below.

- Internal partition walls were modelled as 64 mm uninsulated stud frames sandwiched between 13mm gypsum plasterboard sheets on each side based on the predominant measured thickness.

- Intertenancy walls were modelled with 64 mm stud framing. One side of the frame was contained by one 13 mm gypsum plasterboard sheet and the other side was contained by an air gap and an outer masonry layer. 25 to 50mm of insulation was assumed to occupy the void between adjacent studs to satisfy the intertenancy wall acoustic requirements for all masonry layers options considered.
- External walls were modelled with between 32 to 102 mm of insulation, which was assumed to completely occupy the void between adjacent studs. The inner side of the external wall framing was enclosed by one sheet of 13 mm gypsum plasterboard and on the outer side of the framing it was assumed that there was an air gap present (of nominal thickness 40mm) between the framing and an external masonry layer. The exterior walls of the actual apartments were typically clad with masonry material that was most frequently coated with cement or acrylic render, although two of the apartments featured exposed brickwork. Often, details of the masonry material in the rendered apartments were not able to be ascertained from the walk-through inspections. In such cases, details were sought from the Development Application, if available. Where Development Applications were unavailable, a commercial builder was consulted to facilitate identification of the most likely masonry material. The builder was able to infer the masonry layer by examining the position of control joints in the façade (where present). In total, three types of masonry layers were identified as potential candidate veneers within the cohort of apartments:
  - 140mm concrete blockwork (fully core-filled);
  - 110mm extruded clay brickwork; and
  - 75mm aerated autoclaved concrete (AAC) panels.

Interestingly, this aligns with recent research by the CSIRO that showed that concrete, brick veneer, and AAC were the three most commonly used external wall typologies in apartment buildings across NSW, accounting for 43%, 16%, and 22%, of the apartment developments, respectively, between 2016 and 2020 (CSIRO, 2021a).

It was assumed that a single masonry material was used throughout the building envelope. For cases in which supporting evidence suggested a combination of masonry materials were used, the external wall masonry material specified in **Error! Reference source not found.** was substituted in place of the alternative masonry material to ensure a consistent modelling approach and to reduce simulation permutations.

### Floor and Ceiling Specifications

The floor configuration modelled in each of the apartments was a 100 to 200mm suspended concrete slab.

Above the slab were a number of different flooring configurations including 18mm carpet, 8mm ceramic tiles, or 12mm laminated flooring each with the appropriate underlay. Below the slab was an air gap larger than 66 mm, nominally specified as 90mm wide with high emissivity surfaces, and 13mm of plasterboard that formed the superficial ceiling covering. This specification covered both regular ceiling configurations and suspended ceiling configurations as the nominal size of the air gap was equivalent in both scenarios.

Flooring systems in ground floor apartments suspended above underground car parks were assumed to have additional insulation under the assumption that it was necessary in order for the apartments to comply with the minimum thermal performance requirements. This approach was vindicated by the NatHERS Certificate for Apartment #5, which indicated that the flooring systems of all ground floor apartments in the building had 1.5 m<sup>2</sup>K/W of additional thermal insulation relative to the intermediary floors. This was the sole NatHERS Certificate available amongst the cohort and it should be noted that specific modelling methodology details were not available in the BASIX certificates. The total thermal resistance required for the flooring systems within common areas of class 2 buildings in Climate Zone 7 (Canberra), was also 1.5 m<sup>2</sup>K/W, as specified by Table J1.6 of Volume One of the NCC 2016 (ABCB, 2016). Therefore, 66mm of glass/mineral wool bulk insulation, equivalent to an additional 1.5 m<sup>2</sup>K/W, was chosen as an appropriate amount of additional flooring insulation for ground floor apartments that were above underground car parks.

### Roof Specifications

Apartment #3 was the only apartment on the top floor, and thus had a roof, rather than an intermediary suspended floor above the space. Most of the rooftop was an accessible outdoor area with an exposed concrete upper surface. The roof above the stairway access to the outdoor rooftop area was clad with steel sheeting. Insulation was present within the roof structure as shown in Figure 4-24.

### Building Envelope Radiative Surface Properties

The solar absorptance and emissivity were estimated for each of the external facing surfaces based on the colour and surface finishes of each element using default values within AccuRate Sustainability.

### Thermal Bridging Effects

At the time of writing, the effects of thermal bridging were not included as part of the thermal performance assessment protocol specified by NatHERS. Therefore, thermal bridging effects caused by steel framing within the external walls were not included in the heat transfer models developed for the apartments in this chapter. However, a separate study was carried out on the influence of thermal bridging in the apartment building envelopes, as described in Chapter 6.

#### 5.2.4 Glazing Specifications

The windows were specified in accordance with the 2019 NatHERS Assessor Handbook (Department of the Environment and Energy, 2019b). All windows and glazed sliding doors were aluminium framed. The windows in each of the modelled apartments were single glazed except for Apartment #3, which featured double glazed windows that were assumed to be air filled. There were no special coatings or tinting visible to the naked eye on any of the glazing units during the walk-through inspections, therefore, throughout the modelling the glazing was considered to be clear.

The solar heat gain coefficient (SHGC) and the total thermal resistance of window were classified into two different groups, known as types A and B within AccuRate Sustainability. These vary by the percentage of the window opening occupied by the framing, which is determined from the type of opening mechanism of the window. The maximum opening percentages of the windows, which were specified by default in AccuRate, were also informed by the opening mechanism. Note that since 2013, the NCC requires that windows in apartments above the ground floor restrict the maximum window opening to 125 mm or otherwise have a security screen (ABCB, 2013). A summary of the window properties used is shown in Table 5-2.

*Table 5-2 Window specifications used within the AccuRate building models. Properties were sourced from the built-in AccuRate Sustainability window library.*

Type	Key Characteristics	SHGC	U-value (W/m <sup>2</sup> K)	Maximum Opening Percentage
Sliding window or door	Aluminium single glazing clear	0.70	6.7	45%
Awning/hinged/bi-fold window	Aluminium single glazing clear	0.57	6.7	90%
Sliding window or door	Aluminium double glazing clear	0.59	4.8	45%
Awning/hinged/bi-fold window	Aluminium double glazing clear	0.51	4.8	90%

### 5.2.5 Infiltration and Ventilation Specifications

The default infiltration and ventilation models within the Chenath engine were used to model infiltration and ventilation within the simulated thermal performance assessments. The Chenath engine infiltration model is briefly described below.

Within AccuRate, the Chenath engine calculates the hourly infiltration rate using Equation (5-1), where  $A$  is the stack infiltration factor,  $B$  is the wind infiltration factor and  $v$  is the hourly mean wind speed (m/s) from the weather files multiplied by terrain and geometric factors (Chen, 2013).

$$I = A + B \cdot v \quad (5-1)$$

$A$  and  $B$  are calculated for each zone and are dependent on the building geometry, window seals, and ceiling penetrations specified within the building model (Chen, 2013; AccurateSustainability, 2018b). For a typical detached dwelling, an air change rate at 50 Pa of approximately  $15 \text{ h}^{-1}$  is the airtightness that would result from the use of this method, which was approximately equivalent to the average airtightness of the current existing detached housing stock in Australia (Ambrose and Syme, 2017).

Therefore, in accordance with the default method used in the Chenath engine, the coefficients  $A$  and  $B$  for each zone modelled in the apartments and the resulting modelled airtightness were determined by AccuRate as a function of the ceiling penetrations, window sealing, and building geometry of the apartments.

### 5.2.6 Climate Settings

In accordance with the mandatory NatHERS protocol, the Reference Meteorological Year (RMY) climate files supplied by NatHERS were used for the climate settings within the models.

NatHERS specifies RMY climate files corresponding to 69 Climate Zone classifications across Australia. Each RMY file consists of a concatenation of months taken from different years ranging from the 1970s to the 2000s that have been identified as ‘typical’ months for each Climate Zone to comprise a single year of weather data (Ren and Chen, 2018). The weather data includes dry-bulb air temperature, absolute humidity, atmospheric pressure, wind speed and direction, cloud cover, and direct and diffuse solar irradiation (Ren and Chen, 2018). The study cohort covered 3 different Climate Zone classifications:

- Climate Zone 24 – Canberra;
- Climate Zone 17 – Sydney RO (Sydney CBD); and
- Climate Zone 56 – Mascot (Eastern Sydney and Wollongong).

### 5.2.7 Internal Heat Load Settings

At the time of writing, NatHERS provides default settings for the dwelling internal heat loads that includes both latent and sensible heat generated by occupants, cooking, lighting, and electrical appliances (NatHERS National Administrator, 2019b). The heat loads were categorised for bedrooms, living spaces including kitchens, and living spaces without a kitchen.

In NatHERS, the internal heat loads for the above zone types within a dwelling model are determined by scaling a set of default internal heat loads based on the floor-area of the dwelling (Chen, 2018). The default internal gains in AccuRate are estimated from a 160m<sup>2</sup> dwelling that has 80m<sup>2</sup> of living areas and 80m<sup>2</sup> of bedroom areas. The dwelling is assumed to be occupied by two adults and two children and the internal loads are based on a single repeated daily occupancy profile. Tables for the hourly sensible and latent heat loads from each of the aforementioned sources could be found on the Chenath HSTAR Portal (Chen, 2016). These load settings were not modified within this study.

### 5.2.8 Heating and Cooling Logic

The simulations used the default thermal comfort and associated occupant behavioural strategies specified by NatHERS and were not modified. The thermal comfort zone boundaries and the accompanying heating, cooling, and natural ventilation algorithms set by NatHERS are described below.

#### 5.2.8.1 Heating Settings

The heating thermostat settings in NatHERS are dependent on the zone type and on the time of day. If the temperature in a conditioned zone drops below the heating thermostat settings within the scheduled heating hours, NatHERS software simulation will introduce additional heat into the zone to maintain the zone temperature at the appropriate thermostat temperature. A summary of the heating settings are presented in Table 5-3.

*Table 5-3 NatHERS Heating thermostat settings and heating schedules as a function of zone type.*

<b>Zone Type</b>	<b>Heating Thermostat (°C)</b>	<b>Heating Schedule</b>
Daytime (e.g. living, kitchen, hallway)	20	07:00 – 00:00
Night-time (e.g. bedrooms, ensuite)	18	07:00 – 09:00; 16:00 – 00:00
	15	00:00 – 7:00

#### 5.2.8.2 Cooling Settings

The cooling settings in NatHERS were significantly more sophisticated than the heating settings due to the need to model issues such as the greater potential for cooling using natural ventilation and the effect of indoor air movement (induced by open windows or ceiling fans) on the perceived

comfort of occupants during warmer weather. During simulations, the Chenath engine uses algorithms that maximise the use of natural ventilation, only invoking cooling when natural ventilation cannot maintain zone conditions within the NatHERS thermal comfort regions.

Within NatHERS, the thermal comfort region is based on a combination of the adaptive comfort model and the new effective temperature model (ET\*) described in Auliciems and Szokolay (2007). Together, these models account for the effects of indoor air temperature, relative humidity, air velocity, and mean radiant temperature (Ren and Chen, 2018).

The cooling thermostat temperature is set to the neutral temperature defined by the adaptive comfort model, calculated using the typical mean outdoor temperature in January for each NatHERS Climate Zone (Ren and Chen, 2018; Belusko *et al.*, 2019). Therefore, the cooling thermostat settings vary amongst the 69 NatHERS Climate Zones. The Cooling thermostat settings for each of the Climate Zones included in this study are presented in Table 5-4.

*Table 5-4 Cooling thermostat settings and natural ventilation trigger temperature for each of the NatHERS climate zones in this study (NatHERS National Administrator, 2012)*

<b>Climate Zone</b>	<b>Cooling Thermostat (°C)</b>	<b>Natural Ventilation Trigger Temperature (°C)</b>
17 – Sydney RO (CBD)	25.5	25.0
24 – Canberra	24.0	23.5
56 – Mascot (Wollongong, Sydney)	24.5	24.0

However, the thermal comfort region extends above the neutral temperature. The upper temperature limit is a function of moisture content of the air and the average indoor air speed. For air speeds less than 0.2 m/s, the upper temperature limit is defined as follows:

- Between humidity levels of 4 to 12 g<sub>water</sub>/kg<sub>dry air</sub>, the thermal comfort boundary is defined by the ET\* line passing through the cooling thermostat + 2.5°C at 50% relative humidity. A positive offset of 2.5°C from the neutral temperature corresponds to the upper 90% acceptability limits defined in the adaptive comfort model (ANSI/ASHRAE, 2017; Belusko *et al.*, 2019).
- For absolute moisture concentrations in the zone of less than 4 g<sub>water</sub>/kg<sub>dry air</sub>, the upper temperature limit is confined to the temperature of the aforementioned ET\* line corresponding to an absolute moisture content of 4 g<sub>water</sub>/kg<sub>dry air</sub>.
- The maximum moisture concentration is limited to 12 g<sub>water</sub>/kg<sub>dry air</sub>.

Above indoor air speeds of 0.2 m/s, the maximum moisture concentration is increased to 90% relative humidity and the thermal comfort boundary is recalculated as the ET\* line passing through the cooling thermostat + 2.5°C + ΔT, which is a function of the indoor air speed, v, as shown in Equation (5-2).

$$\Delta T = 6 \times (v - 0.2) - 1.6 \times (v - 0.2)^2 \quad (5-2)$$

To assist in the interpretation of these algorithms, a psychrometric chart depicting the NatHERS comfort region and extended comfort regions for Climate Zone 56 is provided in Figure 5-1 and the heating and cooling conditioning schedules are presented in Figure 5-2.

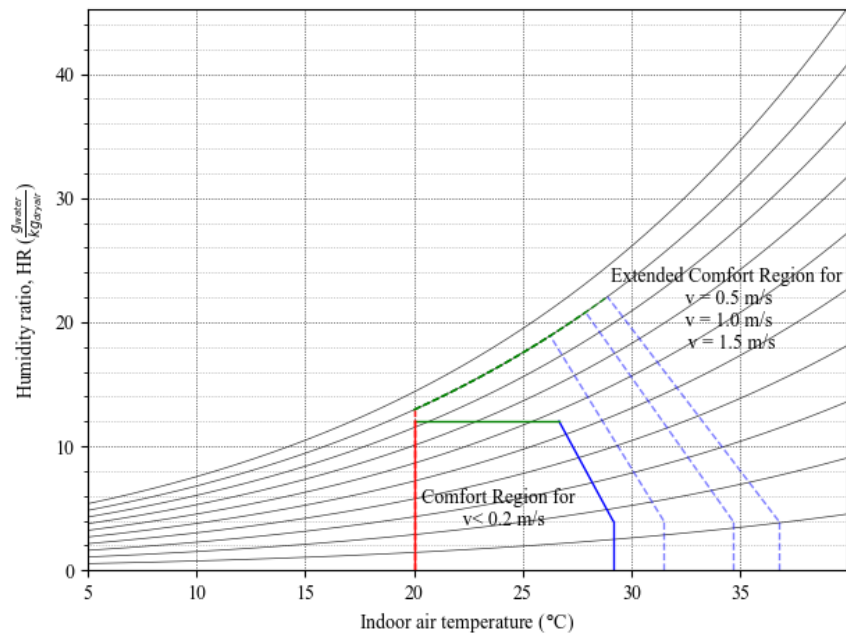


Figure 5-1 NatHERS software thermal comfort boundaries based on the climate in Wollongong and Eastern Sydney (Climate Zone 56; Neutral temperature = 24.5°C) for a living room during daytime active hours (07:00 – 00:00). The comfort region and extended comfort regions are presented for air speeds (v) of 0.2 m/s and 0.5, 1.0, and 1.5 m/s.

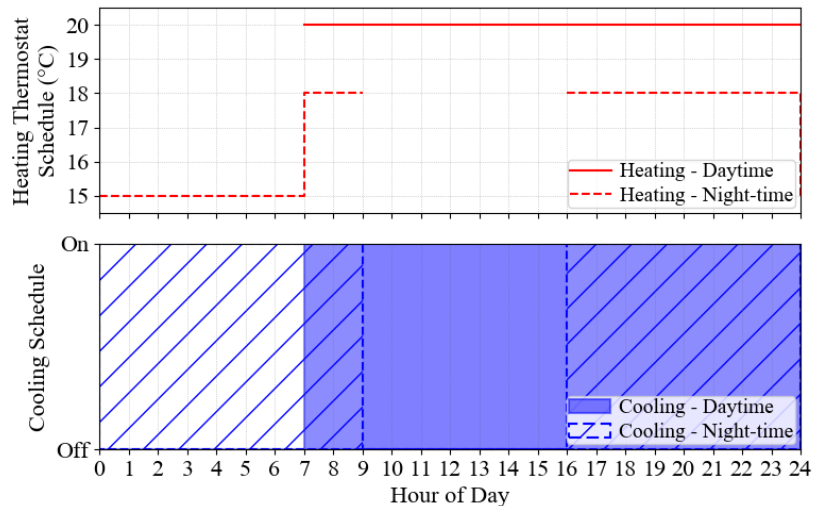


Figure 5-2 Heating and cooling schedules defined in NatHERS for daytime (e.g. living) and night-time (e.g. bedroom) zone types.



The cooling thermostat settings are equivalent for all zone types, although, like heating, the cooling conditioning schedules are governed by zone-type. In addition, the cooling thermostat settings are not defined in terms of a constant temperature set-point. Instead, they are a function of indoor humidity and indoor air speed as depicted (by way of an example) in Figure 5-1.

### Natural ventilation

The capability of natural ventilation to maintain zone conditions within the extended comfort region is evaluated at each time step by the Chenath engine before mechanical cooling is invoked.

Natural ventilation mode is activated when the zone temperature is above the natural ventilation trigger point, which is generally 0.5°C cooler than the cooling thermostat setting as demonstrated in Table 5-4, and when the outdoor temperature is less than 4°C warmer than the indoor temperature. NatHERS considers natural ventilation to be a viable form of cooling despite outdoor temperatures up to 4°C warmer than the zone temperature due to the additional perceived cooling effects of air movement.

If zone conditions still exceed the extended comfort region, any ceiling fans present in the zone are activated to augment the indoor air speed and the zone conditions are re-evaluated, accounting for the increased indoor air speed. If the zone conditions still exceed the extended comfort region then NatHERS considers natural ventilation incapable of maintaining comfort and closes all ventilation openings, deactivates fans, and supplies sufficient mechanical cooling to reduce the zone temperature to the cooling thermostat setting. Natural ventilation openings also have a lock-in period of three hours to eliminate unrealistically frequent opening and closing of windows (Delsante, 2005; AccurateSustainability, 2018a; Ren and Chen, 2018; Belusko *et al.*, 2019)

### Shading

NatHERS also prescribes algorithms for the operation of indoor and outdoor adjustable shading. The indoor shading was set as closed at 18:00 and opened at 07:00. However, if the outdoor temperature exceeded the cooling thermostat settings by more than 2.5°C, the solar irradiance on the glazing exceeded 200W/m<sup>2</sup>, and there was no adjustable outdoor shading, the indoor shading was set to be closed. The outdoor adjustable shading was closed if the outdoor temperature exceeded a given threshold outdoor temperature, which was typically 0.5°C below the cooling thermostat set-point. The outdoor adjustable shading was also closed if the solar irradiance on the glazing exceeded 75W/m<sup>2</sup>.

All windows in the apartments were modelled with 'Holland blinds' for internal adjustable shading as required by NatHERS. None of the windows in the case-study apartments featured outdoor adjustable shading.

### **5.3 Measured vs Simulated Performance Comparison: Methodology**

The measured thermal performance of the apartments characterised and quantified in Chapter 4 was compared against the simulated thermal performance of the apartments, determined using the NatHERS building performance simulation process described in Section 5.2. The primary purpose of the comparison was to understand whether apartments were using more or less energy for heating and cooling in reality than anticipated by NatHERS software, and whether the thermal performance characteristics were well represented by NatHERS default assumptions and settings.

Energy consumption for heating and cooling was the primary metric used to compare the simulated and measured thermal performances. The thorough characterisation of the thermal performance characteristics of the apartments in Chapter 4 then made possible a diagnostic analysis of the causes of the differences between the measured and simulated heating and cooling consumption. This analysis examined the following parameters as possible causes of the difference in the measured and simulated thermal performance of the apartments:

- Indoor environmental conditions;
- Occupant behaviour;
- Weather conditions; and
- Building envelope performance.

The aim was to develop a better understanding of the causes of differences between measured and simulated heating and cooling loads, which would then inform potential changes to the NatHERS assessment process to better simulate real thermal performance of apartments, and improve design guidance/legislation in the NCC.

Due to various operational reasons, the apartments were not monitored for an entire year. Thus, simulated thermal performance results were filtered to align with the corresponding monitoring period for each apartment. (The monitoring periods and the proportion of the heating and cooling season within each has been previously presented in Section 4.2 above.)

#### **5.3.1 Heating and Cooling Energy Methodology**

Energy consumption for heating and cooling was the core metric to assess and compare the measured and simulated thermal performances of the apartments. Both simulated and measured energy consumption were normalised by floor area to allow comparison between dwellings within the present cohort, and to compare with other studies.

The measured electrical energy consumption of the air conditioners over the monitoring period was converted into thermal energy by assuming a constant coefficient of performance (COP) and

energy efficiency ratio (EER). The COP and EER were obtained from the relevant manufacturer specifications for the specific air conditioner model used in each apartment and are provided in Table 5-5. These were based on the Minimum Energy Performance Standards (MEPS) testing conditions of outdoor temperatures of 7°C and 35°C for heating and cooling, respectively. The method used to determine the air conditioner operating mode (i.e. heating or cooling) is described in Section 3.4.2. It should be noted that COP and EER values will vary in reality due to variations in indoor and outdoor environmental conditions as well as the installation details of the air conditioner. The level of variation can be significant. For example, Winkler (2011) determined that the COP of a particular residential heat-pump varied from approximately 2.5 to 3.5 when outdoor temperatures increased from 0°C to 15°C. During testing, indoor temperatures were kept constant at 20°C. However, the MEPS testing used to determine the manufacturer COP and EERs are intended to represent conditions when heat pumps are generally likely to be in use, which reduces the likelihood of significant variations in the COP and EER from the MEPS values in practice.

The electrical energy consumed by the air conditioner during standby operation was omitted from this analysis as the focus was on comparing the measured and modelled thermal energy consumption of the apartments.

*Table 5-5 Manufacturer EER and COP values for the air conditioning systems identified in each apartment.*

<b>Apartment ID</b>	<b>EER</b>	<b>COP</b>
1	2.82	3.42
2	3.89	4.76
3	3.78	4.37
5	3.79	3.95
6	3.28	3.53
7	3.33	4

### **5.3.2 Indoor Environmental Conditions Comparison Methodology**

Heating and cooling use changes the indoor environmental conditions to suit the thermal preferences of occupants. Hence, any differences in the measured and simulated heating and cooling consumption could be a result of different occupant acceptance of indoor environmental conditions rather than as a result of other factors that directly influence the heat balance of the dwelling.

Thus, the differences in the indoor environmental conditions were examined to explore:

- how well the simulated indoor environmental conditions aligned with real conditions during occupied periods; and

- potential links between the indoor environmental conditions chosen (or tolerated) by the occupants and the resulting heating and cooling loads.

The indoor environmental conditions in the living rooms and bedrooms were defined as the hourly average temperature and humidity.

The measured data was filtered to exclude unoccupied periods to reduce the impact of occupancy schedules on the comparison of the indoor environmental conditions chosen (or tolerated) by the occupants. Similarly, the simulated indoor conditions for the bedroom and living room were filtered to only include conditioned hours, which are indicated by the daily schedules presented in Figure 5-2.

Finally, the measured indoor conditions were assessed in terms of the exceedance rates of the upper and lower thermal comfort boundaries defined by NatHERS in order to deduce whether increased or decreased measured heating or cooling consumption relative to the simulated consumption logically aligned with changes in the indoor conditions chosen (or tolerated) by the occupants. The comparison was limited to measurements of the indoor environments to within the NatHERS scheduled conditioned hours for each zone to minimise the impact of diurnal temperature oscillations and occupancy schedules.

### **5.3.3 Occupant Behaviour Impact on Energy Consumption Methodology**

In this context, occupant behaviour refers to comfort management strategies used by occupants in the pursuit of thermal comfort, resulting in the use of heating, cooling, or natural ventilation. However, it is acknowledged that other occupant behaviour such as occupancy schedules and internal heat gains also impact heating and cooling practices.

Therefore, the purpose of this comparison was to evaluate how differences in the comfort management strategies contributed to differences in measured and simulated heating and cooling consumption. This comparison was limited to use of air conditioning and natural ventilation.

While it was likely that differences in the shading usage patterns also contributed to differences in the measured and simulated cooling loads, shading use was not measured. Discussions with occupants indicated that they did adjust shading (such as curtains and blinds) to manage cooling loads, however, it was not possible to specifically quantify the degree to which shading was used.

The internal heat gains caused by appliances, the presence of occupants, and occupant activities were not quantified during the study due to monitoring constraints (i.e. reducing disruption to occupants). Therefore, differences in the measured and simulated internal heat gains assumed within each of the apartments was not evaluated, but was acknowledged as an additional source of difference.

### 5.3.3.1 Air Conditioning and Natural Ventilation Practices

Air conditioning and natural ventilation practices in reality have already been characterised in Section 4.5.1. It was previously established that low utilisation of natural ventilation correlated with high air conditioning use for cooling.

Mechanical heating and cooling use in reality relative to the heating and cooling logic defined in the NatHERS protocol was previously quantified and discussed in Section 4.5.2.

The significance of the assumed use of natural ventilation in the NatHERS protocol on simulated cooling consumption was evaluated by simulating the apartments without natural ventilation and quantifying the resulting increase in simulated cooling consumption.

### 5.3.3.2 Occupancy (Vacant Periods)

While NatHERS assumes that dwellings are always inhabited, and that the zones occupied by occupants shifts as a function of the time of day, as shown in Figure 5-2, it was observed in reality that apartments were intermittently unoccupied. Hence, the measured heating and cooling consumption were attenuated relative to the resulting loads, if the dwellings had been continuously occupied.

It was not possible to extrapolate measured air conditioning consumption to account for unoccupied periods. However, the effect of vacant periods could be accounted for by quantifying the simulated consumption while excluding dates when the apartments were unoccupied. For this comparison, unoccupied periods were considered to be those denoted “holiday periods” as defined in Section 3.9.1.2. The impact of daily occupancy schedules more generally, i.e. those inferred from the Occupancy detection algorithm described in Section 3.9 on the heating and cooling consumption was not explicitly quantified within this study.

## 5.3.4 Weather Data Impact on Energy Consumption Methodology

Actual heating and cooling energy consumption in the apartments would naturally be affected by differences between the weather conditions in reality and those assumed in simulation software.

Thus, the purpose of this analysis was to determine the impact of using weather conditions of the NatHERS RMY files, rather than using actual weather conditions.

The two main tasks involved were as follows.

- To characterise the weather conditions contained in the NatHERS RMY weather files and the real weather conditions measured by the BOM between April 2018 and March 2019.
- To determine the change in simulated heating and cooling consumption as a function of the weather conditions used in the simulation.

### 5.3.4.1 Comparison between Real Weather Conditions and NatHERS Weather files

The nine apartments in the study cohort were located in Canberra, Sydney CBD, Eastern Sydney, and Wollongong. These corresponded to four of the Bureau of Meteorology’s (BOM) Weather Stations across three NatHERS Climate Zones as shown in Table 5-6, from which the real weather data and RMY weather data were sourced.

*Table 5-6 List of weather data sources for the measured weather data (BOM) and NatHERS Climate Zones corresponding to each of the monitored regions.*

Location	BOM Weather Station Location	NatHERS Climate Zone
Canberra	Tuggeranong	CZ 24 – Canberra
Sydney CBD	Sydney – Observatory Hill	CZ 17 – Sydney RO
Eastern Sydney	Sydney Airport	CZ 56 – Mascot
Wollongong	Bellambi	CZ 56 – Mascot

Due to different day-to-day weather conditions, it was not appropriate to compare the two weather sources using time-series or prediction-based assessments such as root-mean-square error (RMSE) or mean absolute error. The most appropriate metric was determined to be the total heating and cooling degree days (HDD/CDD) observed over a period coincident with the monitoring periods. Heating and cooling degree days were calculated using a base temperature of 18°C, which is one of the two base temperatures for cooling and heating specified on the BOM website (Bureau of Meteorology, 2020). The cumulative totals of HDDs and CDDs of the BOM Weather Stations and RMY weather files for the locations listed in Table 5-6 between April 2018 and March 2019 are presented in Figure 5-5.

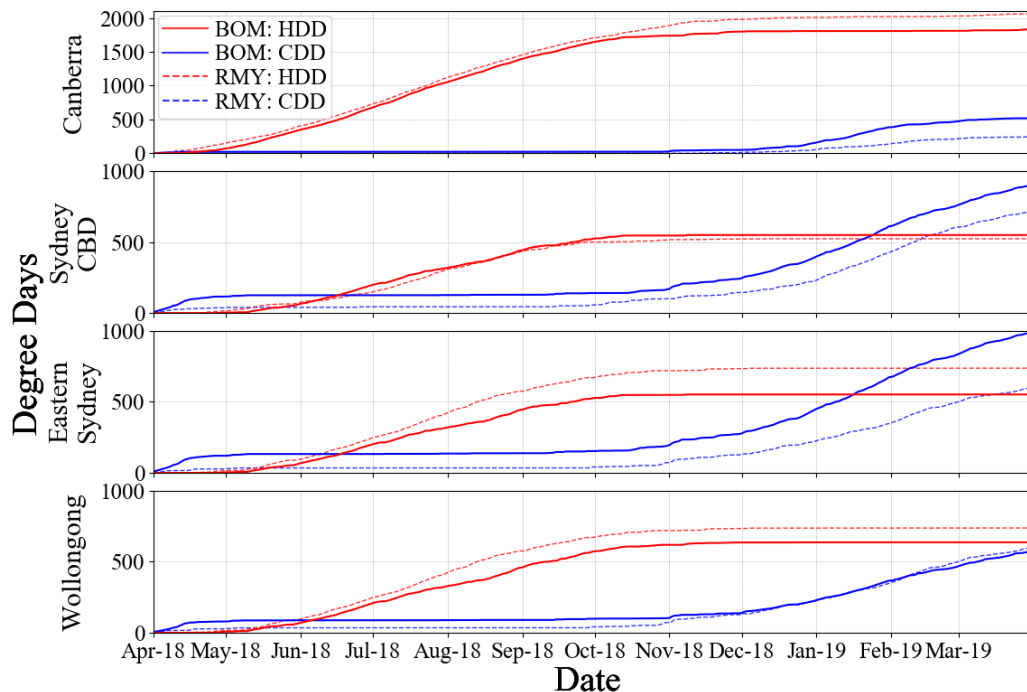


*Figure 5-3 Comparison of the cumulative heating and cooling degree days from BOM data between April 2018 and March 2019 and within the Representative Meteorological Year (RMY) climate files used within NatHERS.*

On average, the real weather measured by the BOM Weather Stations had 51% more cooling degree days (CDDs) and 12% fewer heating degree days (HDDs) within the period between April 2018 and March 2019 as compared to the RMY Weather Files used by NatHERS.

However, there was considerable variance amongst the comparisons for individual locations. For example, Bellambi observed 4% fewer CDDs than included in Climate Zone 56 (Mascot) whilst Sydney Airport observed a 66% increase in CDDs despite also being in Climate Zone 56 (Mascot). In fact, the weather at Sydney Airport aligned much more closely to the RMY file for Sydney CBD (Climate Zone 17) than to Mascot and experienced similar weather to Observatory Hill. Thus, as an aside, the Climate Zone boundaries used within NatHERS may not accurately represent the geographical variation of the climate and may therefore be a potential cause of misalignment between heating/cooling loads predicted by NatHERS and actual loads.

In summary, it was anticipated that the simulated cooling loads would increase substantially in Canberra and Sydney but remain similar in Wollongong and that the simulated heating loads would decrease slightly for all locations except for Sydney CBD under real weather conditions as compared to the NatHERS RMY weather files.

#### 5.3.4.2 Creation of NatHERS Weather Files from Real Weather Data

In order to simulate the apartments using some elements of real weather data within AccuRate, the real weather data was processed to match the file structure of the RMY files. This required a complete set of 8760 hourly measurements of dry-bulb air temperature, absolute humidity, atmospheric pressure, wind speed and direction, cloud cover, and direct and diffuse solar irradiation to comprise a full year for each of the four distinct apartment locations.

The dry-bulb air temperature, absolute humidity, wind speed, and wind direction measurements were sourced directly from the BOM's weather stations nearest to each of the four locations in Table 5-6. Sub-hourly temperature, humidity, wind speed, and wind direction measurements were averaged on an hourly basis.

Global horizontal irradiance (GHI) and direct normal irradiance (DNI) measurements were sourced from hourly solar radiation data in grid format that had been processed by the BOM from satellite images recorded using the Himawari-8 satellite that were provided by the Japan Meteorological Agency (JMA). This data provided high accuracy estimations of solar irradiance across Australia at 0.05° latitude and longitude resolution. Details of how the BOM determined the GHI and the DNI from the satellite images are described in short metadata reports that are available on the BOM website (Bureau of Meteorology, 2019b).

The Direct Horizontal Illuminance (DHI) was calculated using the rearranged form of Equation (5-3), where  $\alpha$  is the solar azimuth angle at the time of the measurement. The solar azimuth angle

for each hour was determined using Python library *PySolar*, which required the local time of measurement and the location latitude, longitude, and elevation. Each of these parameters were provided within the data supplied by the BOM.

$$I_{DNI} = \frac{I_{GHI} - I_{DHI}}{\sin \alpha} \quad (5-3)$$

While the datasets for the dry-bulb air temperature were generally complete, there was missing data for absolute humidity and wind conditions. Missing data was first filled by checking the BOM's next nearest alternative station and extracting the data if it was present. Additional missing data was filled via linear interpolation if the time period of a continuous series missing data was less than 12 hours. Less than 0.104% of the hourly measurements were determined via interpolation. Less than 0.245% of the solar data was missing, of which approximately 50% occurred overnight. Missing solar energy data was substituted by taking the average of the solar radiation at the corresponding time of day within the previous and following week.

The completed sets of real weather data from 01<sup>st</sup> April 2018 to 31<sup>st</sup> March 2019 were compiled then converted into the NatHERS file structure, which were successfully able to be interpreted by AccuRate. The results comparing the measured thermal performance of the apartments to the simulated thermal performance using RMY weather data and using real weather data are presented in Section 5.5.4.

### **5.3.5 Building Envelope Airtightness Impact Methodology**

As previously stated in Section 5.2.5, the typical airtightness resulting from the use of the NatHERS infiltration specification method was around 15 air changes per hour at 50 Pa for a typical Australian detached dwelling. While this value was shown to be representative of the detached dwelling stock of Australia, the on-site blower door testing of the apartments, presented in Section 4.6.1, indicated that the apartments were considerably more airtight than Australian detached dwellings on average. Therefore, the NatHERS default method, described in Section 5.2.5, was anticipated to underestimate the actual airtightness of the apartments, leading to excessive infiltration during the simulations, which would contribute to the differences between the measured and simulated heating and cooling consumption of the apartments.

While the *in-situ* airtightness of a dwelling cannot be known prior to its construction (i.e. for the purposes of an energy performance assessment as part of a Development Application), the underlying proposition to be tested here was that if Australian apartments are significantly more airtight than detached dwellings (as suggested by the findings of this study), then the NatHERS default method may require some modifications to better represent the actual airtightness of apartment dwellings.



The two main tasks to assess the impact of the airtightness specifications on the difference between the measured and simulated thermal performance were therefore:

- to incorporate the airtightness results from the on-site blower door testing into AccuRate; and
- to determine the change in the simulated heating and cooling consumption as a function of the airtightness of the dwellings specified in the simulation.

#### 5.3.5.1 Specification of Airtightness within AccuRate

The procedure described in Building Code Energy Performance Trajectory - Interim Technical Report Appendix G (Bannister *et al.*, 2018) was used to modify the airtightness of the apartments modelled within AccuRate to more closely match the airtightness measured through on-site blower door testing.

For this method, a target natural infiltration rate for each apartment was derived from the air change rate at 50 Pa measured during the blower door tests of each apartment using the relationship determined by Sherman (1987) shown in Equation (5-4), where ACH is the natural air change rate and ACH<sub>50</sub> is the air change rate at 50 Pa provided from the blower door test.

$$ACH = \frac{ACH_{50}}{20} \quad (5-4)$$

Although this is a very simple expression that does not account for many possible influences, this correlation has been widely used in previous studies to provide an estimate of the actual mean infiltration rate.

The Chenath engine then was used to determine initial values of coefficients *A* and *B* in Equation (5-1) for each zone based on the window sealing and ceiling and window penetrations specified within the building model, as performed in the default method.

The hourly natural air change rate for each zone was then calculated using Equation (5-1) using the initial values of the coefficients *A* and *B* and the hourly wind speed extracted from the Climate Zone 56 RMY weather file. Terrain and building geometry factors were also included. The resulting average annual natural air change rate of the dwelling was then calculated as the volume weighted average from each zone. The average annual natural air change rate of the dwelling was then compared to the target natural air change rate, and wall vents and window sealing parameters in the model were modified iteratively until the natural air change rate was within 5% of the desired natural air change rate.

In some cases, the measured air change rates of the apartments were too low to be numerically achieved by modifying infiltration paths within AccuRate . In such cases, it was possible to

manually specify the coefficients  $A$  and  $B$  to achieve the target natural infiltration rate. The appropriate values for coefficients  $A$  and  $B$  to achieve the target average annual natural air change rate were determined by following the same approach as mentioned above, but manual specification enabled the modeller to bypass the minimum values that could be specified within AccuRate using the user interface. In cases where these coefficients were manually specified, the ratio between stack and wind driven infiltration factors (i.e. between coefficients  $A$  and  $B$ ) that was achieved within AccuRate was conserved.

### 5.3.5.2 Comparison of Simulated Apartment Airtightness

The simulated airtightness of the apartments, expressed as air change rates at 50 Pa determined using Equation (5-4), resulting from: i) NatHERS default method and ii) the NCC Trajectory Method are presented in Table 5-7. Also shown is the airtightness of the apartments determined by on-site blower door testing.

*Table 5-7 Simulated airtightness (expressed as air change rates at 50 Pa) for each apartment determined by: i) the NatHERS default method, and ii) NCC Trajectory Project method. Also shown is the measured air change rate at 50 Pa.*

<b>Apartment ID</b>	<b>NatHERS default Method</b>	<b>NCC Trajectory Method</b>	<b>On-site blower door testing</b>
1	11.98	5.05	5.3
2	8.96	4.61	3.2
3	12.87	9.48	9.8
4	10.59	12.4	12.8
5	9.79	4.16	4.3
6	9.12	4.78	2.5
7	15.13	7.12	7.1
8	8.80	3.89	3.5
9	8.50	4.20	4.7

The average air change rates at 50 Pa using the NatHERS default method and the NCC trajectory method were  $10.6 \text{ h}^{-1}$  and  $6.2 \text{ h}^{-1}$ , respectively, which were 80% and 5% greater than the average air change rate at 50 Pa determined via on-site blower door testing. Thus, the NCC Trajectory method was able to substantially improve the alignment between the measured infiltration rate and the infiltration rate assumed within the simulations. The change in the simulated heating and cooling loads resulting from each of the two airtightness specification methods is presented in Section 5.5.5.

## 5.4 Model Validation and Calibration

The Chenath simulation engine has previously been analytically verified for simple cases and has been validated through inter-program performance comparison using the International Energy Agency (IEA) BESTEST protocol (Delsante, 2005; Ren, Chen and James, 2018). The NatHERS protocol, using the Chenath engine, prescribes specific methods to model spaces adjacent to the

apartments (e.g. neighbouring apartments, conditioned and unconditioned corridors, elevator shafts, etc.). These methods were not modified during model calibrations detailed in this section.

The simulation models developed for each of the apartments were calibrated against measured data using a form of parametric analysis to ensure that parameters used in the models closely matched those in the real buildings. This process was based on the calibration procedure provided as part of Option D in the International Performance Measurement and Verification Protocol (IPMVP) (U.S. Department of Energy, 2002), which involves the use of computer simulation software. This procedure was adapted to be applicable to residential buildings rather than commercial buildings, for which the protocol is originally developed. The adaptations included calibrating the simulation models against unoccupied measurement periods and using the deviation between simulated and measured hourly mean zone temperatures as the key metric to quantify the degree of alignment.

Unoccupied periods were used to calibrate the models to remove the effects of occupants, which introduce significant uncertainty, as acknowledged in the IPMVP (U.S. Department of Energy, 2002). This is potentially more important in the case of residential buildings rather than commercial buildings, where occupants are significantly less likely to follow a regular schedule of activities and operations. During unoccupied periods the apartments were free-running. Therefore, indoor temperature difference was used to compare the simulations against measurement data. The exact metric used to assess the fit of the models was the average root mean square error of the hourly indoor temperature in the living room and main bedroom, i.e. where  $RMSE_{ave} = (RMSE_{liv} + RMSE_{bed})/2$ .

In a typical NatHERS simulation, operable windows and shading devices are opened and closed to maintain indoor thermal comfort in accordance with the logic defined in the NatHERS protocol. However, in order to represent an unoccupied period, window and shading controls were disabled. Since the initial state of all windows and all shading devices were not known at the commencement of unoccupied periods, simulation cases were run that assumed windows were either all open or all closed and similarly, that operable shading devices were either all open or all drawn. Modelling the windows and shading devices as either all open or all closed, instead of considering the state of each window and shading device individually, was considered to be a satisfactory way of representing the most likely state of most of the windows and shading devices in the apartment and significantly reduced the required number of simulations.

The method for calibrating the simulation models involved the following steps.

1. Develop the simulation models for each of the apartments using AccuRate in accordance with the NatHERS Assessor Handbook (Department of the Environment and Energy, 2019b). The geometries and initial building envelope characteristics specified in these

models were based on information collected during the energy efficiency inspections to match the actual characteristics of the apartments as much as possible, including airtightness.

2. Simulate the free-running annual thermal performance of the models using actual weather data. Where it was not possible to visually confirm the construction details, in particular the building envelope elements, a range of simulations were run varying the properties of the envelope as shown in Table 5-9. Note that operational parameters controlled by occupants (i.e. the states of operable windows and shading) were assumed to be fixed/constant.
3. Identify the longest period in the measured data when the apartments were unoccupied i.e. the longest “holiday period” as described in Section 3.9.1.2.
4. Calculate the root mean square error (RMSE) between the simulated and measured hourly mean indoor temperatures within monitored zones (living and main bedroom) for each simulation case during the longest unoccupied period, then calculate the average RMSE of the monitored zones.
5. Identify the simulation case with the minimum average RMSE ( $RMSE_{ave}$ ). The building envelope characteristics used in these simulation cases were adopted in the calibrated models. For the apartments where specific details could be visually confirmed during the energy efficiency inspections (e.g. witnessing that the external cladding was brickwork), then the case with the minimum  $RMSE_{ave}$  that contained these known details was selected.

Note that the NatHERS protocol using the Chenath engine prescribes specific methods to model spaces adjacent to the apartments (e.g. neighbouring apartments, conditioned and unconditioned corridors, elevator shafts, etc.). These methods were not modified during the calibration process.

Table 5-8 Parameters varied during calibration to identify the most realistic properties of the building envelope.

Parameter	List of Values
Heating and cooling	Off (i.e. free-running)
Ventilation openings	Always open, always closed
Adjustable shading	Always open, always closed
Internal heat gains	None
Infiltration Rate <sup>1</sup>	NCC Trajectory Method within AccuRate (see Section 5.3.5.1), NCC Trajectory Method with manual specification (see Section 5.3.5.1),
Insulation layer thickness [mm] <sup>2</sup>	External walls: 38, 76, 102; Intertenancy walls: 25, 50; Floors below ground-floor apartments: 33, 66
Thermal mass layer material and thickness	In floors: Concrete: 100 mm, 150 mm, 200 mm In walls <sup>3</sup> : Concrete blockwork: 140 mm unfilled, 140 mm fully core-filled AAC panel: 50 mm, 75 mm Generic extruded brickwork: 110 mm

<sup>1</sup> The infiltration rates used in the models are inferred from the blower door measurements of the apartments. Refer to Section 5.3.5.1 for more information about the method variants used to set the infiltration rate in the models.

<sup>2</sup> Insulation material was assumed to be glass wool batt insulation with a thermal conductivity of 0.044 W/mK.

<sup>3</sup> The thermally massive material was assumed to be the same in external and intertenancy walls.

While the IPMVP does not define an acceptable RMSE between the measured and predicted indoor temperatures when calibrating a building model, it does advise that space temperatures “be examined to ensure they reasonably match the typical range of indoor conditions during occupied and unoccupied days”. In this study, this was taken a step further by comparing the time-series of simulated and measured hourly mean temperatures.

Similar methods have been used in previous studies to calibrate free-running building models. For example, Daniel, Soebarto and Williamson (2015) used the Coefficient of Variation of Root Mean Square Error – CV(RMSE) as their metric to assess the level of agreement between predicted and measured indoor temperatures when calibrating free-running building performance simulation models. CV(RMSE) is a very similar metric to RMSE. The only difference is that CV(RMSE) is calculated by dividing the RMSE by the average measured variable, which was indoor temperature in their study. CV(RMSE) is more commonly applied when comparing modelled and measured energy use (U.S. Department of Energy, 2002; ASHRAE, 2014), where RMSE alone may not adequately describe the agreement in the data because mean energy consumption (for a given time period) may vary by orders of magnitude amongst different buildings and relative differences are significant. Daniel, Soebarto and Williamson (2015) utilised

a CV(RMSE) of 15% as their threshold to assess whether a calibrated model sufficiently matched measured data. Assuming a measured mean indoor temperature of 22°C, this is equivalent to an RMSE of 3.3°C. Similarly, the IPVMP specifies that a CV(RMSE) of between 10 to 20% indicates satisfactory agreement between the energy consumption predicted by a candidate model and measurements. However, temperature, when stated in degrees Celsius or Fahrenheit, is expressed with respect to an arbitrary zero, which means CV(RMSE) in these scales would not express a meaningful relative difference in the view of the present author. For this reason, RMSE, rather than CV(RMSE), has been used as the evaluation metric in this study.

Each apartment was simulated under 1440 different combinations of the parameters stated in Table 5-8, totalling 12,960 simulations. The minimum values of  $RMSE_{ave}$  between the simulated and measured hourly mean indoor temperatures are presented in Table 5-9, and the parameters corresponding to those cases are presented in Table 5-10. In all cases, the minimum  $RMSE_{ave}$  was less than 2.5°C, which is significantly below the indicative threshold of 3.3°C adopted by Daniel, Soebarto and Williamson (2015).

The time-series of the measured and modelled hourly indoor temperatures for the longest unoccupied periods are presented in Figure 5-4.

Potential causes for the remaining differences between the calibrated simulation model and the measured data include the following.

- Internal gains from appliances (such as fridges, etc.) were not considered during the calibration models.
- While the calibration models assumed that operable windows and shading devices were either all fully open or all closed, it is possible that occupants left some blinds partially drawn or some windows open while the apartment was unoccupied.
- Mean natural infiltration rates in apartments may not necessarily be equal to the air change rate at 50 Pa (n50) in the same relationship posed by Sherman (1987), i.e. Equation (5-4). The relationship originally developed by Sherman was derived using experimental data from detached dwellings that may not behave in the same way as apartments.
- NatHERS rules for modelling heat transfer between the apartment being rated and neighbouring apartments and common spaces (which are covered in Section 5.2.2) are simplified to facilitate a fair comparison between ratings of different apartments and do not necessarily represent realistic heat transfer.

Due to these remaining differences, there remains some degree of uncertainty in comparisons between results generated from the calibrated models and measurements from the apartments.

Therefore, as with all comparisons between experimental data and corresponding simulations, these simulation results need to be interpreted with appropriate caution.

*Table 5-9 RMSE between the calibrated models and measurements during the longest unoccupied period for hourly indoor temperatures in the bedroom and living room. Note that the calibrated model corresponds to the parameter set with the minimum value of  $RMSE_{ave}$ .*

Apartment	$RMSE_{bed}$ in bedroom ( $^{\circ}C$ )	$RMSE_{liv}$ in living ( $^{\circ}C$ )	Minimum $RMSE_{ave}$ ( $^{\circ}C$ )
1	1.91	2.91	2.41
2	1.77	1.35	1.56
3	0.62	3.11	1.87
4	2.05	2.25	2.15
5	1.90	1.70	1.80
6	1.74	2.38	2.06
7	1.11	N/A	1.11
8	1.59	0.93	1.26
9	1.63	1.90	1.77

*Table 5-10 Building envelope characteristics for the calibrated models used in each apartment.*

Apartment	Infiltration specification method	Insulation thickness (mm)			Concrete slab thickness (mm)	Primary wall construction material
		External wall	Intertenancy wall	Under-floor		
1	Within AccuRate	102	50	66	200	75 mm AAC panels
2	With manual specification	102	25		150	140 mm Concrete core-filled blockwork
3	Within AccuRate	102	25		200	110 mm Brick
4	Within AccuRate	38	25		200	110 mm Brick
5	With manual specification	38	25	33	100	75 mm AAC panels
6	With manual specification	102	25		150	75 mm AAC panels
7	With manual specification	102	50		100	75 mm AAC panels
8	With manual specification	102	25		200	140 mm Concrete blockwork (fully core-filled)
9	With manual specification	102	25	33	200	140 mm Concrete core-filled blockwork

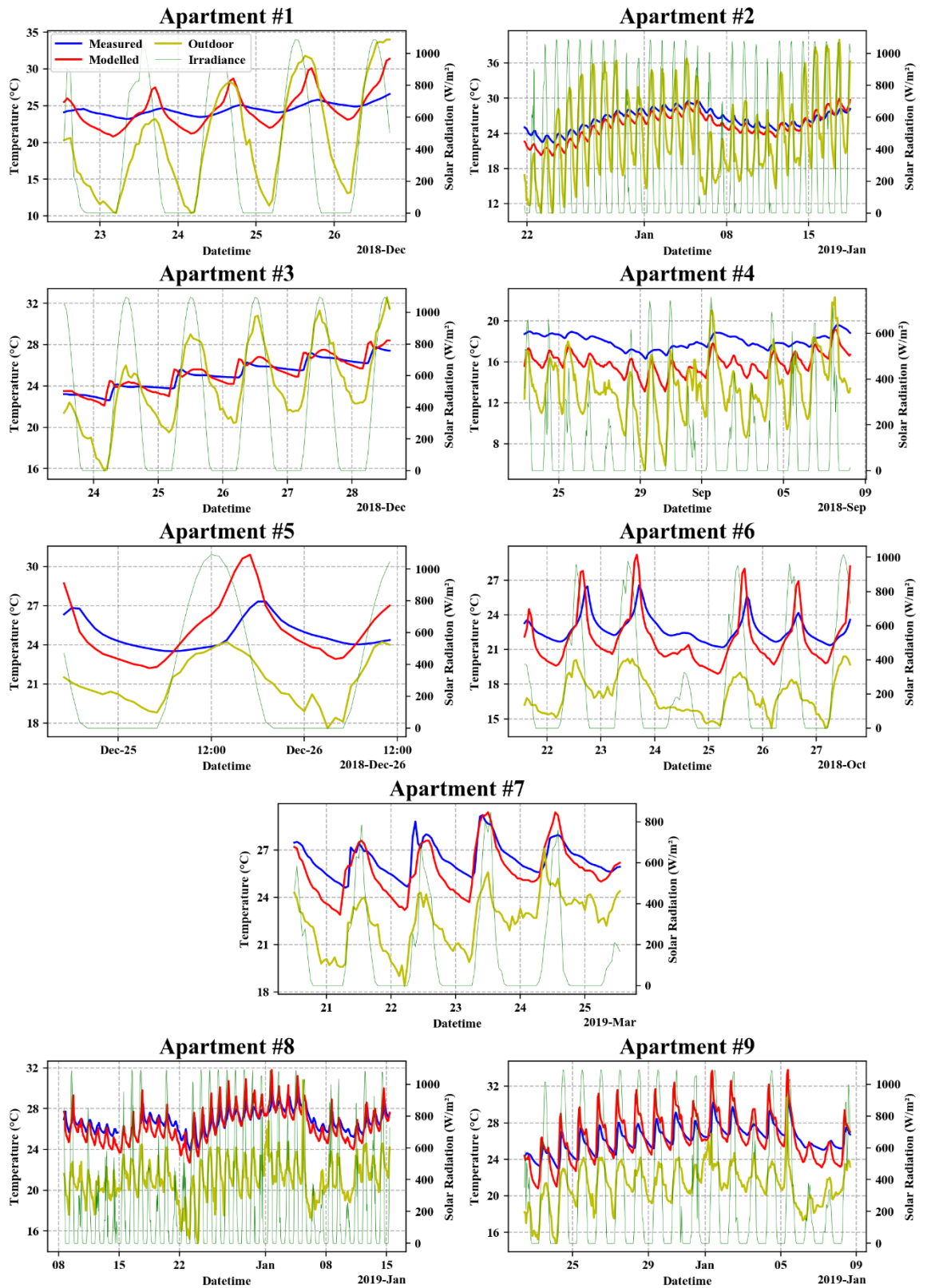


Figure 5-4 Comparison of modelled indoor air temperature from the calibrated models with measured air temperature during the longest unoccupied period in each apartment. Outdoor temperature and global horizontal irradiance are also shown.



## 5.5 Measured vs Simulated Performance Comparison: Results and Discussion

The actual thermal performance of the nine apartments within the study cohort, in particular, the six air conditioned apartments, were compared against the thermal performance of their representative simulated counterpart using default NatHERS simulation assumptions and settings. The primary purpose of the comparison was to quantify the degree to which the actual thermal performance of occupied apartments met or exceeded legislative requirements. The second objective was to assess the level of uncertainty in NatHERS simulations that could be attributed to default assumptions of key inputs specified in the NatHERS protocol.

### 5.5.1 Heating and Cooling Energy Results

Heating and cooling loads were the primary metrics used to compare the measured and simulated thermal performances of the six air conditioned apartments. The average measured and simulated heating, cooling and combined loads are presented in Figure 5-5 and the individual measured and simulated heating and cooling loads for each of the six air conditioned apartments are shown in Figure 5-6. The monitoring period date ranges and the fraction of heating and cooling seasons observed within the monitoring period are presented in Table 4-1.

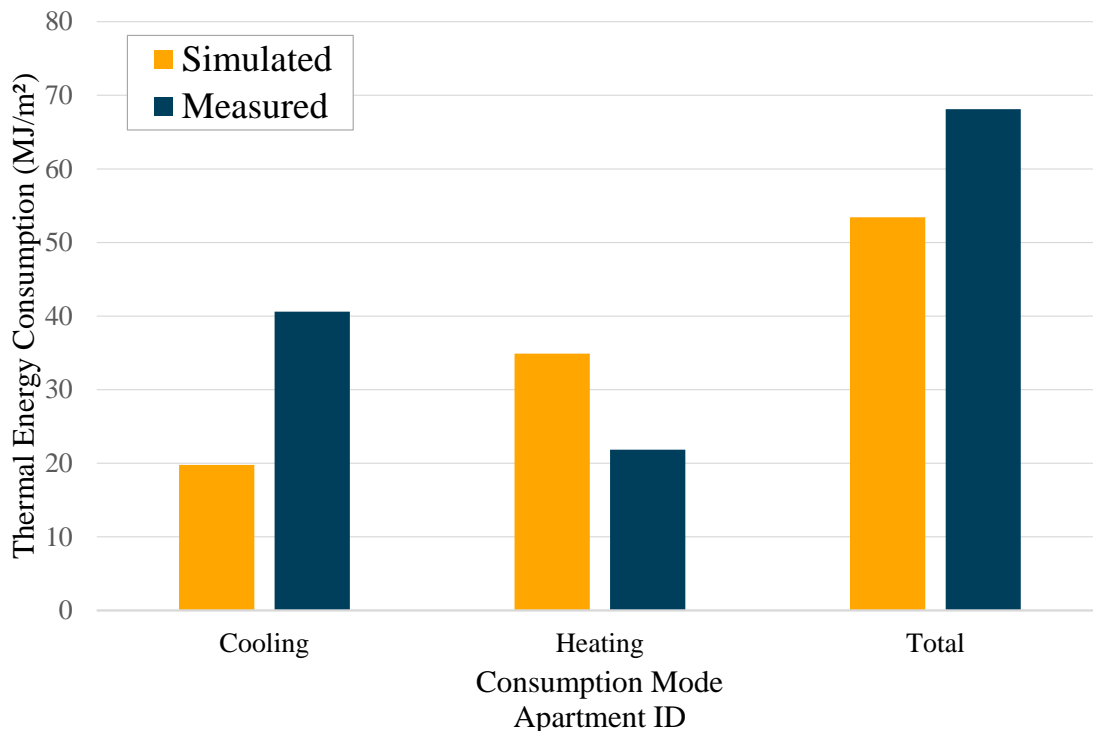


Figure 5-5 Average measured thermal energy consumption of the air conditioned apartments compared to NatHERS simulations performed in accordance with the NatHERS protocol.

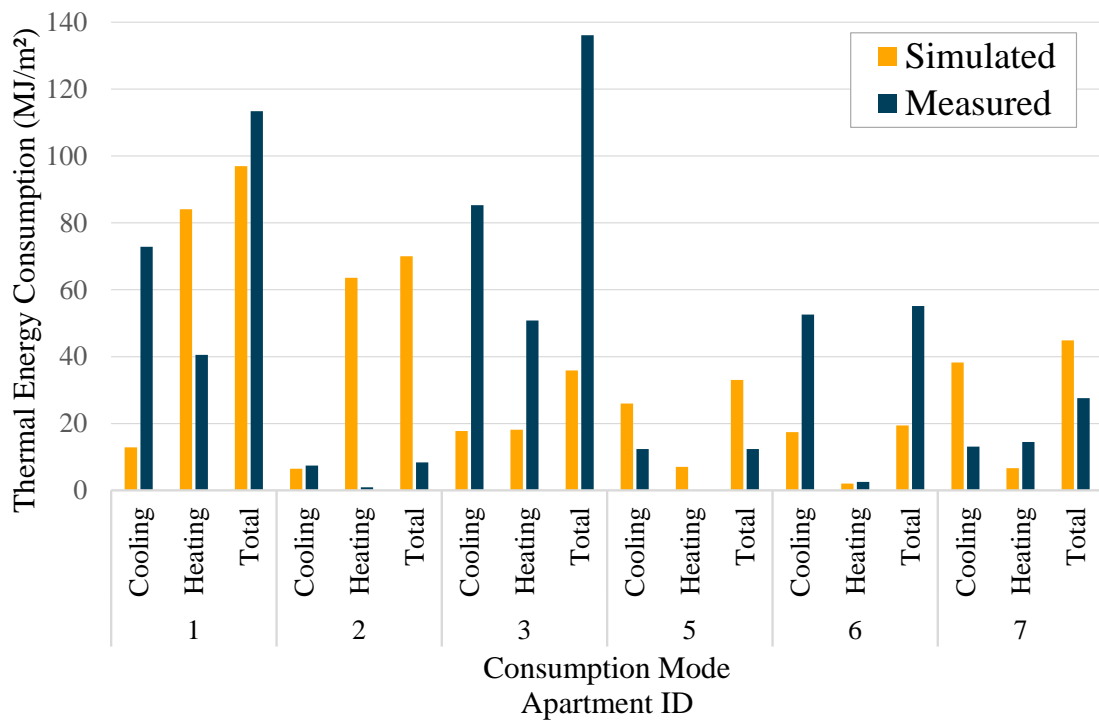


Figure 5-6 Comparison of the measured and simulated thermal energy consumption during the monitoring period using default input assumptions within AccuRate. Only apartments in which the air conditioning energy was individually monitored are shown.

### Cooling

The average measured cooling energy was 2.05 times that determined from NatHERS simulations. Comparing the measured and simulated thermal cooling loads for each apartment, it was observed that:

- Measured cooling loads in two apartments (#5 and #7) were significantly below the simulated cooling loads (i.e. measured cooling loads were 48% and 34% of those simulated, respectively);
- The measured cooling load moderately exceeded the simulations in Apartment #2 (measured cooling load being 15% greater than the simulated cooling load); and
- Measured cooling consumption greatly exceeded the simulated cooling consumption for Apartments #1, #3, and #6, where the measured cooling consumption was 565%, 381%, and 202% greater than of that simulated, respectively.

Thus, while the large deviation observed for three of the apartments greatly increased the difference between the average measured and average simulated cooling loads, on an individual dwelling basis, only half the dwellings actually used more energy for cooling than anticipated by NatHERS.

## Heating

The average measured heating energy was 37% less than that estimated using AccuRate Sustainability with NatHERS default assumptions. However, unlike the cooling season, the monitoring periods were less well aligned with the heating season. Nonetheless, the majority of the heating season was monitored in Apartments #1 and #2 and a substantial proportion of the monitoring period was observed in Apartment #3. The measured heating loads were substantially lower than the simulated heating loads for Apartments #1 and #2, in which measured heating loads were 48% and 1.5%, respectively, of the simulated heating loads. On the other hand, the measured heating loads greatly exceeded the simulated heating loads (by 180%) in Apartment #3. Apartment #5 was excluded from the heating and total energy comparisons as occupants in this dwelling used electric resistance heating, which was not individually monitored.

Thus, while the average measured heating consumption was significantly less than the average simulated heating consumption, the individual comparisons for each dwelling produced mixed results.

## Combined heating and cooling loads

The average measured combined heating and cooling consumption was 27% greater than the average combined simulated consumption. This indicated that to a certain extent, the underestimation of the cooling consumption was partially counteracted by the overestimation of the heating consumption. Individually,

- the measured combined consumption of Apartments #1 was in relatively close agreement with the simulated consumption (i.e. with measured loads that were 17% greater than the simulated loads), despite heavily misaligned proportions of heating and cooling loads;
- the measured combined consumption of Apartments #2, #5 and #7 were significantly below the simulated consumption (i.e. the measured loads were 88%, 63%, and 32% less than the simulated consumption, respectively); and
- the measured combined consumption of Apartments #3 and #6 were significantly greater than the simulated consumption (i.e. the measured loads were 279% and 183% greater than the simulated combined loads).

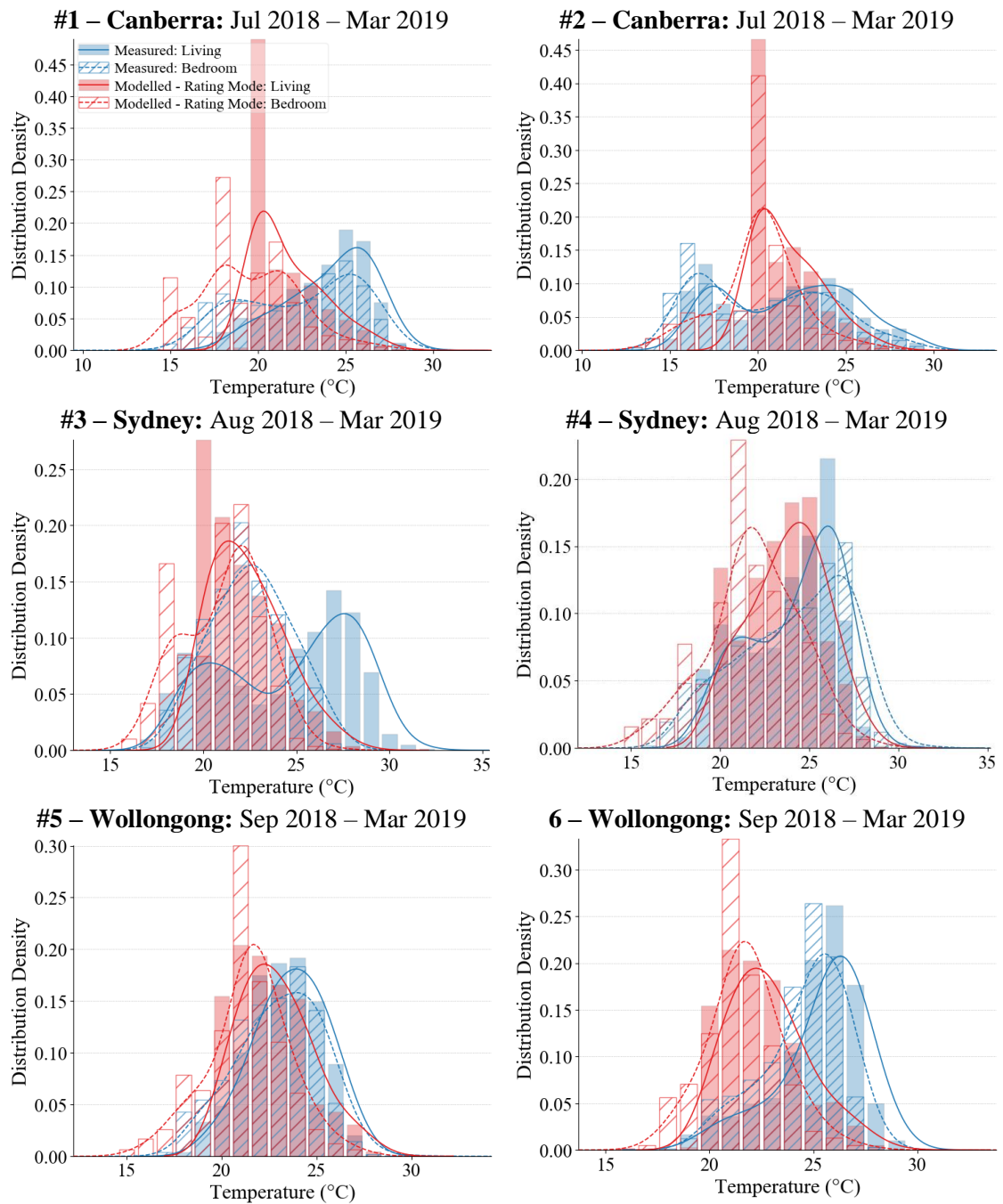
Again, this indicated a mix of results amongst the cohort, despite the underlying trends of the simulated loads underestimating cooling use and overestimating heating use overall.

### **5.5.2 Comparison of Simulated and Actual Indoor Environmental Conditions**

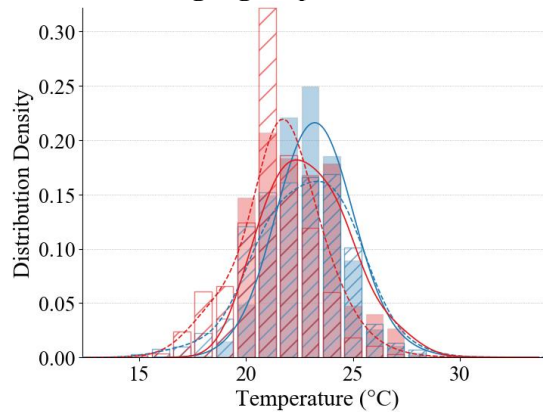
In this section, the differences between the measured and simulated indoor environmental conditions are examined to: a) explore how well the simulation tool represents reality; and b)

explore potential links between the indoor environmental conditions chosen (or tolerated) by the occupants and the resulting heating and cooling loads.

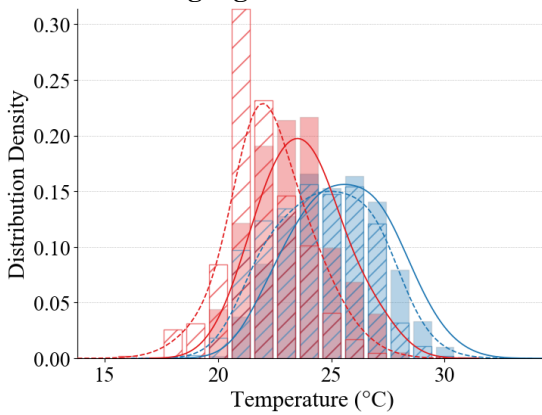
Histograms of the measured and simulated hourly average air temperatures in the living room and bedroom during the monitoring period for each apartment are presented in Figure 5-7. The measured data only includes occupied periods, and the simulated data have been filtered to only include times when the room is considered by NatHERS to be occupied.



**#7 – Wollongong: Sep 2018 – Mar 2019**



**#8 – Wollongong: Oct 2018 – Mar 2019**



**#9 – Wollongong: Dec 2018 – Mar 2019**

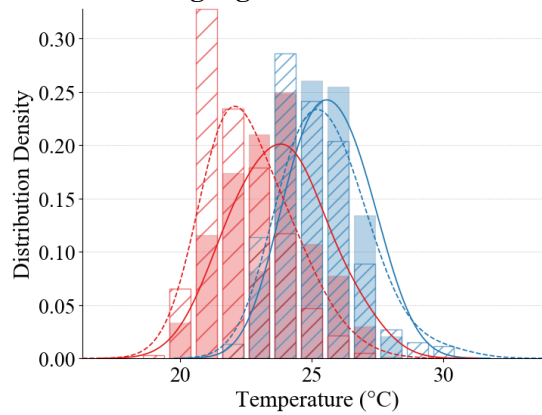


Figure 5-7 Distributions (binned into 1°C intervals) of the hourly air temperature from measurements (blue) and from NatHERS simulations (red) within the monitoring period.

In addition, the proportion of time that the measured indoor conditions were warmer than and cooler than the NatHERS upper and lower comfort region boundaries, respectively, were examined as presented in Table 5-11 and Table 5-12.

Table 5-11 Exceedances rates of the NatHERS thermal comfort region and extended comfort region (assuming an indoor air velocity of 0.5 m/s) for occupied periods within the NatHERS scheduled conditioned hours during: a) the entire monitoring period; and b) exclusively within summer (shown in brackets).

Apartment ID	Living				Bedroom			
	NatHERS Comfort Region Exceedance		Extended Comfort Region Exceedance		NatHERS Comfort Region Exceedance		Extended Comfort Region Exceedance	
#1	20.3%	(38.3%)	2.3%	(5.6%)	6.3%	(17.9%)	0.3%	(0.9%)
#2	15.7%	(46.6%)	5.3%	(18.9%)	7.4%	(25.9%)	2.1%	(7.7%)
#3	55.8%	(92.8%)	22.2%	(39.7%)	23.9%	(28.1%)	0.1%	(0.4%)
#4	35.1%	(52.8%)	0.3%	(0.7%)	44.6%	(73.1%)	0.9%	(2.1%)
#5	67.7%	(92.0%)	5.0%	(10.0%)	49.8%	(70.5%)	1.0%	(1.9%)
#6	67.2%	(72.4%)	10.3%	(15.4%)	17.4%	(18.9%)	0.0%	(0.0%)
#7	51.6%	(86.5%)	0.9%	(3.0%)	40.8%	(69.8%)	0.5%	(1.1%)
#8	80.9%	(92.4%)	27.4%	(46.0%)	58.4%	(67.0%)	9.3%	(17.2%)
#9	69.8%	(68.0%)	10.5%	(13.1%)	72.5%	(70.1%)	4.4%	(5.5%)

*Table 5-12 Exceedance rates of the NatHERS heating thermostat settings for the appropriate zones for occupied periods within the respective NatHERS scheduled heating hours during: a) the entire monitoring period; and b) exclusively within winter (shown in brackets).*

<b>Apartment ID</b>	<b>Living 20°C Exceedance</b>		<b>Bedroom 18°C Exceedance</b>		<b>Bedroom 15°C Exceedance</b>	
#1	5.7%	(24.8%)	7.9%	(27.5%)	0.7%	(3.2%)
#2	35.0%	(99.6%)	35.3%	(98.2%)	2.3%	(5.7%)
#3	10.4%	(45.8%)	0.4%	(2.7%)	0.0%	(0.0%)
#4	5.6%	(27.7%)	1.9%	(3.1%)	0.0%	(0.0%)
#5	2.8%		0.3%		0.0%	
#6	0.7%		0.0%		0.0%	
#7	0.0%		0.7%		0.0%	
#8	0.0%		0.0%		0.0%	
#9	0.0%		0.0%		0.0%	

The measured and simulated distributions of indoor air temperature were compared, together with the measured and simulated heating and cooling consumption to identify whether there was any correlation between the indoor conditions and energy use.

### Cooling

Compared with the average temperatures measured in the living rooms and bedrooms, the simulated results were lower for all nine apartments in summer. This was despite Apartments #1, #2, #3, and #6 using between 15% to 470% more cooling energy. However, the increased cooling use measured in these apartments did coincide with a decrease in the exceedance rates of the upper thermal comfort boundaries defined by NatHERS during summer compared to Apartments #5 and #7, which had lower cooling use than their simulated counterparts.

Therefore, the thermal comfort preferences of occupants were not considered to have contributed significantly to increased measured cooling use in apartments with higher measured cooling use relative to their simulated counterparts. Instead, underutilisation of natural ventilation and shading relative to the NatHERS cooling practices, in combination with warmer weather, were thought to be more important in contributing to higher cooling loads. This issue is examined further in the following sections. However, it was also possible that the measured cooling loads were smaller than the simulated cooling loads in Apartments #5 and #7 due, in part, to higher occupant tolerance of warmer indoor conditions.

### Heating

While there were no prevailing patterns throughout the cohort in relation to heating use and indoor conditions during winter and spring, evidence was found indicating that measured heating use in individual apartments both increased and decreased in response to implied occupant preferences relative to the NatHERS simulated cases.

The most significant observation was that the seasonal average living room and bedroom temperatures measured in Apartment #2 were significantly cooler than those simulated, with a measured average living room temperature that was 2.2°C below the simulated average living temperature, and with 99.6% of all occupied hours in winter below the NatHERS heating thermostat setting. This correlated with significantly lower measured heating consumption compared to the simulated heating consumption, which could thus be partially explained by occupant tolerance of cooler indoor conditions.

In contrast, the difference between the average measured and simulated bedroom temperatures of Apartment #3 in winter was over 2.3°C, and extended to over 2.5°C when confining the measured temperature dataset to hours within the NatHERS bedroom heating schedule. This evidence suggested that the that the increased heating use in Apartment #3 was in part due to warmer bedroom temperatures preferred by occupants.

In Apartment #1, average measured indoor temperatures in winter were slightly warmer than those simulated, despite consuming 32% less energy for heating in winter relative to the simulation. However, approximately 25% of occupied periods in winter were below the NatHERS thermostat settings, indicating that occupants occasionally tolerated cooler indoor conditions than anticipated by NatHERS. The measured heating consumption diminished further relative to the simulated heating consumption in spring, representing just 19% of the simulated heating consumption despite maintaining warmer measured indoor conditions. Overall, occupant tolerance of cooler indoor conditions was considered only a minor cause of reduced heating loads in Apartment #1.

### **5.5.3 Impact of Occupant Behaviour on Energy Consumption**

This section examines the difference in usage patterns for heating, cooling, and natural ventilation as well as differences in occupancy patterns between reality and the NatHERS simulations in order to comprehend how such differences in occupant behaviour may explain differences between the measured and simulated heating and cooling loads. For reference, the NatHERS heating and cooling management logic is presented in Section 5.2.8.

#### **5.5.3.1 Air Conditioning and Natural Ventilation Practices**

The comparison of heating and cooling strategies in reality and the NatHERS protocol have already been presented in Section 4.5. While there were several noted differences between occupant heating and cooling thermostat settings in reality compared to the NatHERS protocol, the key difference was that the ability of natural ventilation to provide cooling appeared to be significantly overestimated by the NatHERS protocol relative to occupant perceptions in reality i.e. NatHERS assumes that natural ventilation can facilitate thermal comfort at higher indoor and/or outdoor air temperatures than occupant perceptions in reality.

As mentioned previously, natural ventilation as a means of cooling a dwelling is prioritised over mechanical cooling within NatHERS simulations to maintain conditions within the thermal comfort boundaries (which vary as a function of indoor air speed). The significance of the use of natural ventilation in NatHERS simulations to reduce cooling loads was quantified by running NatHERS simulations of the apartments without natural ventilation. On average, simulated cooling load intensities increased by 177%; from 23.8 MJ/m<sup>2</sup> to 66.2 MJ/m<sup>2</sup>. Thus, assumptions regarding natural ventilation to provide cooling has a significant impact on simulated cooling loads in NatHERS simulations.

However, the characterisation of natural ventilation practices in reality, presented in Section 4.5.1 and illustrated in Figure 4-16, indicated that the majority of mixed-mode apartments (#1, #2, #5, and #7) also prioritised natural ventilation over artificial cooling in the pursuit of thermal comfort. It was only in Apartments #3 and #6, where artificial cooling was significantly more likely to be in use than natural ventilation for outdoor temperatures above 20°C. Perhaps unsurprisingly then, was that Apartments #3 and #6 had amongst the largest discrepancy between the measured and simulated cooling consumption.

While Apartment #1, which had the greatest relative discrepancy between the measured and simulated cooling loads, appeared to frequently utilise natural ventilation as a form of cooling, it was found that the bedroom or living room sliding door was left at least slightly open for 77% of the time while the air conditioner was in operation, resulting in excessive infiltration (see Section 4.5.1.3).

Thus, underutilisation, and in some cases ineffective or detrimental usage of natural ventilation was considered a major contributing factor to increased measured cooling loads relative to the NatHERS simulated cooling loads. It was not known why some occupants perceived natural ventilation as less appealing than artificial cooling. However, as stated previously, it is also possible that NatHERS overstates the viability of natural ventilation as a form of cooling under some conditions, as even the most sparing users of artificial cooling occasionally contrasted with NatHERS practices.

Natural ventilation opportunities were also less abundant in reality compared to the simulations, as evidenced by the significant increase in cooling degree days in Canberra and Sydney observed in reality compared to their respective NatHERS RMY weather files. The changes in the simulated heating and cooling loads in response to weather conditions is examined in the following section (Section 5.5.4).



### 5.5.3.2 Occupancy (Vacant Periods)

The attenuating effect of such holiday periods on the measured loads was accounted for by quantifying the change in the total simulated heating and cooling loads when excluding these dates.

Overall, excluding dates marked as holiday periods reduced average simulated heating and cooling loads by 1.5% and 7%, respectively. Cooling was affected more than heating because the majority of the holiday periods occurred in summer. Therefore, the impact of holiday periods was not considered a significant cause of differences between the measured and simulated loads for the case-study apartments.

### 5.5.4 Impact of Weather on Energy Consumption

Comparisons of the actual weather conditions during the monitoring periods of the apartments, relative to the NatHERS prescribed representative meteorological year (RMY) weather data, presented in Section 5.3.4.1, indicated that Canberra and Sydney experienced a significantly higher number of cooling degree days (CDD), and Canberra, Sydney, and Wollongong all experienced slightly fewer heating degree days (HDD). Consequently, the NatHERS simulations, using RMY weather, were expected to overestimate heating use and underestimate cooling use. To explore this, NatHERS simulations were performed using weather data derived from the actual weather conditions observed at each of the apartment locations during the monitoring period. A comparison of the space conditioning loads is presented in Figure 5-8.

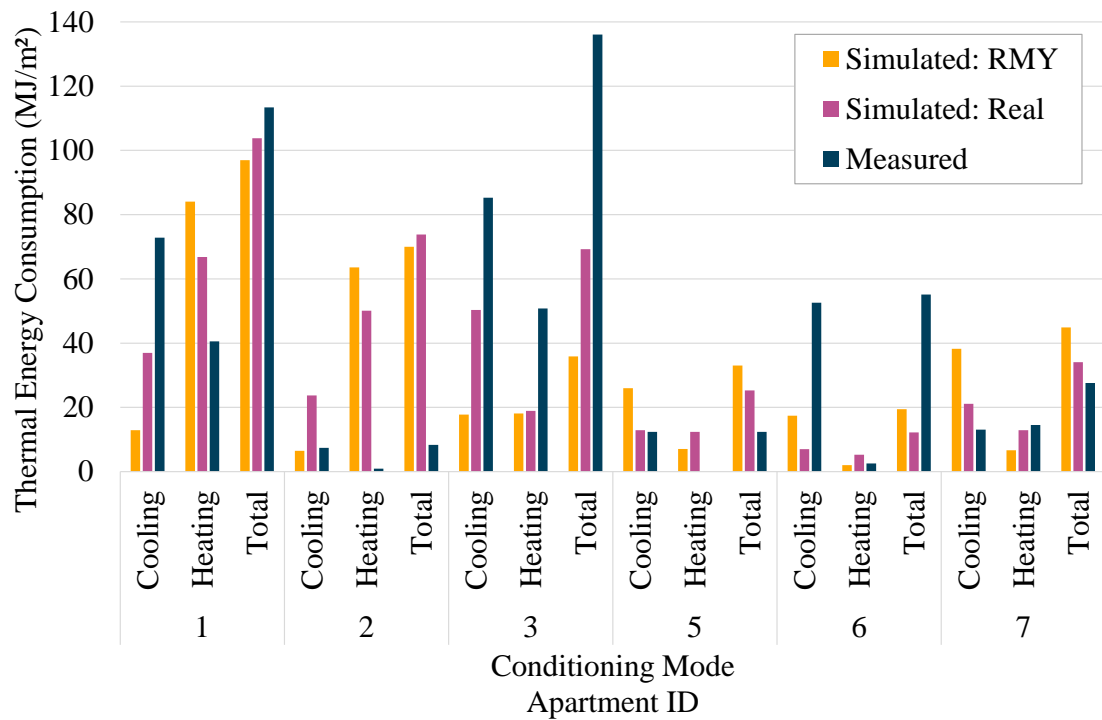


Figure 5-8 Cooling, heating, and total space conditioning intensities as measured compared to NatHERS simulations using different weather conditions based on: i) NatHERS Default RMY climate files (RMY) and ii) climate files derived from real weather data (real). Results presented for the air conditioned apartments during the monitoring period.

### Cooling

The average simulated cooling consumption using the modified climate files derived from real weather conditions was 28% greater than that determined using the NatHERS default climate files within the monitoring period, which improved agreement with the average measured cooling consumption. The average simulated cooling consumption using the default NatHERS climate files and the modified climate files were 51% and 38% less than the measured cooling consumption, respectively.

For each apartment, the change in simulated cooling consumption when the modified climate files were used rather than the default climate file correlated positively with the change in the number of Cooling Degree Days (CDDs) within the climate files. However, the relationship between the two was not entirely consistent. Figure 5-9 shows the percentage change in cooling load as a function of the change in CDDs for each apartment.

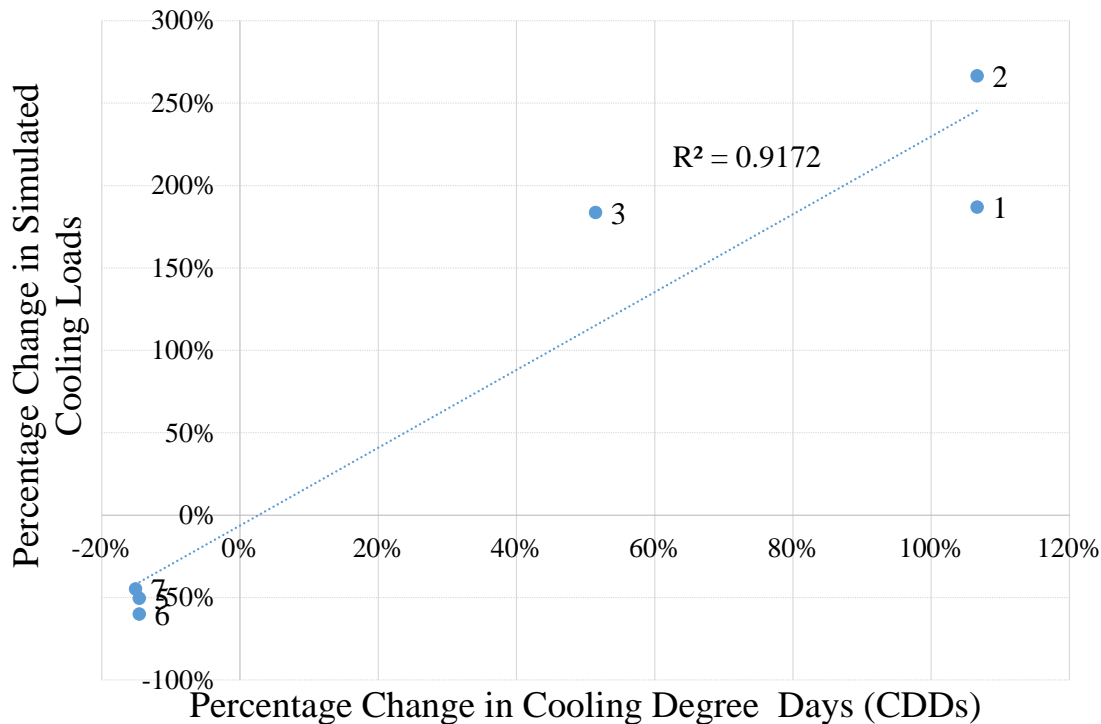


Figure 5-9 Percentage change in simulated cooling load as a function of the change in CDDs for each apartment. The dashed blue line is the linear regression line of best fit.

Within the monitoring period the simulated cooling consumption calculated using the modified climate file rather than the default climate file:

- increased by 187% and 267% in Apartments #1 and #2, respectively, which corresponded to a 107% increase in CDDs;
- increased by 184% in Apartment #3, which corresponded to a 51% increase in CDDs; and
- decreased by 50%, 60%, and 45% in Apartments #5, #6, and #7, respectively, which corresponded to a 15% decrease in the CDDs.

The linear regression curve had a gradient of 2.36 and a y-intercept of -0.06, which indicated that cooling consumption changed by approximately 2.4% for every 1% change in CDDs. The coefficient of determination was 0.917, which indicated a strong correlation. Thus, the simulated cooling consumption was highly sensitive to changes in the number of CCDs within the weather file.

### Heating

The average simulated heating consumption using modified climate files derived from real weather conditions was 8% less than that determined using the NatHERS default climate files within the monitoring period. This improved agreement with the average measured heating

consumption. The average simulated heating consumption overestimated the measured heating consumption by 52% using the modified climate files, an improvement from the 66% overestimation using the default NatHERS climate files.

### Combined

The average simulated combined heating and cooling consumption using the modified climate files increased by just 6% relative to those determined using the default climate files due to both an increase in the average simulated cooling consumption and a decrease in the average simulated heating. The simulated combined heating and cooling consumption calculated using the modified and default climate files were 10% and 15%, respectively, below the average measured combined consumption, resulting in a notable improvement in the agreement between the simulated and measured combined energy consumption.

In summary, performing NatHERS simulations using climate files derived from real weather data was shown to significantly improve the agreement between the measured and simulated heating, cooling and combined consumption amongst the cohort. The use of real weather data led to significantly increased simulated cooling consumption and decreased simulated heating consumption amongst the cohort, which agreed with findings from the majority of other Australian studies examined in Section 2.7.3.1.

### **5.5.5 Impact of Building Envelope Airtightness on Energy Consumption**

The extent to which building envelope air tightness leads to differences in the measured and simulated air conditioning loads is examined in this section.

It has already been established in Section 5.3.5.2 that the NatHERS default method resulted in air change rates at 50 Pa that were on average 80% greater than those measured via on-site blower door testing. Figure 5-10 presents the measured heating, cooling, and combined consumption for each apartment, together with the simulated loads determined with building envelope airtightness specified using: a) the NCC Trajectories method to closely match the actual airtightness of the apartments (BD); and b) the NatHERS default method (Def).

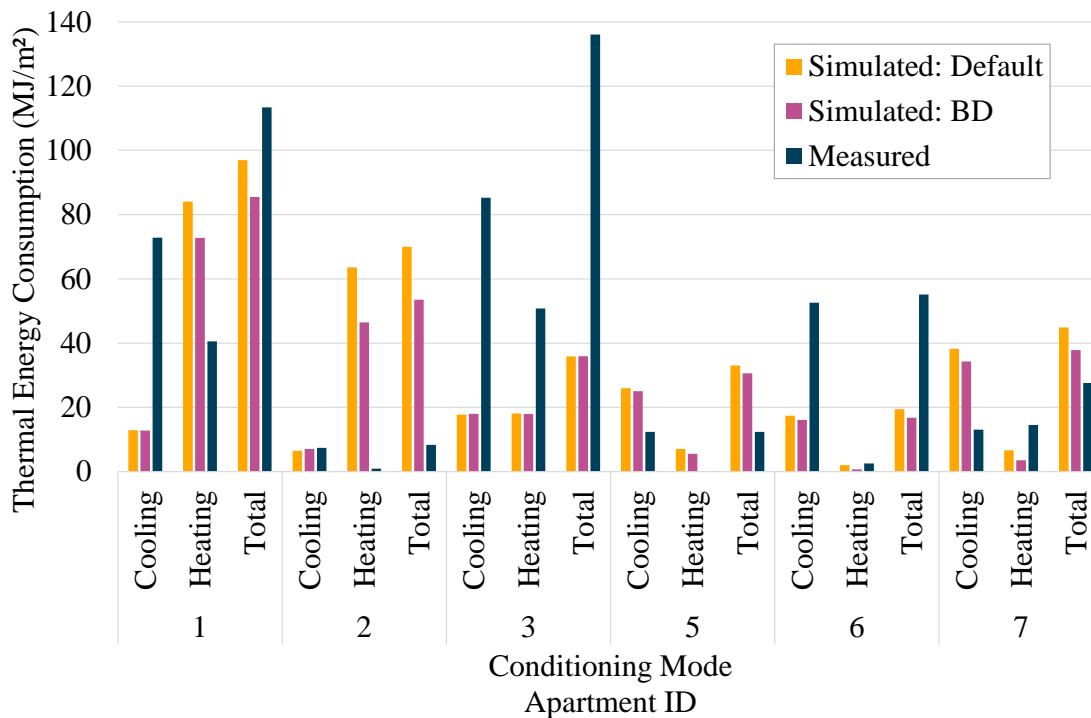


Figure 5-10 Cooling, heating, and total space conditioning intensities as measured compared to NatHERS simulations using different infiltration rates based on: i) the NatHERS Default method (Def) and ii) the blower door test results using the method from the NCC Trajectory Project. Results presented for the air conditioned apartments during the monitoring period.

### Cooling

The average simulated cooling consumption using the infiltration rates derived from the NCC Trajectory method was 5% less than that using the default NatHERS method. This slightly further increased the difference between the simulated and measured average cooling loads. Using infiltration rates derived from the NCC Trajectory method, the average simulated cooling consumption was 47% of the average measured cooling consumption, a decrease from 49% when simulated using infiltration rates determined using the NatHERS default method.

Across the six apartments the simulated cooling consumption changed little in response to the modified infiltration rates. Simulated cooling loads decreased by 10% and 8% in Apartments #6 and #7 when simulated with measured airtightness inputs but varied by less than  $\pm 5\%$  in Apartments #1, #3, and #5. Interestingly, simulated cooling loads increased by 9% Apartments #2 when using measured airtightness inputs (i.e. more airtight than assumed by default). It was not possible to determine why a higher airtightness increased the simulated cooling load without knowing the balance between infiltration air and natural ventilation air in the models. However, it was thought that the natural ventilation algorithm, including the three-hour stickiness period was a contributing factor.

## Heating

The average simulated heating consumption using the infiltration rates derived from the NCC Trajectory method were 26% less than those using the default NatHERS method. As a result, the simulated heating consumption derived using the NCC Trajectory method improved agreement with the measured heating consumption. The discrepancy between the measured and simulated heating loads decreased from a 66% overestimate to a 34% overestimate based on the simulated heating loads calculated with infiltration rates determined using the NatHERS default method and the NCC Trajectory method, respectively.

Apartment #3 was the only apartment in which the simulated heating loads did not differ substantially between the two infiltration models, despite the NCC Trajectory method resulting in a 26% lower infiltration rate than the NatHERS default method.

### **5.5.6 Discussion**

The average measured cooling consumption was 105% greater than the average cooling consumption simulated using NatHERS protocols. Therefore, like the precedent studies based on detached dwellings (refer to Section 2.6.1.1), NatHERS significantly underestimated the cooling consumption in the case-study apartments. Furthermore, the differences in this study were greater than those identified in existing literature. Nonetheless, the scatter in the data was not insignificant, with 2 of the 6 air conditioned apartments using less cooling than simulated using NatHERS protocols.

On the other hand, the average measured heating loads of the case-study apartments were 37% less than the average simulated heating loads, which was beyond the range of findings of previous research (refer to Section 2.6.1.1). However, comparisons between the measured and simulated heating consumption in the literature were less consistent than for cooling. While measured heating in the present study was much less than simulated heating for the two apartments in Canberra (a heating dominated climate), measured heating use was higher than the simulated heating use for the Apartments in Sydney and Wollongong.

In the present study, the greatest cause of misalignment between the measured and simulated cooling loads was considered to be occupant underutilisation, or misuse, of natural ventilation relative to the NatHERS natural ventilation/cooling algorithm assumptions.

Differences in actual and assumed weather conditions also corresponded closely with differences in the measured and simulated cooling consumption. Specifically, greater measured cooling consumption correlated with higher cooling degree days (CDDs) in reality compared to the NatHERS RMY files, and vice versa.

The greater airtightness of the apartments in reality relative to the airtightness assumed by NatHERS only resulted in relative small differences in simulated cooling loads. However, this link was confounded somewhat by window use patterns (see Section 4.5.1.3) including the status of windows that were not monitored as part of the study.

The most significant causes of differences between the measured and simulated heating consumption in individual apartments were occupant tolerance or preference of indoor conditions that were much cooler and much warmer, respectively, than the NatHERS heating thermostat settings.

NatHERS simulations comparing the energy consumption with standard NatHERS airtightness settings against those with the actual, more airtight apartment envelopes, indicated that, on average, a 45% reduction in the simulated air change rate at 50 Pa corresponded to 26% lower simulated heating loads. This indicates that the assumptions around airtightness in NatHERS are not accurate for apartments, and result in significantly overestimated simulated heating loads.

Similar NatHERS simulations comparing the energy consumption with standard RMY weather files against those with the real, warmer weather data observed during the monitoring period indicated that, on average, 11% fewer heating degree days (HDDs) corresponded to 8% lower heating loads.

Overall, comparisons between measured and simulated heating consumption were mixed. A summary of the comparisons is as follows.

- The impact of occupant preferences for warmer conditions in some apartments (#3, #6, and #7) outweighed the counteracting effects of warmer weather conditions and higher airtightness in reality compared to default assumptions in NatHERS, resulting in higher heating consumption in reality.
- However, in other apartments (#1 and particularly #2) occupant tolerance of cooler conditions combined with the effects of warmer weather conditions and higher airtightness, which corresponded to significantly lower heating consumption in reality compared to NatHERS simulations.

As for cooling, it was possible that despite greater airtightness, window use may have resulted in excessive infiltration/ventilation, thereby increasing heating loads.

## **5.6 Legislative Energy Efficiency Performance Assessment**

The objectives of this work were to compare the NatHERS star rating and thermal load simulations carried out by the present author with:

- a) NatHERS star rating and thermal loads provided as part of the original apartment Development Applications, where available; and
- b) legislative building energy efficiency requirements in effect at the time of: i) the development and ii) writing; so as to assess whether the apartments were designed to only meet, rather than exceed, minimum performance requirements

### **5.6.1 Methodology**

#### **5.6.1.1 Simulated Thermal Performance: Development Application vs. Remodelling**

Given the use of the same NatHERS-approved modelling software, it was expected that, ideally, there should be very little variation in the performance between simulations generated in this study to that obtained from the original Development Applications for each apartment. However, as noted in the literature review, the NatHERS Assessor Benchmark Study identified significant variance amongst NatHERS-approved assessors when modelling identical buildings, which was exacerbated when modelling apartment dwellings.

In comparison to the Development Application assessments, the simulations conducted within this study benefitted from a consistent modelling methodology as a single assessor (the author) performed each of the assessments, which were verified by second researcher.

BASIX certificates and occasionally NatHERS certificates from the Development Applications of Apartment #3, and Apartments #5, #6, #8 and #9 were obtained via requests to the Council of the City of Sydney and Wollongong City Council, respectively. Access Canberra was contacted to obtain the NatHERS certificates for Apartments #1 and #2, however Access Canberra no longer retained records for those developments. Apartments #4 and #7 both predated the mandatory inclusion of NatHERS and BASIX into the NCC. While there was no relevant energy efficiency documentation associated with Apartment #4, there was a NatHERS assessment conducted in 2001 for Apartment #7 using a first-generation NatHERS tool.

It should be noted that when evaluating simulations against legislative load limits, simulated loads are modified by an “area-correction factor” to account for naturally occurring bias that benefits larger house designs (Chen, 2012). Henceforth, within this section the term “area-adjusted” refers to simulated heating, cooling, or combined loads that have been adjusted using the area-correction factor.

#### **5.6.1.2 Comparison to Legislative Load Limits**

While the legislative building energy efficiency requirements varied between Australian states and territories, apartment developments in all states and territories were required to use NatHERS approved software to calculate simulated heating and cooling loads to demonstrate compliance with the various thermal performance requirements across each jurisdiction.



For apartments built in the ACT, the primary legislative requirements were the 5 star and 6 star NatHERS star ratings determined using NatHERS approved software for individual apartments and the average of all apartments within a multi-unit development, respectively. While not in effect at the time that any of the apartments were constructed, the thermal loads were also compared to more recent individual heating and cooling limits required in NatHERS introduced in the NCC in 2019 (ABCB, 2019b, 2019c). The relevant NatHERS load limits are provided in Table 5-13.

*Table 5-13 NatHERS legislative thermal performance requirements for apartment developments. The table presents the maximum total load limits and separate heating and cooling load limits for the relevant climate zones. Note that NatHERS does not specify heating and cooling load limits for climate zones within NSW as they have already been included within BASIX.*

Climate Zone	Total load limit (MJ/m <sup>2</sup> /year)		Heating load limit (MJ/m <sup>2</sup> /year)		Cooling load limit (MJ/m <sup>2</sup> /year)	
	Individual (5 star)	Average (6 star)	Individual	Average	Individual	Average
24 Canberra	216	165	194	144	47	31

Apartments built in NSW were subject to BASIX, which replaces NatHERS in NSW. While BASIX is an assessment framework for the overall energy efficiency of buildings in terms of credits for the use of energy efficient features, it also requires that the simulated heating and cooling loads, determined using NatHERS-approved software, for each dwelling in a Class 2 development are below the BASIX maximum load limits. Like NatHERS, BASIX specifies two sets of load limits, those for whole-of-building average performance, and those for individual dwellings. The latter are less stringent than the whole-of-building average performance requirements, to account for poorer performing dwellings resulting from unfavourable orientations or layouts.

The BASIX heating and cooling load limits were updated in July 2017, significantly reducing the maximum heating and cooling load limits for many of the climate zones throughout NSW (NSW Department of Planning and Environment, 2017). The relevant BASIX heating and cooling load limits for units of Class 2 buildings are presented in Table 5-14.

In Climate Zone 56 (Eastern Sydney and Wollongong) the heating and cooling load limits for individual dwellings decreased by 31% and 50%, respectively, whilst the maximum whole-of-building averaged heating and cooling loads decreased by 22% and 42%, respectively. The load limits also decreased for Climate Zone 17 (Sydney CBD), however, the changes were less significant.

Table 5-14 BASIX legislative thermal performance requirements. The table presents the maximum loads for units of multi-unit dwellings for the climate zones considered in the study.

Climate Zone and Region	Heating (MJ/m <sup>2</sup> /year)				Cooling (MJ/m <sup>2</sup> /year)			
	Individual		Average		Individual		Average	
	Pre-2017	Post-2017	Pre-2017	Post-2017	Pre-2017	Post-2017	Pre-2017	Post-2017
17 Sydney CBD	50.0	28.2	40.0	25.0	41.0	31.8	32.0	28.2
56 Mascot	66.0	45.4	51.0	40.0	59.0	29.5	45.0	26.0

## 5.6.2 Results

### 5.6.2.1 Simulated Thermal Performance: Development Application vs. Remodelling

The simulated heating, cooling, and total thermal loads of each of the case-study apartments extracted from the simulations conducted within this study and those obtained from the original Development Applications, where available, were compared to determine how closely the two sources aligned.

The area-adjusted total energy consumption from the original DAs and from the remodelling used to determine the star ratings are presented in Figure 5-11.

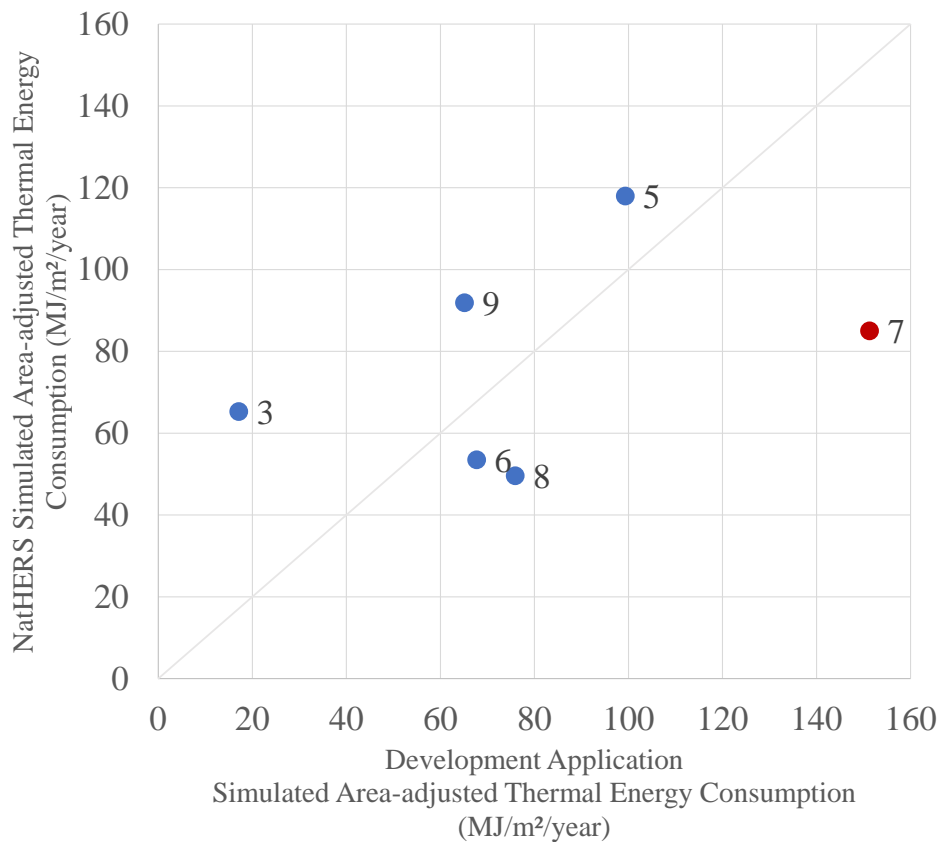


Figure 5-11 Comparison between the area-adjusted thermal energy consumption from the original DAs to the simulations performed in this study for each Apartment where available. Apartment #7 has been marked red to highlight that the DA simulation used outdated first-generation NatHERS tools.

Comparing results produced exclusively using second-generation NatHERS tools (i.e. excluding Apartment #7), the average area-adjusted thermal energy consumption from the original DAs and from the remodelling were 65.0 MJ/m<sup>2</sup>/year and 75.7 MJ/m<sup>2</sup>/year, respectively, and the standard deviations were 26.8 MJ/m<sup>2</sup>/year, and 25.8 MJ/m<sup>2</sup>/year, respectively. Despite similar average loads, the comparisons of the total energy consumption presented in Figure 5-11 portray poor agreement between the DA and remodelling, with significant positive and negative deviation from equivalence and a mean absolute error of 26.8 MJ/m<sup>2</sup>/year. That is despite a mean bias error of 10.6 MJ/m<sup>2</sup>/year.

As illustrated in Figure 5-11, the area-adjusted total thermal energy consumption for Apartment #7 calculated from the remodelling was 56% of that sourced from the original DA. The assessment within the original DA was produced using a first-generation NatHERS tool that therefore lacked the capability to adequately model natural ventilation, amongst other limitations (Delsante, 2005; Williamson, Orkina and Bennetts, 2009). Thus, a significant change in the area-adjusted total thermal energy consumption was expected given the substantial natural ventilation opportunities present in Wollongong (Fiorentini *et al.*, 2019).

The individual heating and cooling load limits presented in Figure 5-12 were compared so as to more thoroughly understand the differences between the thermal loads reported in the original DAs and the remodelling.

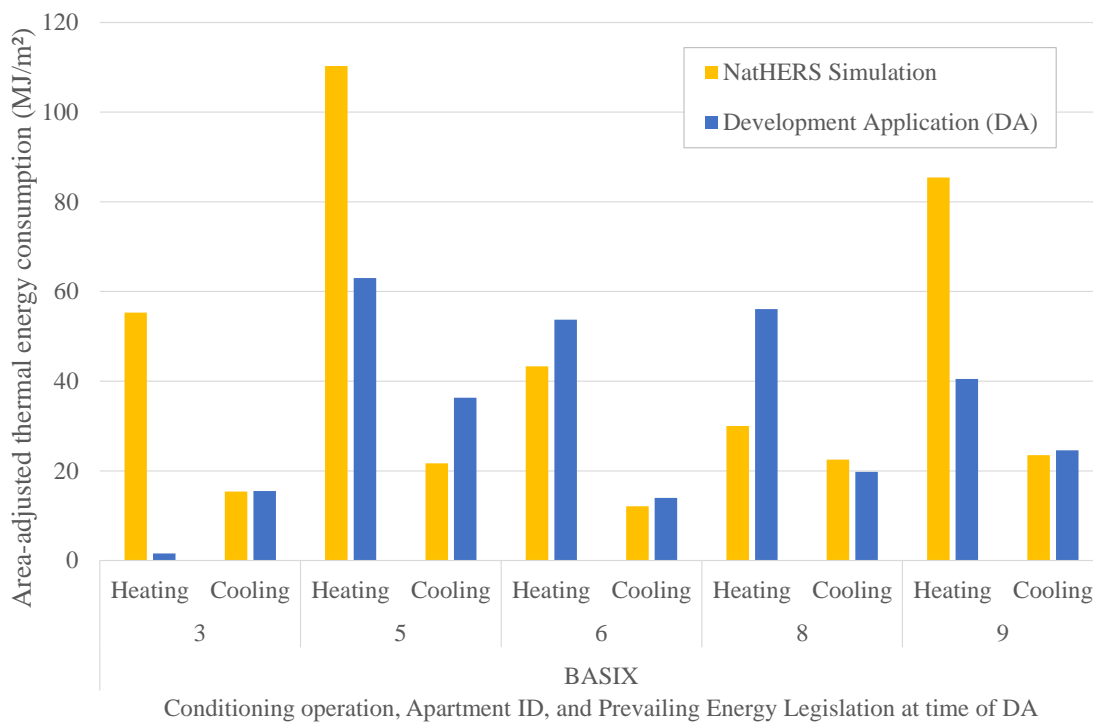


Figure 5-12 Simulated heating and cooling loads obtained from the original Development Applications where available compared with the simulated heating and cooling loads determined from NatHERS remodelling.

The average heating loads from the original DAs and from the remodelling were 43.0 MJ/m<sup>2</sup>/year and 64.9 MJ/m<sup>2</sup>/year, respectively. The average cooling loads from the original DAs and from the remodelling were 22.0 MJ/m<sup>2</sup>/year and 19.0 MJ/m<sup>2</sup>/year, respectively. The cooling loads between the DAs and remodelling matched more closely than the heating loads, with normalised mean absolute errors (nMAE) of 19.7% and 139%, respectively. The nMAEs were determined using Equation (5-5), where  $a$  and  $f$  denoted the DA and remodelled measurements, respectively.

$$nMAE = \frac{\frac{1}{n} \sum |f_t - a_t|}{\frac{1}{n} \sum |a_t|} \quad (5-5)$$

The greatest disparity was observed in Apartment #3, where the remodelled heating load was approximately 35 times greater than that provided in the original DA. As the predicted cooling loads of Apartment #3 demonstrated precise agreement (within 1%), the difference in the NatHERS star ratings between the original DA and remodelling was solely due to the heating load disparity. The large difference in the ratings of Apartment #8 was also attributed to a large difference between the heating loads. However, in this case the heating load from the DA was 87% greater than from the remodelling. Without access to the original models used in the DA, an explanation for the large differences in the heating loads could not be determined, though it was speculated that human error in developing the models was one likely cause, particularly considering that each of these apartments was within the same NatHERS Climate Zone.

In summary, there were significant differences between the DA and remodelling for several individual dwellings. While one of these differences could be attributed to differences in the software used between the DA and the remodelling, other causes cannot be definitively identified. These results are discussed further in Section 5.6.3.

#### 5.6.2.2 Comparison to Legislative Load Limits

The simulated loads from the DAs and from the remodelling of this study were compared to the building energy efficiency requirements: i) in effect at the time of development and ii) in effect at the time of writing. The goal of this comparison was to assess whether the case-study apartments were designed to only meet, or to exceed, minimum performance requirements and whether the increased stringency of subsequent building energy efficiency requirements has impacted apartment design.

As mentioned in the methodology (see section 5.6.1.2), there were different legislative energy performance requirements in ACT, which followed NatHERS, and NSW, which implemented BASIX to supersede NatHERS. Therefore, the subsequent analysis has been conducted separately for the apartments in ACT and NSW.

NatHERS Requirements in the ACT

At the time these apartments were under development, the NatHERS thermal performance requirements in ACT were: a) all apartments had to achieve at least a 5 star rating; and b) on average the apartments in the development had to achieve a 6 star rating overall.

In 2019, the NCC introduced individual heating and cooling load limits in response to concerns that the current assessment of combined heating and cooling loads had contributed to excessively imbalanced heating and cooling loads in recently constructed residential dwellings (Willand, Ridley and Pears, 2016; ABCB, 2019b). Similarly to the NatHERS star rating requirements, less stringent performance requirements were specified for individual dwellings compared to the whole-of-building average.

Figure 5-13 presents the simulated combined thermal energy consumption for Apartments #1 and #2 on the left, together with the load limits corresponding to the NatHERS 5 star and NatHERS 6 star requirements in Climate Zone 24. In addition, the simulated heating and cooling loads, together with the individual heating and cooling load limits introduced in 2019 are shown on the right half of the figure.

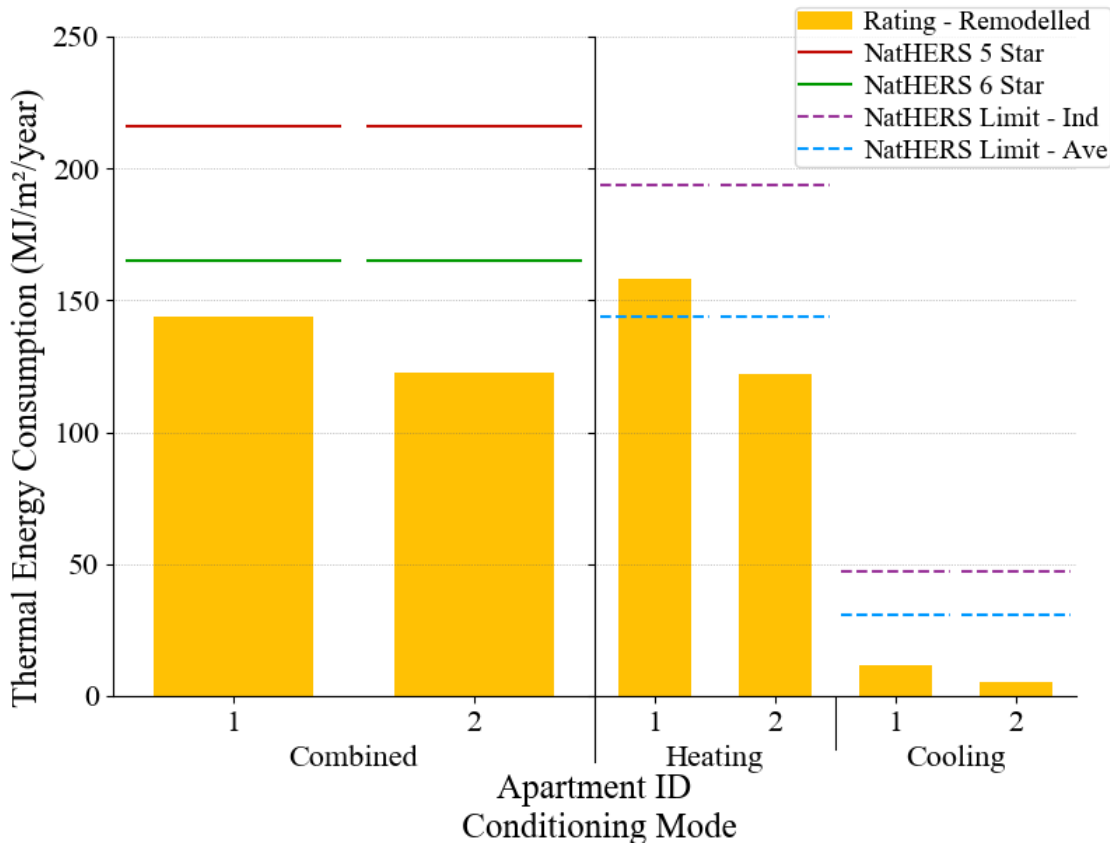


Figure 5-13 Simulated area-adjusted thermal energy consumption of the apartments subject to NatHERS performance requirements (i.e. Apartments #1 and #2 in the ACT). NatHERS heating and cooling limits at the time of construction are shown as horizontal lines. Note: the individual heating and cooling performance and limits shown on the right were introduced in 2019.

The simulated thermal energy consumption was less than the whole-of-building average thermal consumption limits for both apartments, with equivalent NatHERS star ratings of 6.4 and 6.9 stars for Apartments #1 and #2, respectively. The performance of north-facing apartments such as these, generally have enhanced thermal performance in heating-dominant climates such as Canberra due to increased solar exposure relative to apartments without north-facing facades (Stephan, Jensen and Crawford, 2017; Albatayneh *et al.*, 2018). This aids in achieving the whole-of-building averaged performance requirements by compensating for the additional heating input required by apartments with less than optimal orientations (Heffernan *et al.*, 2017).

Despite both apartments being designed and constructed at least 5 years before the implementation of the individual heating and cooling load limits within NatHERS, the simulated heating and cooling loads were within the 2019 individual dwelling limits for both apartments and only the simulated heating loads of Apartment #1 exceeded the whole-of-building limits. This indicated that the balance in the simulated heating and cooling load limits was within the range expected by the NCC within Climate Zone 24.

#### BASIX Requirements in NSW

As all the case-study apartments within the cohort were constructed prior to July 2017, the heating and cooling load limits for each of these dwellings at the time of development follow the original BASIX requirements for apartments introduced in 2005. In July 2017, the BASIX heating and cooling load limits were updated, and resulted in a significant reduction in the maximum loads across many Climate Zones, as shown in Table 5-14.

Figure 5-14 summarises the simulated heating and cooling loads from the modelling conducted in this study and those from the DAs where available, together with the both the heating and cooling load limits in effect at the time of development and those introduced in July 2017.

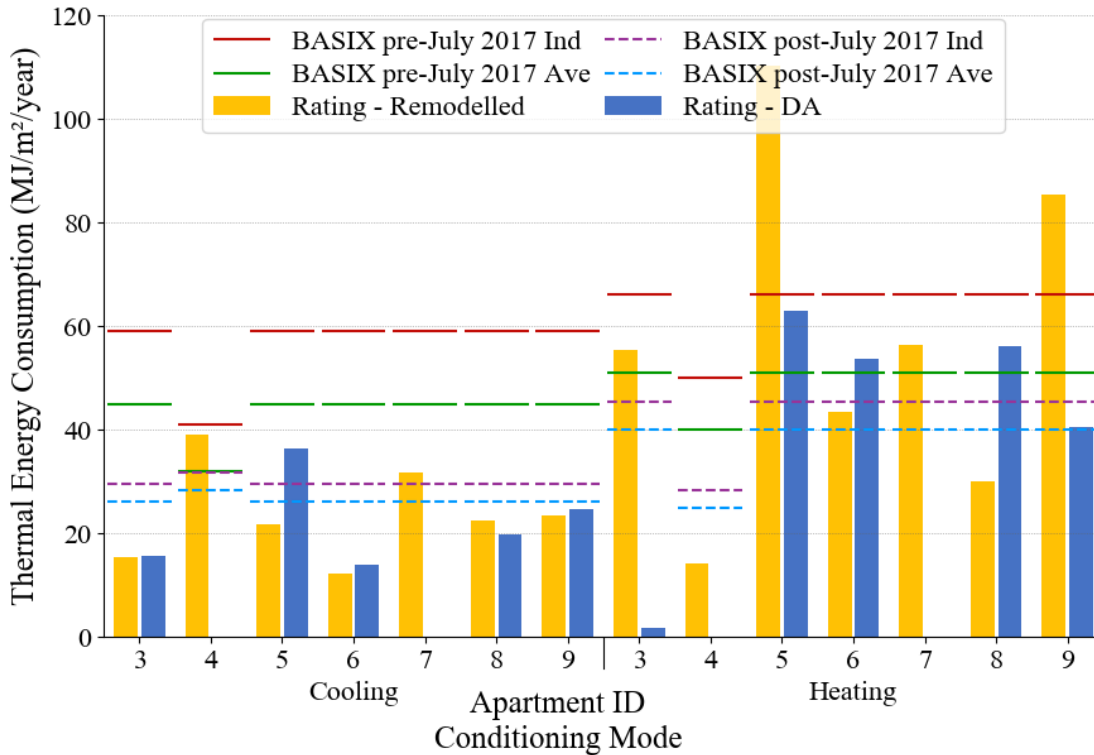


Figure 5-14 Comparison of the simulated heating and cooling loads from the modelling conducted in this study and those from the original Development Application. The BASIX heating and cooling load limits are shown as horizontal lines.

Load limits at the time of development (Pre-July 2017)

None of the heating or cooling loads sourced from the DAs exceeded the pre-July 2017 maximum allowable heating or cooling limits for individual dwellings (i.e. all were compliant). This was to be expected given the DAs were approved and the buildings were constructed. However, the whole-of-building averaged heating load limits were exceeded in the DAs of Apartment #5, #6, and #8, indicating that these apartments were amongst the poorer performing apartments within the multi-unit development. In fact, the heating load from the DA of Apartment #5 was within 5% of the individual dwelling heating load limit and was therefore barely within the legislative limits.

Examining the NatHERS simulations performed in this study, however, the maximum allowable heating load limit for individual dwellings was exceeded in Apartments #5 and #9, indicating that these would not have passed DA inspections without design modifications. In addition, the whole-of-building averaged heating limits were exceeded in Apartments #3 and #7.

Apartments #4 and #7 were developed and constructed prior to the introduction of BASIX load limits for apartments in 2005 and were therefore not required to demonstrate compliance with the BASIX heating and cooling load limits.

### Load Limits in effect at the time of writing (Post-July 2017)

The updated and more stringent load limits resulted in three of the five available DAs exceeding the individual dwelling heating load limits and four of the five DAs exceeding the whole-of-building averaged heating load limits. Only the DA for Apartment #5 exceeded the updated cooling load limits, in which both the whole-of-building average and individual dwelling limits were exceeded. Similar rates of non-compliance were demonstrated for the remodelled loads, although all apartments passed the cooling load limits.

In summary, the majority of the thermal performance assessments included as part of the Development Applications of the apartments that participated in this study, which were designed and constructed between 2012 and 2016, would fail to pass the requirements of today due to the more stringent heating and cooling load limits introduced in July 2017. This implies that the updated regulations are significantly improving the thermal performance of the new building stock within Climate Zone 56.

### **5.6.3 Discussion**

The results above indicated that there was poor alignment between the remodelled loads and those from the Development Applications for the majority of the case-study apartments. This reinforces findings from the NatHERS Benchmark Study (Floyd, Isaacs and Hills, 2014), in which it was found that NatHERS assessments of apartment dwellings produced the highest margin of error amongst experienced NatHERS assessors for any building typology. Within the NatHERS Benchmark study, less than half of the assessors obtained a rating within 1 star of the correct result. For comparison, the following distribution in the differences between the star ratings obtained from the simulations conducted within this study and those obtained from the DAs were observed:

- One apartment (17%) was within 0.5 stars;
- Two apartments (33%) were within 1 star; and
- Five apartments (83%) were within 2 stars.
- One apartments had a difference of 3.7 stars.

Thus, a similar proportion of the assessments were within 1 star of the ‘correct’ rating, and one apartments produced a significantly different star rating. While, it cannot be known with absolute certainty whether the simulations conducted within this study could be considered the ‘correct’ result, it is assured that the models were meticulously constructed in accordance with the NatHERS Assessor handbook, were checked by a highly experienced user of AccuRate, and were calibrated against measurements.



The misalignment (1.7 stars) for one of the apartments was due to the use of first-generation NatHERS modelling tools for the assessment included in the Development Application. A similar observation was uncovered within the Residential Baseline Energy Efficiency Study (RBEE) performed by CSIRO, in which NatHERS assessments from Development Applications of older dwellings were biased towards lower star ratings than their reanalysed counterpart, using second-generation tools (Ambrose *et al.*, 2013).

The cause of misalignments amongst the remaining apartments of the present study could not be definitively determined, however human error would have been a very likely cause. More specifically, it was thought that incorrect zone specifications and incorrect shading specifications probably contributed most significantly to the misalignments, as the NatHERS benchmark study identified these issues as the most common factors leading to assessment inaccuracy. It should be noted, perhaps in response to such issues, that in 2020 the zoning specifications for apartment dwellings were updated within the Chenath Engine to improve the consistency and accuracy of predicted energy consumption for apartments (Department of the Environment and Energy, 2019b, 2019c).

The RBEE study also found that the average star rating increased for more recently built dwellings, as expected, due to increased stringency in the building performance requirements. Similarly, the current study found that the majority of the case-study apartment assessments, including those performed within this study and those included in the original Development Applications, which were produced between 2013 and 2016, no longer complied with the BASIX heating and cooling load limit requirements, due to increases in the stringencies in July 2017. This implied that the increased stringencies are expected to enhance the energy efficiency of the apartment building stock in NSW. So far, this appears to be the case. Average NatHERS star ratings for apartments in NSW have increased from 5.2 stars between 2011/12 and 2016/17 (NSW Department of Planning and Environment, 2020), to 6.2 stars between 2017/18 and 2019/20 (CSIRO, 2021b). The average NatHERS star rating for apartments in NSW between 2011/12 and 2016/17 quoted above aligned closely to the average NatHERS star ratings of the case-study apartment cohort within this study, which were also developed between 2011/12 and 2016/17. The average star ratings were 5.4 stars for the ratings sourced from the Development Applications and 5.2 stars for the ratings derived from simulations performed within this study.

## **5.7 Summary**

Representative numerical simulation models for each of the case-study apartments were developed using the second-generation NatHERS tool, AccuRate Sustainability. The models were constructed using data collected from the energy performance inspections conducted at each

apartment, and where appropriate from details within the Development Applications, and the relevant version of the NCC at the time of construction.

Comparisons between measured and simulated building thermal performance showed that on average the *measured cooling consumption was 105% greater* than the average simulated cooling consumption. However, there was significant scatter across the cohort. Individual comparisons highlighted very significant discrepancies for 3 of the 6 apartments, whereas 2 of the remaining 3 apartments actually used less cooling in reality than predicted using the NatHERS software with default settings.

On the other hand, the average *measured heating consumption was 37% lower* than the average simulated heating consumption. Individual comparisons highlighted significantly lower in heating use in reality compared with the simulated models for 2 Apartments in Canberra (a heating-dominated climate) and significantly higher use for 1 Apartment in Sydney.

The causes of mismatch between the measured and simulated *cooling* loads were, in order of impact/importance, deduced from simulations in this study to be as follows.

1. Occupant underutilisation of natural ventilation relative to the NatHERS protocol.
2. Warmer weather in reality compared to the NatHERS representative weather files.
3. Misuse of natural ventilation leading to excessive ventilation/infiltration was, i.e. leaving doors and window open when air conditioning was in operation.
4. Greater airtightness in the apartments in reality compared to NatHERS default settings did not appear to contribute significantly to greater cooling loads.
5. Occupant preferences of indoor conditions did not appear to significantly contribute to differences between reality and NatHERS.

The most significant causes of discrepancies between the measured and simulated *heating* consumption were, in order of significance/impact, thought to be as follows.

1. Occupant tolerance or preference of indoor conditions that were cooler or warmer, respectively, than the NatHERS heating thermostat settings.
2. Greater airtightness in the apartments in reality compared to the NatHERS default settings contributed to lower simulated heating loads.
3. Warmer weather in reality compared to the NatHERS representative weather files also contributed to lower simulated heating loads.

However, in reality, occupant preferences outweighed the combined effects of greater airtightness and warmer weather. Thus, while apartments with occupants that tolerated cooler indoor air temperatures than the NatHERS heating settings had significantly lower heating consumption, apartments with occupants that preferred warmer indoor temperatures than the NatHERS heating settings had higher heating consumption.

There were also large differences between the simulated loads calculated in this study and those obtained from the available Development Applications. This finding aligned with previous studies that demonstrated large variance in NatHERS assessment outputs amongst assessors, particularly for apartment-type dwellings. This implies that the current assessment methodology and regulatory framework may result in the approval of some dwellings with sub-standard thermal performance.

Finally, the thermal performance of the 2 apartments in the ACT appeared to exceed the minimum NCC requirements at the time of development (2013 and 2014), and even met the more recent the heating and cooling requirements introduced in 2019. However, around half the case-study apartments in NSW were near the minimum required thermal performance at the time of development and more than half would have failed to comply with the increased stringency introduced in July 2017.

## Chapter 6

# 6 Thermal Bridging of External Walls in Apartment Buildings

## 6.1 Introduction

### 6.1.1 Background

Thermal bridges can be defined as localised two-dimensional and three-dimensional heat transfer features, or elements, between interior and exterior sides of the thermal envelope of a building. Thermal bridges may generally be classed as either material or geometric in nature, and can be a combination of both. Common thermal bridges present in the thermal envelope of apartment buildings in Australia include:

- framing within the walls, ceiling, and floors that form the external envelope of the building, particularly framing that penetrates through a layer of insulation;
- window framing;
- fixings such as wall ties, nails, and bolted connections that fix masonry or plasterboard layers to the frame; and
- structural elements that abut, obstruct, or penetrate the building envelope such as a structural column, slab edge, or balcony protrusion.

Thermal bridges decrease the total thermal resistance of the building envelope, which may result in increased energy loads required to maintain thermal comfort. In addition, thermal bridges disrupt the temperature profile across the envelope, which may increase the likelihood of surface or interstitial condensation, which can lead to mould growth and reduced indoor air quality.

Steel framing was present in all nine of the case-study apartments, which were constructed using reinforced concrete structures, and effects of thermal bridging were evident as shown in Section 4.6.2. The prevalent use of steel framing in the construction of non-load bearing elements within Australian apartment buildings suggests that thermal bridging may be a significant and emerging issue as apartments become more prevalent and as the minimum required thermal performance of buildings continues to increase.

The 2019 edition of the National Construction Code (NCC) Volume One introduced several changes to the calculation processes for the thermal resistance of the building envelope, including new approaches for the treatment of thermal bridges. The NCC 2019 Volume One stipulates that

thermal bridging effects must be considered for building envelope elements that are required to achieve a minimum total thermal resistance as specified in Section J1 of the NCC (ABCB, 2019c). The total thermal resistance must be calculated in accordance with AS/NZS 4859.2:2018 *Thermal insulation materials for buildings; Part 2: Design*, which references NZS 4214:2006 *Methods of determining the total thermal resistance of parts of buildings* for the treatment of thermal bridges. However, these new requirements do not apply to sole-occupancy units (SOU) in Class 2 buildings (i.e. apartment dwellings) and Class 4 buildings (sole residences within buildings that are otherwise non-residential in nature), as the building envelopes of such building classes are not required to achieve a minimum total thermal resistance.

In SOUs of Class 2 and Class 4 buildings, thermal bridging is only addressed where lightweight external wall cladding or metal roofing attaches directly to metal framing without lining or with lining attached directly to the frame. In such cases, a thermal break with an equivalent resistance of no less than  $0.2 \text{ m}^2\text{K/W}$  must be installed at all points of contact between the external cladding and the metal frame. This requirement previously applied to all NCC Volume One building classifications since at least as early as 2009, but was superseded in NCC 2019 Volume One for non-residential building classifications by the aforementioned requirement that thermal bridging effects must be considered when evaluating whether building envelope elements achieve a minimum required total thermal resistance.

Thermal bridging is not currently considered when evaluating the heating and cooling loads of apartment dwellings within Section J (energy efficiency) of the NCC 2019 Volume One. As examined in Chapter 5, for the reduction of heating and cooling loads, compliance with the NCC is demonstrated for SOU's of Class 2 buildings by individually achieving a NatHERS rating of not less than 5 stars, and achieving an average NatHERS rating of not less than 6 stars, including the separate heating and cooling load limits. NatHERS does not currently consider the effects of thermal bridging during calculation of the simulated annual heating and cooling loads. This is despite AccuRate Sustainability, one of the three software tools accredited under NatHERS, featuring a simplified method to integrate the effects of thermal bridging in building envelope elements.

### **6.1.2 Aims and Objectives**

The primary aim of this chapter was therefore to determine the significance of thermal bridging effects caused by metal framing within external walls that conform to current building practices and codes for Australian apartments. The secondary aim was to determine whether the treatment of thermal bridging using the simplified methods currently adopted by Australian regulatory bodies is satisfactory relative to more thorough methods.

This involved the following objectives.

- Quantify and compare the total thermal resistances calculated for a representative external wall assembly commonly erected in Australian apartment dwellings when:
  - accounting for the effects of thermal bridging by direct calculation;
  - accounting for the effects of thermal bridging using the simplified methods referenced in the NCC and AccuRate; and
  - neglecting the effects of thermal bridging.
- Identify whether, and through which mechanisms, thermal bridging affects heat transfer and fluid dynamics within the air cavity layer in the wall.

## **6.2 Methodology**

The total thermal resistance of an external wall assembly that represents typical external wall assemblies commonly found in apartment buildings was calculated using three-dimensional steady-state conjugate heat transfer CFD simulations. Two distinct cases of the wall assembly were simulated, one including the effects of thermal bridging and the other ignoring the effects of thermal bridging. The results were compared to the total thermal resistance calculated using a variety of simple methods that are described in Section 2.8.3 of the literature review.

A comparison of the thermal characteristics of the air cavity between the thermally bridged and unbridged cases, determined using CFD, was performed to identify the impact of thermal bridging on the thermal characteristics of the air cavity.

### **6.2.1 Base Case (Case 1)**

A brick veneer wall with steel framing was nominated as the base case to represent a typical external wall assembly used in Australian apartment buildings.

#### **6.2.1.1 Selection Rationale**

Brick veneer was examined in this study despite being less common in apartment buildings than concrete block or autoclaved aerated concrete (AAC) wall systems as this analysis could then also be applied to brick veneer construction in detached dwellings (which is the more common construction system in that typology), as shown in Table 6-1. Although it should be noted that timber framing is currently significantly more common than steel framing in detached homes, the proportion of detached dwellings built with steel framing is increasing (Australian Construction Insights, 2018).

*Table 6-1 Prevalence of the three most common external wall systems used in apartment buildings in Australia between 2016 and 2021. Data sourced from the Australian Housing Data portal (CSIRO, 2021a).*

<b>External Wall System</b>	<b>Class 1 (Detached Dwellings)</b>	<b>Class 2 (Apartments)</b>
Concrete block	3%	30%
AAC	4%	17%
Brick veneer	52%	13%

Brick veneer was also considered to be similar thermally to concrete block veneer; the thermal resistances of 110 mm brickwork and 140 mm dense concrete block are 0.14 m<sup>2</sup>K/W and 0.16 m<sup>2</sup>K/W, respectively (ABCB, 2019c). In addition, both wall systems use wall ties to fix the masonry leaf to the frame. On the other hand, a 75 mm AAC panel has a much greater thermal resistance (between 0.3 to 0.75 m<sup>2</sup>K/W) and is typically fastened to the frame using horizontal battens (Hebel, 2015), which changes the air flow pattern within the cavity.

#### 6.2.1.2 Construction Details

A plan view cross section of the representative wall system is presented in Figure 6-1. The brick veneer wall assembly featured the following components:

- 110 mm clay brick and mortar external façade;
- 40 mm enclosed, unventilated air cavity;
- 0.4 mm pliable membrane;
- 76 mm insulation layer bridged by steel studs located at 600 mm spacing; and
- 13 mm plasterboard internal lining.

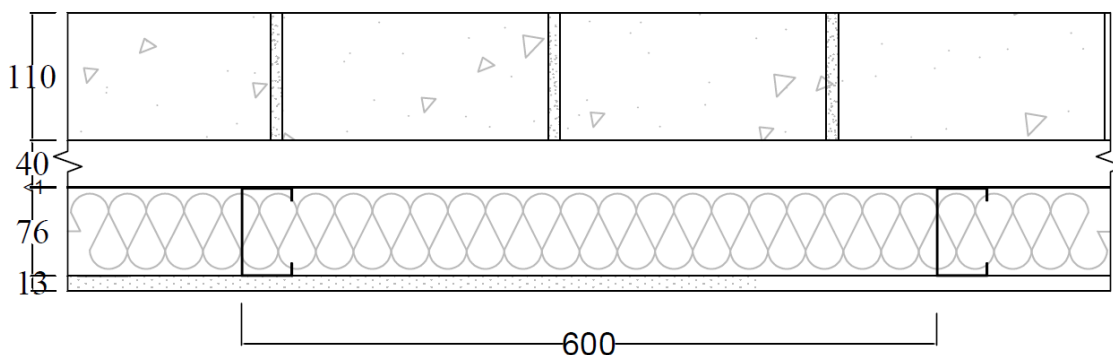


*Figure 6-1 Cross-section of the brick veneer wall assembly examined in this study. Dimensions given in millimetres.*

The wall was modelled with a height of 2.7 m. This is the minimum required ceiling height for habitable rooms within the Apartment Design Guide (NSW Department of Planning and Environment, 2015), which governs apartment design requirements in NSW via SEPP 65.

However, the total vertical rise in between concrete slab floors is likely to be slightly larger to allow for services and frame tracks.

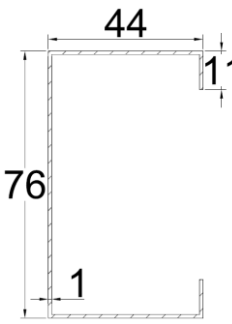
It should be noted that this construction assembly model was a typical and necessary simplification of a real wall assembly. Additional construction details and assumptions are provided in the following sub-sections.

### Frame Details

Metal framing was the sole source of thermal bridging that was considered within this representative external wall. The stud dimensions are provided in Table 6-2. It was assumed that insulation completely filled the concave region formed by the stud without being compressed. In adherence with literature discussed in Section 2.8.3, contact thermal resistances of 0.03 m<sup>2</sup>K/W were assumed at the interface between the inner stud flange and the plasterboard internal lining and between the outer stud flange and the pliable membrane.

*Table 6-2 Specifications of the steel stud used in the wall assembly.*

Stud dimensions (mm)	
Depth	76
Web width/BMT	1
Flange width	44
Lip length	11
Centre distance	600



The diagram shows a cross-section of a C-shaped steel stud. The vertical dimension is labeled 76. The horizontal dimension of the top flange is labeled 44. The vertical dimension of the lip on the top flange is labeled 11. The horizontal dimension of the web is labeled 1.

Horizontal framing members (i.e. noggings, top tracks, and bottom tracks) were not included within this simplified representative wall assembly to reduce the geometric complexity and the corresponding number of mesh elements required in the CFD simulations.

### Membrane Layer

The thermal resistance of the pliable membrane was assumed to be negligible as it was a homogeneous layer that provided an extremely small thermal resistance due to its very small thickness (approximately 0.4 mm). However, the membrane influenced the heat transfer within the wall assembly in the following ways.

- It was assumed that a non-reflective membrane surface was facing the air cavity in accordance with manufacturer installation instructions. Thus, the emissivity of the interior surface of the cavity) was assumed to be 0.9 in accordance with AS/NZS 4859.2.
- The membrane was assumed to be fixed to the steel frame using broad headed washers at 300mm centres in accordance with AS 4200.2:2017 *Pliable building membranes and*



*underlays; Part 2: Installation.* Thus, while the thermal resistance of the membrane was considered negligible, it was assumed that the contact resistance between the stud flange and the membrane was not negligible, as previously indicated, and between the insulation layer and the membrane, which was included to minimise heat conduction flanking the contact resistance applied to the steel stud.

### Fixings

The thermal bridging effects of fixings such as screws and wall ties were not considered in this study. Gorgolewski (2007) demonstrated empirically that fixings that do not penetrate insulation layers cause only a very minor increase (less than  $0.008 \text{ W/m}^2\text{K}$ ) in the total thermal transmittance of brick veneer wall elements. Thus, the overall magnitude of the effect of fixings on the total thermal resistance of the wall assembly was anticipated to be small relative to the uncertainty introduced by their inclusion in the CFD simulations. This uncertainty stemmed from the lack of quantitative data concerning contact resistances between fixings and adjacent elements.

### Cavity Ventilation

For the purposes of comparison, the cavity in the representative wall was assumed to be unventilated, i.e. there was no infiltration of external air into the cavity. This represents a simplified case for the purposes of comparing the treatment of thermal bridging effects between the simple methods and the CFD simulations.

However, in reality, brick veneer cavities are ventilated to a degree due to the mandatory presence of weepholes (formed by open head vertical joints between bricks) at centres not exceeding 1200 mm to remove excess moisture (Standards Australia, 2015, 2018). Nonetheless, drain holes in the form of open vertical joints in the outer leaf of a masonry cavity wall are stated in ISO 6964 to usually conform to the unventilated cavity criteria, and so are not regarded as ventilation openings within ISO 6946 (British Standards Institution, 2017c).

### **6.2.2 Alternative Case (Case 2)**

Only one alternative case was examined in this study. This case was defined based on the base case, but was modified by removing the steel stud and the associated contact resistances to exclude the influence of thermal bridges. To ensure the mesh was otherwise equivalent in the CFD simulations, a new mesh for the alternative case was not generated. Instead, the material properties of steel stud section of the mesh were replaced with those of insulation, thereby forming a homogeneous layer within the wall assembly.

## 6.2.3 Material Properties

### 6.2.3.1 Solids

Material Properties for solids were sourced from Specification J1.2 of NCC 2019 Volume One where available. Supplementary material property information was obtained from the AIRAH Technical Handbook 5<sup>th</sup> Edition (AIRAH, 2013). The relevant material properties of the solid materials are presented in Table 6-3.

*Table 6-3 Material properties of the solid materials used in the wall assembly.*

<b>Material</b>	<b>Density (kg/m<sup>3</sup>)</b>	<b>Thermal conductivity (W/mK)</b>	<b>Specific heat capacity (kJ/kgK)</b>
Steel	7850	47.5	490
Mineral wool insulation	22	0.035	880
Gypsum plasterboard	880	0.17	1050
Clay brick – 3.75 kg	1950	0.78	960

### 6.2.3.2 Fluids

For the CFD simulations, the fluid properties of air were extracted from Table A-4 in *Fundamentals of Heat and Mass Transfer, Sixth Edition* (Incropera *et al.*, 2006) assuming constant fluid properties obtained at a temperature of 303 K. This temperature was selected as it was the average of the free-stream temperatures on the interior and exterior sides of the wall.

## 6.2.4 Boundary Conditions

Boundary conditions for the film convection coefficients and free-stream temperature at the interior and exterior boundaries of the wall are presented in Table 6-4. These boundary conditions were specified in accordance with AS/NZS 4859.2 for design summer conditions in Australia.

*Table 6-4 Boundary conditions specified in accordance with AS/NZS 4859.2 for summer conditions in Australia.*

<b>Boundary</b>	<b>Free-stream temperature (°C)</b>	<b>Film resistance (m<sup>2</sup>K/W)</b>
Interior	24	0.12
Exterior	36	0.04

The horizontal surfaces at the top and bottom of the domain were adiabatic. The lateral vertical surfaces were modelled as periodic boundary conditions such that the domain was periodically repeating in the wall-planar direction, effectively forming an infinitely long wall that was not influenced by edge effects. In this way, heat and mass flow were linked between the lateral vertical sides. A summary of the boundary conditions is shown schematically in Figure 6-2.

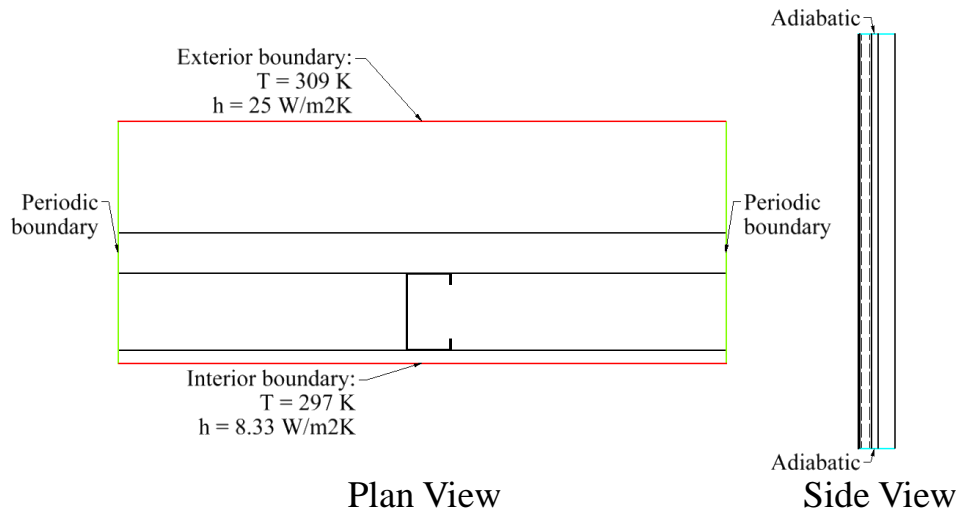


Figure 6-2 Graphical representation of boundary conditions within the numerical simulation. Note that the plan view and side view are not in comparable scales.

## 6.2.5 Simulation Methodology

Simulations were conducted using ANSYS Fluent 18.1 using the pressure-based solver with the pressure-velocity coupling scheme.

### 6.2.5.1 Computational Domain and Mesh

A three-dimensional periodically repeating section of the wall was modelled. The dimensions of the simulated domain were 0.239 m x 0.6 m x 2.7 m. Periodicity occurred in the wall-planar direction. The domain geometry is presented in Figure 6-3.

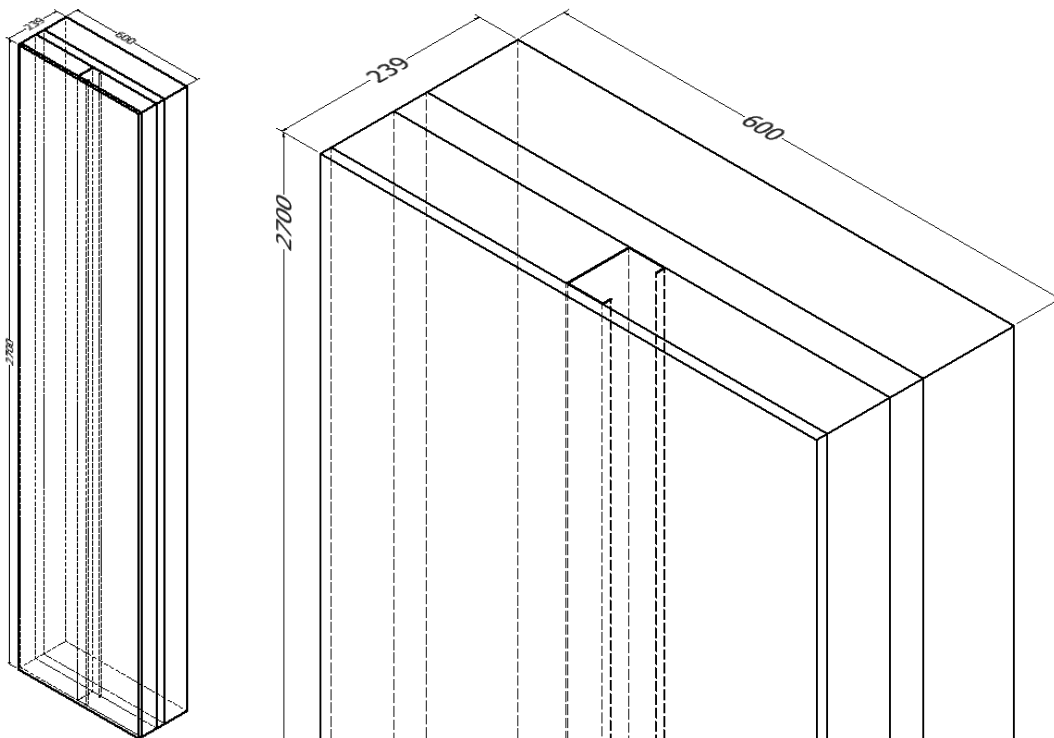


Figure 6-3 External wall geometry used in the CFD simulations. The full domain is shown on the left and a close-up is shown on the right.

A conformal mesh was generated to numerically represent the geometry. The mesh was refined in the cavity near the walls, maintaining a dimensionless near-wall distance,  $y^+$ , less than one, to accurately resolve thermal and velocity boundary layers in this critical section of the domain. A grid sensitivity analysis was conducted using a total of four versions of the mesh, which were incrementally refined according to a node count ratio of approximately 1.5.

#### 6.2.5.2 Cavity Flow Model

Natural convection was the primary mechanism driving flow within the cavity. The temperature difference of the air within the cavity was sufficiently small (i.e. less than 28.6°C) that the Boussinesq approximation could be used (Gray and Giorgini, 1976). The Boussinesq approximation treats density as constant in all inertial equations of motion except for the buoyancy term within the momentum equation (de Vahl Davis, 1968; ANSYS, 2009).

For Case 2 (no thermal bridging), flow was modelled with the laminar flow model in ANSYS Fluent (i.e. no turbulence modelling), as it was apparent from previous characterisations of flow within differentially heated enclosed cavities discussed in Section 2.8.4.2, that fluid motion in Case 2 was likely to occur within the laminar regime, despite not having strictly isothermal cavity walls (Yin, Wung and Chen, 1978; Chenoweth and Paolucci, 1986; Xamán *et al.*, 2005).

However, there was no guidance in terms of the expected flow regime in Case 1, where the temperature on the cold side of the wall varied significantly in the wall-planar direction, resulting in complex three-dimensional fluid movement. Based solely on the maximum temperature difference across the cavity due to the presence of thermal bridging, but otherwise assuming the fluid flow to behave as it would in a differentially heated cavity indicated that flow would remain in the laminar regime.

However, initial simulations using the laminar model showed the presence of localised weak turbulent effects, such as the formation of vortices, and fluid velocities in the cavity were significantly higher than anticipated based on reference studies of the differentially heated cavity for the same Rayleigh number. Thus, Case 1 was simulated again using the Shear Stress Transport (SST)  $k-\omega$  RANS turbulence model available within ANSYS Fluent. Wu and Lei (2015) compared the performance of turbulence models for natural convection flow within a three-dimensional square cavity, including the effects of surface radiation. They concluded that while all turbulence models were capable of capturing the main features of the flow, the SST  $k-\omega$  RANS model had the best overall performance in terms of modelling the time-averaged quantities of the flow. The SST  $k-\omega$  RANS model also provided the advantage of being able to accurately model laminar flow in regions where turbulence was absent.

Both the laminar model and the SST k- $\omega$  RANS model demonstrated close agreement in terms of heat flux through the cavity, maximum velocity within the cavity, and the primary flow paths throughout the cavity.

### 6.2.5.3 Radiation Model

The Discrete Ordinates (DO) radiation model available within ANSYS Fluent was used to model radiative heat transfer occurring within the air cavity. It was assumed that the air in the cavity was a non-participating medium. Thus, the radiative heat exchange examined in this study was purely surface-to-surface interactions. The DO model has been used in previous studies modelling radiative heat exchange within a differentially heated cavity with a high aspect ratio (Wu and Lei, 2015) and has been recommended by other similar studies (Benyahia *et al.*, 2020).

It was assumed that all surfaces facing the cavity were opaque, grey, and diffuse, with an emissivity of 0.9. This was in accordance with AS 4859.2 for non IR reflective products. Note that the stud and insulation faces were obscured from the cavity by a non-reflective pliable membrane.

## 6.2.6 Analysis of Results

The total thermal resistance of the representative wall assembly,  $R_T$ , was determined from the CFD simulations using Equation (6-1)

$$R_T = \frac{\Delta T}{q} \quad (6-1)$$

where  $\Delta T$  is the temperature difference between the free-stream temperature boundary conditions and  $q$  is the simulated heat flux intensity through the domain.

Similarly, the thermal resistance of the air cavity,  $R_{cav}$ , within the wall determined in the CFD simulations was calculated using Equation (6-2)

$$R_{cav} = \frac{T_H - T_C}{q} \quad (6-2)$$

where  $T_H$  is the area-weighted average temperature on the exterior side of the cavity,  $T_C$  is the area-weighted average surface temperature on the interior side of the cavity, and  $q$  is the average heat flux intensity through the cavity, including radiation and convection, which was equal to that through the domain due to steady-state boundary conditions.

### 6.2.6.1 Comparison with Simple Calculations

#### Thermal Resistance of the Wall Assembly

The total thermal resistance of the representative wall assembly was also calculated using the following simple methods for treating thermal bridges:

- the NZS 4214 version of the isothermal planes method; and

- the Gorgolewski method.

These methods were selected from the available simple methods described in Section 2.8.3 as a) they are specifically intended for steel-framed assemblies, and b) the NZS 4214 method and the Gorgolewski method have been referenced in the NCC and in NatHERS software AccuRate Sustainability, respectively, for the treatment of thermal bridges. These methods were applied to the thermally bridged case only (Case 1). The total thermal resistance of the non-thermally bridged case (Case 2) was determined using conventional one-dimensional heat transfer calculations.

The total thermal resistances of Case 1 and Case 2 calculated using these simplified methods were compared, including comparison with the CFD simulations.

#### Thermal Resistance of the Air Cavity

The thermal resistance of the air cavity determined by CFD simulations was compared with the thermal resistance of the cavity calculated using the semi-analytical model that is provided as part of ISO 6946 and adopted in AS/NZS 4859.2, which was used in the simple methods to determine the thermal resistance of the air cavity. Following this method, the thermal resistance of an unventilated air cavity is given by Equation (6-3)

$$R_{cav} = \frac{1}{h_a + h_r} \quad (6-3)$$

where  $R_{cav}$  is the thermal resistance of the cavity ( $m^2K/W$ ),  $h_a$  is the convection coefficient ( $W/m^2K$ ) and  $h_r$  is the radiative coefficient ( $W/m^2K$ ).

The convection coefficient is determined using Equation (6-4)

$$h_a = MAX \left( \frac{0.025}{d}, 1.25 \quad \text{if } \Delta T \leq 5 \right. \\ \left. 0.73 \cdot \Delta T^{1/3} \quad \text{if } \Delta T > 5 \right) \quad (6-4)$$

where  $d$  is the cavity width (m), and  $\Delta T$  is the temperature difference across the cavity (K); and the radiative coefficient is given by Equation (6-5)

$$h_r = 4 \cdot \sigma \cdot T_{ave}^3 \cdot \frac{1}{\frac{1}{\varepsilon_1} + \frac{1}{\varepsilon_2} - 1} \quad (6-5)$$

where  $\sigma$  is the Stefan-Boltzmann constant ( $W/m^2K^4$ ),  $T_{ave}$  is the average cavity temperature (K), and  $\varepsilon_1$  and  $\varepsilon_2$  are the emittances of the surfaces bounding the air cavity.

### 6.2.6.2 Thermal Characterisation of the Air Cavity Layer

A comparison of the CFD simulations of the air cavities in Case 1 and Case 2 were examined more thoroughly to identify whether thermal bridging effects in a layer adjacent to an air cavity influenced the thermal characteristics of the cavity itself.

This involved qualitative characterisation of discernible differences in the key flow characteristics between the two cases. This was facilitated by comparison of the flow fields and velocity profiles within the cavity using vector maps and streamlines.

The component heat transfer mechanisms through the cavity were also specifically quantified. The net radiative heat transfer across the cavity was available as an output of the CFD program. This was compared to the general solution for the net radiative heat exchange between two planar surfaces, given by Equation (6-6)

$$q_{rad} = \frac{\sigma(T_H^4 - T_C^4)}{\frac{1}{\varepsilon_H} + \frac{1}{\varepsilon_C} - 1} \quad (6-6)$$

where  $\sigma$  is the Stefan-Boltzmann constant, the subscripts  $H$  and  $C$  correspond to the hot and cold planar surfaces,  $T$  is the area-weighted average surface temperature, and  $\varepsilon$  is the surface emissivity.

The convective heat transfer in the cavity was characterised using the Nusselt number, which was calculated using (6-7)

$$Nu_L = \frac{q_{conv} \cdot L}{k(T_H - T_C)} \quad (6-7)$$

where  $q_{conv}$  is the heat flux through the cavity excluding surface to surface radiative heat transfer,  $L$  is the characteristic length, taken as the width of the cavity, and  $k$  is the thermal conductivity of the air.

## 6.3 Results and Discussion

### 6.3.1 Mesh Sensitivity

Case 1 was simulated using coarse, medium-coarse, medium-fine, and fine mesh sizes to assess whether the solution was sufficiently independent of mesh size. The coarse, medium-coarse, medium-fine and fine meshes had  $0.61 \times 10^6$  nodes,  $0.91 \times 10^6$  nodes,  $1.3 \times 10^6$  nodes, and  $2.2 \times 10^6$  nodes, respectively.

Figure 6-4 demonstrates the variation in a number of key variables, including those used to identify convergence, as a function of node count.

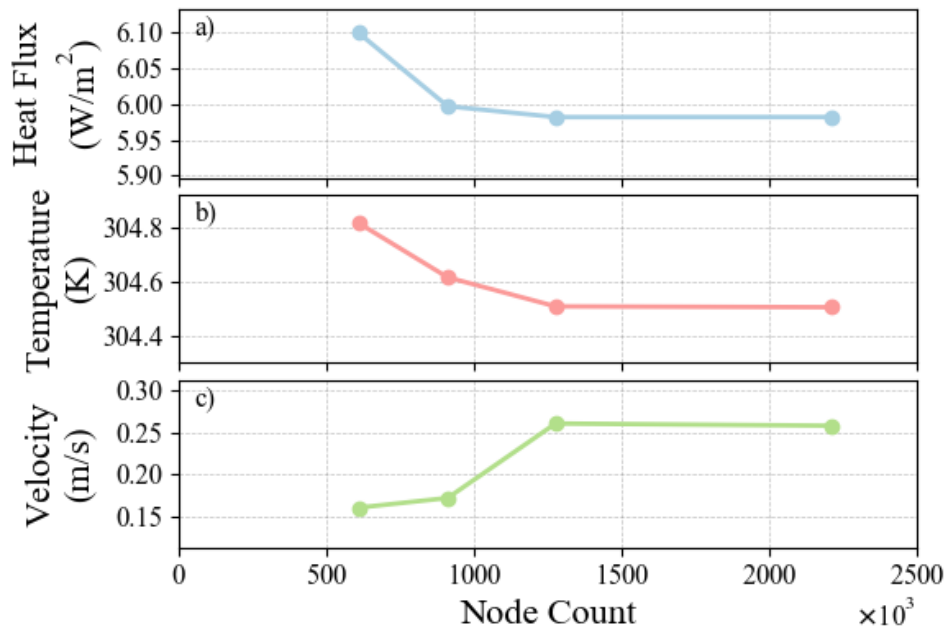


Figure 6-4 A collection of key variables as a function of mesh size. Plot a) corresponds to the heat flux at the interior boundary; b) corresponds to the temperature at the interface between the steel stud flange and the air cavity; and c) corresponds to the maximum air velocity magnitude within the air cavity.

There was very little variation between the medium-fine and fine meshes in each of the monitored variables as evidenced in Figure 6-4. However, the variation increased as the node count decreased below a critical threshold node count, which occurred between  $0.91 \times 10^6$  and  $1.3 \times 10^6$  nodes.

The area-weighted average heat flux through the inlet boundary using the medium-fine mesh was 0.0012% lower than when using the fine mesh. This increased to 0.25% and 2.0% higher heat fluxes when using the medium-coarse and coarse meshes, respectively. Similarly, at the interface between the steel stud flange and the air cavity, the mean surface temperature using the medium-fine mesh was  $0.0030^\circ\text{C}$  warmer than when using the fine mesh but was  $0.11^\circ\text{C}$  and  $0.31^\circ\text{C}$  warmer when using the medium-coarse and coarse meshes, respectively.

Flow behaviour within the cavity simulated using the medium-fine and fine meshes were qualitatively very similar. However, there was substantial differences in the flow behaviour between the two fine and two coarse meshes. Quantitatively, the maximum velocity within the cavity using the medium-fine, medium-coarse, and coarse mesh sizes was 1% higher, 33% lower, and 38% lower, respectively, than the maximum velocity when using the fine mesh.

The medium-fine mesh therefore provided an acceptable level of agreement with the fine mesh; the results from the medium-fine mesh were therefore considered sufficiently independent of the mesh sizing. The medium-fine mesh was used in the subsequent reporting of results generated from the CFD simulations.



### 6.3.2 Total Thermal Resistance

The total thermal resistance of the wall assembly, calculated using each of the methods examined in this study, is presented in Table 6-5.

*Table 6-5 Total thermal resistance of the brick veneer wall assembly calculated using the examined methods with and without consideration for thermal bridges.*

Case	Method	Total Thermal Resistance (m <sup>2</sup> K/W)
1 (Including thermal bridging)	CFD simulation	2.00
	AS/NZS 4859.2	1.90
	Gorgolewski	1.87
2 (Ignoring thermal bridging)	CFD simulation	2.74
	AS/NZS 4859.2	2.73

A comparison between the total thermal resistances calculated using the CFD simulation method for Case 1 and Case 2 indicated that including the steel stud in the model reduced the total thermal resistance of the wall by 27%. In other words, the insulation efficiency of this wall assembly was 73%, where insulation efficiency is defined as the ratio of the actual total thermal resistance to the ideal (i.e. unbridged) total thermal resistance. A comparison of the temperature distributions for each case is presented in Figure 6-5.

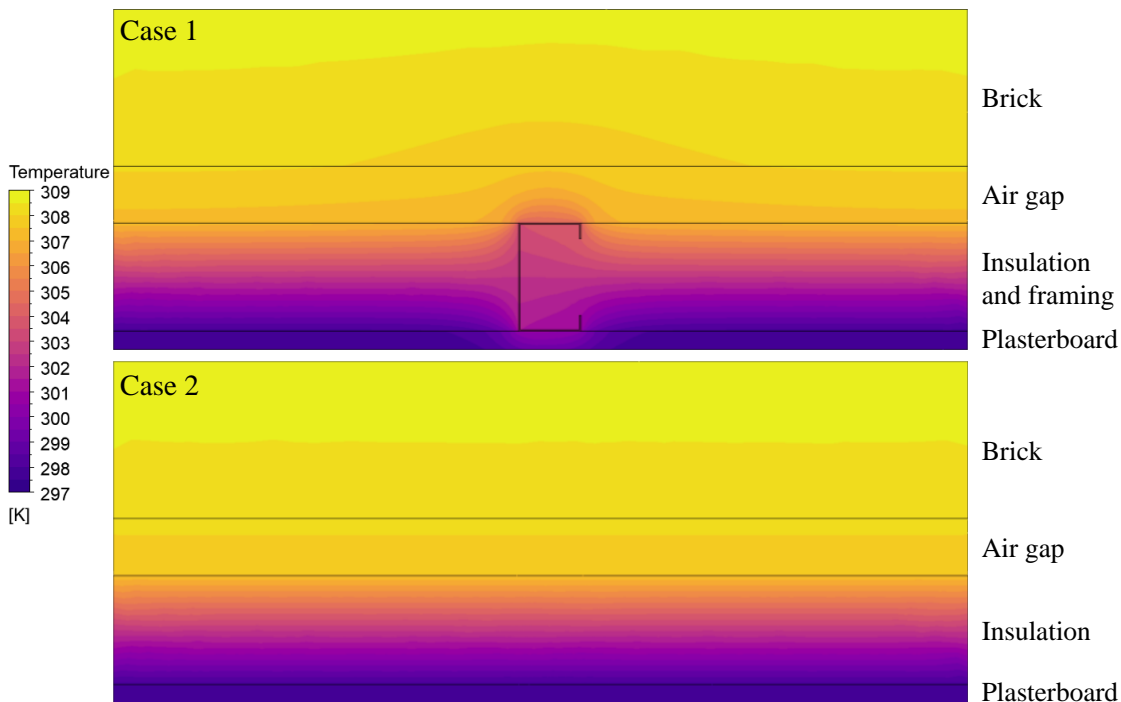


*Figure 6-5 Comparison of temperature distributions for Case 1 (bridged) and Case 2 (unbridged) at a cross-section of the wall assembly corresponding to the mid-height of the cavity (y=1.35m).*

The simplified methods, i.e. AS/NZS 4859.2 and the Gorgolewski method, underestimated the total thermal resistance of the wall assembly examined in the present study by 5% and 6.5%, respectively, relative to that calculated using the numeric simulation method. This suggests that these methods provide slightly conservative estimates of the actual total thermal resistance of the wall. This is supported by accounts from Trethewen (1998), who found the NZ 4214 adaptation of the isothermal planes method to be slightly conservative, but found the parallel paths method to be rather optimistic.

The estimate produced by the NZS 4214 adaptation of the isothermal planes method was within the margin of error reported for the method during its development (Trethewen, 1995), but the estimate produced by the Gorgolewski method exceeded the anticipated margin of error. Gorgolewski reported that his method produced an average absolute error of 2.7% relative to finite-element modelling. However, both Gorgolewski's simplified method and the finite-element analysis he used to calibrate his method did not appear to consider contact resistances. Thus, the Gorgolewski method can be expected to underestimate the total thermal resistance when contact resistances are considered.

For the unbridged case (Case 2), the total thermal resistance calculated using CFD simulation and AS/NZS 4859.2 methods demonstrated close agreement. The slight difference in the total thermal resistance between the two methods was attributed to the resistance of the cavity, which was 10% greater in the CFD model compared to that predicted using the semi-analytical method provided in AS/NZS 4859.2.

### **6.3.3 Thermal Characteristics of the Air Cavity**

Results from the CFD simulations provided interesting insights into the nature of natural convection within an unventilated cavity with and without consideration of thermal bridging effects within layers adjacent to the cavity.

#### **6.3.3.1 Flow Patterns**

When the stud was not included in the simulation, the flow was characterised by a single convection cell with symmetrical boundary layers on the cold and hot sides of the cavity. The flow was effectively two-dimensional.

Surface-to-surface radiation was the dominant heat transfer mechanism across the cavity. It is important to note however that Xamán *et al.* (2008) previously demonstrated that surface-to-surface radiation does not significantly affect the flow pattern of air within an enclosed cavity. While convective heat transfer was apparent at the top and bottom extremities of the cavity, the temperature gradient across the width of the cavity was linear throughout the majority of the cavity, indicating that conductive heat transfer was significant. The average Nusselt number,

calculated using Equation (6-7) was 1.07, indicating that heat transfer was almost exclusively via conduction.

The flow pattern described above is similar to the flow regime of conduction previously reported by Yin, Wung and Chen (1978) and shares the defining characteristic of having a dimensionless horizontal temperature gradient of -1 at the mid-plane across the cavity. The flow pattern in the cavity also resembles the “fully developed merged boundary layer” flow regime described by Chenoweth and Paolucci (1986), which is described by a single convection cell with universal velocity and temperature profiles across the width of the cavity occupying the majority of the cavity region that are independent of their position along the height of the cavity.

The inclusion of the stud, and thereby the effect of thermal bridging in the wall, resulted in several key differences in the flow patterns within the air cavity compared to the unbridged case.

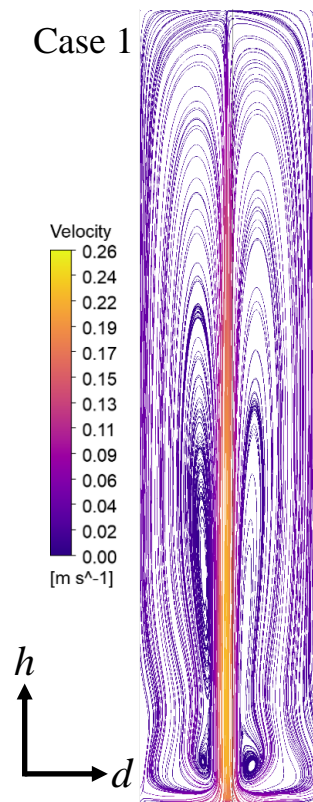


Figure 6-6 Two-dimensional flow streamlines in a plane at the mid-width of the cavity (Case 1).

The primary difference was the formation of coupled convection cells rather than unicellular flow as illustrated in Figure 6-6. These coupled convection cells were arranged such that downward flow occurred in the vicinity of the stud flange and upward flow occurred in the regions in between repeated studs. This is more clearly visualised in the three-dimensional vector map at the mid-height of the cavity depicted in Figure 6-7. Thus, in the thermally bridged case, the coupled convection cells were oriented approximately perpendicular to the cell orientation that typically occurs in enclosed cavities.

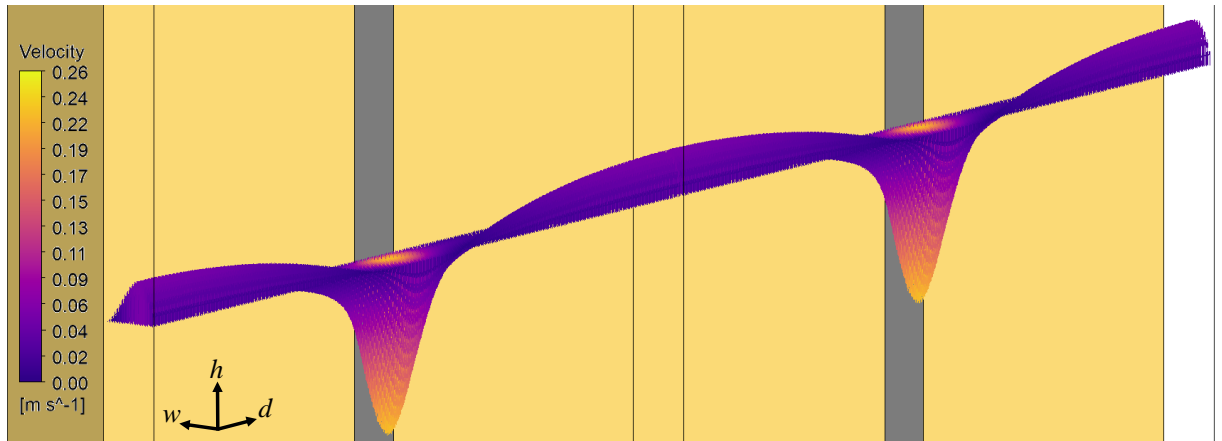


Figure 6-7 Three-dimensional visualisation of the air cavity flow vectors at the mid-height of the cavity (Case 1). The geometry and vectors have been repeated to highlight the flow in between adjacent studs. The stud flange and insulation surfaces of the interior wall have been indicated in grey and yellow, respectively. Note that the interior side of the cavity is cooler than the exterior side (not shown).

The concentration of upward and downward flows in the regions in between and adjacent to the stud, respectively, also resulted in significantly higher fluid velocities within the cavity compared to the unbridged case. Figure 6-8 presents a to-scale comparison of the velocity profiles across the width of the cavity between the thermally bridged and unbridged cases. The figure demonstrates that the peak of the downward and upward flows were slightly skewed to the cool and warm sides of the cavity, respectively, as expected, and that maximum downward and upward velocities in Case 1 were 12.2 and 3.2 times, respectively, those in Case 2.

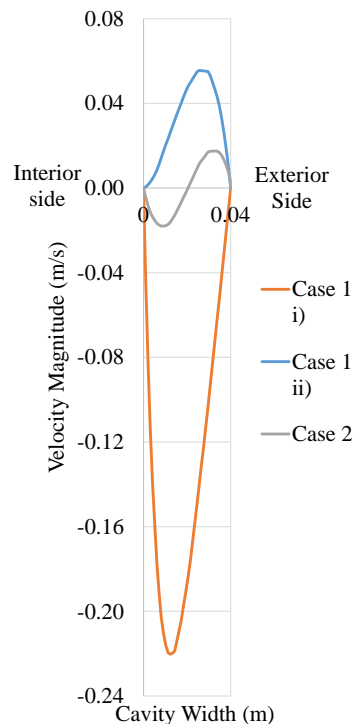


Figure 6-8 Velocity profiles at the mid-height of the cavity ( $y=1.35\text{m}$ ) for Case 1 and Case 2. The two profiles shown for Case 1 represent the velocity profiles at the stud centroid plane (i) and at the mid-plane between adjacent studs (ii).

The relatively greater momentum of the fluid in the thermally bridged case resulted in vortices occurring at the bottom of the cavity as the downward flow impinged the bottom surface of the cavity as shown in Case 1 i) c) of Figure 6-9. The vortices facilitated the lateral dispersion of air in the transition to upward flow. However, despite the higher velocity in Case 1 compared to Case 2, flow remained laminar for the majority of the cavity.

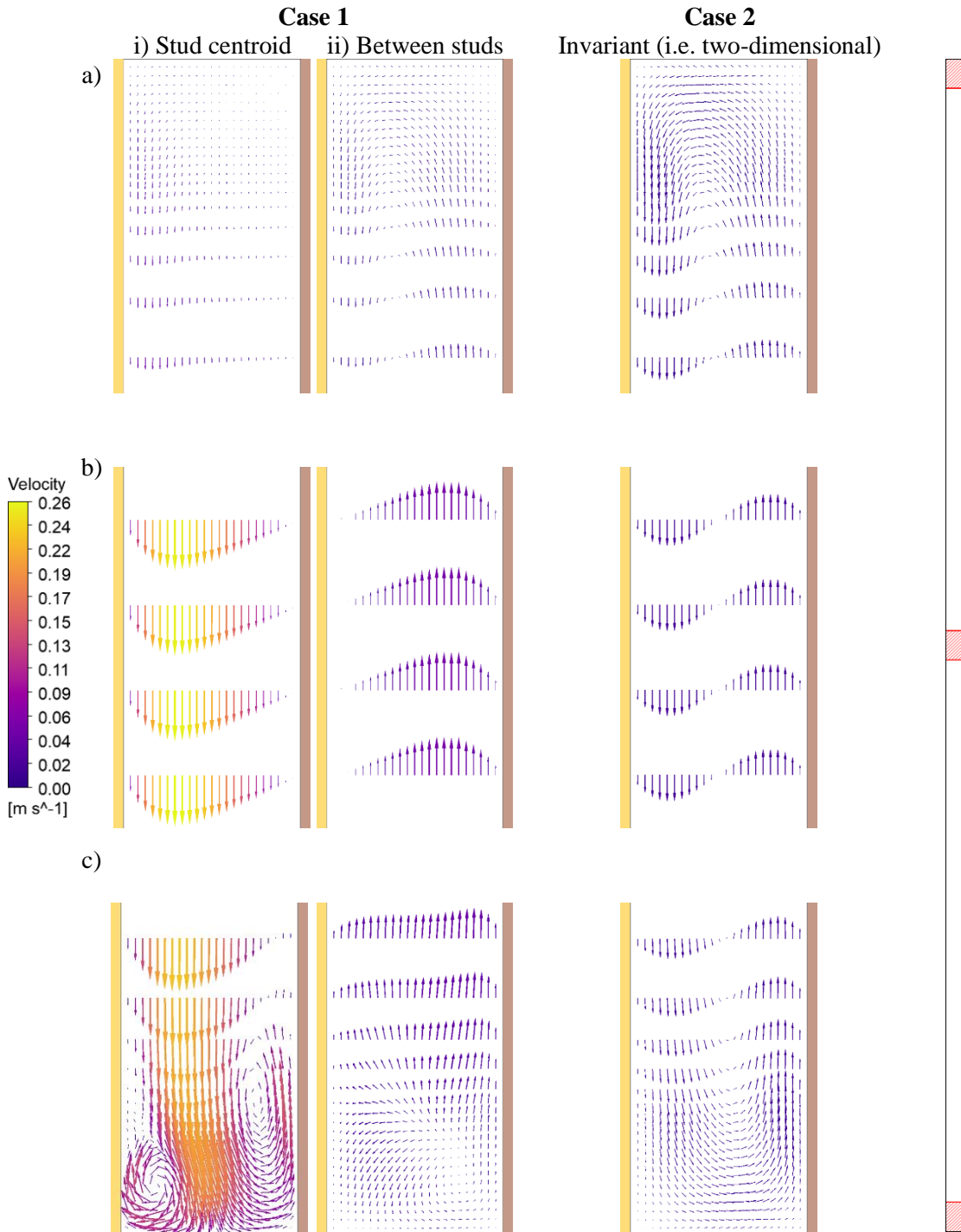


Figure 6-9 Field vectors for flow at the top (a), central (b), and bottom (c) regions of the air cavity indicated by the red, shaded regions on the right side of the figure. The vectors in Case 1 ii) and Case 2 have been enlarged by a factor of 3 and 6, respectively, relative to Case 1 i), to better illustrate key features of the flow.

### 6.3.3.2 Thermal Performance

The thermal resistance of the air cavity was calculated to determine whether the various flow patterns observed in the cavity impacted the thermal performance of the cavity, with results presented in Table 6-6.

*Table 6-6 Thermal characteristics of the air cavity determined using CFD.*

Case	Area-weighted average surface temperature (K)		Thermal resistance (m <sup>2</sup> K/W)	Total heat flux (W/m <sup>2</sup> )	Radiative heat flux (W/m <sup>2</sup> )	Convective Nusselt Number
	Interior	Exterior				
1	307.92	306.94	0.163	5.98	5.21	1.21
2	308.21	307.49	0.164	4.37	3.87	1.07

Including thermal bridging effects within layers adjacent to the air cavity slightly reduced the thermal resistance of the air cavity and ultimately had an insignificant impact (<0.7% change).

In both cases radiation was the dominant heat transfer mechanism, accounting for 87% and 89% of the heat transfer in Case 1 and Case 2, respectively. The difference in radiative heat flux between Case 1 and Case 2 corresponded solely to differences in the interior and exterior surface temperatures between the two cases, and could be approximated by radiative heat transfer between planar surfaces given by Equation (6-6).

Convective and conductive heat transfer increased by a greater magnitude than predicted by the temperature difference alone. Thus, it was apparent that convection within the cavity increased. The Nusselt number of the cavity, defined using Equation (6-7), increased by 14% for Case 1 compared to Case 2. Therefore, the change in convective heat transfer was significant, but ultimately did not significantly impact the total heat transfer across the cavity. This was thought to be because radiation was the dominant heat transfer mechanism across the cavity and that convective effects were still relatively weak as conduction was still significant.

Overall, this comparison of a simplified cavity model suggests that: a) convection in the cavity is affected by the changed flow dynamics resulting from thermal bridging effects in a building layer adjacent to the cavity; and b) that this change in convection is not significant to the total heat flux through the cavity. However, in reality, it is anticipated that convective heat transfer effects can be more significant for a number of reasons. Firstly, including the effects of surface roughness, particularly of the brick wall, may increase the convective heat transfer coefficient; secondly, the presence of brick ties fixed to the studs along the height of the cavity are likely to disrupt the formation of developed flow paths, thereby enhancing mixing; and thirdly, infiltration of external air through the open head joints in the brick wall may enhance natural convection and/or result in forced convection in or through the cavity. In addition, convective heat transfer would have a larger relative impact in wall cavities where IR-reflective membranes have been installed to

reduce the radiative heat transfer across the cavity. However, the examination of additional cases was outside of the scope of this project but is recommended for future work.

## **6.4 Summary**

This chapter provides a comparative analysis of different methods used to determine the total thermal resistance of a steel-framed brick veneer external wall assembly that is representative of those that are prevalent in recently constructed apartment buildings throughout Australia.

The findings indicate that the method adopted by the Australian NCC Volume One in 2019 and the method currently available in the NatHERS approved software, AccuRate, but not yet used for regulatory assessments both slightly underestimated the total thermal resistance of the wall assembly compared to conjugate heat transfer CFD simulation method. Thus, for the representative wall examined, these methods were conservative in their treatment of thermal bridges.

A comparison of CFD simulations of the wall assembly indicated that the inclusion of thermal bridges reduced the total thermal resistance of the wall by 27% compared to the case where thermal bridging effects were not considered and heat transfer was considered to be one-dimensional.

The CFD simulation of the wall assembly also demonstrated that there were considerable differences in the flow dynamics occurring within the air cavity of the wall when thermal bridging effects were considered versus when they were ignored. Specifically, the presence of the stud resulted in the formation of high velocity downward air flow at the vicinity of the stud flange and upward flow occurring in between adjacent studs. In effect, this created a coupled-convection cell system that was almost orthogonally oriented relative to the net direction of heat flux through the wall, which was in contrast to two-dimensional, symmetric, unicellular flow in the unbridged case.

While the significant difference in flow dynamics occurring within the cavity enhanced convective heat transfer, it did not significantly affect the overall thermal resistance of the cavity, since radiation dominated in the representative case chosen. However, enhanced convection in the thermally bridged case may become significant when radiative heat transfer is less prominent, such as in walls with the reflective surface of a membrane facing into the cavity.

## Chapter 7

### 7 Conclusions

The primary aim of this study was to understand and quantify the thermal performance of apartments in Australia, particularly with respect to the simulated thermal performance determined in accordance with the Australian Nationwide House Energy Rating Scheme (NatHERS). This is thought to be the first study to have measured the thermal performance of a cohort of occupied, residential buildings in Australia that consisted exclusively of apartments.

The literature review presented in this thesis details the context and motivations for this study and identified significant knowledge gaps. In particular, it highlighted the fact that there is very little quantitative evidence of the actual thermal performance of apartments despite the introduction of simulation-based energy efficiency regulations (i.e. NatHERS) for Australian apartments in 2005 and the significant number of apartments constructed since then.

The review also revealed that there was previously only a relatively limited understanding of the link between the actual and simulated thermal performance of residential dwellings generally. Differences between actual and simulated thermal performance were most commonly attributed to uncertainties regarding thermal comfort perceptions and occupant behaviour followed by weather conditions and building envelope performance.

The impacts of thermal bridging, which is not accounted for in the NatHERS protocol and has historically been considered negligible in building performance simulation studies generally, was also regarded as a contributing factor to differences between the actual and simulated thermal performance.

Thus, there were three primary research activities described within this thesis as follows.

- Determination of thermal performance (i.e. energy consumed for heating and cooling) and the associated thermal conditions, occupant behaviour, local weather conditions, and building envelope performance for a set of occupied apartments.
- Comparison of measured and simulated thermal performance of the set of apartments.
- Determination of the impact of thermal bridging in apartments.

Nine case-study apartment dwellings located in Wollongong, Sydney, and Canberra were evaluated. Seven of the apartments had air conditioning, however air conditioning was only able to be independently monitored in six apartments. Data collection involved longitudinal monitoring of circuit-level electricity consumption, window state, and indoor environmental



conditions for a period of up to nine months. A comprehensive energy efficiency audit was conducted at each apartment including airtightness testing via the fan pressurisation method and a thermographic survey.

In terms of energy consumption in apartments the primary findings were as follows.

- The mean daily electricity consumption of the case-study apartments was 9.4 kWh, which was comparable to, but 0.6 kWh lower than that of apartments monitored in Sydney as part of the Smart Grid Smart City (SGSC) project.
- Air conditioning consumption accounted for 19% of the total electricity consumption across the cohort. Average daily air conditioning consumption amongst the apartments with air conditioning was 2.2 kWh, which was approximately 50% less than observed in a cohort of predominately detached dwellings in Western Sydney (Ding *et al.*, 2019).
- A new rule-based algorithm was developed to automatically classify air conditioning electricity consumption data as being either ‘standby’ or ‘active’ consumption, and the latter was further automatically classified as heating or cooling. This method demonstrated improved classification accuracy compared to methods applied in previous studies.
  - Across the six apartments in which air conditioning consumption was independently monitored, 25% of the electricity consumed by air conditioning was when systems were in ‘standby’ operation. However, in three apartments, overall energy consumed during standby operation was comparable to or even exceeded energy consumed in active operation.
  - Of the energy consumed in active operation, 74% was used for cooling and 26% was used for heating.

New research related to indoor thermal conditions within Australian apartments were as follows.

- A new analysis tool was developed to identify periods when apartments were occupied using a combination of rule-based and machine-learning algorithms.
- Thermal conditions were evaluated against the adaptive thermal comfort model.
  - The two naturally ventilated apartments exhibited the greatest proportion of occupied hours in summer when internal conditions exceeded the adaptive thermal comfort 80% acceptability bands. This implies that natural ventilation may be insufficient to maintain comfort for such dwellings in their particular climate zone (i.e. NatHERS Climate Zone 56) and aligns with findings from Jensen *et al.* (2017), which were that Australian apartments are not designed to maintain acceptable thermal conditions during heat wave events without air conditioning.

- More than 50% of the occupied hours in winter for one apartment were below the 80% acceptability limits of the adaptive comfort model. This apartment had the lowest heating consumption amongst the cohort despite being located in Canberra, which has a substantially colder climate than Sydney and Wollongong. The conditions observed in this apartment are considered by the World Health Organization (WHO) to pose health risks to vulnerable individuals (e.g. infants and the elderly), however none of the regular occupants of this apartment were considered to be vulnerable.
- The remaining apartments were considered comfortable, with over 90% of occupied hours within the 80% acceptability limits of the adaptive comfort model.

Analysis of occupant management of the indoor environment via operation of heating, cooling, and window systems revealed significant differences with respect to NatHERS heating and cooling assumptions and also had significant implications for space conditioning consumption. The key findings regarding occupant behaviour are presented below.

- There were two distinct occupant cooling strategies observed amongst the cohort. Occupants in four of the air-conditioned apartments prioritised natural ventilation and only used air conditioning when natural ventilation was deemed unsuitable. Occupants in the two other air-conditioned apartments preferred to use air conditioning to provide cooling regardless of outdoor conditions and did not utilise natural ventilation opportunities.
- A comparison of observed occupant cooling strategies with the cooling strategy assumed by NatHERS indicated that only 9% of occupant air conditioning usage events satisfied the indoor and outdoor conditions defined in NatHERS to invoke cooling. 56% of cooling-on events partially met such conditions, although these conditions also met the requirements to utilise natural ventilation to provide cooling. The remaining 35% of cooling-on events did not meet any of the conditions required to invoke cooling. This suggests that the NatHERS protocol either overestimates the cooling potential of natural ventilation or that the definition of thermal comfort used by NatHERS does not reflect occupant perceptions/practices. In any case, the implication is that cooling energy consumption is likely to be underestimated by NatHERS.
- During summer, occupants cooled their bedrooms to lower temperatures than their living rooms. This differs from NatHERS assumptions in which cooling thermostat settings are equivalent between all zone-types and only vary by schedule.

- Occupants heated their apartments to between 2 and 4°C above the NatHERS heating thermostat settings, again indicating that occupant preferences differed from the assumptions used by NatHERS.

Previously, there was little published data on the airtightness of apartments in Australia, despite indications from international studies that apartments are generally more airtight than detached dwellings. Findings from airtightness testing of the case-study apartments were as follows.

- The average air change rate of the apartments was 5.9 h<sup>-1</sup> at 50 Pa, which was significantly less than the reported national average of 15.5 h<sup>-1</sup> at 50 Pa for recently constructed detached dwellings.
- This suggests that recently constructed apartments in Australia are significantly more airtight than recently constructed detached dwellings, which aligns with studies conducted internationally.
- If these results are representative of apartments across Australia, then the infiltration model used in NatHERS could not be considered as accurate for apartment dwellings. Literature indicates that uncertainty of infiltration rates has been regarded as the leading cause of uncertainty in simulated heating loads (de Wilde and Tian, 2009). Thus infiltration losses might be overestimated by NatHERS default assumptions resulting in excessive simulated apartment heating loads.

The thermographic inspections of the apartment building envelopes revealed the following.

- Generally, external wall insulation was well installed. However, thermal bridges caused by steel studs were prevalent. This suggests that thermal bridging may be an important issue in apartments that warrants additional treatment in NatHERS and NCC.
- Installation defects of ceiling insulation were present in the penthouse apartment as evidenced by large gaps in the insulation coverage in the ceiling. This is likely to have been a contributing factor to overheating of the upper floor of this apartment.

Comparison of weather conditions during the monitoring period of the apartments relative to the NatHERS prescribed representative meteorological year (RMY) weather data indicated that of the climate zones observed, on average, there were 51% more cooling degree days (CDDs) in reality compared to the RMY files and 12% less heating degree days (HDDs). This agreed with the trend observed in other studies that average temperatures in Sydney and surrounding areas have increased in recent years relative to historic norms. Thus, the RMY files, which represent historic norms, might no longer represent current weather patterns.

## **Simulated Thermal Performance Evaluation**

Building performance simulation models were developed for each of the apartments, which were calibrated against measured indoor temperature data and local weather conditions to infer visually obscured building envelope details. Comparison between field measurements and NatHERS simulations performed with these models in accordance with the NatHERS protocol showed significant differences between the actual and simulated heating and cooling consumption. A large fraction of these differences could be explained by differences between assumptions in the NatHERS protocol relative to observations made of the apartments during the field study. The relative impact of these differences were quantified by running NatHERS simulations using modified inputs that matched with field observations and examining the corresponding change in simulated heating and cooling consumption. The key findings are listed below.

- Measured cooling consumption was 105% greater than cooling loads determined by NatHERS and measured heating consumption was 37% lower than heating loads determined by NatHERS. The overall space conditioning consumption over the monitoring period was 27% greater in reality than simulated.
- This suggests that NatHERS has a propensity to underestimate cooling consumption in apartments. This finding aligns with comparisons conducted in detached dwellings, and therefore indicates underestimating cooling consumption by NatHERS is consistent across both dwelling types.
- The greatest cause of underestimated cooling loads were differences in occupant behaviour, i.e. a combination of occupants foregoing natural ventilation opportunities and NatHERS overestimating the cooling potential of natural ventilation during warm outdoor conditions. Warmer weather in reality compared to NatHERS weather data had the second most significant influence on overestimated cooling consumption.
- As in previous studies performed in detached dwellings, comparisons of heating consumption were inconsistent. The most significant uncertainties were regarding occupant thermal comfort preferences and infiltration rates.

## **Thermal Bridging**

The impact of thermal bridging in apartments was investigated to determine the impact of steel framing on the total thermal resistance of masonry-clad walls. This external wall assembly was considered typical of Australian apartment construction practices based on CSIRO metadata of NatHERS assessments and inspections of the case-study apartments (CSIRO, 2021a).

While NatHERS does not currently consider the effects of thermal bridging, simplified methods for the treatment of thermal bridging have been adopted by the NCC or proposed for future

versions of NatHERS. The accuracy of such simplified treatments was investigated relative to comprehensive computational fluid dynamics (CFD) simulations involving steady-state conjugate heat transfer. The key findings from these comparisons are summarised below.

- CFD simulations showed that the total thermal resistance of the wall was reduced by 27% by the steel framing compared to the one-dimensional heat-transfer case without thermal bridges.
- The NZS 4214 Isothermal Planes method and the Gorgolewski method both underestimated the total thermal resistance of the thermally bridged wall by approximately 5% relative to total thermal resistance calculated using CFD simulations. Thus, use of these methods to account for thermal bridging is likely to result in walls that exceed the minimum required total thermal resistance in reality.

Thermal bridges that occur adjacent to air cavities result in periodic temperature variations along the inside surfaces of the cavity. The impact of such phenomenon on the thermodynamics of enclosed air cavities did not appear to have been investigated in previous literature.

The presented CFD study demonstrated the following.

- Including thermal bridging resulted in significantly higher air velocities and substantial differences in air flow patterns, as well as increased convective heat transfer coefficients in the cavity.
- For the circumstances modelled in the present study, heat transfer across the cavity was dominated by surface-to-surface radiation. Nusselt numbers were 1.21 and 1.07 in the bridged and unbridged cases, respectively, resulting in a negligible difference in the overall thermal (convection and radiation) resistance across the air cavity between the bridged and unbridged cases. However, the impact would likely be significantly more prominent in reality, particularly when reflective membranes were used to significantly reduce radiation heat transfer across the cavity.

In summary, this study has provided an in-depth understanding of the actual thermal performance of a small cohort Australian apartment dwellings. It also provides insights into indoor environmental conditions within occupied apartments, associated occupant preferences, and occupant strategies used to maintain their preferred indoor environmental conditions. It is also hoped that this thesis makes a significant contribution to our knowledge of heating and cooling energy consumption in apartments as simulated with the NatHERS protocol as compared with reality; which therefore has an important impact on appropriate thermal design of apartment buildings.

## 7.1 Recommendations for Future Work

Some suggested areas for future research are summarised below.

- More research is needed to determine the thermal performance of a larger sample of apartments covering a broader range of climatic conditions to determine how apartments perform across Australia so as to verify the key findings within this study and provide additional insight that may inform regulatory changes to improve comfort and energy efficiency in Australian apartment buildings.
- Further research is required to better understand occupant thermal comfort preferences in Australian apartments. While the current study assumed that occupant thermal perceptions aligned with the adaptive comfort model, collection of thermal sensation votes would lead to a better characterisation of occupant perceptions, and their impact on heating and cooling usage behaviour. In turn, updating the definition of thermal comfort used by NatHERS would enable more accurate estimation of heating and cooling loads.
- While the impact of thermal bridging in apartments was quantified via steady state simulation in this study, further work is required to understand the impact of thermal bridging under transient conditions, particularly for thermally massive thermal bridges such as balconies. This should be undertaken through both simulation and experiments

## List of References

- ABCB (2009) 'Building Code of Australia 2009 Volume One'.
- ABCB (2013) 'National Construction Code 2013 Volume One'.
- ABCB (2016) 'National Construction Code 2016 Volume One'.
- ABCB (2019a) *Energy efficiency: NCC 2022 and beyond*. Canberra.
- ABCB (2019b) *NatHERS heating and cooling load limits*. Canberra.
- ABCB (2019c) 'National Construction Code 2019 Volume One'.
- AccurateSustainability (2018a) 'AccuRateSustainability Help File: Heating and cooling Operation'.
- AccurateSustainability (2018b) 'AccuRateSustainability Help File: Infiltration & Ceiling Penetration'.
- Acil Allen Consulting (2017) *Energy Consumption Benchmarks: Electricity and Gas for Residential Customers*.
- Acil Allen Consulting (2021) *Consulation Regulation Impact Statement for a Proposal to increase residential building energy efficiency requirements, Australian Building Codes Board*. Available at: <https://ncc.abcb.gov.au/practitioners/history>.
- AIRAH (2013) *AIRAH Technical Handbook*. 5th edn.
- Albatayneh, A. *et al.* (2018) 'The significance of the orientation on the overall buildings thermal performance-case study in Australia', *Energy Procedia*, 152, pp. 372–377. doi: 10.1016/j.egypro.2018.09.159.
- Allison, P. (2013) *What's the best R-squared for Logistic Regression, Statistical Horizons*. Available at: <https://statisticalhorizons.com/r2logistic> (Accessed: 27 January 2020).
- Ambrose, M. *et al.* (2013) *The Evaluation of the 5-Star Energy Efficiency Standard for Residential Buildings*. Australia.
- Ambrose, M. and James, M. (2014) *Natural ventilation and air conditioning use*. Australia.
- Ambrose, M. and Syme, M. (2015) *House Energy Efficiency Inspections Project - Final report*. Australia.
- Ambrose, M. and Syme, M. (2017) 'Air tightness of new Australian residential buildings', *Procedia Engineering*, 180, pp. 33–40. doi: 10.1016/j.proeng.2017.04.162.

Andersen, R. V. *et al.* (2009) ‘Survey of occupant behaviour and control of indoor environment in Danish dwellings’, *Energy and Buildings*, 41(1), pp. 11–16. doi: 10.1016/j.enbuild.2008.07.004.

ANSI/ASHRAE (2017) *ANSI/ASHRAE Standard 55-2017. Thermal Environmental Conditions for Human Occupancy*.

ANSYS (2009) ‘Natural convection and Bouyancy-driven flows’. Available at: <https://www.afs.enea.it/project/neptunius/docs/fluent/html/ug/node470.htm>.

ASHRAE (2014) *Guideline 14-2014 Measurement of Energy, Demand, and Water Savings, ASHRAE Guideline 14-2014*.

ASHRAE (2017) *2017 ASHRAE Handbook - Fundamentals (SI Edition)*.

Attia, S. and Carlucci, S. (2015) ‘Impact of different thermal comfort models on zero energy residential buildings in hot climate’, *Energy and Buildings*, 102, pp. 117–128. doi: 10.1016/j.enbuild.2015.05.017.

Auliciems, A. and Szokolay, S. V (2007) *Thermal comfort: DESIGN TOOLS AND TECHNIQUES*.

Ausgrid (2020) *Your energy use: Save energy at home*. Available at: <https://www.ausgrid.com.au/Your-energy-use/Save-energy-at-home> (Accessed: 15 June 2021).

Australian Bureau of Statistics (2017) *2071.0 - Census of Population and Housing: Reflecting Australia - Stories from the Census , 2016*. Available at: [https://www.abs.gov.au/ausstats/abs@.nsf/Lookup/by Subject/2071.0~2016~Main Features~Snapshot of Australia, 2016~2](https://www.abs.gov.au/ausstats/abs@.nsf/Lookup/by+Subject/2071.0~2016~Main+Features~Snapshot+of+Australia,+2016~2) (Accessed: 16 June 2021).

Australian Bureau of Statistics (2019) ‘8731.0 - Building Approvals, Australia, Mar 2019’, pp. 8–9. Available at: [https://www.abs.gov.au/AUSSTATS/abs@.nsf/Lookup/8731.0Main+Features1Mar 2019?OpenDocument](https://www.abs.gov.au/AUSSTATS/abs@.nsf/Lookup/8731.0Main+Features1Mar+2019?OpenDocument).

Australian Construction Insights (2018) *Framing material use in residential construction*.

Australian Energy Regulator (2020) *Guidance on energy consumption benchmarks on residential customers' bills*. Melbourne.

Balvedi, B. F., Ghisi, E. and Lamberts, R. (2018) ‘A review of occupant behaviour in residential buildings’, *Energy and Buildings*, 174, pp. 495–505. doi: 10.1016/j.enbuild.2018.06.049.

Bannister, P. *et al.* (2018) ‘Building Code Energy Performance Trajectory - Interim Technical



Report'. Available at:

[http://www.lowcarbonlivingcrc.com.au/sites/all/files/publications\\_file\\_attachments/sp0016\\_trajectory\\_interim\\_technical\\_report.pdf](http://www.lowcarbonlivingcrc.com.au/sites/all/files/publications_file_attachments/sp0016_trajectory_interim_technical_report.pdf).

Belusko, M. *et al.* (2019) *RP1024 : Informing the Next Generation Residential Energy Assessment Tools*.

Benyahia, N. *et al.* (2020) 'Coupling turbulent natural convection-radiation-conduction in differentially heated cavity with high aspect ratio', *International Journal of Thermal Sciences*, 158(June), p. 106518. doi: 10.1016/j.ijthermalsci.2020.106518.

Betts, P. L. and Bokhari, I. H. (2000) 'Experiments on turbulent natural convection in an enclosed tall cavity', *International Journal of Heat and Fluid Flow*, 21(6), pp. 675–683. doi: 10.1016/S0142-727X(00)00033-3.

British Standards Institution (2017a) *BS EN ISO 10077-2:2017 Thermal performance of windows , doors and shutters - Calculation of thermal transmittance - Part 2: Numerical method for frames*.

British Standards Institution (2017b) *BS EN ISO 10211:2017 Thermal bridges in building construction - Heat flows and surface temperatures - Detailed calculations*.

British Standards Institution (2017c) *BS EN ISO 6946:2017 Building components and building elements - Thermal resistance and thermal transmittance - Calculation methods*.

Building Research Establishment (2013) *Guidance Standard Assessment Procedure, Department for Business, Energy, & Industrial Strategy*. Available at: <https://www.gov.uk/guidance/standard-assessment-procedure> (Accessed: 20 April 2022).

Bureau of Meteorology (2019a) *2018–19 was Australia's hottest summer on record, with a warm Autumn likely too*. Available at: <http://www.bom.gov.au/climate/updates/articles/a032.shtml> (Accessed: 4 May 2020).

Bureau of Meteorology (2019b) *Australian Hourly Solar Irradiance Gridded Data*. Available at: <http://www.bom.gov.au/climate/how/newproducts/IDCJAD0111.shtml> (Accessed: 19 September 2020).

Bureau of Meteorology (2020) *Annual and monthly heating and cooling degree days. Documentation*. Available at: <http://www.bom.gov.au/climate/map/heating-cooling-degree-days/documentation.shtml> (Accessed: 29 February 2020).

Carter, G. and Kosasih, B. (2018) 'Not so cool roofs', *AIRAH Ecolibrium*.

Chaudhuri, T. *et al.* (2016) 'On assuming Mean Radiant Temperature equal to air temperature

- during PMV-based thermal comfort study in air-conditioned buildings’, *IECON Proceedings (Industrial Electronics Conference)*, (April 2018), pp. 7065–7070. doi: 10.1109/IECON.2016.7793073.
- Chen, D. (2012) ‘Area Correction Factors in AccuRate v1.1.4.1’, (October), pp. 1–7. Available at: <https://www.hstar.com.au/Chenath/files/AreaAdjustment20121030.pdf>.
- Chen, D. (2013) *Infiltration Calculations in AccuRate V2.0.2.13*. Available at: <https://hstar.com.au/Home/Chenath>.
- Chen, D. (2016) *AccuRate and the Chenath Engine for Residential House Energy Rating*. Available at: <https://hstar.com.au/Home/Chenath> (Accessed: 27 March 2020).
- Chen, D. (2018) ‘Internal Heat Gain Estimation from Occupants and Appliances’, (May), pp. 1–5.
- Chenoweth, D. R. and Paolucci, S. (1986) ‘Natural convection in an enclosed vertical air layer with large horizontal temperature differences’, *Journal of Fluid Mechanics*.
- City of Sydney (2015) ‘Residential Apartments Sustainability Plan’, (February).
- City of Sydney (2017) ‘Environmental action 2016 – 2021: Strategy and action plan’, (March).
- ClimateWorks (2010) *Low Carbon Growth Plan for Australia*. Available at: <http://www.climateworksaustralia.org/project/national-plan/low-carbon-growth-plan-australia>.
- COAG Energy Council (2015a) *National Energy Productivity Plan: Work Plan*. Canberra. Available at: <https://assets.ecca.org.au/library/Reports/NEPP-2015-Work-Plan-COAG-4-Dec-2015.pdf>.
- COAG Energy Council (2015b) *National Energy Productivity Plan 2015–2030*. Canberra. Available at: <http://www.scer.gov.au/workstreams/energy-market-reform/national-energy-productivity-plan/>.
- COAG Energy Council (2018) *Trajectory for low energy buildings*. Available at: [http://coagenergycouncil.gov.au/sites/prod.energycouncil/files/publications/documents/Trajectory for Low Energy Buildings.pdf](http://coagenergycouncil.gov.au/sites/prod.energycouncil/files/publications/documents/Trajectory%20for%20Low%20Energy%20Buildings.pdf).
- Coleman, S. (2017) *Australia State of the Environment 2016: Built Environment*. Canberra.
- Commonwealth of Australia (2005) *The Private Cost Effectiveness of Improving Energy Efficiency: Productivity Commission Inquiry Report, Productivity Commission*.
- Cooper, P. et al. (2016) *EE3A: Pathways and initiatives for low-income older people to manage energy: Final Report*.

- Cozza, S. *et al.* (2020) ‘Do energy performance certificates allow reliable predictions of actual energy consumption and savings? Learning from the Swiss national database’, *Energy and Buildings*, 224, p. 110235. doi: 10.1016/j.enbuild.2020.110235.
- Cozza, S. *et al.* (2021) ‘In search of optimal consumption: A review of causes and solutions to the Energy Performance Gap in residential buildings’, *Energy and Buildings*, 249, p. 111253. doi: 10.1016/j.enbuild.2021.111253.
- CSIRO (2021a) *Dashboards: Construction, Australian Housing Data Portal*. Available at: <https://ahd.csiro.au/dashboards/construction/> (Accessed: 29 January 2021).
- CSIRO (2021b) *Dashboards: Energy Rating, Australian Housing Data Portal*. Available at: <https://ahd.csiro.au/dashboards/energy-rating/> (Accessed: 15 February 2021).
- Cuerda, E. *et al.* (2020) ‘Understanding the performance gap in energy retrofitting : Measured input data for adjusting building simulation models’, *Energy & Buildings*, 209, p. 109688. doi: 10.1016/j.enbuild.2019.109688.
- D’Oca, S. *et al.* (2014) ‘Effect of thermostat and window opening occupant behavior models on energy use in homes’, *Building Simulation*, 7(6), pp. 683–694. doi: 10.1007/s12273-014-0191-6.
- Daniel, L. *et al.* (2015) ‘Learning from thermal mavericks in Australia: Comfort studies in Melbourne and Darwin’, *Architectural Science Review*, 58(1), pp. 57–66. doi: 10.1080/00038628.2014.976537.
- Daniel, L., Soebarto, V. and Williamson, T. (2015) ‘House energy rating schemes and low energy dwellings: The impact of occupant behaviours in Australia’, *Energy and Buildings*, 88, pp. 34–44. doi: 10.1016/j.enbuild.2014.11.060.
- de Dear, R. and Brager, G. (2002) ‘Thermal comfort in naturally ventilated buildings: Revisions to ASHRAE Standard 55’, *Energy and Buildings*, 34(6), pp. 549–561. doi: 10.1016/S0378-7788(02)00005-1.
- de Dear, R., Brager, G. and Cooper, D. (1997) *Developing an Adaptive Model of Thermal Comfort and Preference, ASHRAE RP-884*. Available at: [https://www.sydney.edu.au/architecture/documents/staff/richard\\_de\\_dear/RP884\\_Final\\_Report.pdf](https://www.sydney.edu.au/architecture/documents/staff/richard_de_dear/RP884_Final_Report.pdf).
- de Dear, R., Kim, J. and Parkinson, T. (2018) ‘Residential adaptive comfort in a humid subtropical climate—Sydney Australia’, *Energy and Buildings*, 158, pp. 1296–1305. doi: 10.1016/j.enbuild.2017.11.028.

- Delghust, M. *et al.* (2015) 'Regulatory energy calculations versus real energy use in high-performance houses', *Building Research and Information*, 43(6), pp. 675–690. doi: 10.1080/09613218.2015.1033874.
- Delsante, A. (2005) 'Is the new generation of building energy rating software up to the task? - a review of AccuRate', in *ABCB Conference 'Building Australia's Future 2005'*. Available at: [http://www.hearne.com.au/attachments/Accurate Reviewer's Guide.pdf](http://www.hearne.com.au/attachments/Accurate%20Reviewer's%20Guide.pdf).
- DELWP (2016) *Better Apartments Design Standards*.
- Department of Industry (2021) *International climate change commitments*. Available at: <https://www.industry.gov.au/policies-and-initiatives/australias-climate-change-strategies/international-climate-change-commitments> (Accessed: 10 May 2021).
- Department of the Environment and Energy (2019a) *Australian Energy Update 2019*. Canberra.
- Department of the Environment and Energy (2019b) 'NatHERS assessor handbook'. Canberra.
- Department of the Environment and Energy (2019c) 'NatHERS Technical Note: June 2019'. Canberra.
- Deuble, M. P. and de Dear, R. J. (2012) 'Mixed-mode buildings: A double standard in occupants' comfort expectations', *Building and Environment*, 54, pp. 53–60. doi: 10.1016/j.buildenv.2012.01.021.
- DEWHA (2008) *Energy Use in the Australian Residential Sector: 1986-2020*. Canberra.
- Ding, L. *et al.* (2019) *Validating and Improving the BASIX Assessment Tool for Low-Carbon Dwellings*.
- Eames, M., Kershaw, T. and Coley, D. (2012) 'The appropriate spatial resolution of future weather files for building simulation', *Journal of Building Performance Simulation*, 5(6), pp. 347–358. doi: 10.1080/19401493.2011.608133.
- EnergyConsult (2015) *Residential Energy Baseline Study: Australia*.
- Erba, S., Causone, F. and Armani, R. (2017) 'The effect of weather datasets on building energy simulation outputs', *Energy Procedia*, 134, pp. 545–554. doi: 10.1016/j.egypro.2017.09.561.
- Ewing, R. and Rong, F. (2008) 'The impact of urban form on U.S. residential energy use', *Housing Policy Debate*, 19(1), pp. 1–30. doi: 10.1080/10511482.2008.9521624.
- Fabi, V. *et al.* (2012) 'Occupants' window opening behaviour: A literature review of factors influencing occupant behaviour and models', *Building and Environment*, 58, pp. 188–198. doi: 10.1016/j.buildenv.2012.07.009.

- Fan, H., Macgill, I. F. and Sproul, A. B. (2015) 'Statistical analysis of driving factors of residential energy demand in the greater Sydney region , Australia', *Energy & Buildings*, 105, pp. 9–25. doi: 10.1016/j.enbuild.2015.07.030.
- Fanger, P. . (1970) *Thermal Comfort. Analysis and applications in environmental engineering*. Copenhagen: Danish Technical Press.
- Farah, S. *et al.* (2019) 'Integrating climate change into meteorological weather data for building energy simulation', *Energy and Buildings*, 183, pp. 749–760. doi: 10.1016/j.enbuild.2018.11.045.
- Feijó-muñoz, J., González-lezcano, R. A., *et al.* (2019) 'Airtightness of residential buildings in the Continental area of Spain', *Building and Environment*, 148(November 2018), pp. 299–308. doi: 10.1016/j.buildenv.2018.11.010.
- Feijó-muñoz, J., Pardal, C., *et al.* (2019) 'Energy impact of the air infiltration in residential buildings in the Mediterranean area of Spain and the Canary islands', *Energy & Buildings*, 189, pp. 226–238. doi: 10.1016/j.enbuild.2019.02.023.
- Ferdyn-Grygierek, J. *et al.* (2018) 'Analysis of Accuracy Determination of the Seasonal Heat Demand in Buildings Based on Short Measurement Periods', *Energies*. doi: 10.3390/en11102734.
- Fiebig, F. *et al.* (2017) 'Detecting occupancy in smart buildings by data fusion from low-cost sensors', *e-Energy 2017 - Proceedings of the 8th International Conference on Future Energy Systems*, pp. 259–261. doi: 10.1145/3077839.3081675.
- Finch, G., Wilson, M. and Higgins, J. (2013) 'Thermal Bridging of Masonry Veneer Claddings and Energy Code Compliance', in *12th Canadian Masonry Symposium*. Vancouver, British Columbia.
- Fiorentini, M. *et al.* (2019) 'Development of an enthalpy-based index to assess climatic potential for ventilative cooling of buildings: An Australian example', *Applied Energy*, 251(May), p. 113169. doi: 10.1016/j.apenergy.2019.04.165.
- Floyd, W., Isaacs, T. and Hills, R. (2014) *NatHERS Benchmark Study*. Canberra. Available at: <https://www.nathers.gov.au/sites/default/files/Research%2520Rep%2520-%2520Assessor%2520Benchmark%2520Study.pdf>.
- Foo, G. (2020) *Climate Change – Impact on Building Design and Energy*.
- GBCA (2009) 'Green Star - Multi Unit Residential v1: Fact Sheet & Business Case'. Green Building Council Australia. doi: 10.3992/jgb.2.3.32.

- Gorgolewski, M. (2007) 'Developing a simplified method of calculating U -values in light steel framing', 42, pp. 230–236. doi: 10.1016/j.buildenv.2006.07.001.
- Gray, D. D. and Giorgini, A. (1976) 'The validity of the boussinesq approximation for liquids and gases', *International Journal of Heat and Mass Transfer*, 19(5), pp. 545–551. doi: 10.1016/0017-9310(76)90168-X.
- Greater Sydney Commission (2018) 'Greater Sydney Region Plan, March 2018 (updated June 2018)', (March). Available at: <https://gsc-public-1.s3.amazonaws.com/s3fs-public/greater-sydney-region-plan-0618.pdf>.
- Gupta, R. and Kotopouleas, A. (2018) 'Magnitude and extent of building fabric thermal performance gap in UK low energy housing', *Applied Energy*, 222(October 2017), pp. 673–686. doi: 10.1016/j.apenergy.2018.03.096.
- Gyprock (2021) *THE RED BOOK: Book 3: Commercial & Multi-Residential Installation Guide - Class 2-9 buildings*. Available at: <https://www.gyprock.com.au/resources/redbook>.
- Haldi, F. and Robinson, D. (2008) 'A comparison of alternative approaches for the modelling of window opening and closing behaviour', *Air Conditioning and the Low Carbon Cooling Challenge*, (July), pp. 27–29.
- Haldi, F. and Robinson, D. (2009) 'Interactions with window openings by office occupants', *Building and Environment*, 44(12), pp. 2378–2395. doi: 10.1016/j.buildenv.2009.03.025.
- Han, B., Yan, G. and Yu, J. (2019) 'Refrigerant migration during startup of a split air conditioner in heating mode', *Applied Thermal Engineering*, 148(December 2018), pp. 1068–1073. doi: 10.1016/j.applthermaleng.2018.11.126.
- Hatvani-Kovacs, G. *et al.* (2018) 'Heat stress-resistant building design in the Australian context', *Energy and Buildings*, 158, pp. 290–299. doi: 10.1016/j.enbuild.2017.10.025.
- Hebel (2015) 'High Rise Facades: Design and Installation Guide'. Available at: [www.hebel.com.au](http://www.hebel.com.au).
- Heffernan, E. *et al.* (2017) 'Energy efficiency within mid-rise residential buildings: A critical review of regulations in Australia', *Energy Procedia*, 121, pp. 292–299. doi: 10.1016/j.egypro.2017.08.030.
- Henkes, R. A. W. M. and Quere, P. Le (1996) 'Three-dimensional transition of natural-convection flows'.
- Hitchin, R. and Knight, I. (2016) 'Daily energy consumption signatures and control charts for air-conditioned buildings', *Energy & Buildings*, 112, pp. 101–109. doi:

10.1016/j.enbuild.2015.11.059.

Hopfe, C. J. and Hensen, J. L. M. (2011) ‘Uncertainty analysis in building performance simulation for design support’, *Energy and Buildings*, 43(10), pp. 2798–2805. doi: 10.1016/j.enbuild.2011.06.034.

IEA (2018) *2018 Energy Efficiency Indicators Highlights*. doi: 10.1080/10511482.1993.9521135.

Incropera, F. *et al.* (2006) *Fundamentals of Heat and Mass Transfer*. Sixth. John Wiley & Sons, Inc.

Infrastructure Australia (2016) *Australian Infrastructure Plan: Priorities and reforms for our nation’s future*. Available at: [http://infrastructureaustralia.gov.au/policy-publications/publications/files/Australian\\_Infrastructure\\_Plan.pdf](http://infrastructureaustralia.gov.au/policy-publications/publications/files/Australian_Infrastructure_Plan.pdf).

IPART (2007) *Residential energy and water use in Sydney, the Blue Mountains and Illawarra*.

ISO (1998) ‘ISO 7726: 1998 Ergonomics of the Thermal Environment - Instruments for measuring physical quantities’. International Organization for Standardization.

Jensen, C. *et al.* (2017) *Living Well: Apartments, Comfort and Resilience in Climate Change*. Available at: [https://msd.unimelb.edu.au/\\_\\_data/assets/pdf\\_file/0003/3040095/Living-Well-Report-Final-for-issue-080317.pdf](https://msd.unimelb.edu.au/__data/assets/pdf_file/0003/3040095/Living-Well-Report-Final-for-issue-080317.pdf).

Jokisalo, J. *et al.* (2009) ‘Building leakage, infiltration, and energy performance analyses for Finnish detached houses’, 44, pp. 377–387. doi: 10.1016/j.buildenv.2008.03.014.

Jones, R. V., Fuertes, A. and De Wilde, P. (2015) ‘The gap between simulated and measured energy performance: A case study across six identical New-Build flats in the UK’, *14th International Conference of IBPSA - Building Simulation 2015, BS 2015, Conference Proceedings*, (December), pp. 2248–2255.

Kang, Y. *et al.* (2021) ‘Performance gap in a multi-storey student accommodation complex built to Passivhaus standard’, *Building and Environment*, 194(November 2020), p. 107704. doi: 10.1016/j.buildenv.2021.107704.

Kaschuba-holtgrave, A. *et al.* (2020) ‘Individual unit and guard-zone airtightness tests of apartment buildings’. doi: 10.1177/1744259118786977.

Kelly, S. (2011) ‘Do homes that are more energy efficient consume less energy?: A structural equation model of the English residential sector’, *Energy*, 36(9), pp. 5610–5620. doi: 10.1016/j.energy.2011.07.009.

- Khoury, J., Alameddine, Z. and Hollmuller, P. (2017) 'Understanding and bridging the energy performance gap in building retrofit', *Energy Procedia*, 122, pp. 217–222. doi: 10.1016/j.egypro.2017.07.348.
- Kim, J. *et al.* (2016) 'Field Study of Air Conditioning and Thermal Comfort in Residential Buildings', (April), pp. 7–10.
- Kim, J. *et al.* (2017) 'Understanding patterns of adaptive comfort behaviour in the Sydney mixed-mode residential context', *Energy and Buildings*, 141, pp. 274–283. doi: 10.1016/j.enbuild.2017.02.061.
- Kim, J. *et al.* (2019) 'Thermal comfort in a mixed-mode building: Are occupants more adaptive?', *Energy and Buildings*, 203, p. 109436. doi: 10.1016/j.enbuild.2019.109436.
- Kissock, J. K., Haberl, J. S. and Claridge, D. E. (2003) *Inverse Modeling Toolkit: Numerical Algorithms*.
- Kleiminger, W., Beckel, C. and Santini, S. (2015) 'Household occupancy monitoring using electricity meters', *UbiComp 2015 - Proceedings of the 2015 ACM International Joint Conference on Pervasive and Ubiquitous Computing*, pp. 975–986. doi: 10.1145/2750858.2807538.
- Korpi, M., Vinha, J. and Kurnitski, J. (2008) 'Airtightness of single-family houses and apartments', in *Proceedings of the 8th Symposium on Building Physics in the Nordic Countries NSB2008*. Copenhagen, pp. 1397–1404.
- Lawson, R. M., Way, A. G. J. and Sansom, M. R. (2018) *Thermal Bridging in Light Steel Framing & Modular Construction*.
- LBNL (2020) *Residential Leakage Database, Residential Building Systems*. Available at: <http://resdb.lbl.gov/> (Accessed: 23 February 2020).
- Li, Y., Delsante, A. and Symons, J. (2000) 'Prediction of natural ventilation in buildings with large openings', *Building and Environment*, 35(3), pp. 191–206. doi: 10.1016/S0360-1323(99)00011-6.
- Liu, Y. *et al.* (2017) 'Comparing micro-scale weather data to building energy consumption in Singapore', *Energy & Buildings*, 152, pp. 776–791. doi: 10.1016/j.enbuild.2016.11.019.
- Louviere, J. J. *et al.* (2000) *Stated Choice Methods: Analysis and Applications*. Cambridge University Press.
- Mahdavi, A. *et al.* (2021) 'The role of occupants in buildings' energy performance gap: Myth or reality?', *Sustainability*, 13(6), pp. 1–44. doi: 10.3390/su13063146.



Majcen, D., Itard, L. C. M. and Visscher, H. (2013) ‘Theoretical vs . actual energy consumption of labelled dwellings in the Netherlands : Discrepancies and policy implications’, *Energy Policy*, 54, pp. 125–136. doi: 10.1016/j.enpol.2012.11.008.

Manz, H. (2003) ‘Numerical simulation of heat transfer by natural convection in cavities of facade elements’, *Energy and Buildings*, 35(3), pp. 305–311. doi: 10.1016/S0378-7788(02)00088-9.

Marchese, J. (2005) *Refrigerant Migration Can Cause Problems*, *ACHR News*. Available at: <https://www.achrnews.com/articles/92910-refrigerant-migration-can-cause-problems> (Accessed: 5 November 2020).

Martins, C., Santos, P. and Da Silva, L. S. (2016) ‘Lightweight steel-framed thermal bridges mitigation strategies: A parametric study’, *Journal of Building Physics*, 39(4), pp. 342–372. doi: 10.1177/1744259115572130.

Mirsadeghi, M. *et al.* (2013) ‘Review of external convective heat transfer coefficient models in building energy simulation programs : Implementation and uncertainty’, *Applied Thermal Engineering*, 56(1–2), pp. 134–151. doi: 10.1016/j.applthermaleng.2013.03.003.

Mitchel, L. M. (2010) *Energy Efficient Cities: Assessment Tools and Benchmarking Practices. Chapter 5: Green Star and NABERS: Learning from the Australian Experience with Green Building Rating Tools*. Edited by R. K. Bose. doi: 10.1596/978-0-8213-8104-5.

Moeller, S. *et al.* (2020) ‘Apartment related energy performance gap – How to address internal heat transfers in multi-apartment buildings’, *Energy and Buildings*, 215. doi: 10.1016/j.enbuild.2020.109887.

Moore, T., Berry, S. and Ambrose, M. (2019) ‘Aiming for mediocrity: The case of Australian housing thermal performance’, *Energy Policy*, 132(January), pp. 602–610. doi: 10.1016/j.enpol.2019.06.017.

Muncey, R. W. (1953) ‘The calculation of temperatures inside buildings having variable external conditions’, *Aust. J. Appl. Sci.*, p. 189.

Munsami, K., Prasad, D. and Ding, L. (2017) ‘The Role of Post Occupation Evaluation in Achieving High Performance Buildings through Diagnostics’, in *Procedia Engineering*. Elsevier B.V., pp. 356–364. doi: 10.1016/j.proeng.2017.04.194.

Myors, P., O’Leary, R. and Helstroom, R. (2005) *Multi Unit Residential Buildings Energy & Peak Demand Study*.

NABERS (2018a) ‘NABERS Energy and Water for Apartment Buildings’.

- NABERS (2018b) ‘NABERS for Apartment Buildings: Rating Process - User Guide V1.0’.
- Narkhede, S. (2018) *Understanding AUC-ROC Curve, Towards Data Science*. Available at: <https://towardsdatascience.com/understanding-auc-roc-curve-68b2303cc9c5> (Accessed: 24 February 2021).
- NatHERS National Administrator (2012) ‘Nationwide House Energy Rating Scheme - Software Accreditation Protocol’. Available at: [http://www.nathers.gov.au/files/publications/NatHERS Software Accreditation Protocol-June 2012.pdf](http://www.nathers.gov.au/files/publications/NatHERS%20Software%20Accreditation%20Protocol-June%202012.pdf).
- NatHERS National Administrator (2015) *Nationwide House Energy Rating Scheme (NatHERS): Administration and Governance*. Canberra.
- NatHERS National Administrator (2019a) *NatHERS Certificate: A guide to the NatHERS Certificate*. Available at: <https://www.nathers.gov.au/owners-and-builders/nathers-certificate> (Accessed: 27 April 2021).
- NatHERS National Administrator (2019b) ‘Nationwide House Energy Rating Scheme - Software Accreditation Protocol’. Available at: [https://www.nathers.gov.au/sites/default/files/2019-10/2019 NatHERS Software Accreditation Protocol.pdf](https://www.nathers.gov.au/sites/default/files/2019-10/2019%20NatHERS%20Software%20Accreditation%20Protocol.pdf).
- NatHERS National Administrator (2021) *The National Construction Code and State and Territory Regulations*. Available at: <https://www.nathers.gov.au/governance/national-construction-code-and-state-and-territory-regulations> (Accessed: 15 April 2022).
- Newton, P. (2017) *Becoming more urban: attitudes to medium-density living are changing in Sydney and Melbourne, The Conversation*. Available at: <https://theconversation.com/becoming-more-urban-attitudes-to-medium-density-living-are-changing-in-sydney-and-melbourne-84693> (Accessed: 10 May 2021).
- NHSC (2013) *State of Supply Report: Changes in how we live*. Available at: <https://treasury.gov.au/publication/state-of-supply-report-changes-in-how-we-live>.
- Nicol, J. F. (2001) ‘Characterising occupant behaviour in buildings: Towards a stochastic model of occupant use of windows, lights, blinds, heaters, and fans’, in *Building Simulation*.
- Nicol, J. F. and Humphreys, M. A. (2002) ‘Adaptive thermal comfort and sustainable thermal standards for buildings’, *Energy and Buildings*, 34(6), pp. 563–572. doi: 10.1016/S0378-7788(02)00006-3.
- Nicol, J. F., Humphreys, M. A. and Olesen, B. (2004) ‘A stochastic approach to thermal comfort - Occupant behavior and energy use in buildings’, *ASHRAE Transactions*, 110 PART I, pp.

554–568.

Nordström, G., Lidelöw, S. and Johnsson, H. (2012) ‘Comparing energy signature analysis to calculated U-values in wooden houses in a cold climate’, *WIT Transactions on Ecology and the Environment*, 165, pp. 411–419. doi: 10.2495/ARC120361.

Norford, L. K. *et al.* (1994) ‘Two-to-one discrepancy between measured and predicted performance of a “low-energy” office building: insights from a reconciliation based on the DOE-2 model’, *Energy and Buildings*, 21(2), pp. 121–131. doi: 10.1016/0378-7788(94)90005-1.

NSW Department of Planning (2011) *2006-09 Multi-Dwelling Outcomes BASIX Ongoing Monitoring Program*.

NSW Department of Planning and Environment (2015) *Apartment Design Guide*.

NSW Department of Planning and Environment (2016) ‘Basix Thermal Comfort Protocol’, 2014(May), pp. 1–20. Available at: <https://www.basix.nsw.gov.au/iframe/about-basix/news/articles/518-updates-to-the-thermal-comfort-protocol-may-2016.html>.

NSW Department of Planning and Environment (2017) ‘BASIX Thermal Comfort Protocol’. Available at: <https://www.basix.nsw.gov.au/iframe/about-basix/news/articles/518-updates-to-the-thermal-comfort-protocol-may-2016.html>.

NSW Department of Planning and Environment (2019) *Which BASIX tool suits my project?* Available at: <https://basix.nsw.gov.au/iframe/new-to-basix/which-basix-tool-suits-my-project.html> (Accessed: 20 May 2019).

NSW Department of Planning and Environment (2020) ‘BASIX Certificate Data 2011/12 to 2018/19’. Available at: <https://www.planningportal.nsw.gov.au/opendata/dataset/basix-new-single-dwelling-2011-12-to-2018-19> (Accessed: 1 May 2021).

NSW Department of Planning Industry and Environment (2021) *BASIX: Dwelling types - Multi-dwelling*. Available at: <https://pp.planningportal.nsw.gov.au/basix/about-basix/dwelling-types/multi-dwelling> (Accessed: 29 January 2021).

NSW Environmental Protection Authority (2018) *NSW State of the Environment 2018*. Available at: <https://www.soe.epa.nsw.gov.au/> (Accessed: 17 June 2019).

O’Leary, T. *et al.* (2016) ‘Comparing the energy performance of Australian houses using NatHERS modelling against measured household energy consumption for heating and cooling’, *Energy and Buildings*, 119, pp. 173–182. doi: 10.1016/j.enbuild.2016.03.025.

Pan, W. (2010) ‘Relationships between air-tightness and its influencing factors of post-2006

- new-build dwellings in the UK’, *Building and Environment*, 45(11), pp. 2387–2399. doi: 10.1016/j.buildenv.2010.04.011.
- Paolucci, S. and Chenoweth, D. R. (1989) ‘Chaos in a Differentially Heated Vertical Cavity’, *Journal of Fluid Mechanics*, 201.
- Park, J. and Choi, C. S. (2019) ‘Modeling occupant behavior of the manual control of windows in residential buildings’, *Indoor Air*, 29(2), pp. 242–251. doi: 10.1111/ina.12522.
- Peng, C. *et al.* (2012) ‘Quantitative description and simulation of human behavior in residential buildings’, *Building Simulation*, 5(2), pp. 85–94. doi: 10.1007/s12273-011-0049-0.
- Peterman, K. D. *et al.* (2016) ‘Experimental Seismic Response of a Full-Scale Cold-Formed Steel-Framed Building. I: System-Level Response’, *Journal of Structural Engineering*, 142(12), p. 04016127. doi: 10.1061/(asce)st.1943-541x.0001577.
- Pitt&sherry (2016) *Initial Scoping Work for Implementation of NEPP # 31 – Advancing the National Construction Code Final Report Prepared by : Reviewed by : Authorised by :*
- Ren, Z. and Chen, D. (2018) ‘Modelling study of the impact of thermal comfort criteria on housing energy use in Australia’, *Applied Energy*, 210(October 2017), pp. 152–166. doi: 10.1016/j.apenergy.2017.10.110.
- Ren, Z., Chen, D. and James, M. (2018) ‘Evaluation of a whole-house energy simulation tool against measured data’, *Energy & Buildings*, 171, pp. 116–130. doi: 10.1016/j.enbuild.2018.04.034.
- Ren, Z. and Chen, Z. (2010) ‘Enhanced air flow modelling for AccuRate - A nationwide house energy rating tool in Australia’, *Building and Environment*, 45(5), pp. 1276–1286. doi: 10.1016/j.buildenv.2009.11.007.
- Rickwood, P. (2009) ‘Residential Operational Energy Use’, *Urban Policy and Research*, 27(2), pp. 137–155. doi: 10.1080/0811114092950495.
- Rijal, H. B. *et al.* (2007) ‘Using results from field surveys to predict the effect of open windows on thermal comfort and energy use in buildings’, *Energy and Buildings*, 39(7), pp. 823–836. doi: 10.1016/j.enbuild.2007.02.003.
- Rijal, H. B., Humphreys, M. A. and Nicol, J. F. (2019) ‘Adaptive model and the adaptive mechanisms for thermal comfort in Japanese dwellings’, *Energy and Buildings*, 202, p. 109371. doi: 10.1016/j.enbuild.2019.109371.
- Roberts, M. B. *et al.* (2019) ‘Characterisation of Australian apartment electricity demand and its implications for low-carbon cities’, *Energy*, 180(2019), pp. 242–257. doi:

10.1016/j.energy.2019.04.222.

Rosewall, T. and Shoory, M. (2017) *Houses and Apartments in Australia*. Available at: <https://rba.gov.au/publications/bulletin/2017/jun/pdf/bu-0617-1-houses-and-apartments-in-australia.pdf>.

Ryan, E. M. and Sanquist, T. F. (2012) 'Validation of building energy modeling tools under idealized and realistic conditions', *Energy and Buildings*, 47, pp. 375–382. doi: 10.1016/j.enbuild.2011.12.020.

Saman, W. *et al.* (2008) *Study of the Effect of Temperature Settings on AccuRate Cooling Energy Requirements and Comparison with Monitored Data*.

Saman, W. *et al.* (2013) *A framework for adaptation of Australian households to heat waves, National Climate Change Adaptation Research Facility (NCCARF)*. Gold Coast: National Climate Change Adaptation Research Facility. Available at: <http://eprints.qut.edu.au/62001/>.

Samaratunga, M. *et al.* (2017) 'Modelling and Analysis of Post-occupancy Behaviour in Residential Buildings to Inform BASIX Sustainability Assessments in NSW', *Procedia Engineering*, 180, pp. 343–355. doi: 10.1016/j.proeng.2017.04.193.

Santamouris, M. *et al.* (2017) 'Urban Heat Island and Overheating Characteristics in Sydney , Australia . An Analysis of Multiyear Measurements'. doi: 10.3390/su9050712.

Scanada Consultants Limited (1997) *Field Investigations of Indoor Environment and Energy Usage in Mid-Rise Residential Buildings*. Ottawa, Ontario.

Sherman, M. H. (1987) 'Estimation of infiltration from leakage and climate indicators', *Energy and Buildings*, 10(1), pp. 81–86. doi: 10.1016/0378-7788(87)90008-9.

Shoory, M. (2016) *The Growth of Apartment Construction in Australia*.

Sinnott, D. (2016) 'Dwelling airtightness: A socio-technical evaluation in an Irish context', *Building and Environment*, 95, pp. 264–271. doi: 10.1016/j.buildenv.2015.08.022.

Soares, N. *et al.* (2017) 'Energy efficiency and thermal performance of lightweight steel-framed (LSF) construction: A review', 78(February), pp. 194–209. doi: 10.1016/j.rser.2017.04.066.

Soebarto, V. (2000) 'A low-energy house and a low rating: What is the problem?', *ANZAScA 2000: Proceedings of the 34th conference of the Australia and New Zealand Architectural Science Association*, pp. 111–118.

Standards Australia (2015) *AS 4773.2:2015 Masonry in small buildings - Part 2: Construction*.

Standards Australia (2018) *AS 3700:2018 Masonry structures*.

- Standards Australia and Standards New Zealand (2015) *AS/NZS ISO 9972:2015 Thermal Performance of Buildings - Determination of Air Permeability of Buildings - Fan Pressurisation Method*.
- Stein, J. R. (1997) *Accuracy of Home Energy Rating Systems*. Berkeley, CA.
- Stein, J. R. and Meier, A. (2000) 'Accuracy of home energy rating systems', *Energy*, 25(4), pp. 339–354. doi: 10.1016/S0360-5442(99)00072-9.
- Stephan, A., Jensen, C. A. and Crawford, R. H. (2017) 'Improving the life cycle energy performance of apartment units through façade design', *Procedia Engineering*, 196(June), pp. 1003–1010. doi: 10.1016/j.proeng.2017.08.042.
- Stevenson, F. and Rijal, H. B. (2010) 'Developing occupancy feedback from a prototype to improve housing production', *Building Research and Information*, 38(5), pp. 549–563. doi: 10.1080/09613218.2010.496182.
- Taylor, J. *et al.* (2014) 'The relative importance of input weather data for indoor overheating risk assessment in dwellings', *Building and Environment*, 76, pp. 81–91. doi: 10.1016/j.buildenv.2014.03.010.
- Tomczyk, J. (2018) *Crankcase Heaters Can Help to Prevent Refrigerant Migration*, *ACHR News*. Available at: <https://www.achrnews.com/articles/136837-crankcase-heaters-can-help-to-prevent-refrigerant-migration> (Accessed: 5 November 2020).
- Tony Isaacs Consulting (2005) *Evaluation of the findings of the Productivity Commission Inquiry into Energy Efficiency with specific focus on the Building Industry*.
- Trethowen, H. A. (1989) 'Thermal insulation and contact resistance in metal-framed panels', in *ASHRAE Transactions*. Ottawa, Ontario.
- Trethowen, H. A. (1995) 'Validating the isothermal planes method for R-value predictions', in *ASHRAE Transactions*, pp. 755–765.
- Trethowen, H. A. (1998) *Calculating R-Values using the Isothermal Planes Method*.
- Trethowen, H. A. (2004) *Effect of Thermal Bridging on Heat losses of walls in Australian Houses*.
- Trethowen, H. A. and Cox-Smith, I. (1996) 'Contact Resistance in a Steel-Framed Wall', *Journal of Thermal Insulation and Building Envelopes*, 20(October).
- Trombley, J. and Halawa, E. (2017) 'Can further energy reductions be achieved through behaviour changes in low income households?', *Energy Procedia*, 121, pp. 230–237. doi:

10.1016/j.egypro.2017.08.022.

Tsoka, S. *et al.* (2018) ‘A method to account for the urban microclimate on the creation of “typical weather year” datasets for building energy simulation, using stochastically generated data’, *Energy and Buildings*, 165, pp. 270–283. doi: 10.1016/j.enbuild.2018.01.016.

U.S. Department of Energy (2002) *International Performance Measurement & Verification Protocol Concepts and Options for Determining Energy and Water Savings*.

Upadhyay, A. K., Munsami, K. and Smith, C. L. (2019) *RP1041: Improving the thermal performance of dwellings for carbon positive and healthy homes*. Sydney.

de Vahl Davis, G. (1968) ‘Laminar natural convection in an enclosed rectangular cavity’, *International Journal of Heat and Mass Transfer*, 11(11), pp. 1675–1693. doi: 10.1016/0017-9310(68)90047-1.

Vela, A. *et al.* (2020) ‘Estimating Occupancy Levels in Enclosed Spaces Using Environmental Variables: A Fitness Gym and Living Room as Evaluation Scenarios’, *Sensors (Basel, Switzerland)*, 20(22), pp. 8–10. doi: 10.3390/s20226579.

Versteeg, K. H. and Malalasekera, W. (2007) *An Introduction to Computational Fluid Dynamics*. 2nd edn. Essex: Pearson Education.

Walsh, P. J. and Delsante, A. (1983) ‘Calculation of the thermal behaviour of multi-zone buildings’, *Energy and Buildings*, 5(4), pp. 231–242. doi: 10.1016/0378-7788(83)90011-7.

Wang, L., Mathew, P. and Pang, X. (2012) ‘Uncertainties in energy consumption introduced by building operations and weather for a medium-size office building’, *Energy and Buildings*, 53, pp. 152–158. doi: 10.1016/j.enbuild.2012.06.017.

Wang, W., Chen, J. and Hong, T. (2018) ‘Occupancy prediction through machine learning and data fusion of environmental sensing and Wi-Fi sensing in buildings’, *Automation in Construction*, 94(October), pp. 233–243. doi: 10.1016/j.autcon.2018.07.007.

Way, A. G. J. and Kendrick, C. (2008) *Avoidance of Thermal Bridging in Steel Construction*, *SCI publication P380*.

Wilcox, S. and Marion, W. (2008) *Users Manual for TMY3 Data Sets*. Golden, Colorado.

De Wilde, P. (2014) ‘The gap between predicted and measured energy performance of buildings: A framework for investigation’, *Automation in Construction*, 41, pp. 40–49. doi: 10.1016/j.autcon.2014.02.009.

de Wilde, P. and Coley, D. (2012) ‘The implications of a changing climate for buildings’,

*Building and Environment*, 55, pp. 1–7. doi: 10.1016/j.buildenv.2012.03.014.

de Wilde, P. and Tian, W. (2009) ‘Identification of key factors for uncertainty in the prediction of the thermal performance of an office building under climate change’, *Building Simulation*, 2(3), pp. 157–174. doi: 10.1007/s12273-009-9116-1.

Willand, N., Ridley, I. and Pears, A. (2016) ‘Relationship of thermal performance rating, summer indoor temperatures and cooling energy use in 107 homes in Melbourne, Australia’, *Energy and Buildings*, 113, pp. 159–168. doi: 10.1016/j.enbuild.2015.12.032.

Williamson, T. (2005a) *DR133: Submission to Productivity Commission Public Enquiry into Energy Efficiency*.

Williamson, T. (2005b) *DR78: Submission to Productivity Commission Public Enquiry into Energy Efficiency*.

Williamson, T., Orkina, N. and Bennetts, H. (2009) ‘A comparison of accredited second generation NatHERS software tools’, in *43rd Annual Conference of the Architectural Science Association*.

Winkler, J. (2011) ‘Laboratory Test Report for Fujitsu 12RLS and Mitsubishi FE12NA Mini-Split Heat Pumps’.

World Health Organization (1987) ‘Health Impact of Low Temperatures’. Copenhagen.

Wu, T. and Lei, C. (2015) ‘On numerical modelling of conjugate turbulent natural convection and radiation in a differentially heated cavity’, *International Journal of Heat and Mass Transfer*, 91, pp. 454–466. doi: 10.1016/j.ijheatmasstransfer.2015.07.113.

Xamán, J. *et al.* (2005) ‘Numerical study of heat transfer by laminar and turbulent natural convection in tall cavities of façade elements’, *Energy and Buildings*, 37(7), pp. 787–794. doi: 10.1016/j.enbuild.2004.11.001.

Xamán, J. P. *et al.* (2008) ‘Effect of the surface thermal radiation on turbulent natural convection in tall cavities of façade elements’, *Heat and Mass Transfer/Waerme- und Stoffuebertragung*, 45(2), pp. 177–185. doi: 10.1007/s00231-008-0393-5.

Yan, D. *et al.* (2017) ‘IEA EBC Annex 66: Definition and simulation of occupant behavior in buildings’, *Energy and Buildings*, 156, pp. 258–270. doi: 10.1016/j.enbuild.2017.09.084.

Yan, D. and Hong, T. (2018) *International Energy Agency, EBC Annex 66 Definition and Simulation of Occupant Behavior in Buildings Annex 66 Final Report*.

Yang, Z. *et al.* (2014) ‘A systematic approach to occupancy modeling in ambient sensor-rich



buildings’, *Simulation*, 90(8), pp. 960–977. doi: 10.1177/0037549713489918.

Yao, M. and Zhao, B. (2017) ‘Factors affecting occupants’ interactions with windows in residential buildings in Beijing, China’, *Procedia Engineering*, 205, pp. 3428–3434. doi: 10.1016/j.proeng.2017.09.857.

Yin, S. H., Wung, T. Y. and Chen, K. (1978) ‘Natural convection in an air layer enclosed within rectangular cavities’, *International Journal of Heat and Mass Transfer*, 21(3), pp. 307–315. doi: 10.1016/0017-9310(78)90123-0.



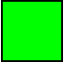


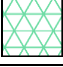
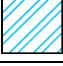
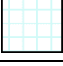


## Appendix A – Case-study apartment floor plans and sensor locations

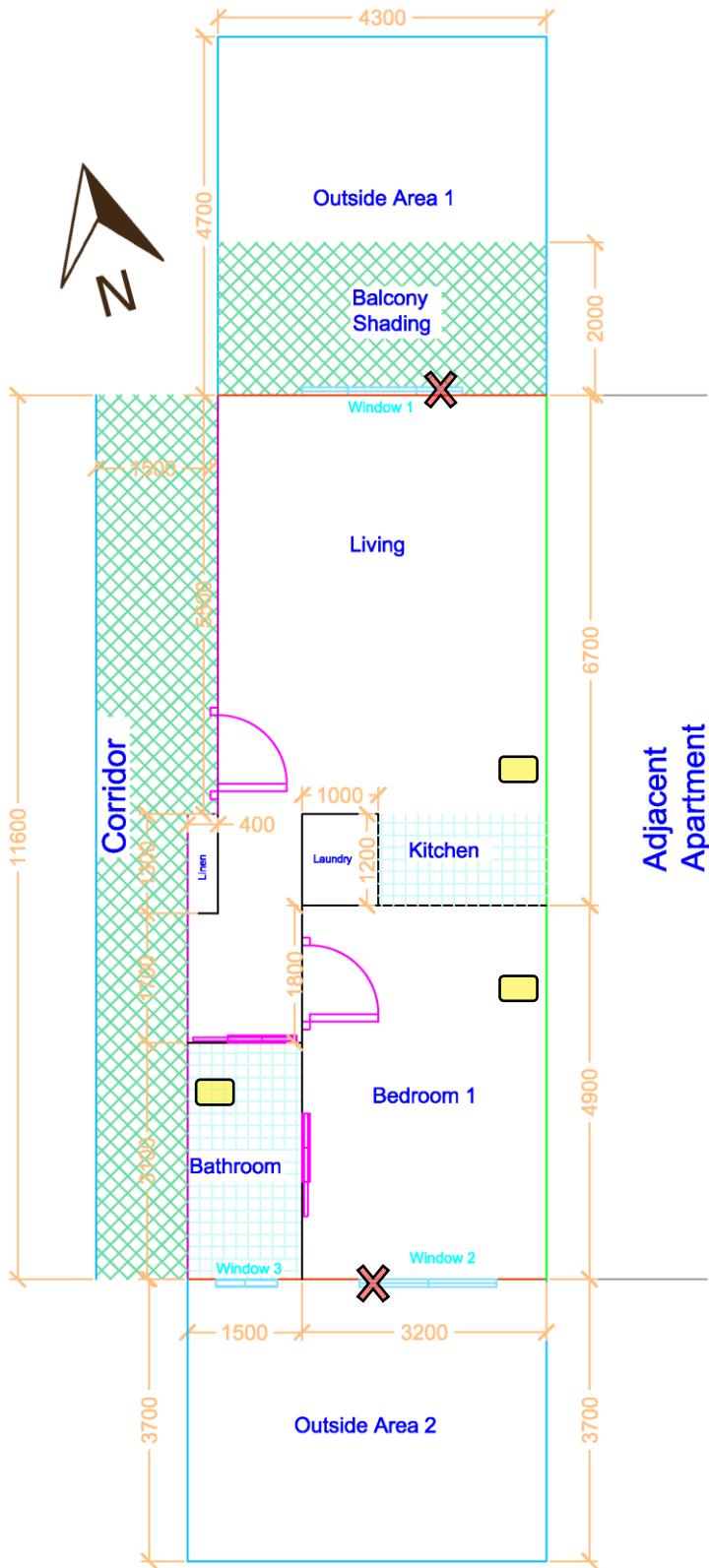
This appendix contains floor plan diagrams of the nine case study apartments investigated in this thesis. The diagrams include the locations of the sensors that were installed as part of the monitoring performed in this study and also highlights the primary shading elements included in the building performance simulation models.

Note that shading elements may include naturally ventilated corridors (in accordance with NatHERS technical notes) and walls of neighbouring apartments, including those on other floors. Apartment #9 was also shaded by a neighbouring building. The shading provided by the neighbouring building was included in the models in accordance with NatHERS, but is not presented in the floor plans supplied below.

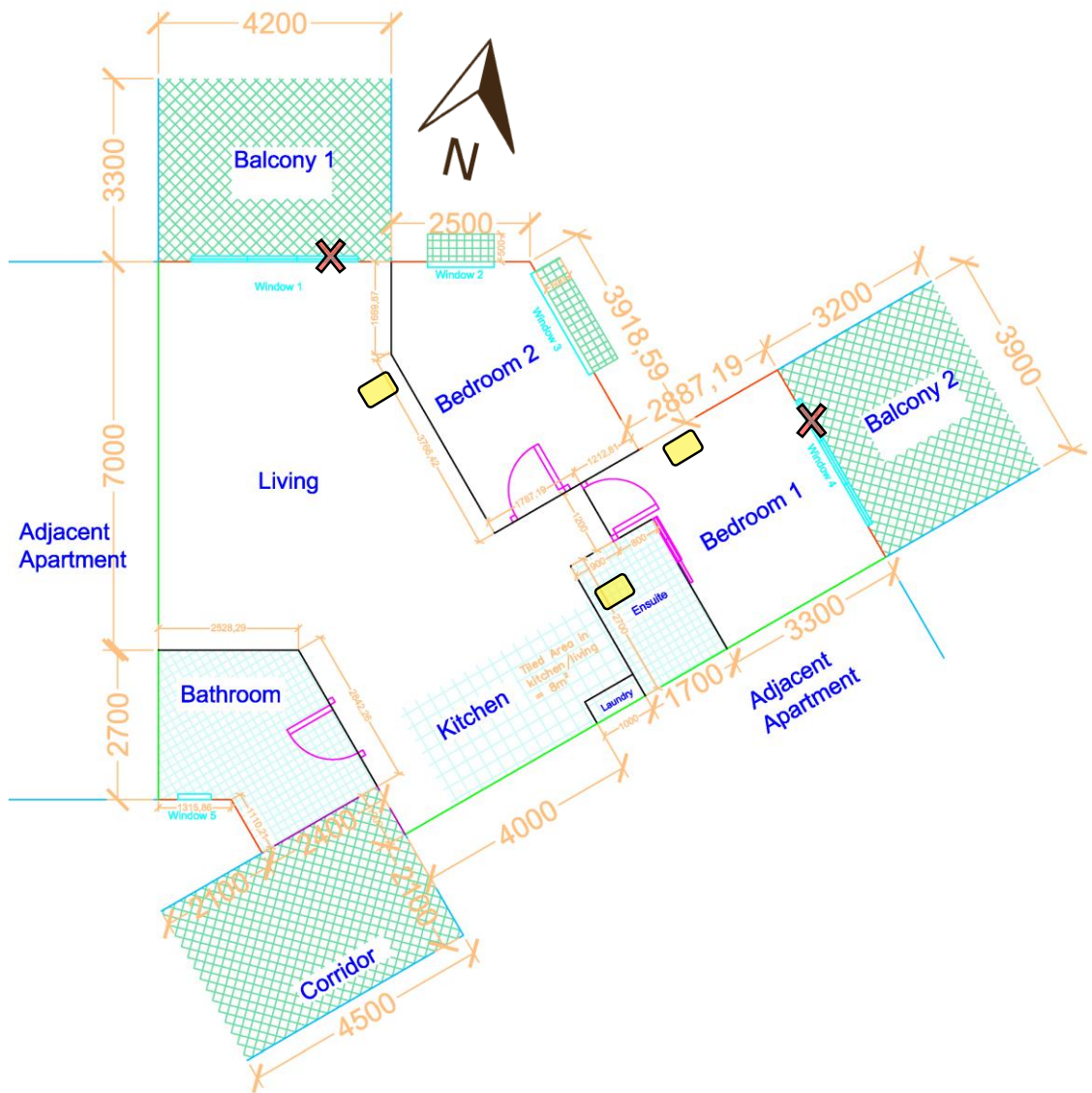
The different wall types and shading elements in the diagrams can be distinguished by line colour. The legend is provided below.

*Key for floor plan diagrams.*

Colour	Wall Type
	External
	External – intertenancy
	Internal – intertenancy (neighbour)
	Internal
	Wing walls and vertical shading
	Horizontal shading
	Vertically shading structures
	Tile floor covering
<b>Sensors</b>	
	Temperature/Relative Humidity/IEQ
	Reed switch

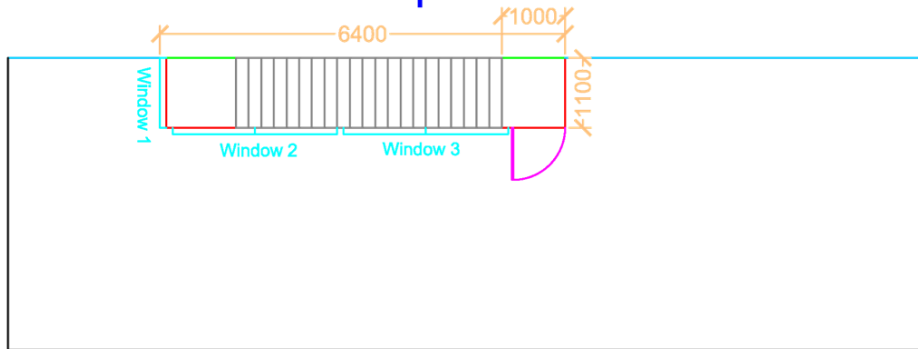


*Floor plan for Apartment #1.*

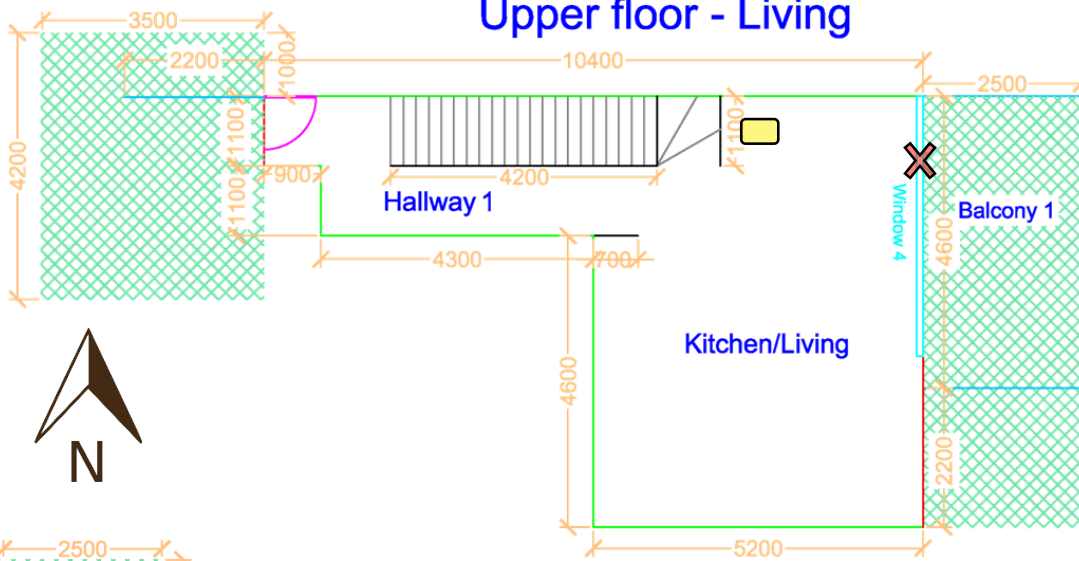


Floor plan for Apartment #2.

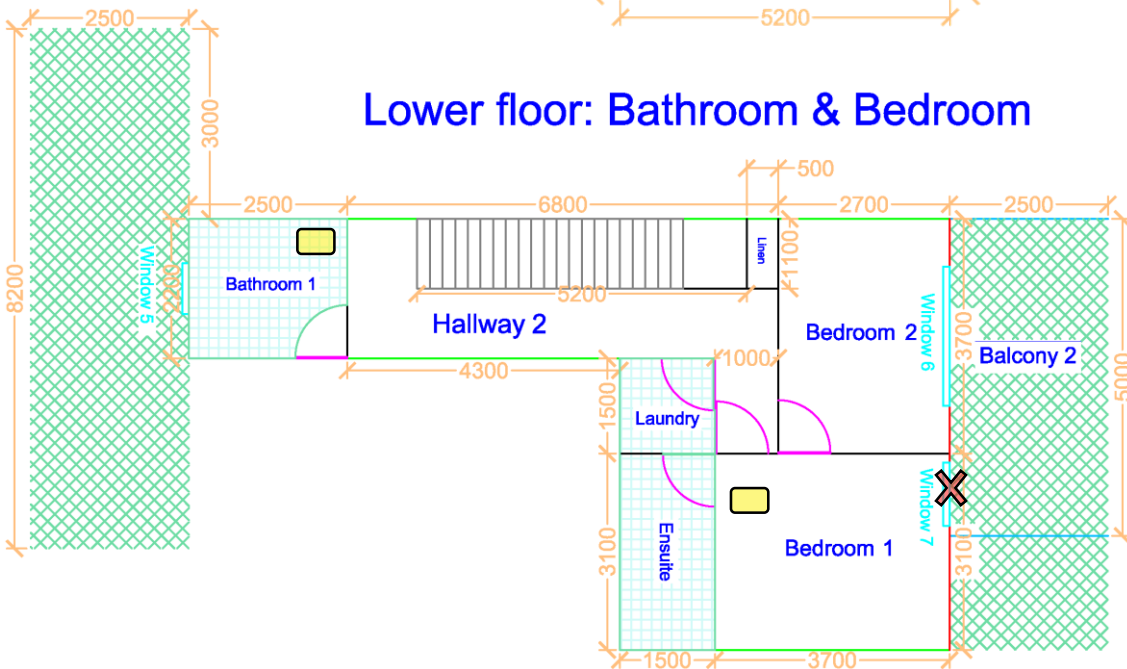
### Rooftop



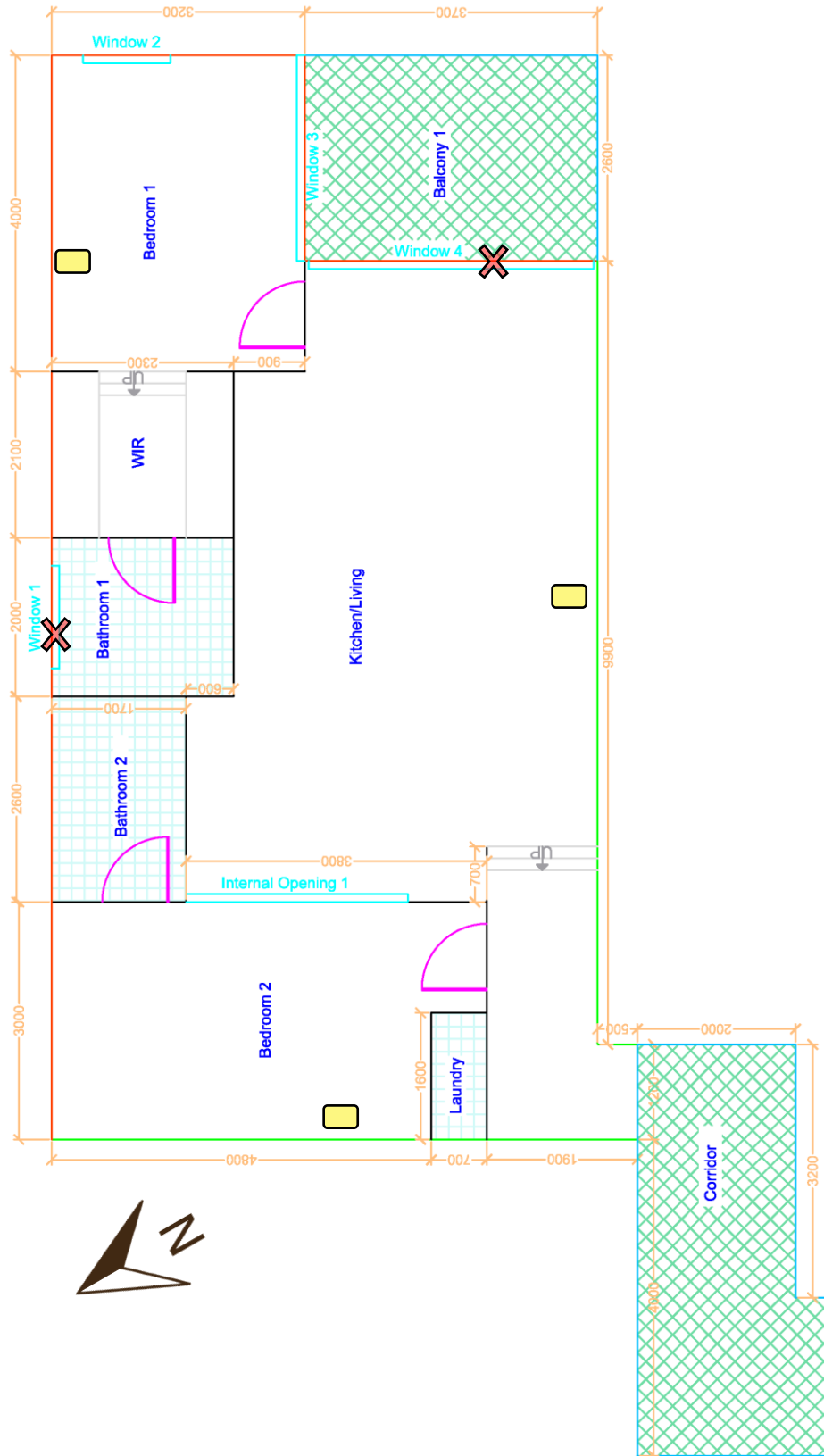
### Upper floor - Living



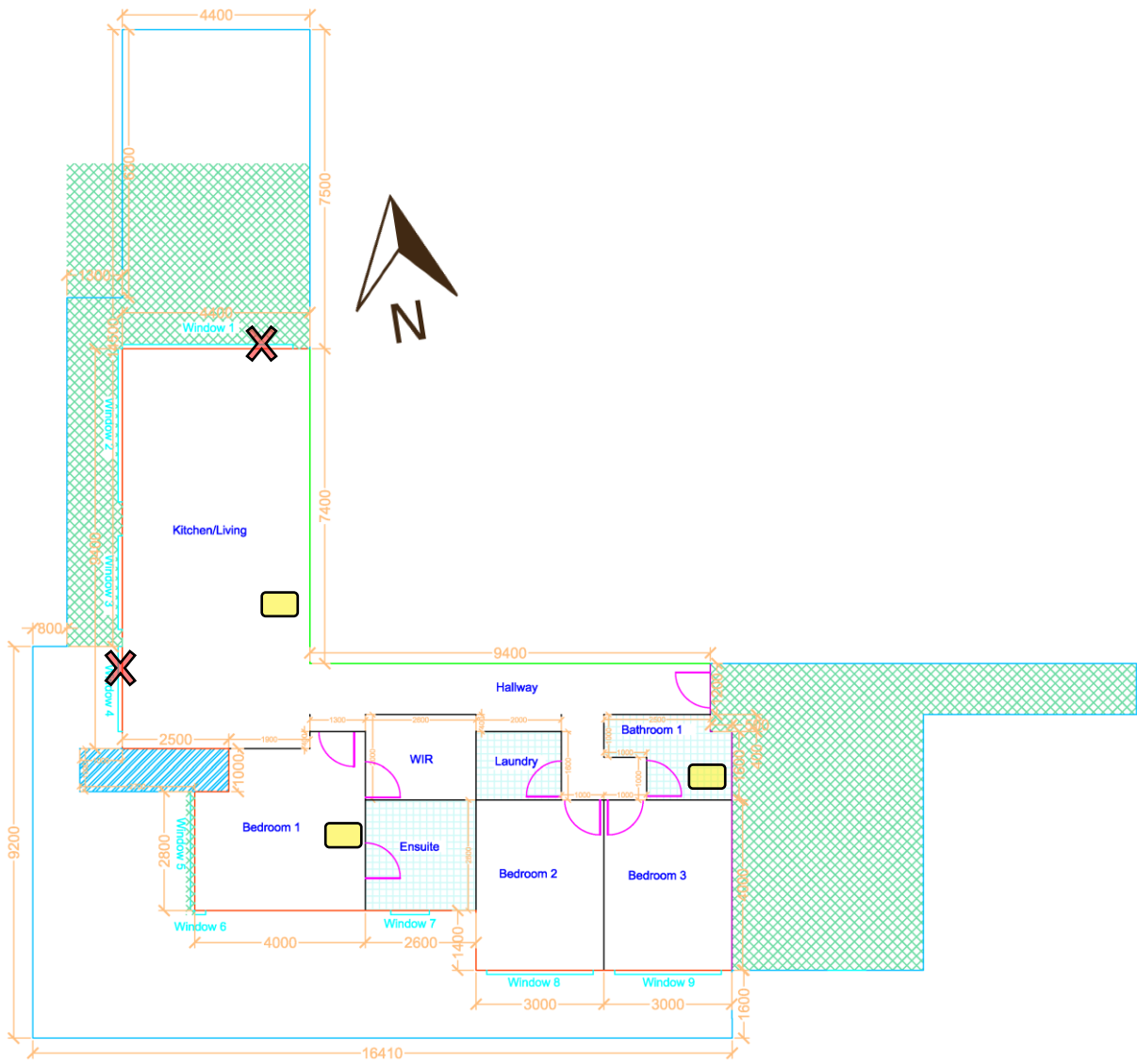
### Lower floor: Bathroom & Bedroom



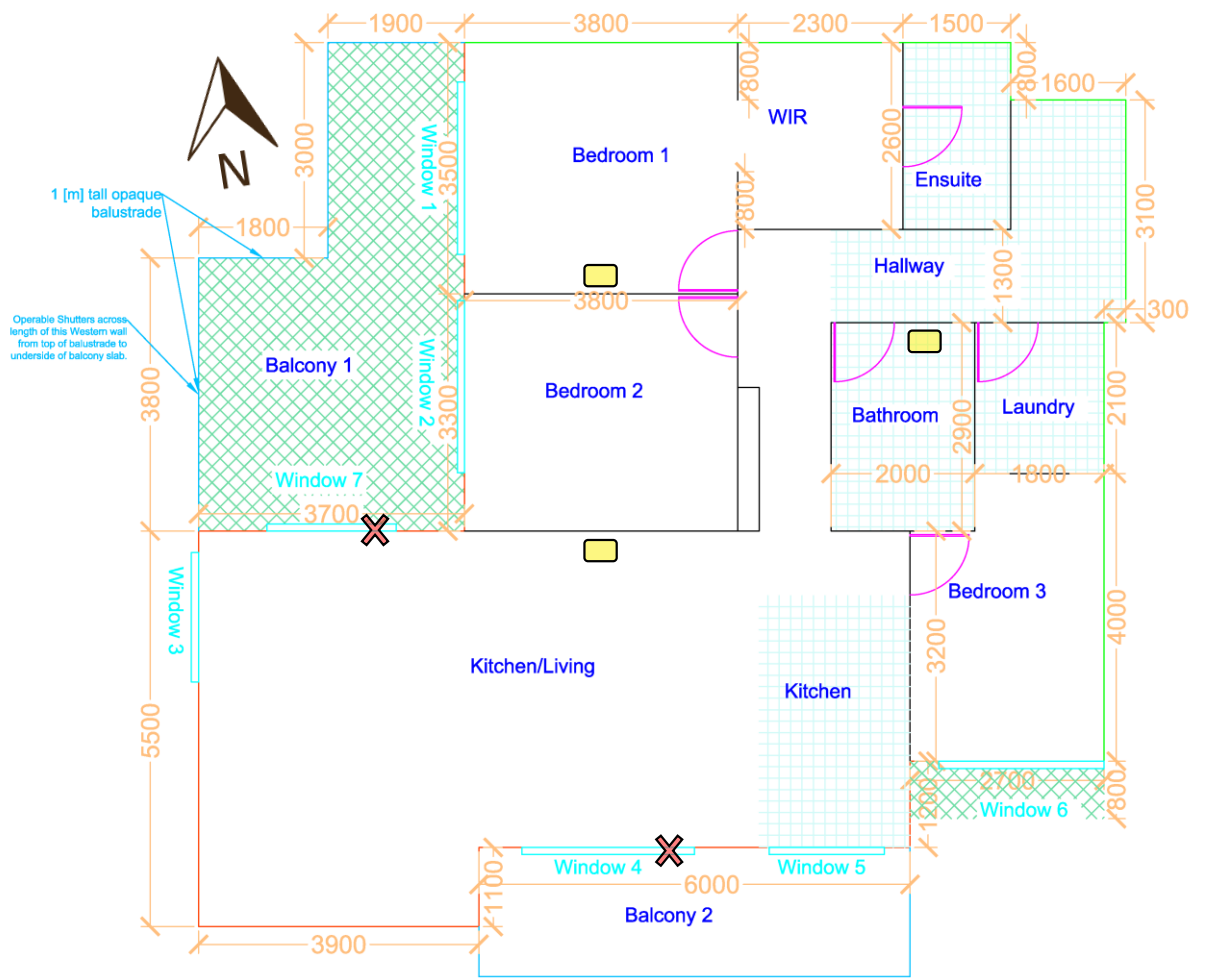
Floor plan for Apartment #3.



Floor plan for Apartment #4.

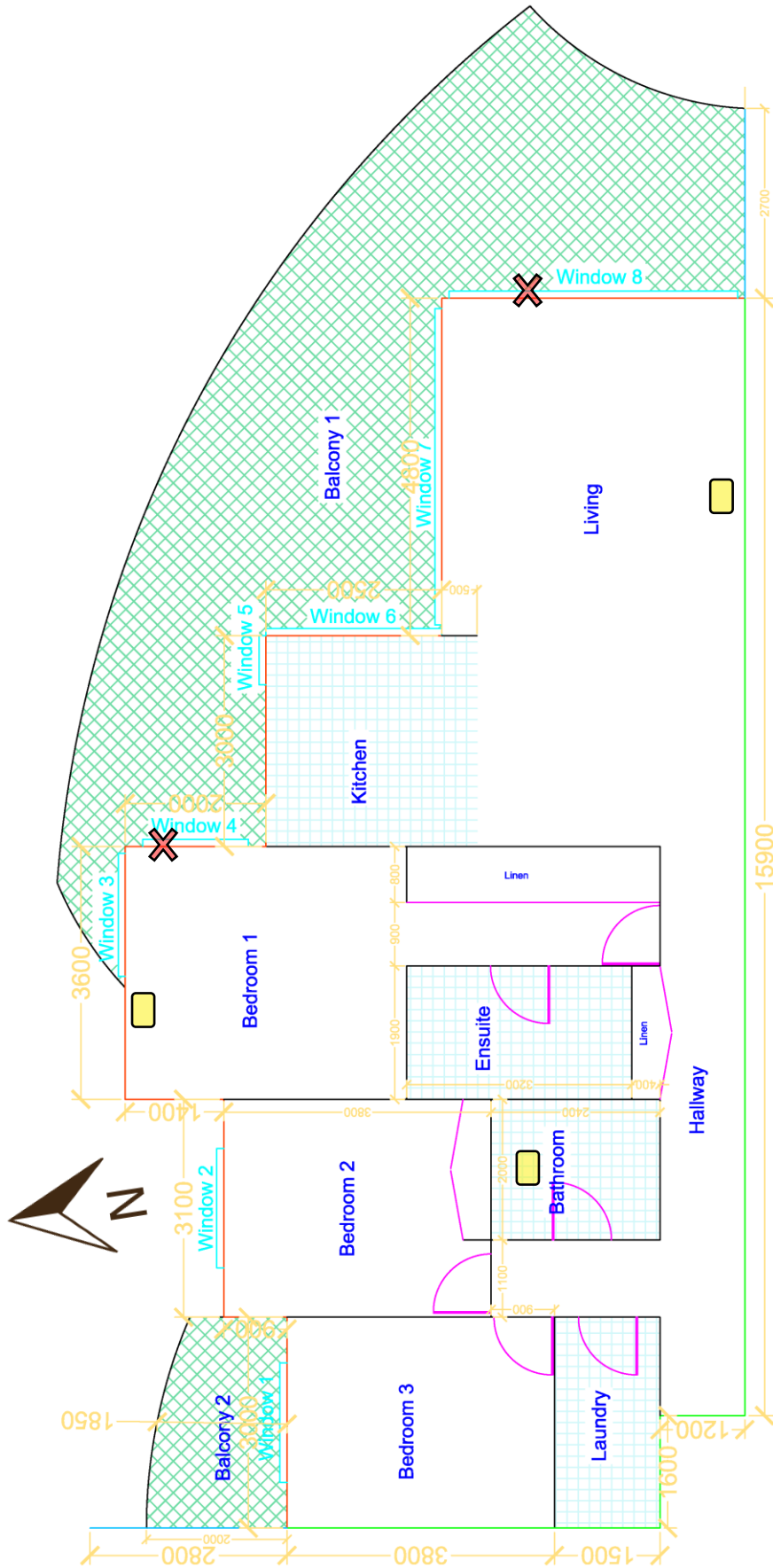


*Floor plan for Apartment #5.*

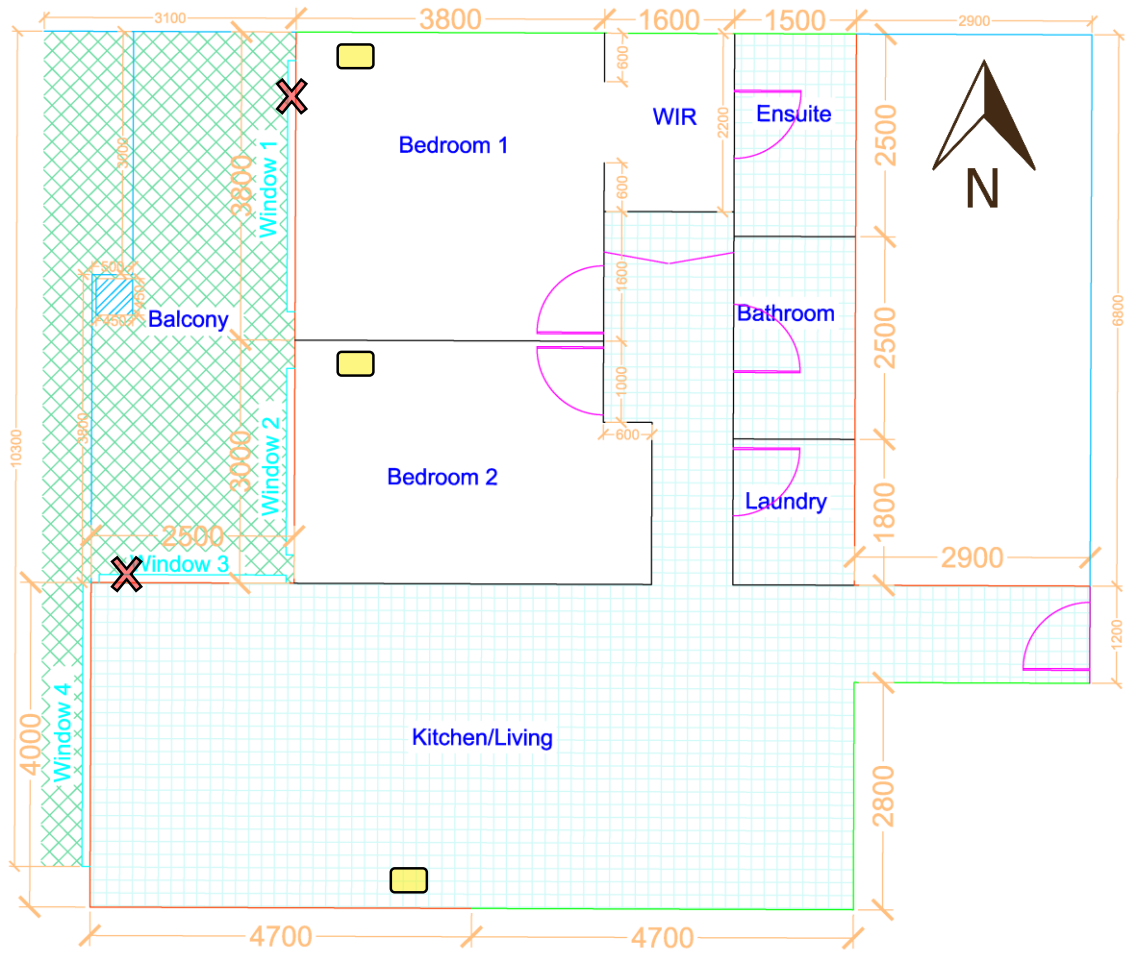


Floor plan for Apartment #6.

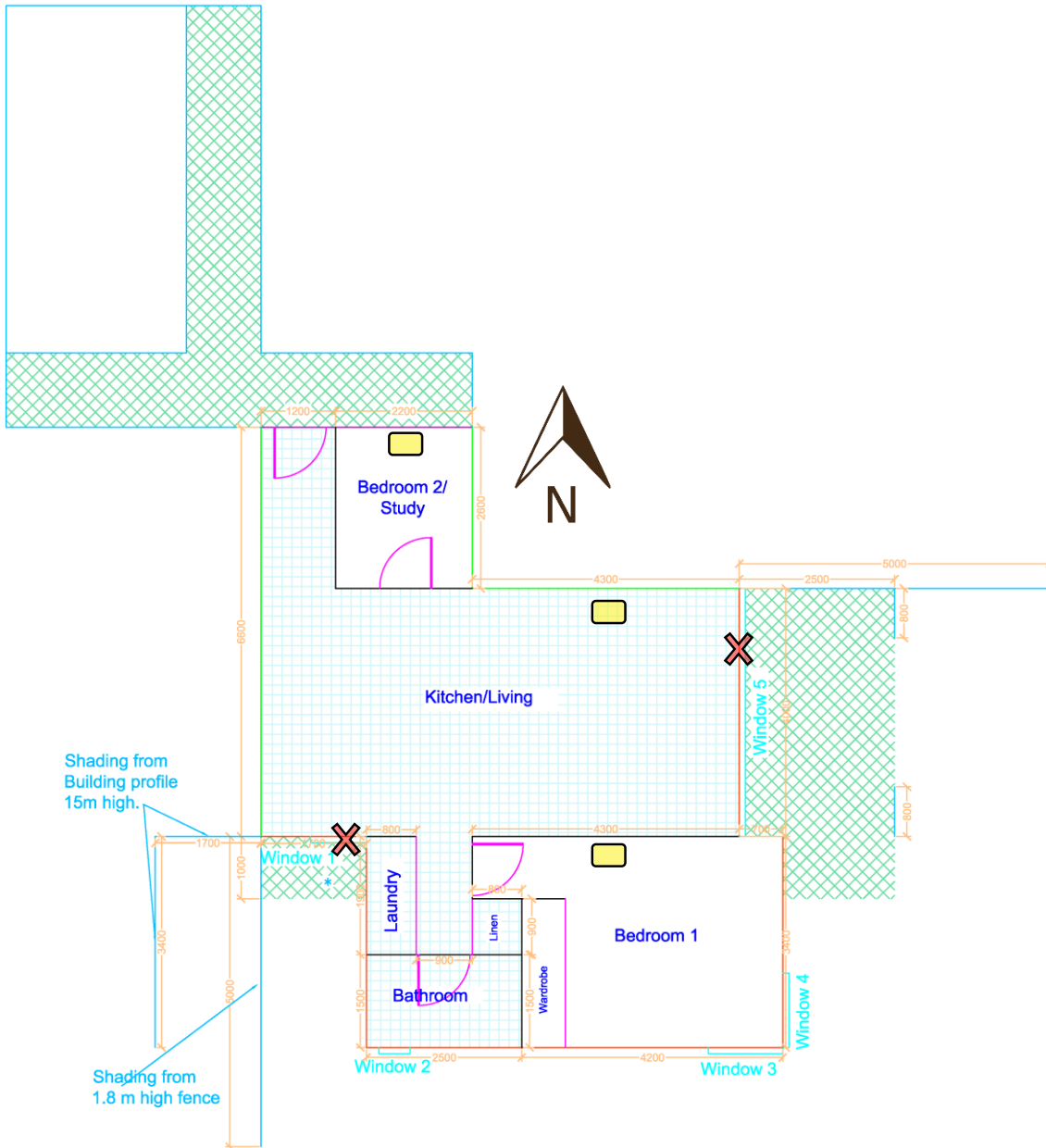




Floor plan for Apartment #7.



*Floor plan for Apartment #8.*



*Floor plan for Apartment #9.*